CCL2/CCR2 chemokine signaling modulates ductal breast cancer progression by enhancing glycolysis and c-MET activation

Diana Sofía Acevedo

M.Sc. Emporia State University, 2012
B.Sc., Truman State University, 2010

Submitted to the graduate degree program in Pathology and the Graduate Faculty of the University of Kansas in partial fulfillment of the requirements for the degree of Doctor of Philosophy.

_____

Dissertation Chair: Nikki Cheng, PhD

_____

Lisa Zhang, PhD

_____

Nika Gloyeske, MD

_____

Russell Swerdlow, MD

_____

Roy Jensen, MD

Date Defended: April 27th, 2021

The dissertation committee for Diana Sofía Acevedo certifies
that this is the approved version of the following dissertation:

CCL2/CCR2 chemokine signaling modulates ductal breast cancer progression by enhancing glycolysis and c-MET activation

_____

Chair: Nikki Cheng, PhD

_____

Graduate Director: Soumen Paul, PhD

Date Approved: May 2nd, 2021

Abstract

Despite therapeutic advancement, ductal carcinoma in situ (DCIS) remains the most common form of pre- invasive breast cancer diagnosed among women with 60,000 cases every year. Treatment for DCIS involves a combination of lumpectomy and radiotherapy in which 10-35% of patients experience disease recurrence that is often accompanied by invasive ductal carcinoma. By developing a molecular approach to evaluate the prognosis of DCIS we can identify biomarkers for DCIS patients capable of predicting which cases will become invasive and potentially spare women from non-necessary surgeries.

The CCL2/CCR2 chemokine signaling is overexpressed in breast cancer biopsies and malignant breast cell lines. Here we demonstrated additional molecular factors by which CCL2/CCR2 might drive DCIS progression, by RPPA analysis on DCIS.com breast cancer cells we identified that CCL2 induction phosphorylated c-MET tyrosine kinase. By PLA we confirmed that CCR2 interacts with c-MET and by CO-IP we demonstrated that this interaction is potentially mediated by SRC dependent mechanisms.

Additionally, global metabolomic analysis revealed that CCL2 alters glycolysis. Specifically, CCL2/CCR2 regulate glycolysis by enhancing glucose consumption, intracellular lactate, and upregulation of Hexokinase 2. In vitro studies targeting c-MET induced by CCL2 with the c-MET pharmacological Merestinib, resulted in blocked cellular migration, proliferation, survival, growth, and glycolysis in basal like breast cancer cells.

By injecting SUM225 CCR2 overexpressing cells via the MIND Mammary Intraductal Injection model and dosing the animals orally with Merestinib, we demonstrated that c-MET inhibition mediated by CCL2/CCR2 resulted in decreased lesion mass, proliferation, and expression of glycolytic enzymes associated with formation of fewer invasive lesions compared to vehicle control. To investigate the effects of inhibiting c-MET pathway on metabolites involved in the glycolytic pathway in vivo, MIND model lesions were analyzed by IC-MS and showed that Merestinib blocked consumption of glycolytic intermediates.

Lastly, we identified the physiological and clinical relevance of the CCR2 and c-MET receptors in normal, DCIS and IDC (invasive ductal carcinoma). By datamining analysis of TCGA data sets we found positive and significant mRNA correlations between CCR2 and c-MET. We further analyzed the protein expression in TMAs from DCIS and DCIS patient samples and identified that there was a positive and significant correlation between CCR2 and c-MET in DCIS and IDC tissues. Co-staining of CCR2 and c-MET demonstrated that co-expression of these receptors is higher in IDC tissues compared to DCIS and normal. These data indicate that CCR2 and c-MET mRNA, and protein expression have an important role in DCIS transition to IDC and that can potentially be identified as biomarkers use to predict DCIS progression.

Implications: This project identifies a unique association between CCL2/CCR2 expression, c-MET activity, and enhancement of glycolysis with important implications into prognosis and potential management of DCIS progression. These associations can be considered as novel molecular targets for alternative therapeutic for DCIS patients expressing high levels of CCR2 and c-MET.

Acknowledgements

As a first-generation immigrant and the first in my family to pursue higher education in the United States, my academic journey has been very challenging. However, I have been privileged to have encounter very special people that have guided, encouraged, and helped so I can be here today.

To start, I want to express my gratitude to my mentor, Dr. Nikki Cheng, since my first interaction with her as I was applying to a part- time and temporal position in her lab as a research technician, she was extremely supportive on my journey. I remember that as part of the interview she asked what was my long-term plan? I told her I wanted to reapply and obtain entrance to the Ph.D. program since I had faced multiple rejections to this program due to my GRE scores. Dr. Cheng gave me something I did not have; the confidence to believe in myself so I could reach my full potential and reach my academic goals. She encouraged me through my application process and has been key in my academic success.

Dr. Cheng has provided and supported many professional development opportunities by including me in reviews, taking active roles in peer publications, teaching me grantsmanship skills, and demanding nothing but the best. Her managing and teaching style have shaped me in how I think and work as a scientist and overall have helped me built self-confidence and strengthen my work ethic. Dr. Cheng has also encouraged me and supported my vision of giving back to the Hispanic community by allowing me to mentor highly motivated Latina students interested in science and research by giving them the opportunity to conduct research in her lab.

To my committee members, Dr. Roy Jensen for his support and patience even during the times that I was not able to be very effective in communicating my findings. I appreciate his time and input into my proposal revisions and encouraging comments as I started to show progress. To Dr. Lisa Zhang, who has been very helpful, supportive and very generous with her time. Numerous times she has shared her cancer metabolism knowledge and experience with me to help me identify aspects of my studies that I did not considered before. To Dr. Nika Gloyeske, thank you for accepting to be part of my committee, for your flexibility and time to provide me positive feedback on my progress reports. To Dr. Russell Swerdlow, you have made a great impact in my academic and professional career. I cannot thank you enough for being very tough by challenging me with very complex questions but being very fair and guiding me during the times where I seemed lost in the metabolic pathways. I also, will forever appreciate the time that you stood up for me and encouraged me to keep going. I remember one time I walked into your office and you shared a difficult time you went through in medical school, it made me realize we all go through it and that is part of our journey.

To the past and present members of the Cheng lab. Fellow students Min Yao, Gage Brummer and Nadia Alissa who have shown me support, encouragement and solidarity during my time and my lab. To Wei Fang Ph.D., thank you for all you technical support, your data analysis, and critical thinking skills have helped me shaped the way I think and talk about the data. My interactions with you have helped me to become a better scientist by improving ways to plan and design my experiments in a more efficient manner. To Benford Mafuvadze who trained me and guided my way around Dr. Cheng's lab during the first 6 months. To Curtis Smart, Meghan, Mike, Kyle, Tina,

Brandon, Baolin, and Paige who have made my time at the lab very enjoyable and have helped me throughout this journey.

I want to thank my mentees because they have challenged me to be the mentor I did not have when I first started my career. To Gabriela Acosta who was the first student that I worked with. Seeing you transition from an undergraduate to now a clinical laboratory scientist professional fills me with joy and a lot of motivation. To Marcela Medrano, the first high school student that we hosted in the lab and that now is a full-time research assistant. Your perseverance and commitment to improve yourself has fueled me during times I did not want to keep going. To Hannah Leyva, you display the work ethic of a senior scientist. Thank you for being so patient during times where I was very ill, and I could not work with you. To Kyla Vasquez who inspires me with her outstanding academic performance and commitment to science. Your drive and focus have motivated me many times. Thank you all for teaching me that this journey is and has not been solely about myself but about the future generations that are coming behind.

To Ms. Zöe Baldwin, thank you for your friendship and support. I appreciate you guiding every semester through the requirements of the Pathology department and logistics through my time at KUMC. Thank you for your service to the Pathology students.

To Dr. Larry Long, thank you for your time and ability to help me own my narrative. Thank you for teaching me how to embrace the personal hardships that I faced during my Ph.D. journey and to develop coping skills to manage difficult situations.

To my parents who sacrificed so much to invest in me by providing an educational trip initially to study English. Thank you for believing in me and supporting me during all these years even when reaching this dream of completing my education seemed unattainable. Soon enough we will see and enjoy the fruits of all our sacrifices.

To my daughter Sofía. You are the most successful biologic and genetic experiment I have ever been part of! You are my dear darling sweetheart, and the best daughter a mother could ever have. Your hunger for knowledge and kind heart makes you an exceptional being. Thank you for being patient and supporting my journey. I am so proud of you, and the sweet little niña you have become.

To my husband Daniel, words cannot describe the gratitude an appreciation I have for you. Thank you for your encouragement, support, and patience during my journey. You have been there for me all the step of the way; reading rejection letters, crying with me but you have always believed in me even when I thought I would never get into a Ph.D. program. You have been to my side in every single award ceremony and every obstacle I have faced. I would not have been able to navigate this without you.

To the Self-graduate fellowship program. Thank you for granting me the opportunity to be considered and selected for this prestigious fellowship. The professional development opportunities that I have obtained through this program have helped me become the professional I am today. Thank you!

To the NIH Administrative Diversity Supplement grant to help me fund my first year of training as a graduate student in the project “Progression of DCIS to invasive breast cancer through CCR2 chemokines signaling”

To the Pathology department for granting us two basic science Pathology awards that helped fund some experiments to provide preliminary data on metabolism.

To the Geographical Management of Cancer Health Disparities Program (GMap) Region 3 Research Completion Award. NIH, NCI. University of New Mexico Comprehensive Cancer Center. Thank you for granting me the award to fund the in vivo portion of my dissertation “Effect of c-MET inhibition in CCL2/CCR2 mediated DCIS progression in vivo”

Table of Contents

Figures and Tables

Chapter I. Introduction

Chapter II. Chemokine Signaling Facilitates Early Stage Breast Cancer Survival and Invasion through Fibroblast dependent Mechanisms

Chapter III. CCL2/CCR2 chemokine signaling enhances glycolysis in human breast cancer cells by upregulating Hexokinase 2 expression

Chapter IV. Activation of the c-MET receptor tyrosine kinase by CCL2/CCR2 chemokine signaling is important for DCIS progression

Chapter V. Targeting c-MET by Merestinib inhibited CCR2 mediated DCIS growth, proliferation, and expression of glycolytic enzymes associated with decreased invasion in the MIND model

Chapter VI. Clinical relevance of the c-MET tyrosine kinase receptor in DCIS progression to IDC

List of Abbreviations

ADH	Atypical Ductal Hyperplasia
ALDH1	Aldehyde Dehydrogenase 1
α -SMA	Alpha Smooth Muscle Actin
ANOVA	Analysis of Variance
ATP	Adenosine triphosphate
BSA	Bovine Serum Albumin
BRCF	Biospecimen Repository Core Facility
CCL2	C-C Chemokine Ligand 2
CCR2	C-C Chemokine Receptor 2
CK	Cytokeratin
CO-IF	Co-Immunofluorescence
CRISPR	Clustered Regularly Interspaced Short Palindromic Repeats
DAB: 3,3’	Diaminobenzidine
DAPI: 4’,6’	Diamidino-2-Phenylindole Dihydrochloride
DCIS:	Ductal Carcinoma in Situ
DMEM	Dulbecco’s Modified Eagle Medium
DMFS	Distance Metastasis Free Survival
DMSO	Dimethyl sulfoxide
E-Cadherin	Epithelial Cadherin
EDTA	Ethylenediaminetetraacetic Acid
EGFR	Epidermal Growth Factor Receptor
ELISA	Enzyme-Linked immunosorbent assay
EMT	Epithelial – Mesenchymal Transition

ER	Estrogen Receptor
ERK	Extra cellular Signal-Regulated Kinases ½
ETC	Electron Transport Chain
FACS	Flow Assorted Cell Sorting
FAS	Fatty Acid Synthesis
FBS	Fetal Bovine Serum
Fsp1	Fibroblast Specific Protein 1
G Protein	Guanine nucleotide-binding Protein
GCPR	Guanine Protein Coupled Receptors
GC-MS	Gas Chromatography Gas Spectroscopy
GFP	Green Fluorescent Protein
HTRA2	High Temperature Requirement Protein A2
H&E	Hematoxylin and eosin
h	Hours
HGF	Hepatocyte Growth Factor
HR	Hazard Ratios
HRP	Horseradish peroxidase
IC-MS	Ion Chromatography Mass Spectroscopy
IDC	Invasive Ductal Carcinoma
IHC	Immunohistochemistry
IP	Immunoprecipitation
IRB	Institutional Review Board
IRES:	Internal Ribosome Entry Site
KD	Knockdown
KO	Knockout

KUMC	University of Kansas Medical Center
MAPK	Mitogen- Activated Protein Kinases
Min	Minutes
MIND	Mammary Intra-ductal Injection
MOM	Mouse on Mouse
mRNA	Messenger RNA
NOD-SCID	Non-Obese Diabetic Severe Combined Immunodeficient Interleukin receptor-γ2
MRI	Magnetic Resonance Imaging
MRS	Magnetic Resonance Spectroscopy
NP-40	Noni dent P-40
OXPHOX	Oxidative Phosphorylation
PAGE	Polyacrylamide Gel Electrophoresis
PBS:	Phosphate Buffered Saline
PCNA	Proliferating Cell Nuclear Antigen
PCR	Polymerase Chain Reaction
PI3K	Phosphatidylinositol-3 kinase
PKC	Protein Kinase C
PPP	Pentose Phosphate Pathway
PR	Progesterone receptor
RTK	Receptor Tyrosine Kinase
SD	Standard Deviation
SEM	Standard Error of the Mean
SF	Serum Free
ShRNA	Short Hairpin RNA

SH2	Src Homology 2 Domain
SDS	Sodium Dodecyl Sulfate
TCA	Tricarboxylic acid cycle
TMA	Tissue Microarray
TNBC	Triple Negative Breast Cancer
WT	Wild Type
VW8	Von Willebrand Factor 8

Chapter I: Introduction

Ductal Carcinoma i*n Situ* (DCIS)

Epidemiology and Natural History

Ductal carcinoma in *situ* (DCIS) refers to the abnormal growth of the epithelial cells that have become “cancerous” but are still confined within the duct and lobule of the breast. If left untreated, DCIS can progress to invasive ductal carcinoma (IDC). DCIS is the most common type of pre- invasive breast cancer, with 63,410 cases diagnosed, an approximate of 252,710 new cases of invasive breast cancer, and 40,610 expected deaths in 2017 in the United States [1].

A normal breast duct is a hollow tube made from epithelial cells and surrounded by myoepithelia and a basal membrane. DCIS is a heterogeneous group of lesions characterized for abnormal growth but that are still confined within the basal membrane and myoepithelia of the breast duct which serve as structural barriers between the stroma and duct. Progression from DCIS to IDC is characterized by the disappearance of the myoepithelium and appearance of invading ductal carcinoma cells into the surrounding stroma.

DCIS represents an advanced or late stage tumor progression with malignant potential, and it is the known to be the direct precursor of most invasive breast cancers (IBCs). Some evidence that supports the idea that DCIS is nonobligatory precursor of most invasive breast cancers (IBC) is the fact that most IBCs are accompanied by DCIS and foci of histological continuity [2, 3]. Wellings and Jensen established a model for human breast cancer evolution. The model suggests that in humans, DCIS lesions start to develop in the terminal duct lobular units (TDLUs) and that there is a continuous from TDLUs to cancer through a series of acquired mutations that make increasingly

“abnormal: stages over time [4]. Currently, is well known that most IBCs evolved through a nonobligatory series of stages such as hyperplasia, also known as hyperplastic lobular units (HELU), atypical ductal hyperplasia (ADH), ductal carcinoma in situ (DCIS) and lobular carcinoma *in situ* (LCIS) [3, 4] (Fig.1).

Laboratory and clinical data indicate that DCIS can progress to invasive disease. A study reported that from 179 DCIS cases of patients, if left untreated, the average progression rate was (~43%) to develop invasive disease [5]. Further studies demonstrate that the major risks for developing IBC are the same for DCIS and that they both share many genetic abnormalities, especially when they are in the same breast [2-4, 6]. Therefore, if not completely removed, DCIS diagnosis represents a strong risk factor for developing IBC in the future. Thus, there is an urgent need in the field to identify molecular biomarkers and mechanisms that drive DCIS progression to IDC so we can accurately predict disease progression.

The clinical conundrum of DCIS overtreatment and undertreatment

One of the current clinical challenges is that the standard diagnostic method for DCIS, the mammogram, cannot predict disease progression. Since the current treatment for DCIS involves mastectomy or lumpectomy with or without radiation and hormonal treatment, there is not a clinical available tool to predict which DCIS cases will become invasive. About 5 to 30% of DCIS patients who are treated with breast-conserving therapy experience local recurrence on the same breast, about one half of the recurrences are invasive [7].

Magnetic Resonance Spectroscopy as an alternative diagnostic approach for DCIS

Due to the lack of an assertive prognostic tool, using a non-invasive molecular imaging approach to study the progression of DCIS in an animal model would be very useful. With the new and improved magnetic resonance imaging (MRI) and spatial resolution, as many as 98% DCIS cases are detected with MRI. Additionally, 6-23% lesions that cannot be detected via mammogram can be detected with MRI due to the enhancement of non-calcified DCIS which remain undetected with the standard mammogram [8]. MRI detects lesions as small as 2mm in transgenic mouse models of breast cancer and it is capable of differentiate between *in situ* mammary lesions from invasive mammary tumors [9, 10].

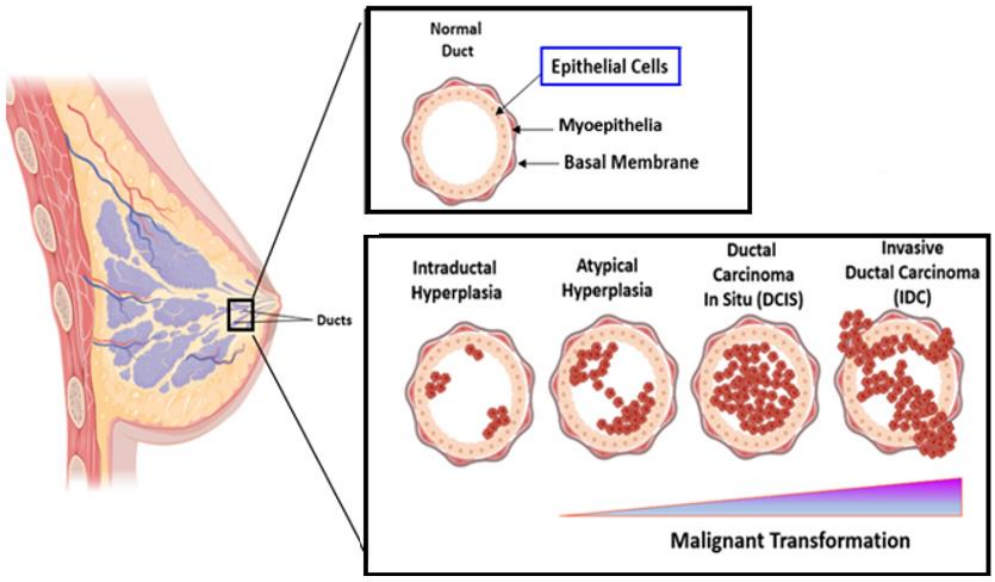

Figure 1. Current model of DCIS transition to IDC. A normal breast duct is a hollow tube made with epithelial cells and surrounded with myoepithelia and basal membrane. DCIS progression and transition to invasive disease through a series of mutations that make abnormal stages over time.

Even though, MRI can provide image acquisition and identifying radiological characteristics that might help identify which neoplasias will likely become invasive or will progress, this image base method has the limitation that does not provide data on the molecular mechanisms that might be involved in cancer progression. However, Magnetic Resonance Spectroscopy (MRS) coupled with MRI can provide data on metabolite profiles relative to tissue morphology. Therefore, using MRI along MRS is used to study the metabolism of tumors and or cells by the detection of different metabolites and biochemicals that are involved in different metabolic pathways in vivo [11]. Therefore, the capability of MRS to non-invasively determine concentration of metabolites in certain tissues provides powerful biological information not given by any other current imaging diagnostic method [12].

Challenges to assess DCIS progression in vivo

DCIS is a multi- stage process in which genetic and molecular heterogeneity are involved at different steps making it a great challenge to obtain tissue samples from all stages of progression. This presents a great obstacle for studying the molecular mechanisms that could mediate the transition from pre- invasive DCIS to IDC. Therefore, the lack of suitable in vivo models to study DCIS makes it even more challenging to understand the pathobiology of DCIS. For instance, mammary fat pad injection and subcutaneous transplant models do not represent the heterogeneity of breast cancer and do not mimic DCIS progression and transition to invasive disease [13-16].

Transplant models fail to grow primary DCIS cells elucidating another challenge in making it difficult to translate potential predictors of the disease or therapeutic targets to the clinic. Even though the establishment of molecular subtypes in IDC and the use of

the hormonal Estrogen (ER) and Progesterone (PR) in addition to the HER2 biomarkers to guide treatment has been recognized, [17 - 20] subtype alone is not a direct or significant predictor od DCIS progression or transition to IDC [21 - 23].

To overcome some of these limitations, the mouse intra ductal (MIND) model was developed [24]. This model consists of injecting DCIS cell lines and patient derived DCIS epithelial cells into the mammary ducts of immunosuppressed mice (Fig. 2). The MIND model mimics the progression of human DCIS and can be observed in definable stages including ductal growth of in situ lesions that is followed by the invasion of surrounding microenvironment (stroma) as cancer cells cross the myoepithelial and basal membrane [25, 26].

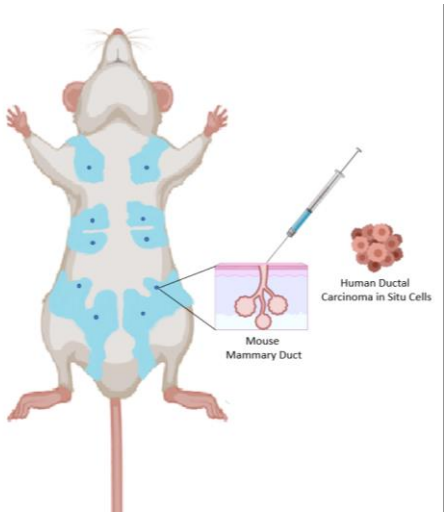

Figure 2. The MIND (Mouse Mammary Intraductal Injection) model mimics DCIS progression. The MIND model is the most physiological and clinically relevant model for DCIS available until this day because the cells are seeded within their native environment and it resembles the heterogeneity and natural progression of human disease.

Chemokines

Chemotactic cytokines which are also referred to as chemokines, are a family of small soluble proteins (8-17 kDa). Chemokines have been recognized as critical mediators of the inflammatory response by forming molecular gradients to mediate the movement of cells from the innate and adaptive immune system to the site of injury or inflammation [27]. Additionally, chemokines have long been recognized as regulators of biological processes such as angiogenesis, immune cell trafficking during embryonic development, wound healing, and infection [28, 29].

Currently, about 47 chemokine ligands and 23 chemokine receptors have been identified and are classified into several categories according to the spacing of two NH2 - terminal cysteines. Current classes of the chemokine family are referred to as CC, CXC, and CX3 in which the X is a non-cysteine amino acid residue [30]. While the CXC class of chemokines regulate recruitment of neutrophils and T cells, the CC chemokine regulate both T and B cells as well as the recruitment of dendritic cells and those derived from the bone marrow [28, 31].

Structure and function of the CCL2 chemokine ligand

CCL2, also known as Monocyte Chemotactic Protein 1 (MCP1) is a small chemokine that belongs to the C-C class of chemokines that has been shown to be a critical regulator of immunological processes including inflammation, macrophage recruitment during wound healing and autoimmune diseases [32,35]. CCL2 is well known for its role during inflammation or infection since it recruits monocytes, T cells and dendritic cells. Studies reveal that even though CCL2 can bind to CCR2-CCR5, it has the highest binding affinity for the receptor CCR2 [39].

Structure and function of the CCR2 Chemokine receptor

The chemokine receptor CCR2 is a G Protein Coupled Receptor (GPCR) that regulates macrophage recruitment during wound healing, infection, and inflammation [27, 38]. Even though CCR2 is expressed as two spliced isoforms (A and B) in humans, one isoform is expressed in mice. CCR2A is primarily expressed in macrophages, while CCR2B regulates T cell signaling [39]. CCR2 signaling is activated through the binding of three different ligands: CCL2, 7 and 8 chemokines. However, chemokines also activate downstream pathway targets independently of G proteins including p38 MAPK [40], and JAK2/STAT3 pathway [41].

In normal tissues, chemokine receptor levels are maintained at low levels. In macrophages, prolonged binding of the ligand to the chemokine receptor leads to β-arrestin which is a negative regulator of G- Proteins Coupled Receptors that promotes receptor internalization, causing desensitization and thus downregulating downstream signaling [42]. However, during acute inflammation, CCL2 mRNA expression and secretion is induced by IL6 [43], and TNF-Ƙ [44].

Significance of the CCL2/CCR2 chemokine signaling in cancer

Signaling of CCL2 through CCR2 leads to the activation of downstream signaling pathways including p42/44 MAPK, phospholipase C-γ, and PKC through G-protein dependent mechanisms which regulate cellular adhesion and motility in macrophages [45]. Recent studies on the signaling pathway as it related to breast cancer has found that CCL2 enhances expression activity of RhoA through Smad3 and MEK signaling

through p42/p44 MAPK signaling to regulate breast cancer cell motility and survival [46] (Fig. 3).

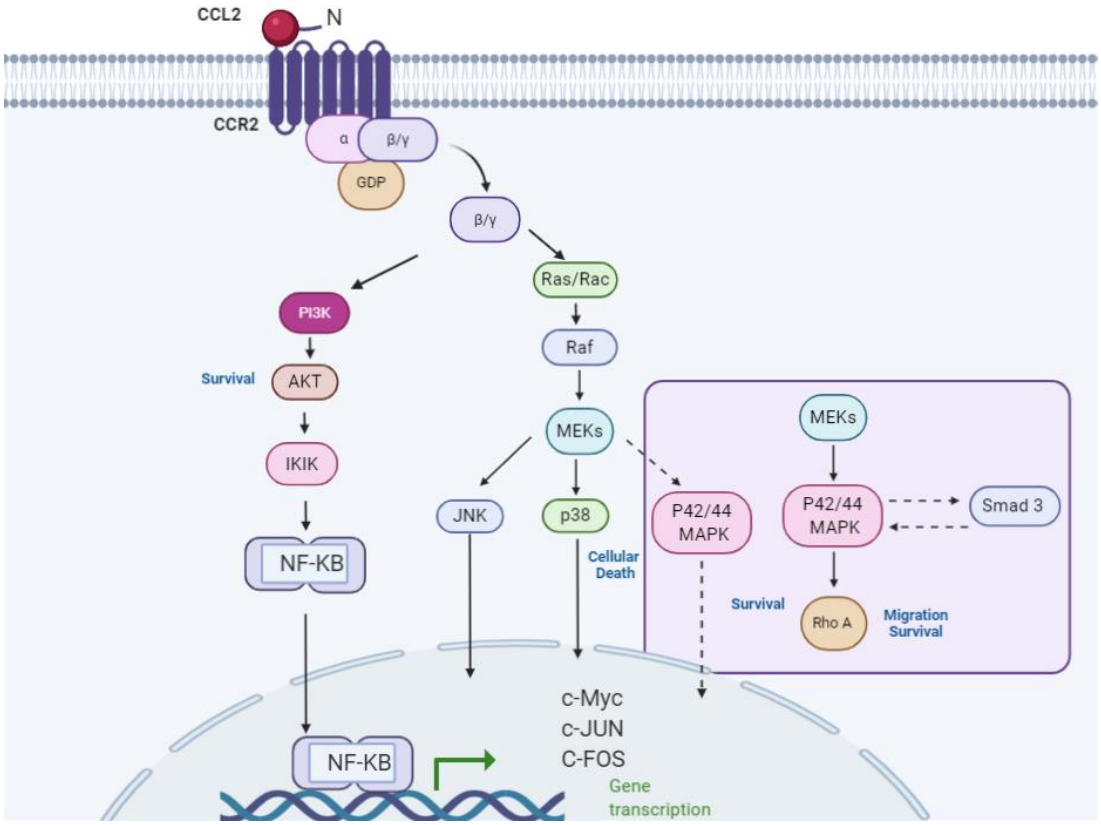

Figure 3. CCL2/CCR2 Chemokine signaling pathways. Chemokine signal transduction starts by the binding of the CCL2 ligand at the NH2 terminus to the seven transmembrane CCR2 G protein coupled receptor. Binding leads to phosphorylation of the intracellular region at the serine/threonine residues which results in conformational changes and activation on the heterotrimeric G protein complex that includes the subunits Gα, Gβ, and Gγ. Following activation of the G protein complex to a GTP bound state, dissociation of the Gα subunit from the Gβ and Gγ, thus activating downstream pathways. Activated pathways include PI-3 kinase (PI-3K), Rho family of GTPases, and p42/44 MAPK.

The significance of this chemokine CCL2 and its receptor CCR2 is that they are both overexpressed in multiple cancer types including pancreatic, brain, prostate, colon and breast cancer [47-51]. Over expression of CCL2 correlated with tumor grade and poor patient prognosis in glioma, prostate, breast, and ovarian cancers [50-53].

Mechanisms of CCL2/CCR2 in regulating breast cancer

The CCL2/CCR2 chemokine signaling is highly regulated in breast cancer at different levels including genetic, RNA, protein and signaling via autocrine and paracrine mechanisms. To start, at the genomic levels, single nucleotide polymorphisms of CCL2 (MCP1), have been associated with the risk of breast cancer development. Such variations in the genome exist in the regulatory regions of the MCP-1 gene. Results indicate that independently of initial stage, breast cancer patients that carry at least one G allele were at an increased risk for metastasis [54]. On the other hand, the single nucleotide polymorphism in CCR2 has been implicated with an increased risk for developing Her2+ breast cancer and poor prognosis [55].

In breast cancer, CCL2/CCR2 are highly expressed in DCIS compared to normal tissue. In breast cancer cells, epithelial CCR2 corresponds to invasive potential [46, 56] and it is associated with the development of sporadic breast cancer [57].

Protein and RNA expression level alterations of CCL2 have been implicated in breast cancer. High expression of CCL2 correlates with tumor grade and poor patient prognosis demonstrated by flow cytometry studies of cell suspensions from tumor biopsies [58]. Increased expression of CCL2 in breast tumors by immunohistochemistry in the epithelium and stroma contributes to disease progression and it is highly correlated with increase macrophage recruitment [52].

Analysis of blood serum levels from breast cancer patients revealed that increased CCL2 levels correlated with tumor stage and lymph node involvement [59]. CCL2 has been proposed as a potential alternative target for metastatic breast cancer

because high expression of CCL2 correlates with a decrease in survival in breast cancer patients [60,61]. On the other hand, the CCR2 chemokine receptor is highly upregulated in breast ductal carcinoma in cells in IDC correlates tumor grade and decreased long-term patient survival [46]. These studies indicate that CCL2 plays a role in breast cancer progression by influencing growth and metastatic spread.

Further evidence indicates that stromal CCL2 and epithelial CCR2 expression in breast cancer correlates with poor patient prognosis [62, 63]. CCL2/CCR2 signaling in breast cancer promotes invasion during early stage breast cancer progression. Ex vivo tissue models and in vivo mouse models have demonstrated that CCR2 expression in breast cancer cells is important for DCIS progression, cancer stem cell renewal and breast cancer survival and invasion.

De regulated CCL2/CCR2 signaling has been implicated in inflammatory [64], metabolic as well as immune diseases that indicate that CCL2/CCR2 regulate monocyte recruitment and M2 polarization through MAPK pathways [32]. In terms of autocrine and paracrine signaling mechanisms, studies demonstrate that CCL2 expression in fibroblasts significantly reduced mammary tumor metastasis associated with decreased survival independently from tumor growth or macrophage recruitment [65]

An important role for autocrine and paracrine CCL2/CCR2 chemokine signaling in breast cancer cells in promoting DIS progression was demonstrated using the MIND model and co- transplant models. The CCL2/CCR2 chemokine regulates breast cancer progression by signaling to breast cancer cells in promoting DCIS progression by using a murine mammary intra-ductal injection (MIND) to mimic DCIS progression, CCR2

overexpression in SUM225 breast cancer cells enhanced formation of invasive lesions associated with the increase presence of CCL2 expressing fibroblasts. CCR2 KD and knockout in DCIS.com breast cancer cells inhibited the invasive potential as well as the decreased presence of CCL2 expressing fibroblasts [62, 63, 66].

Functional Studies for CCL2/CCR2

Animal studies elucidate roles of CCL2/CCR2 in breast cancer development by demonstrating that blocking CCL2 activity with neutralizing antibodies in mammary tumor bearing mice decreases tumor growth, angiogenesis, metastasis and M2 macrophage recruitment. [52, 65, 67]. These studies suggest that CCL2 signaling through CCR2 may play a unique role in tissue homeostasis and that CCL2 regulates tumor progression through macrophage dependent mechanisms.

The receptor CCR2 and its ligand, CCL2 knockout mice show similar defects in macrophage recruitment when inflammation is induced without any compensatory upregulation of CCL7 or 8 [34, 35]. Other expression analysis has shown significant correlations between CCL2 expression and macrophage levels [52, 66].

Emerging roles for CCL2/CCR2 signaling in breast cancer

The standard model for CCL2/CCR2 in cancer has been to regulate metastatic progression through the recruitment of immune cells to tumor tissue [48]. However, this paradigm has been challenged by different studies that elucidate novel roles by which CCL2 regulates tumor progression through additional mechanisms that are independent of macrophage recruitment [65, 68].

Recent studies have identified molecular mechanism by which CCL2 enhanced phosphorylation of Smad3 and MEK p-42/p44 MAPK associated with increased cell migration and survival and RhoA expression. An alternative mechanism for survival revealed that MEK-p42/44MAPK signaling induced by CCL2 function independently from Smad3 and therefore and alternative mechanism for cell survival [46].

Additionally, in an ex vivo culture model that CCL2 knockdown inhibited PyVmT tumor cell proliferation and survival and enhanced cell necrosis and cellular autophagy, ultimately decreasing cell viability [66]. These studies suggest that CCL2 regulates cellular migration, invasion, through a variety of mechanisms that involve programmed cell death.

In summary, evidence demonstrate that CCL2/CCR2 is a clinically relevant target. Since CCL2 regulates cell motility, growth, and survival, targeting the CCL2/CCR2 chemokine signaling pathway can be a potential therapeutic target with direct implications in tumor ablation by downregulating key biological processes that occur during breast cancer progression and metastasis.

The c-MET receptor

The c-Met receptor is part of the receptor tyrosine kinase family (RTK). This family is characterized by having proteins that have a transmembrane protein domain with both extracellular binding domains and an intracellular tyrosine kinase domain. Upon ligand binding, there is a conformational change in the intracellular domain that is followed by phosphorylation of tyrosine residues in the kinase domain. Therefore, the activation of the kinase domain increases accessibility of ATP and substrate binding sites. Activation

of tyrosine residues results in recruitment of adaptor proteins to exert specific signal transduction functions. In general, downstream signaling for RTKs involve many cellular functions that include growth, motility, invasion, differentiation, survival, and proliferation.

Structure and function of the HGF ligand and c-MET receptor

The receptor tyrosine kinase is the protein product of *c-MET* (mesenchymal-epithelial transition factor), proto- oncogene. Under normal conditions, c-MET along its ligand, HGF/SF (Hepatocyte Growth Factor/ Scatter Factor), exert fundamental biological processes such as embryogenesis, wound healing, tissue regeneration, and formation of nerve and muscle tissue which is controlled regulated by p53 [69]. The known HGF/SF ligand was independently identified by two different groups and named based on their biological functions [70-72].

The protein c-MET forms a heterodimer at the extracellular binding site with 50kD α and 145 kD β subunits which are linked by a disulphide bond. The extracellular portion of the c-MET receptor is made from domains that include SEMA (SEMA homology region) which is the HGF binding site, PSI (plexin-semaphorin-integrin) that stabilizes binding, and four IPT (immunoglobulin-like regions in plexins and transcription factors). These are followed by a transmembrane domain and the intracellular domains including, juxtamembrane, a tyrosine kinase, and a C-terminal docking site [69] (Fig. 4).

HGF and c-MET expression in breast cancer

Studies have shown that the expression of scatter factor (SF) and c-MET are both higher in the in *situ* and invasive ductal carcinomas than in the normal breast and benign proliferating lesions. Infiltrating ductal cancers expressed even higher SF and c-MET

levels than intraductal cancers [73]. Others have demonstrated with both a co-culture and *in vivo* models that HGF secreted from fibroblasts, activates c-MET and increases the percentage of DCIS structures with invasiveness outgrowths and degradation of Collagen IV [74]. These studies suggest that the paracrine mechanism of HGF(SF)/c-MET signaling with fibroblasts enhances the transition to invasive carcinomas and provides further evidence of targeting the c-MET axis. Additionally, it has been reported that c-MET is highly associated with ductal cells and ductal structures and that an imbalance of c-MET expression in tumor and normal tissue is associated with an aggressive DCIS phenotype [75]. The clinical significance of investigating c-MET is that it is overexpressed in 20–30% of breast cancer cases and correlates with high risk of metastasis and poor prognosis making it a promising therapeutic target [76, 77].

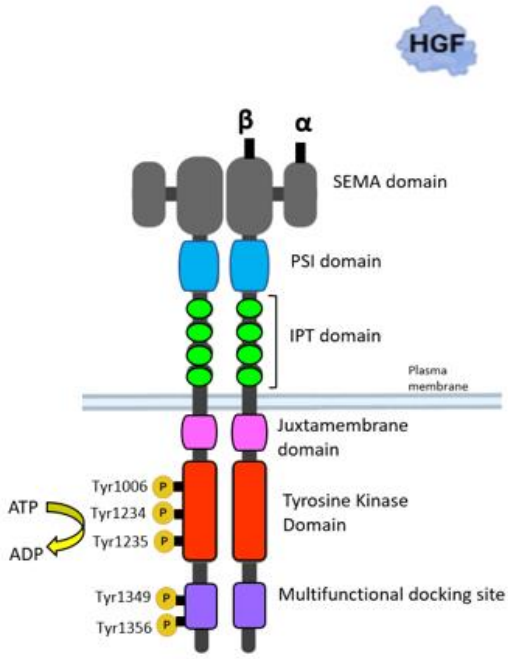

Figure 4. Structure of the c-MET receptor Tyrosine kinase

c-MET signal transduction

The kinase domain of c-MET, upon HGF binding, undergoes a conformational change that includes the dimerization of the tyrosine residues Y1234-1235 and Y1349 in the C terminal tail. Receptor phosphorylation recruits proteins such as Grb2 to activate different signaling downstream pathways including Ras/CDC42, Stat3 and p42/44_MAPK which facilitate breast cancer cell survival invasion, proliferation and scattering [78-80]. (Fig. 5).

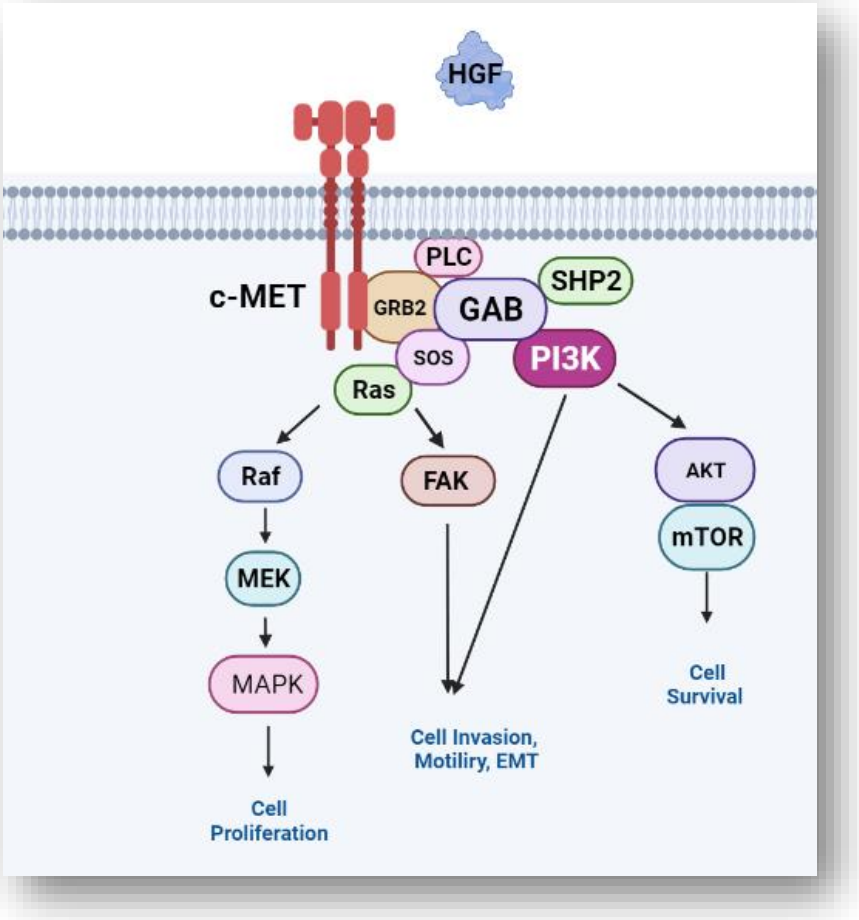

Figure 5. Signaling transduction pathways for the c-MET receptor.

Mechanisms of c-MET regulation

Signal transduction of c-MET is highly regulated to prevent prolonged activation on downstream signaling. Specifically, c-MET signaling is regulated by the degradation and internalization of the receptor [81]. For instance, the ubiquitin ligase Cbl plays a key role in the downregulation of the receptor activity. Although Cbl can be recruited by the Grb2 adaptor protein, it can directly phosphorylate the docking site Y1003 which is a negative regulator of the biological activity of c-MET. Direct phosphorylation of Y1003 leads to ubiquitination and degradation of the c-MET receptor. Ubiquitination of the receptor is very important to maintain physiological activation levels. Studies have demonstrated that mutations in the Cbl domain result in oncogenic phenotypes [82].

Additional there are several other mechanisms of c-MET regulation. At the gene level it can be regulated by epigenetics events such as histone methylation or acetylation that are modulated by DNA methyltranferases (DNMT) and histone (de)acetylases (HDAC). Transcription factors such as Sp-1, AP-1, and PAX can act as regulators of gene transcription. At the mRNA level, alternative splicing which results in mature RNAs of different lengths leading to different products that affect biological activities. The Untranslated region (3' UTR) of the MET RNA is recognized in the cytoplasm by microRNAs (miR-1, miR-34) that act as inhibitors of MET mRNA translation. An additional mechanism of regulation can occur during the translation initiation step in which EIf4b, Eif4e EIf3 have shown to play a role in transcriptional control. On the other hand, cleavage and glycosylation regulate c-MET at the protein level which occurs in the Golgi apparatus where the MET protein undergoes N and O linked glycosylation events before translocating to the membrane. Ligand binding dependent events leads to

phosphorylation of other RTKs including EGFR, and Src. Lastly, desensitization of the receptor occurs via internalization and it is recycled through endosomes or degraded by the ubiquitin proteosome. These events result in a complete halt of the signal transduction in response to biochemical cues [83].

Mechanisms of c-MET regulation in breast cancer

Unlike other cancer types, in breast cancer the mechanisms of c-MET regulation are mainly aberrant signaling and activity. Studies have shown by in situ hybridization that HGF mRNA was detected in ductal epithelial hyperplasia, adipocytes, endothelial cells, and stromal fibroblasts. These studies also identified HGF and c-MET mRNA co expression in benign ductal epithelium as well as in cases of ductal carcinoma in situ and infiltrating carcinoma. Even though the pattern of expression was heterogenous, at tumor zones such as advanced margins, there was a strong expression of HGF and c-MET which potentially suggest an autocrine signaling mechanism [84].

Other have reported by IHC and in situ hybridization that expression patterns of HGF and c-MET was detected in cancer and stromal cells demonstrating autocrine and paracrine patterns. By IHC and autocrine expression pattern was detected in 46.6% of the breast tumors. Further analysis showed that co expression of HGF and c-MET was correlated with clinical features including histologic grade, high Ki67, and reduced patient survival [85].

Another molecular mechanism of c-MET regulation is phosphorylation. Previous studies have investigated by mass spectroscopy protein phosphorylation events in basal breast cancer cell lines including MDA_MB_231, T-47D and MCF-7. Their findings

showed increased levels of tyrosine phosphorylation of c-MET, epidermal growth factor receptor (EGFR), and Src family kinase (SFK). This family of kinases phosphorylates the c-MET and EGFR receptor tyrosine kinase which promotes migration. Further evidence shows that inhibiting SFK reduced cellular proliferation, survival, and motility in basal breast cancer cell lines [86].

By using reverse phase protein arrays, Raghav et al, measured protein levels of c-MET and p-c-MET in a cohort of 257 patients with invasive breast cancer. Their results showed that a total of 123 (47.9%) of the samples displayed high expression of p-c-MET (Y1235). c-MET phosphorylation was significantly correlated to clinical features including age (>50 years) and grade III tumors. To identify relationships between subtype and outcome, this group identified that both high c-MET and p-c-MET levels were associated with worse relapse free survival (RFS), and overall survival (OS) in HER-2 positive breast cancers. Overall, high levels of p-c-MET resulted in a higher risk of tumor recurrence [87].

Role of energetic metabolic pathways and its intermediates in cancer progression

Cancer cells are very distinctive in their cellular roles compared to normal cells. One of the most common characteristics is their ability to modify their metabolism. For instance, in normal mammalian cells, glucose is catabolized in several biochemical steps to generate pyruvate. This three-carbon molecule is oxidated and converted into acetyl CoA which is further metabolized in the tricarboxylic acid (TCA) cycle in the mitochondria. In the TCA cycle, through a series of enzymatic reactions, NADH and FADH2 which are reducing equivalents are generated. These molecules are essential for the transfer of electrons to the electron transport chain (ETC). Thus, electrons pass

through the ETC complexes to generate a mitochondrial membrane potential to produce ATP and bi products such as CO_2 and water. Since this process requires oxygen, it is also known as oxidative phosphorylation (OXPHOS). The mitochondrial complex I, replenishes NAD which is produced when α-ketoglutarate is converted to succinyl CoA by alpha-ketoglutarate dehydrogenase. On the other hand, complex II replaces FAD from the conversion of succinate to fumarate by succinate dehydrogenase, which is the only enzyme that takes an active role in the TCA cycle and the ETC [88].

Along with glycolysis, the TCA cycle generates building blocks for lipid, amino acids, and nucleotide biosynthesis. In normal cells, the balance between energy production and utilization is maintained to perform biological processes. However, in cancer cells, the rate of glucose uptake significantly increases, and pyruvate is mostly converted to lactate rather than converted to Acetyl CoA to enter the TCA cycle and ETC in the mitochondria even in the presence of Oxygen [89]. This process, known as the Warburg effect, which was initially observed in the 1920s by Otto Warburg. He questioned the source tumor cells to get energy, respiration and fermentation. He was the first scientist to determine that cancer cells were using glucose and fermenting (splitting it) to produce lactate, a process that usually occurs when Oxygen is depleted. Warburg also found that respiration which is the process where organic materials are burned to produce water and CO_2 was enough for the cells to maintain tumor viability. Therefore, he concluded that to eradicate cancer cells, both Oxygen and glucose had to be removed [90].

Breast cancer metabolism

To identify specific metabolic programs of breast cancer cells, Richardson et al, performed analyses of carbon flux metabolism in cells that represent stages of breast malignant progression. These cells included the MCF10 which progresses to a malignant phenotype and that was obtained by different transformation events cycling in tumor in nude mice. MCF10-AT cells which are transformed with H-ras and that in vivo display a phenotype that is characterized by being mildly hyperplastic. The other cells include MCF10-AT1 which forms atypical hyperplasia and carcinoma in situ and the MCF10-CA1a which have a high metastatic potential. These cells were derived from the spontaneously immortalized MCF10-A cell line which means that they have the same genetic background. Therefore, these cells represent different stages of tumor progression (MCF10 transformation, MCF10-AT1 tumorigenicity, and MCF10-AT1 metastasis).

By using 3D NMR mass spectrometry, changes in central carbon metabolism related to cellular transformation were identified. These changes included an increased carbon flux through the pentose phosphate pathway (PPP), TCA cycle, and synthesis of glutamate, glutathione, and fatty acids. Additionally, de novo synthesis of glycine and proline were detected as major metabolic shifts upon malignant transformation. In contrast, in the non-transformed parental cell line MCF10 catabolized only minor fraction of glucose via the PPP which seemed to be significantly elevated in the transformed cell lines [91]. These studies demonstrate the ability of cancer cells to shift their nutrient preference to fuel biological processes needed to generate energy, survival, and

proliferation. However, these studies do not take into account the tumor microenvironment and might not be representative of physiological conditions.

Morandi and Chiarugi, discuss in a very comprehensive review metabolic alterations during breast cancer progression in both cancer and stromal cells. In normal breast tissue, the epithelium and stroma undergo OXPHOS and TCA cycle. As malignant transformation occurs and in situ breast cancer starts to form, the tumor increases glucose uptake which is usually accompanied by overexpression of the glucose transporter GLUT1 and PKM1/2 activity. Other metabolic pathways including PPP, fatty acid synthesis (FAS), phosphoglycerate dehydrogenase (PHDGH) which catalyzes the first step of the serine biosynthesis pathway, and glutaminolysis. At this stage, the stroma keeps undergoing OXPHOS but an increase in glycolysis is observed and no longer undergoing the TCA cycle or using it as the main fuel for energy.

During invasive breast cancer, the tumor decreases glucose uptake but it “preferentially” switches to other metabolic pathways including the TCA cycle, glutaminolysis, Cav-1, FAS, NADH/NAD+ as well as increases in proline and glycine fluxes. On the other hand, the stroma displays increase in glucose uptake, glycolysis and monocarboxylate transporter 4 (MCT4) which is a lactate transporter that facilitates lactate efflux from highly glycolytic cells. In contrast, there is a marked decreased in Cav-1 in the stroma [92]. These findings are very important because they help us to understand that the crosstalk between tumor and stroma is very important in the metabolic preferences of the cells that lead to tumor progression. It also reveals important metabolic pathways that can be used as potential therapeutic target at specific stages of breast cancer progression and how it affects drug resistance.

On The other hand, during IDC progression, studies have revealed that the Warburg effect contributes via AKT/mTOR/HIF1α tamoxifen resistance in luminal breast cancers [93]. In other cancer subtypes, the Warburg effect drives growth through PI3-AKT dependent mechanisms in Her2+ breast cancers [94] and promotes growth through EGFR and c-Myc dependent mechanisms in basal like breast cancers [95,96]. Lactate serves as a signal transducer to promote growth and metastasis which are highly associated with stromal reactivity [97].

In summary, in tumor cells, even when oxygen in the environment is sufficient, cells tend to convert glucose into lactate to support the mitochondria oxidative phosphorylation [98]. This is because the pyruvate produced in the glycolytic pathway is more abundant than the cycle can process [90]. Therefore, in tumor cells, the production of pyruvate is replaced by lactate. This reaction is catalyzed by the lactate dehydrogenase enzyme (LDH) leading to no ATP production [99, 100].

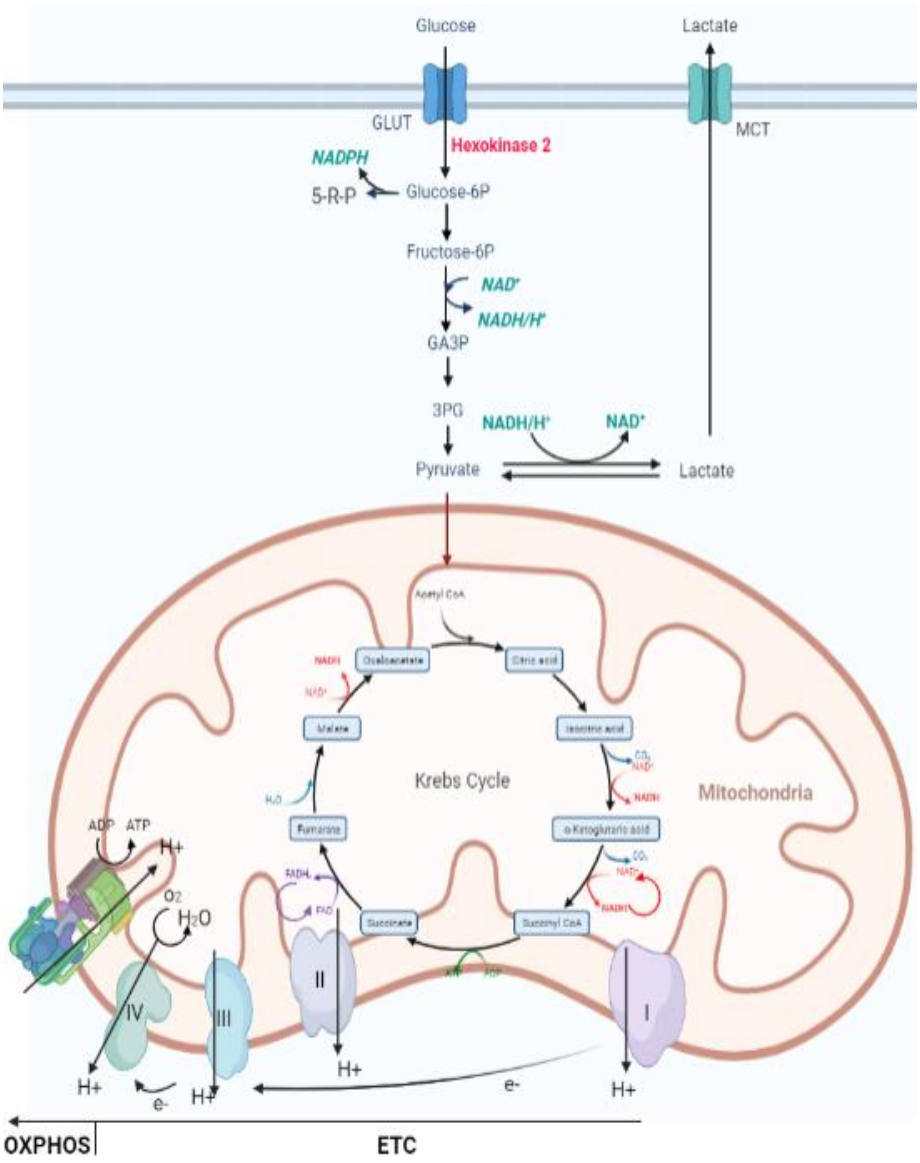

Figure 6. Overview of glycolysis in breast cancer cells

Project goal and Scientific Question

The goal of this project is to explore the functional role of c-MET mediated by CCL2/CCR2 in DCIS progression.

The overall scientific question that this project seeks to answer is:

How does the CCL2/CCR2 chemokine signaling cooperate with other molecular factors to promote DCIS progresion?

Hypothesis

To achieve this goal and based on preliminary studies, I hypothesize that c-MET activity mediated by CCL2/CCR2 chemokine signaling enhances cell proliferation, migration, survival, and growth promoting DCIS progression. (Fig 7).

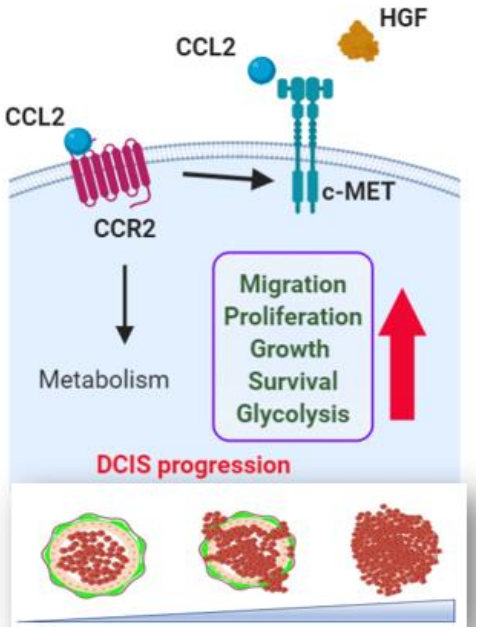

Figure 7. Hypothesis and model of the research project

Aims and outline contents

To test the hypothesis, and based on the considerations above, the following chapters will examine different aspects of this study though in vitro, in vivo studies using the MIND (Mouse Mammary Intraductal Injection) that mimics DCIS progression. Lastly, we include analysis of breast ductal human databases and samples. Therefore, this dissertation is organized by five chapters that discuss the specific aims of this study and that are summarized below:

Chapter II. Chemokine Signaling Facilitates Early Stage Breast Cancer Survival and Invasion through Fibroblasts dependent Mechanisms.

Chapter III. CCL2/CCR2 chemokine signaling enhances glycolysis in human breast carcinoma cells by upregulating Hexokinase 2 expression.

Chapter IV. Activation of the c-MET receptor by CCL2/CCR2 chemokine signaling is important for breast cell migration, proliferation, survival, growth, and glycolysis.

Chapter V. Targeting c-MET by Merestinib inhibited CCR2 mediated DCIS growth, proliferation, and expression of glycolytic enzymes associated with decreased invasion in vivo.

Chapter VI. Physiological and clinical relevance of the c-MET tyrosine kinase receptor in DCIS progression to IDC.

Chapter VII. Concluding remarks and Conclusions.

Chapter II. Chemokine Signaling Facilitates Early Stage Breast Cancer Survival and Invasion through Fibroblast dependent Mechanisms

This chapter has been published as a peer reviewed open access article and it is reprinted here without adaptations as: Brummer, G*., Acevedo, D. S*., Hu, Q., Portsche, M., Fang, W. B., Yao, M., Zinda, B., Myers, M., Alvarez, N., Fields, P., Hong, Y., Behbod, F., & Cheng, N. (2018). “Chemokine Signaling Facilitates Early-Stage Breast Cancer Survival and Invasion through Fibroblast-Dependent Mechanisms.” *Molecular cancer research: MCR*, *16*(2), 296–308.

Author Contributions: G. Brummer* and D.S. Acevedo* contributed equally to this article.

Abstract

Ductal carcinoma in situ (DCIS) is the most common form of breast cancer, with 50,000 cases diagnosed every year in the United States. Overtreatment and undertreatment remain significant clinical challenges in patient care. Identifying key mechanisms associated with DCIS progression could uncover new biomarkers to better predict patient prognosis and improve guided treatment.

Chemokines are small soluble molecules that regulate cellular homing through molecular gradients. CCL2-mediated recruitment of $CCR2^+$ macrophages are a well-established mechanism for metastatic progression. Although the CCL2/CCR2 pathway is a therapeutic target of interest, little is known about the role of CCR2 expression in breast cancer.

Here, using a mammary intraductal injection (MIND) model to mimic DCIS formation, the role of CCR2 was explored in minimally invasive SUM225 and highly invasive DCIS.com breast cancer cells. CCR2 overexpression increased SUM225 breast cancer survival and invasion associated with accumulation of CCL2 expressing fibroblasts. CCR2-deficient DCIS.com breast cancer cells formed fewer invasive lesions with fewer $CCL2^+$ fibroblasts. Cografting CCL2-deficient fibroblasts with DCIS.com breast cancer cells in the subrenal capsule model inhibited tumor invasion and survival associated with decreased expression of aldehyde dehydrogenase (ALDH1), a proinvasive factor, and decreased expression of HTRA2, a proapoptotic serine protease.

Through data mining analysis, high expression of CCR2 and ALDH1 and low HTRA2 expression were correlated with poor prognosis of breast cancer patients. **Implications:** This study demonstrates that CCR2 overexpression in breast cancer drives early-stage breast cancer progression through stromal-dependent expression of CCL2 with important insight into prognosis and treatment of DCIS.

Introduction

Ductal carcinoma in situ (DCIS) is the most common form of pre-invasive breast cancer in the United States, with over 50,000 cases diagnosed every year. Standard treatment for DCIS involves a combination of lumpectomy and radiation therapy [101,102]. Yet, 10 to 35% of patients experience disease recurrence, often accompanied by invasive ductal carcinoma (IDC) [103,104], indicating that under-treatment and over-treatment remain significant concerns in patient care. Few approaches exist to evaluate prognosis of DCIS. Compared with IDC, the use of biomarkers in DCIS has not been well studied. Small or low-grade lesions may still become invasive [104,105]. Estrogen receptor (ER), Her2, Ki67, p16 and Cox2 are associated with disease recurrence but not with development of invasive breast cancer [106]. Identifying key mechanisms associated with DCIS progression could lead to better prognostic factors and tailored treatments for patients with DCIS.

Chemokines are small soluble molecules (8kda), which form molecular gradients to mediate homing of immune cells to tissues during inflammation. Chemokine signal to seven transmembrane receptors that couple to G protein dependent and independent pathways to promote cell migration [107,108]. CCL2/CCR2 chemokine signaling is a

critical regulator of macrophage recruitment during wound healing and infection [109]. CCL2 and CCR2 are overexpressed in multiple cancer types including: pancreatic, prostate, and colon cancers and breast cancer correlating with poor patient prognosis [110,111]. In breast cancer, animal models have demonstrated that CCL2 recruits CCR2+ macrophages to promote tumor growth and metastasis [111,112]. The CCL2/CCR2 pathway is a current therapeutic target of interest [111]; but little is known about mechanisms of this pathway in cancer beyond signaling in immune cells.

We recently found that CCR2 is overexpressed in breast cancer cells and regulates CCL2-induced cell survival and migration [113], indicating a macrophage independent role for CCL2 in breast cancer. Using a novel Mammary Intraductal injection (MIND) model of DCIS, we demonstrate that CCR2 overexpression in DCIS lesions enhances invasive progression associated with accumulation of CCL2 expressing fibroblasts. Using the subrenal capsule model, we demonstrate that fibroblasts derived from DCIS promote breast cancer survival and invasion through CCL2 dependent mechanisms. Furthermore, increased CCL2/CCR2 signaling in DCIS is associated with increased expression of ALDH1, a pro-invasive factor, and decreased expression of HTRA2, a pro-apoptotic serine protease, factors associated with poor prognosis of breast cancer patients [114,115]. These studies identify a key mechanism of DCIS progression involving CCL2/CCR2 signaling between fibroblasts and breast epithelial cells, with important clinical implications.

Materials and Methods

Cell culture

Human fibroblasts were isolated from reduction mammoplasty or DCIS tissues obtained from the Biospecimen Core Facility at the University of Kansas Medical Center (KUMC) and immortalized by expression of human teleromerase reverse transcriptase as described [116]. Fibroblasts were authenticated by expression of: Platelet Derived Growth Factor Receptor-α (PDGFR-α, Fibroblast Specific Protein 1 (Fsp1) and α-smooth muscle actin (α-sma) and absence of pan-cytokeratin. DCIS.com cells originated from Dr. Fred Miller's laboratory [117]. These cell lines were cultured in DMEM containing 10% FBS (Atlas Biological cat no. FR-0500-A), 2 mmol/L L-glutamine (Cellgro cat no. 25-005-CI), 100 IU/mL penicillin, and 100 µg/ml streptomycin (Cellgro cat. no. 10-080). SUM225 cells originated from Dr. Steven Ethier's laboratory, Medical University of South Carolina, Charleston, SC [118], and were cultured in Ham F12 media containing 10% FBS, 5 µg/mL insulin, 1 µg/ml cortisone, and antibiotics. Cells were passaged no longer than 6 months, and tested for mycoplasma after thawing using the MycoAlert Plus Kit (Lonza cat no. LT07-701).

Lentiviral transduction

For CCR2 overexpression, full length CCR2 cDNA was obtained from University of Missouri-Rolla cDNA Resource Center (clone ID no. CCR200000), and subcloned into pHAGE–CMV-MCS-IRES-zsgreen lentiviral plasmid (PLASMID, Harvard University) using NHEI and XbaI restriction sites. pHAGE empty vector was used as a vehicle control. CCR2 and non-silencing control shRNAs in pGFP-c-shlenti lentivirus vectors were purchased from Origene (cat no. TL321181). The CCR2 targeting sequence was: 5'-TATTGTCATTCTCCTGAACACCTTCCAGG3'. CCL2 and non-silencing control

shRNAs in pGFP-c-shlenti lentivirus vectors were obtained from OriGene (cat no. TL316716). The CCL2 targeting sequence (OriGene) was: 5'-ACTTCACCAATAGGAAGATCTCAGTGCAG-3'. CCL2 and non-silencing control shRNAs in GIPZ shRNA lentivirus vectors were obtained from Dharmacon (cat no. V2LHS31298). The CCL2 targeting sequence was: 5'-TAAGTTAGCTGCAGATTCT-3'.

To generate lentivirus, 3.33 µg of PMD2G (Addgene cat no.12260), 6.66µg PDPAX2 (Addgene cat no.12259), and 10ug target vectors were co-transfected in HEK 293T cells using Lipofectamine 2000 (ThermoFisher cat no. 11668027). Medium was removed 48 hours later and used to transduce cells, which were sorted for Green Fluorescent Protein (GFP) expression by FACS.

Gene deletion by clustered regularly interspaced short palindromic repeats

The CCR2 guide RNA was cloned into the pSpCAs9(BB)-2A-GFP(PX458) vector (Addgene cat no.48318) using *Bsm*BI enzyme. The CCR2 guide RNA sequence was: 5'-TTCACAGGGCTGTATCACATCGG-3', which targeted the exon encoding the extracellular loop between the second and third transmembrane domains of human CCR2. The vector was transfected into DCIS.com breast cancer cells using jetPei transfection reagent (Polyplus cat no. 101-01), with N/P 7.5. Forty eight hours later, GFP positive cells were FACS sorted, cultured as single cell clones in 96 well plates, and expanded into 6 well plates. Genomic DNA of individual colonies was screened by PCR to detect mutant colonies. The detection primer pair spanning the CCR2 targeting site was: 5'- ACATGCTGGTCGTCCTCATC, 3'-AAACCAGCCGAGACTTCCTG. The PCR product of the wildtype (WT) gene was 901bp, and contained one D*de*I enzyme digestion

site to yield 231 and 670bp fragments. Exon excision introduced an additional D*de*I restriction site resulting in fragment sizes of 181, 231 and 468 bp upon D*de*I restriction.

ELISA

A total of 40,000 cells/well were seeded in 24 well plates in DMEM/10% FBS for 24 hours, washed in PBS and incubated in serum free DMEM for 24 hours in 500 µLl/well. Conditioned media were assayed for human CCL2 by ELISA (PeproTech, catalog no.900-M31). Reactions were catalyzed using tetramethylbenzidine substrate (catalog no. 34028, Pierce). Absorbance was read at OD450 nmol/L using a BioTek Microplate Reader.

MIND model

NOD-SCID IL receptor-γ2 null female mice 8 to 10 weeks of age were purchased from The Jackson Laboratory. MIND injections were performed as described [119]. Briefly, 4,000 cells/µL breast epithelial cells were prepared in 50 µL PBS containing 0.1% Trypan blue. A Y incision was made on the abdomen of mice anesthetized with ketamine/xylazine [100mg/Kg(K)+10mg/kg(X)] to expose the 4-5 and 9-10 inguinal glands. The inguinal nipples were snipped. A 30-gauge Hamilton syringe with a blunt-ended 0.5-inch needle was used to deliver 5 µL (20,000) cells/nipple. Skin flaps were closed with wound clips. Mice were palpated for lesions twice weekly. SUM225 injected mice were sacrificed 7 weeks post-injection. DCIS.com injected mice were sacrificed 4 weeks post-injection.

Subrenal graft

Transplantation into subrenal capsules of NOD–SCID female mice (6-8 weeks old) was performed as described [120]. Briefly, 250,000 fibroblasts were re-suspended

with 100,000 DCIS.com cells in 50 µL rat tail collagen I (BD Pharmingen), and cultured in DMEM/10% FBS for 24 hours. Mice were anesthetized by ketamine/xylazine, a 1 to 1.5 cm midline incision was made in the back 3 cm from the base of the tail, and the lateral or contralateral kidney was exposed. A small incision was made in the capsule layer using forceps and small spring-loaded scissors. The graft was inserted using a glass pipette. The body wall was closed with gut absorbable sutures and the skin was closed with wound clips. Mice were monitored twice weekly and sacrificed 3 weeks post-transplantation.

DAB immunostaining

Tissues were fixed in 10 % neutral formalin buffer and embedded in wax as described [121]. For DAB immunostaining, 5µm sections were dewaxed and heated in 10 mmol/L sodium citrate buffer pH 6.0 for 2 minutes. Endogenous peroxidases were quenched in PBS/60 % methanol/3% H_2O_2, blocked in PBS/3% FBS, and incubated with primary antibodies (1:100) overnight at 4^{o}C: Collagen IV (Novus Biologicals NB120-6586SS), cleaved caspase-3 Asp175 (Cell Signaling Technology catalog no. 9579), Von Willebrand Factor 8 (VWF8) (Millipore, catalog no. Ab7356), PDGFR-α (Cell Signaling Technology, catalog no. 5241), KI67 (Santa Cruz Biotechnology catalog no. 1307), HTRA2 (Cell Signaling Technology, catalog no. 2176), CCL2 (Santa Cruz Biotechnology, catalog no. 1304), or F4/80 (Abcam, catalog no. ab6640). Fsp1 antibodies (Abcam, catalog no. 27427) were diluted 1:3. Slides were incubated for 2 hours at 1:1,000 with: anti-rabbit-biotinylated (Vector Laboratories, catalog no. BA-5000), anti-goat biotinylated (Vector Laboratories catalog no. BA-5000), or anti-rat-biotinylated (cat no.BA-9401, Vector Laboratories). For Laminin staining, slides were treated with 20

µg/ml Proteinase K for 1 hour at 37^0C prior to incubation with 1:100 pan-specific antibodies (Novus Biologicals, catalog no. NB300-144AF700). Slides were incubated with streptavidin peroxidase (Vector Laboratories catalog no. PK-4000), developed with 3,3'-diaminobenzidine (DAB) substrate (Dako, catalog no. K346711), counterstained with Mayer hematoxylin and mounted with Cytoseal. Proliferating Cell Nuclear Antigen (PCNA) (catalog no. sc25280, Santa Cruz Biotechnology) and ALDH1A1 (R&D Systems, catalog no. MAB5869) proteins were detected using the Mouse on Mouse (MOM) kit (Vector Laboratories, catalog cat no. BMK-2202).

Immunofluorescence

For CK/α-sma co-staining, slides were heated in 10 nmol/L sodium citrate buffer pH 6.0 for 2 minutes. Slides were incubated with antibodies 1:100 overnight at 4°C to: α-sma, (Spring Biosciences, catalog no. SP171) and CK5 (Thermo Fisher Scientific, cat no. MA5-12596) or CK19 (Thermo Fisher Scientific, cat no. MS198). Slides were incubated for 2 hours at 1:200 with anti-rabbit-IgG-Alexa Fluor 568 (Thermo Fisher Scientific, catalog no. A10042) and anti-mouse IgG-Alexa Fluor 488 (Thermo Fisher Scientific, cat no. A-11001). For pan-cytokeratin/phalloidin costaining, slides were heated in 10 mmol/L sodium citrate pH 6.8 for 5 minutes. Slides were incubated with 1:100 Alexa Fluor 488-phalloidin (Thermo Fisher Scientific catalog no. A12379) and anti-pan-cytokeratin (Santa Cruz Biotechnology, catalog no. 8018) overnight at 4°C, and incubated with secondary anti-mouse-Alexa Fluor 647 (Thermo Fisher Scientific, catalog no. 31571) using the MOM kit. Sections were counterstained with 4',6-diamidino-2-phenylindole,dihydrochloride (DAPI) and mounted with PBS/glycerol.

Image quantification

Five random fields/section were captured at 10x magnification using the FL-Auto EVOS System (Invitrogen). DAB staining was quantified as described previously [110]. Briefly, images were imported into Adobe Photoshop, DAB staining was selected using the Magic Wand tool, copied and saved a separate file. Images were opened in Image J (NIH, Bethesda, MD), and converted to grey scale. Background pixels were removed by threshold adjustment. Images were subject to particle analysis. Positive DAB values were normalized to total area values, expressed as arbitrary units. To quantify stromal staining, epithelial tissues were cropped out in Adobe Photoshop. DAB staining was selected in stroma, copied to a new window, and saved as a separate file. Images were opened in Image J and quantified. Stromal DAB values were normalized to total stromal values.

Scoring of tumor invasion

Tissues were sectioned at three depths approximately 50 µm apart. Two to three serial sections per depth were stained. Images were captured at 4x and 10x magnification and scored in a blinded fashion: 1 (non- invasive), 2 (lowly invasive), or 3 (highly invasive). For CK/α-sma CO-IF, 1 indicated no invasion, with intact α-sma+ myoepithelium and confinement of epithelial cells within the duct; 2 indicated 50% or less disappearance of the α-sma surrounding the duct and/or appearance of three or fewer cells invading through the duct; 3 indicated more than 50% α-sma disappearance, with appearance of more than three cells invaded through the duct and making contact with the periductal stroma. For Collagen IV and Laminin immunostaining: 1 indicated well defined expression in the basement membrane, 2 indicated additional low-level expression in lesion; 3 indicated higher expression in epithelium, with poor definition

between epithelium and stroma. For phalloidin/pan-cytokeratin staining: 1 indicated a well-defined border between tumor and kidney, with a few tumor cells invaded into kidney tissue; 2 indicated some tumor cell invasion, characterized by viable tumor cells present in kidney tissue; the border between kidney and tumor tissue was less defined; and 3 indicated high invasion characterized by extensive number of tumor cells in kidney tissue; tumor was embedded in kidney, and the border between kidney tissue and tumor were undefined.

Flow cytometry

Flow cytometry staining for CCR2 expression was conducted as described [113]. Briefly, adherent cells were detached from plastic by Accutase (Thermo Fisher Scientific catalog no. A1110501), washed in PBS, and incubated with anti-CCR2-PE for 1 hour on ice. Samples were washed in PBS three times and analyzed on a LSRII Flow cytometer, normalized to unstained controls.

Fibroblast proliferation assay

Fibroblasts were seeded 30,000/well in 24 well plates overnight. DCIS.com cells (500,000) were seeded in 10 cm dishes and incubated with 5 mL serum free DMEM for 24 hours. Fibroblasts were treated with 500 µL of DMEM or tumor conditioned medium for 24 or 48 hours. Fibroblasts were detached through trypsinization, quenched in DMEM/10% FBS and pelleted by microcentrifugation. Fibroblasts were re-suspended in 50 µL PBS and counted by hemocytometer.

Statistical Analysis

Cell culture experiments were repeated a minimum of three times. Data are expressed as mean$\pm$ SEM. Statistical analysis was determined using two-tailed *t*-test or

ANOVA with Bonferroni *post-hoc* comparisons for normal distributions and Kruskall-Wallis test with Dunn *post-hoc* comparison for non-Gaussian distributions. Statistical analysis was performed using GraphPad Software. Significance was determined by $P<0.05$. (*P <0.05, ** P <0.01, *** P <0.0001, n.s., not significant or P >0.05).

Ethics approval and consent to participate:

All animal experiments were performed at KUMC according to guidelines from the Association for Assessment and Accreditation of Laboratory Animal Care. Experiments were approved by the Institutional Animal care and Use Committee. Patient samples were collected under approval by Institutional Review Board (IRB) at KUMC. All samples were de-identified by the Biospecimen Core, an IRB approved facility, prior to distribution.

Results

CCR2 overexpression in SUM225 cells enhances DCIS progression

In DCIS, cancer cells grow, but remain within the boundaries of ducts and lobules, which are lined by α-sma+ myoepithelial cells and basement membrane, structural barriers between the stroma and duct. Progression from DCIS to IDC is characterized by disappearance of the myoepithelium and appearance of invading ductal carcinoma cells into the surrounding stroma [122]. To clarify the role of epithelial CCR2 expression in DCIS progression, we utilized MIND models established through injection of SUM225 and DCIS.com breast cancer cells. SUM225 breast cancer cells are lowly invasive, of a luminal/Her2+ subtype [123]. DCIS.com breast cancer cells, a basal-like subtype, are more highly invasive [119]. By flow cytometry, CCR2 expression was significantly lower

in SUM225 cells compared to DCIS.com breast cancer cells (Figure 8A). We first examined the effects of CCR2 overexpression on progression of SUM225 lesions. By lentivirus transduction, two different SUM225 cell lines were generated to overexpress CCR2 (CCR2-L and CCR2-H) and compared with SUM225 cells expressing pHAGE vehicle control (Figure 8A). These cells were MIND injected into NOD-SCID mice, and examined 7 weeks post-injection, when lesions were palpable. CCR2 overexpressing xenografts showed no significant changes in mammary tissue mass compared to pHAGE control (Figure 8B).

Extent of epithelial invasion in the mammary gland or breast tissue has been determined by evaluating myoepithelial integrity through α-sma expression and examining for presence of carcinoma cells contacting the surrounding stroma [119, 124-126]. To evaluate the effects of CCR2 overexpression on ductal invasion, we co-stained for α-sma to define ductal myoepithelium, and for human specific CK19 to define SUM225 cells. Lesions were scored for invasiveness. Noninvasive lesions had intact α-sma+ myoepithelium, lowly-invasive lesions showed reduced α-sma expression, lining the breast duct, and a few invasive cancer. Highly invasive lesions showed minimal α-sma expression and multiple invasive cancer cells. In the pHAGE controls, 21 % were noninvasive, 51% were lowly invasive and 28% were highly invasive. Of CCR2-L MIND lesions, 12% were non-lowly invasive, 57% were medium invasive and 31% were highly invasive. Of CCR2-H MIND lesions, 8% were noninvasive, 66% were lowly invasive, and 26% were highly invasive (Figure 8C). The decrease in lowly invasive lesions and increase in lowly invasive lesions indicate a shift towards invasion.

To further characterize invasion, through basement membrane, mammary tissues were stained for laminin and collagen IV, which are basement membrane proteins associated with invasiveness in breast cancer [127, 128]. In non-invasive lesions, Laminin and Collagen IV were expressed in the basement membrane and surrounding stroma. In lowly invasive lesions, laminin and collagen IV were also detected in the epithelium, correlating with a few invading epithelial cells. In highly invasive lesions, laminin and collagen IV expression in lesions resulted in poorly defined borders between stroma and epithelium. consistent with α-asma /CK19 CO-IF, laminin and collagen IV staining revealed that CCR2 overexpression in SUM225 cells decreased the number of lowly invasive lesions and increased the number of highly invasive lesions (Figure 9A-B). CCR2 overexpression was also associated with increased cell proliferation and decreased apoptosis as indicated by Ki67 and cleaved caspase-3 staining (Figure 8D-E). These data indicate that CCR2 overexpression in SUM225 cells enhances the progression of MIND xenografts.

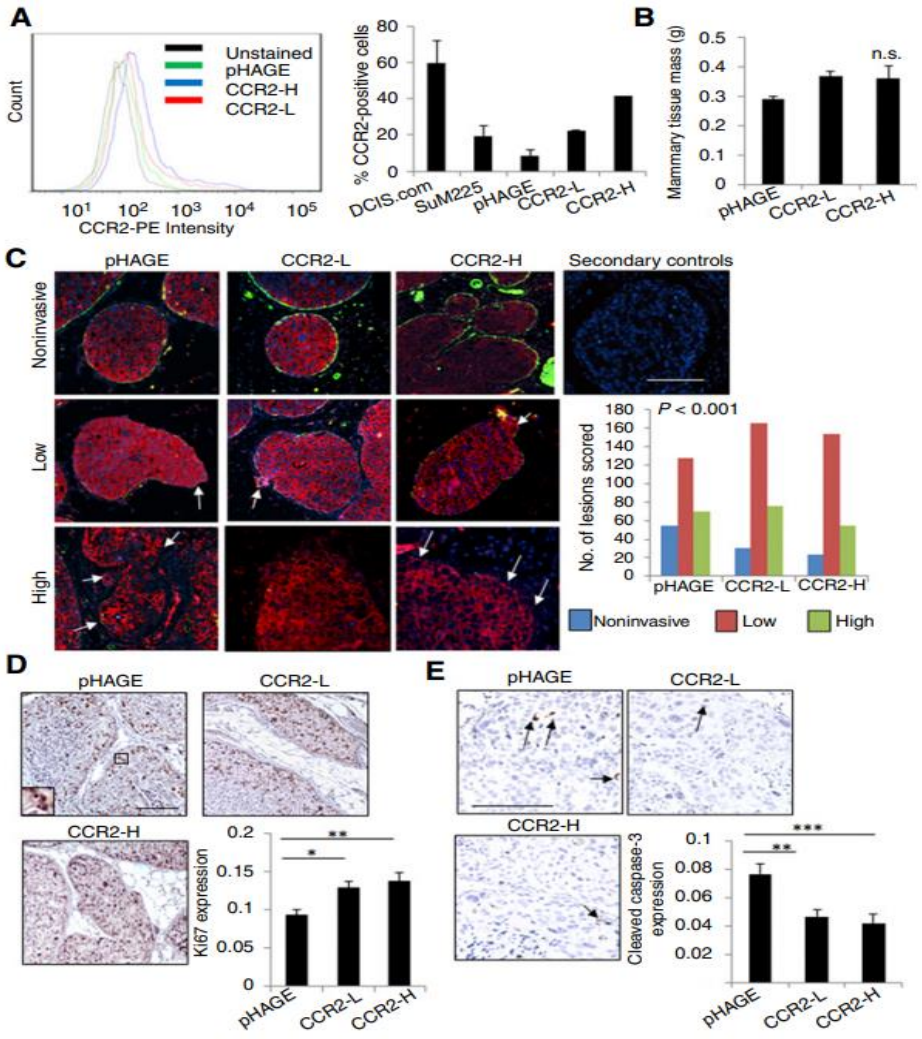

Figure 8. CCR2 overexpression in SUM225 breast cancer cells enhances invasive progression. A, Flow cytometry analysis for CCR2 expression in parental DCIS.com or SUM225 parental cells or SUM225 cells expressing vehicle pHAGE control or CCR2 (CCR2-L, CCR2-H). Histogram analysis shown on left. Graph shows percentages of positive cells. **B,** Tissue mass of SUM225 MIND injected mammary glands **C.** SUM225 lesions were co-stained for CK-19 (red) and α-sma (green), and scored for the number of invasive lesions *n*=252 lesions for control pHAGE, 272 lesions for CCR2-L and *n*=231 for CCR2-H group. Representative images are shown with secondary antibody control panel of anti-rabbit-Alexa-fluor488/anti-mouse-Alexa-fluor-568/DAPI overlay. Arrows indicate invasive foci. **D** and **E,** Image J quantification of immunostaining for Ki67 **(D)** or cleaved caspase-3 **(E)** in SUM225 lesions (arbitrary units). Arrows point to examples of positive staining. Statistical analysis was performed using One-way ANOVA with Bonferroni *post-hoc* comparison (**B, D, E**) or χ^2 test **(C).** Statistical significance was determined by P<0.05. *P<0.05. ns, not significant. Mean±SEM values are shown. Scale bar=200 μm

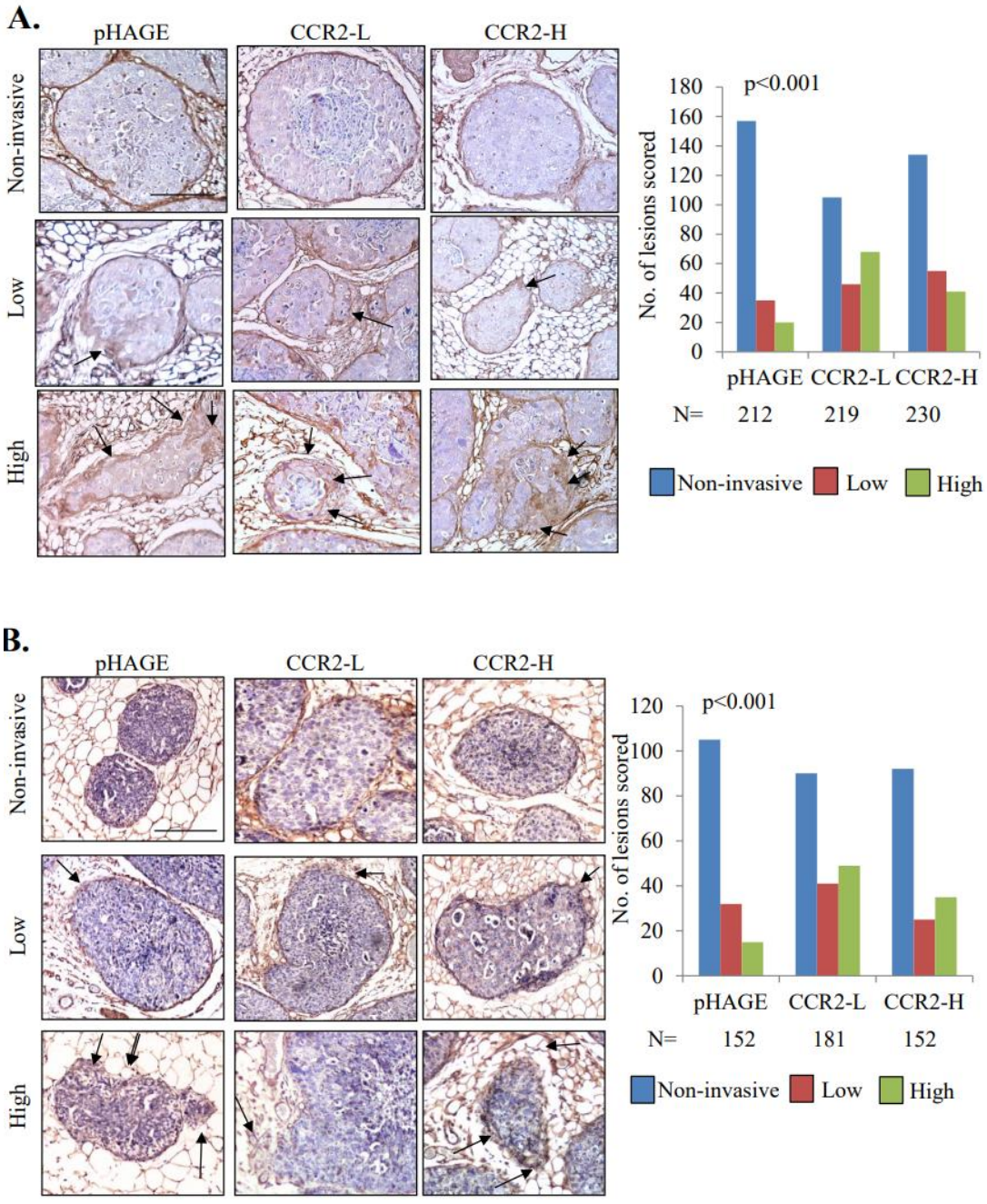

Figure 9. Collagen and laminin expression in SUM225 MIND lesions. CCR2 overexpressing or control SUM225 MIND lesions were immunostained for **A**. collagen IV or **B.** laminin expression. Lesions were scored for invasiveness based on collagen or laminin expression. Arrows point to areas of invasiveness. Total sample size per group (N) are shown below graphs. Scale bar= 200 microns. Statistical analysis was performed using χ^2 test. Statistical significance was determined by $P<0.05$.

Knockdown or knockout of CCR2 in DCIS.com cells inhibits DCIS progression

We next examined the effects of CCR2 deficiency on progression of DCIS.com lesions. Of the four shRNA sequences tested, one induced significant knockdown of CCR2 expression in DCIS.com cells (Figure 10A). MIND injection of DCIS.com cells in NOD-SCID mice resulted in palpable mammary lesions at 4 weeks. CCR2 knockdown (CCR2-KD) decreased mammary tissue tumor growth compared to control shRNA expressing xenografts (Figure 10B). To examine for changes in ductal invasion, sections were CO-IF stained for α-sma and human specific CK5 to identify DCIS.com cells and scored. Although the percentage of lowly invasive lesions (75%) was higher in the CCR2-KD group compared with control (68%), the percentage of highly invasive lesions dropped from 20% in the control shRNA group to 6% in the CCR2-KD group. The percentage of noninvasive lesions increased from 12% in controls to 19% in the CCR2-KD group. These data indicated a shift from high to less invasive lesions with CCR2-KD (Figure 10C). This trend was also observed in analysis of collagen IV and laminin expression in DCIS.com MIND lesions (Figure 11A-B). CCR2-KD was also associated with decreased tumor cell proliferation and increased apoptosis (Figure 10D-E).

To validate the effects of CCR2-KD on DCIS.com progression, the CCR2 gene was knocked out by CRISPR. Two WT clones and one homozygous knockout clone (CCR2-KO) were identified from 70 clones (Figure 12A). By flow cytometry, WT clones showed similar CCR2 expression levels to parental cells, while CCR2-KO cells showed a significant reduction in CCR2 expression (Figure 12B). MIND injection of CCR2-KO cells resulted in a significant reduction in mammary tissue mass and fewer invasive lesions (Figure 12C-D), compared to WT xenografts. These data indicate that CCR2 KD or KO inhibits progression from DCIS to IDC in DCIS.com MIND xenografts.

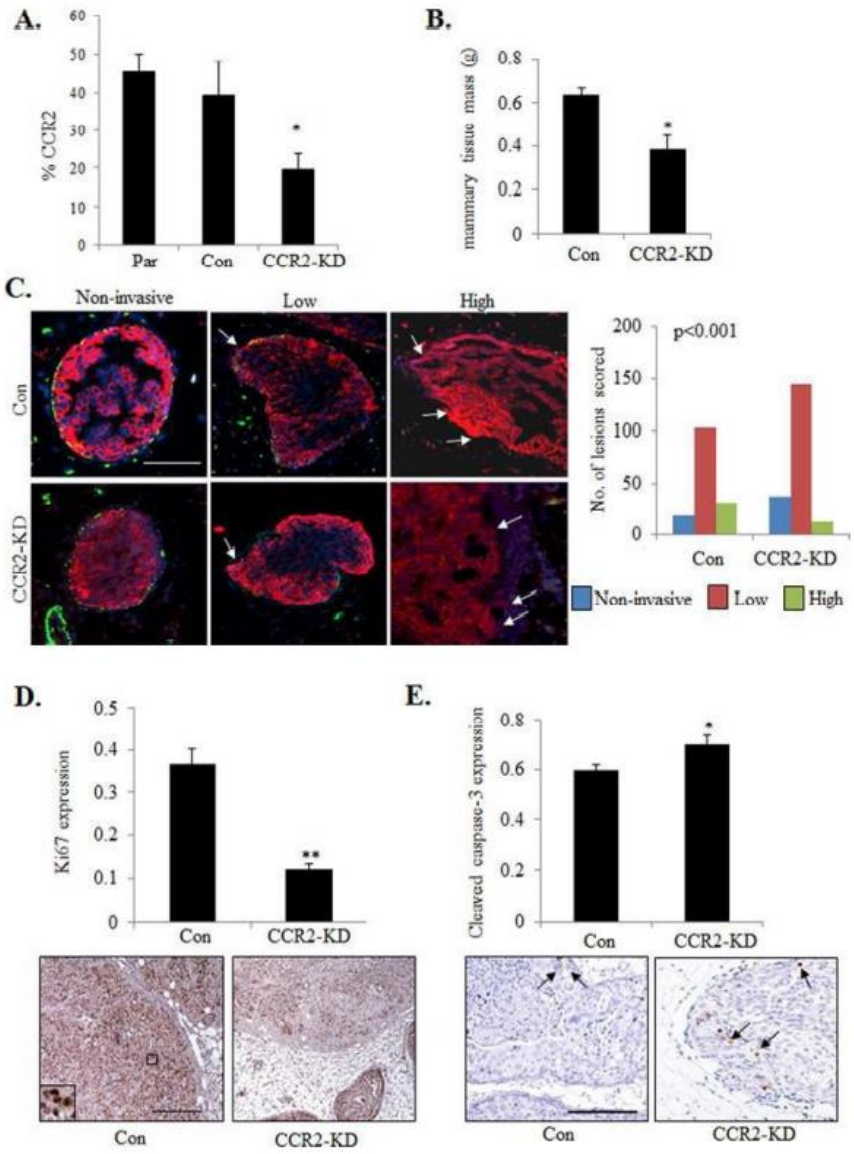

Figure 10. shRNA mediated CCR2-KD in DCIS.com breast cancer cells inhibits invasive progression. A. Flow cytometry analysis for CCR2 expression in Parental (Par) or DCIS.com cells expressing control (Con) or CCR2 shRNA (CCR2-KD). **B,** Tissue mass of DCIS.com MIND injected mammary glands **C,** DCIS.com MIND lesions were co-stained for CK5 (red) and α-sma (green) and counterstained with DAPI (blue)**.** Representative images are shown with arrows pointing to invading tumor cells. Lesions were scored for invasiveness. *n*=152 lesions for control shRNA group, 193 lesions for CCR2-KD group. n=8 mice/group. **D** and **E**. Image J quantification of Ki67 **(D)** or cleaved caspase-3 **(E)** immunostaining in DCIS.com lesions. Arbitrary units are shown. Arrows point to examples of positive staining. Statistical analysis was performed using one way ANOVA with Bonferroni *post-hoc* comparison (**B, D, E**) or χ^2 test (**C**). Statistical significance was determined by P<0.05. *P<0.05, **P<0.01. Scale bar=200μm.

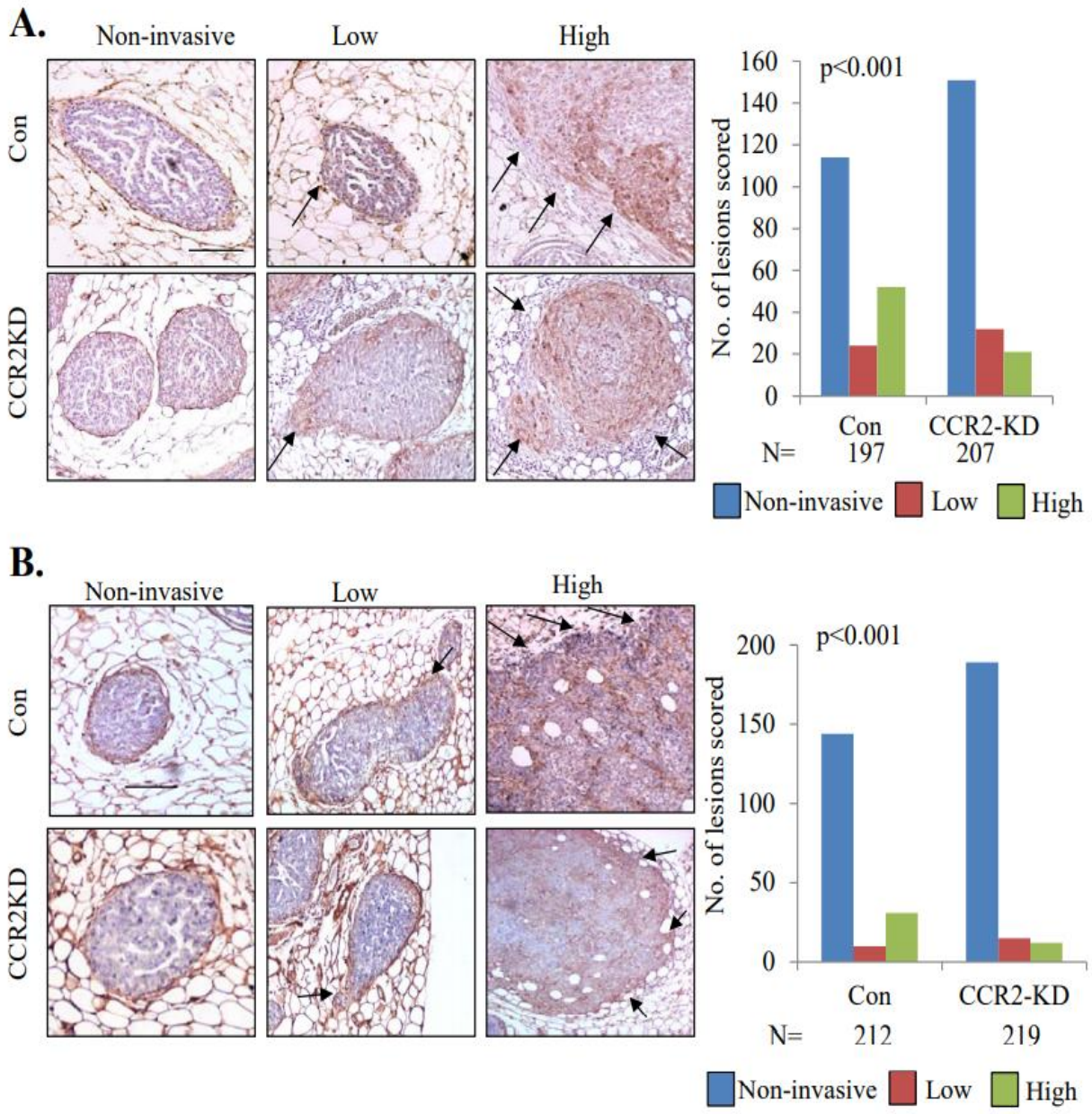

Figure 11.Collagen and laminin expression in DCIS.com MIND lesions. CCR2 or control shRNA expressing DCIS.com MIND lesions were immunostained for **A.** collagen IV or **B.** laminin expression. Lesions were scored for invasiveness based on collagen or laminin expression. Total sample size per group (N) are shown below graphs. Arrows point to areas of invasiveness. Scale bar= 200 microns. Statistical analysis was performed using χ^2 test. Statistical significance was determined by $P<0.05$.

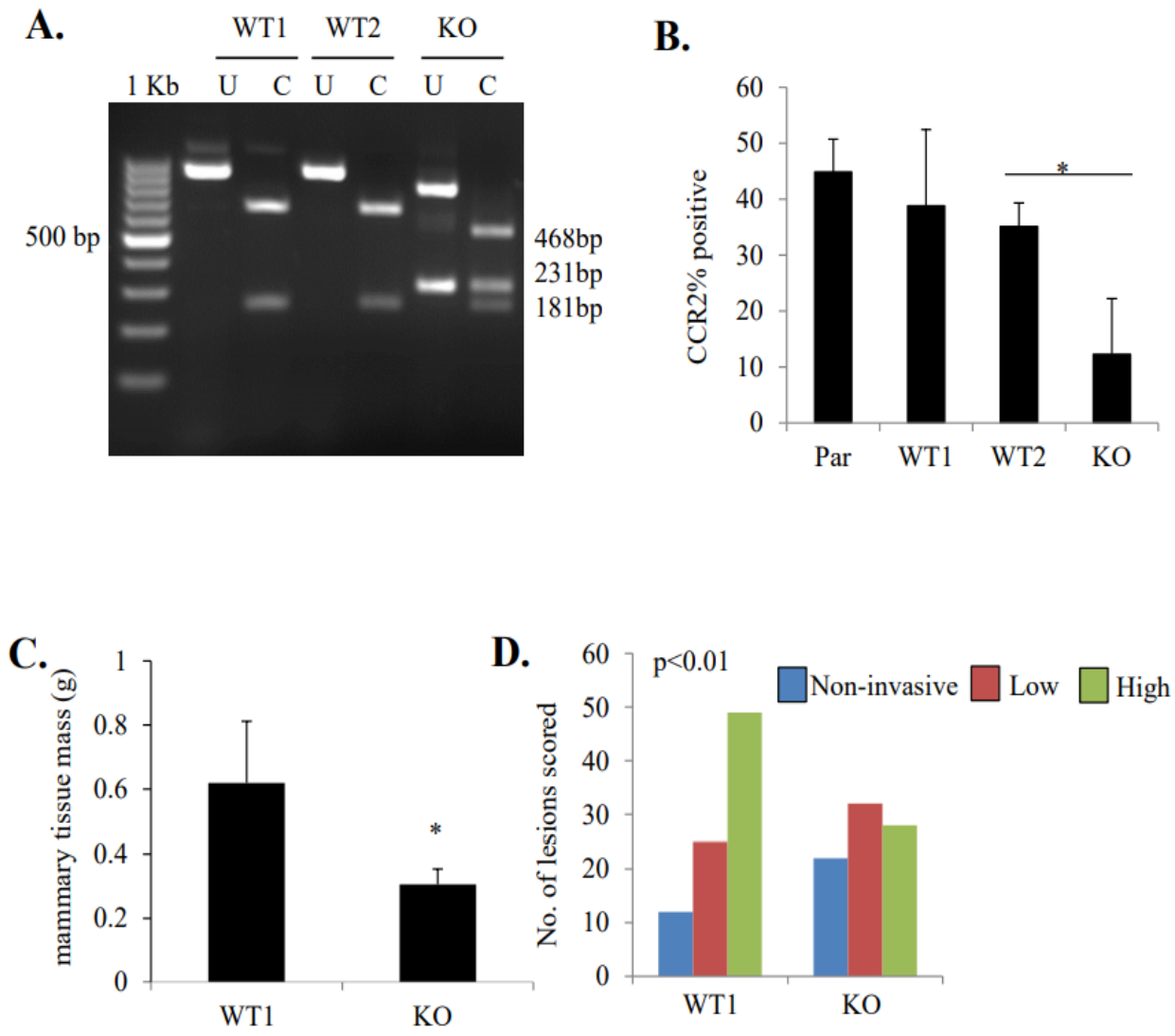

Figure 12. CRISP/R mediated knockout of CCR2 inhibits DCIS.com breast cancer progression. A. PCR identification of wildtype (WT1, WT2) or CCR2 knockout (KO) cut (C) or uncut (U) clones. The presence of fragments, 468, 231and 181 bp in size indicates exon excision. **B.** Flow cytometry analysis of WT and KO cells in comparison with parental (Par) cells. **C-D**. MIND model injection of WT1 or KO cells were examined for changes in mammary gland weight (C) or invasion (D). Statistical analysis was performed using One-way ANOVA with Bonferroni *post-hoc* comparison **(B),** Two Tailed test **(C),** or χ^2 test **(D).** Statistical significance was determined by $p<0.05$. *$P<0.05$. Mean±SEM values are shown.

Increased angiogenesis, fibrosis and macrophage recruitment are associated with invasive breast cancer [122]. To determine how epithelial CCR2 expression affected the surrounding mammary stroma, immunostaining was performed to analyze expression of biomarkers for macrophages (F4/80) and endothelial cells (VWF8). To account for fibroblast heterogeneity, we immunostained for two different markers: Fsp1 and PDGFR-α [129, 130]. DAB expression of stromal biomarkers was quantified by pixel density analysis and normalized to total stromal area, using an Image J protocol described previously [110]. There were no significant changes in VWF8 or F4/80 expression with CCR2 overexpression or knockdown (Figure 13A-B). Fsp1 and PDGR-α were expressed in fibroblastic stroma and in epithelial cells, consistent with studies showing mesenchymal marker expression in breast cancer cells [110, 131]. CCR2 overexpressing SUM225 xenografts showed increased stromal expression of Fsp1 and PDGFR-α (Figure 14A-B), associated with stromal CCL2 expression (Figure 14C). Conversely, CCR2 deficient DCIS.com MIND xenografts showed a significant decrease in fibroblastic cells and decreased CCL2 expression in the stroma (Figure 15A-B). These data indicate that CCR2 overexpression or knockdown is associated with changes in CCL2 expressing fibroblasts in the DCIS stroma.

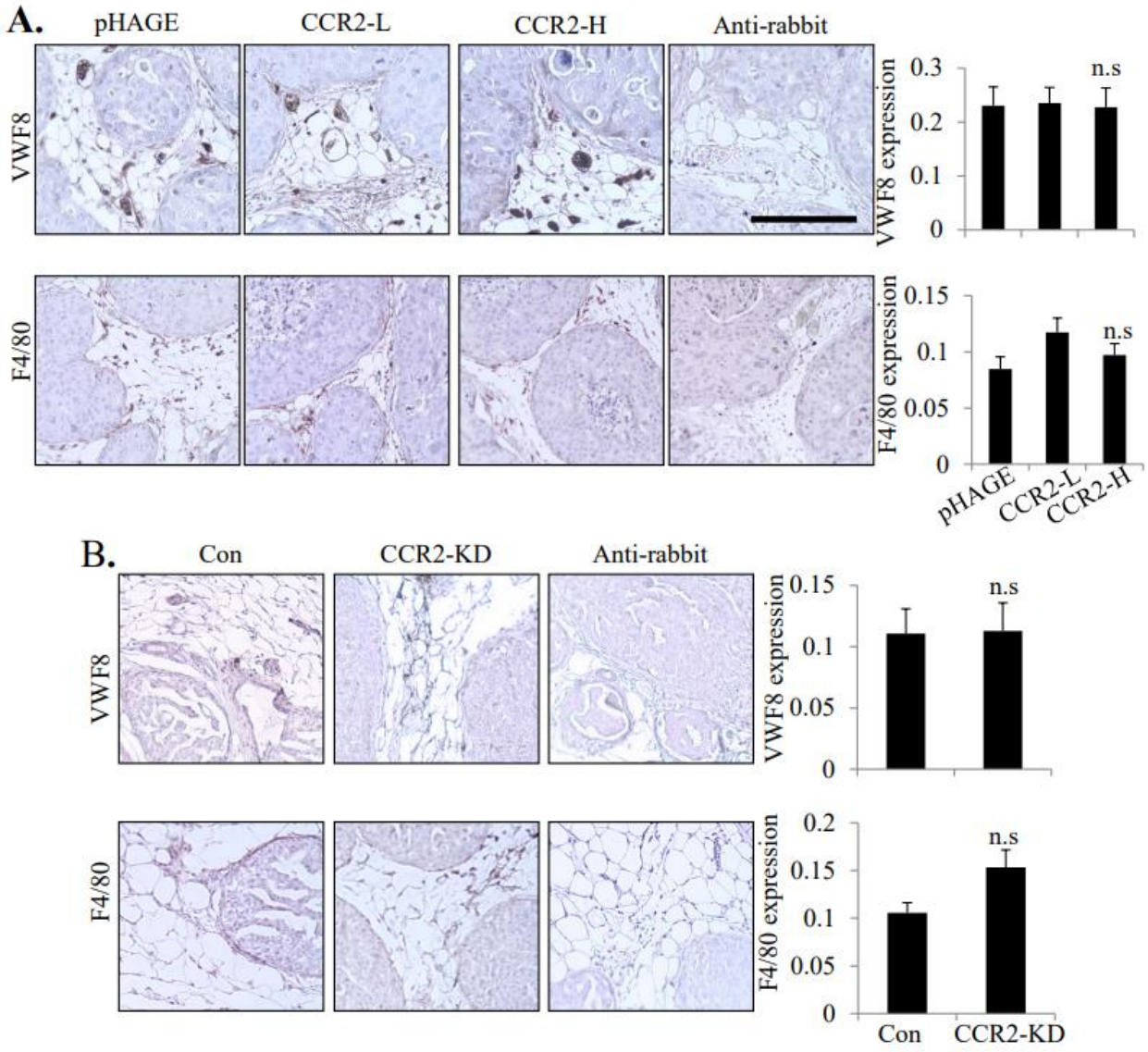

Figure 13. Effect of CCR2 overexpression and knockdown on stromal reactivity. Immunostaining for VWF8 or F4/80 expression was performed in **A.** SUM225 MIND lesions or **B.** DCIS.com MIND lesions. Secondary rabbit biotinylated antibody staining shown as a control. Scale bar=200 microns. Statistical analysis was determined using One Way ANOVA with Bonferroni *post-hoc* comparisons to all groups. Statistical significance was determined by $p<0.05$. n.s=not significant. Mean±SEM values are shown.

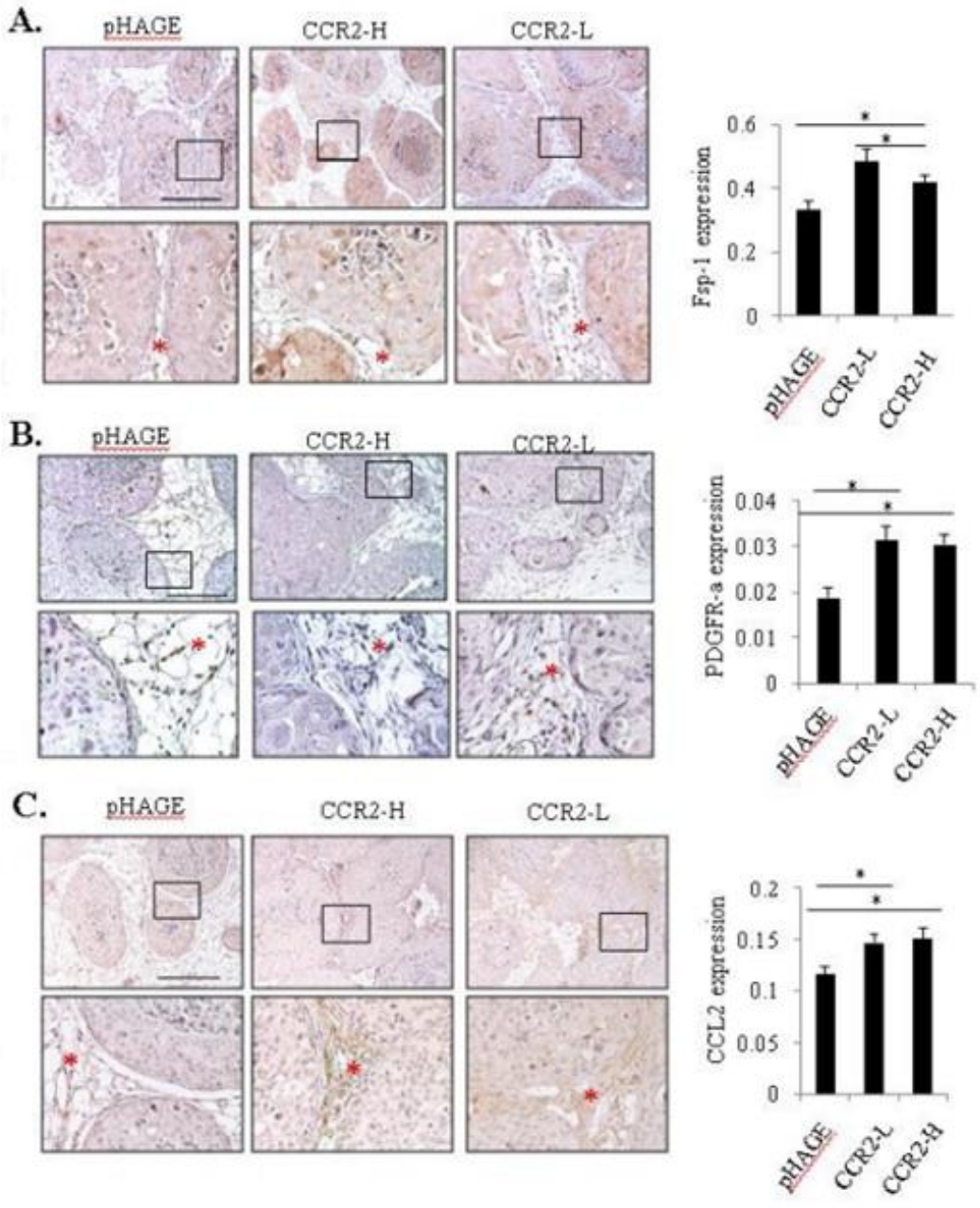

Figure 14. CCR2 overexpression in SUM225 MIND xenografts increases the levels of CCL2 expressing fibroblasts. Sum 225 MIND lesions were immunostained for Fibroblast Specific Protein 1 (Fsp1; **A.**) and Progesterone Growth Factor Receptor-α (PDGFR-α; **B**); or CCL2 expression **(C).** Representative images are shown with magnified image underneath. The stroma is marked with an asterisk in the magnified image. Expression in the stroma was quantified by Image J, in arbitrary units. Statistical analysis was performed using one-way ANOVA with Bonferroni *post-hoc* comparison. Statistical significance was determined by $P<0.05$. *$P<0.05$, ***$P<0.001$. Mean±SEM values are shown. Scale bar=400 microns.

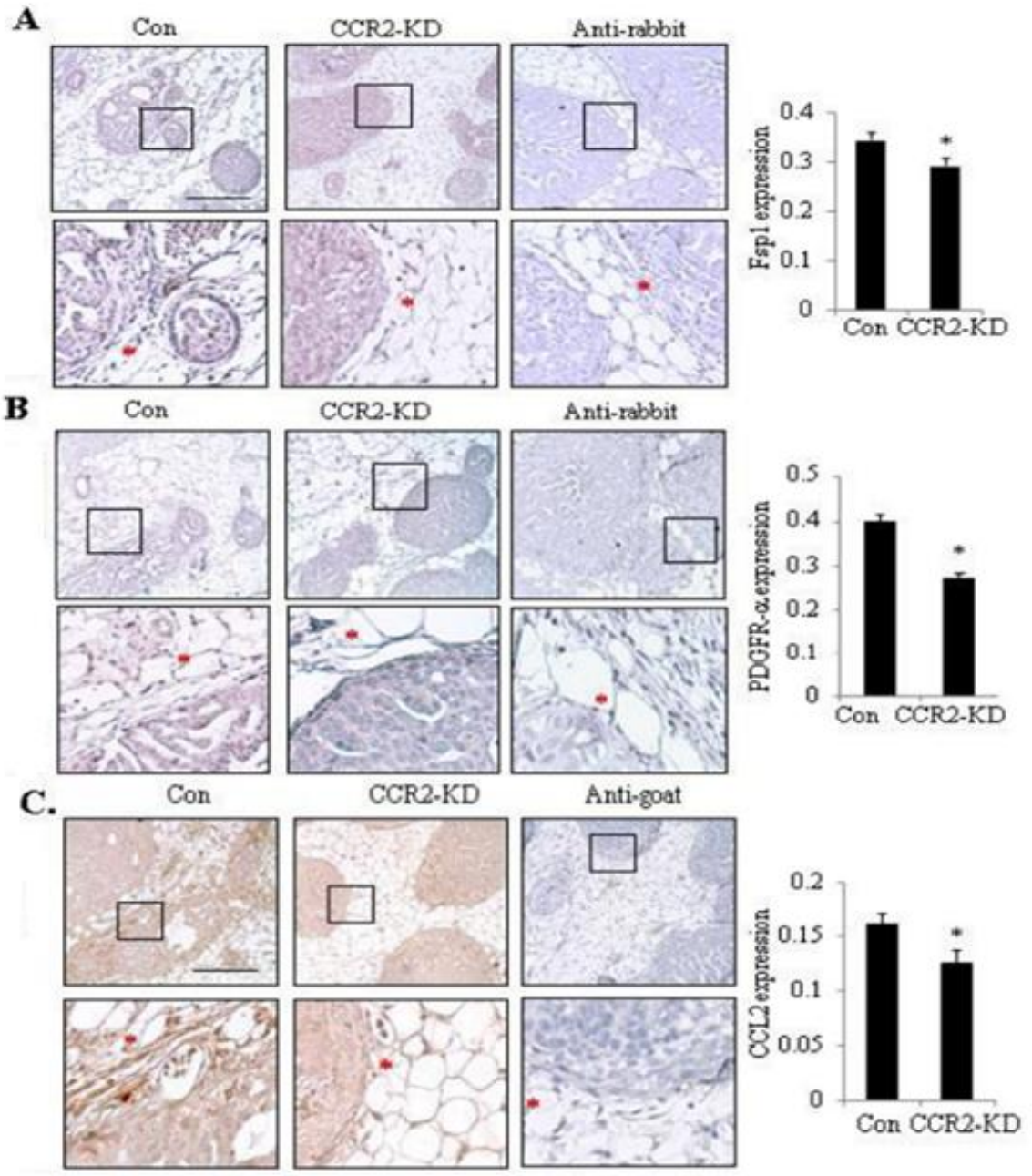

Figure 15. CCR2 shRNA knockdown in DCIS.com MIND xenografts reduces the levels of CCL2 expressing fibroblasts. DCIS.com MIND lesions were immunostained for Fibroblast Specific Protein 1 (Fsp1; **A.**), Progesterone Growth Factor Receptor-α (PDGFR-α; **B)** or CCL2 expression **C.** Representative images are shown with magnified image underneath. The stroma is marked with an asterisk in the magnified image. Expression in the stroma was quantified by Image J, in arbitrary units. Statistical analysis was performed using two-tailed *t*-test (**B**). Statistical significance was determined by $P<0.05$. *$P<0.05$. Mean$\pm$SEM values are shown. Scale bar= 400 µm.

CCL2 from DCIS fibroblasts is important for CCR2 mediated breast cancer survival and invasion

To further characterize the expression of CCL2 in DCIS stroma, fibroblasts were isolated from patient samples of normal breast or DCIS tissues and analyzed for CCL2 expression. By ELISA, two out of three DCIS fibroblast lines (1213-249, 80H) expressed higher levels of CCL2 compared to normal fibroblasts (hNAF2525, hNAF8727) and DCIS.com breast cancer cells (Figure 16A). Although previous studies have established an important role for carcinoma associated fibroblasts from invasive breast cancers [132, 133], the role of fibroblasts derived from DCIS tissues remain poorly understood. To determine the functional role of CCL2 derived from DCIS fibroblasts to CCR2 mediated breast cancer progression, we utilized the subrenal capsule model. The advantage of this model is that it is devoid of fibroblasts, enabling us to determine the relative contribution of cografted fibroblasts without interference from host stroma. Mammary carcinoma cells grafted in the subrenal capsule form tumors consistently and similarly to orthotopic injection [134,135]. 1213-249 DCIS derived fibroblasts, which showed the highest level of CCL2, were co-grafted with DCIS.com breast cancer cells in the renal capsule of NOD-SCID mice and analyzed for changes in tumor growth and invasion. Fibroblasts co-grafted with parental DCIS.com cells showed increased tumor mass compared to DCIS.com cells grafted alone (Figure 16B). CCR2 deficient DCIS.com cells co-grafted with 1213-249 fibroblasts showed a significant 20% decrease in tumor mass compared with fibroblasts co-grafted with control DCIS.com cells (Figure 16B).

To examine for changes in tumor invasion into normal kidney tissue, we performed CO-IF staining for pan-cytokeratin and phalloidin to distinguish tumor cells from kidney tissues. In the subrenal capsule model, pan-cytokeratin antibodies stained

DCIS.com tumors more clearly than CK5 antibodies used in the MIND model. Pan-cytokeratin antibodies recognized CK: 4, 5, 6, 8, 10, 13 and 18, and preferentially stained breast cancer cells over kidney tissues, which expressed fewer of the cytokeratins [136]. Using this approach, tumor invasion was characterized by a lack of defined border between tumor and kidney tissues, and scattering of tumor cells throughout the kidney, as observed in control lesions (Figure 16C). CCR2 deficient cells co-grafted with fibroblasts showed a reduction in tumor invasion, characterized by more cohesive tumors and a clearer delineation between tumor and kidney tissues (Figure 16C). Decreased invasiveness was associated with decreased tumor cell proliferation and increased apoptosis as indicated by PCNA and cleaved caspase-3 immunostaining (Figure 16D-E). CCR2-KD DCIS.com cells grafted alone did not show significant differences in tumor growth or invasion compared to control shRNA cells grafted alone (Figure. 17 A-C). These studies indicate that CCR2 KD in DCIS.com breast cancer cells inhibit fibroblast mediated tumor growth and invasion.

To determine the relevance of CCL2 expression in DCIS fibroblasts, fibroblasts were immortalized by hTERT expression to enable stable shRNA expression. Two CCL2 deficient fibroblast lines were generated from two different shRNA systems. A 47% decrease in CCL2 expression was observed using the GFP-c-shLenti OriGene system (CCL2-pLenti). A 30% decrease in CCL2 expression using the GIPZ Dharmacon system (CCL2/GIPZ) (Figure 18A). CCL2 deficient or control fibroblasts were co-grafted with DCIS.com breast cancer cells in the kidney capsule and analyzed for changes in tumor progression. CCL2 deficient fibroblasts co-grafted with DCIS.com cells resulted in smaller tumors and reduced tumor invasion, associated with decreased tumor cell

proliferation and increased apoptosis (Figures 18B-C). These studies indicate that CCL2 derived from DCIS fibroblasts modulates progression of DCIS.com breast cancer cells.

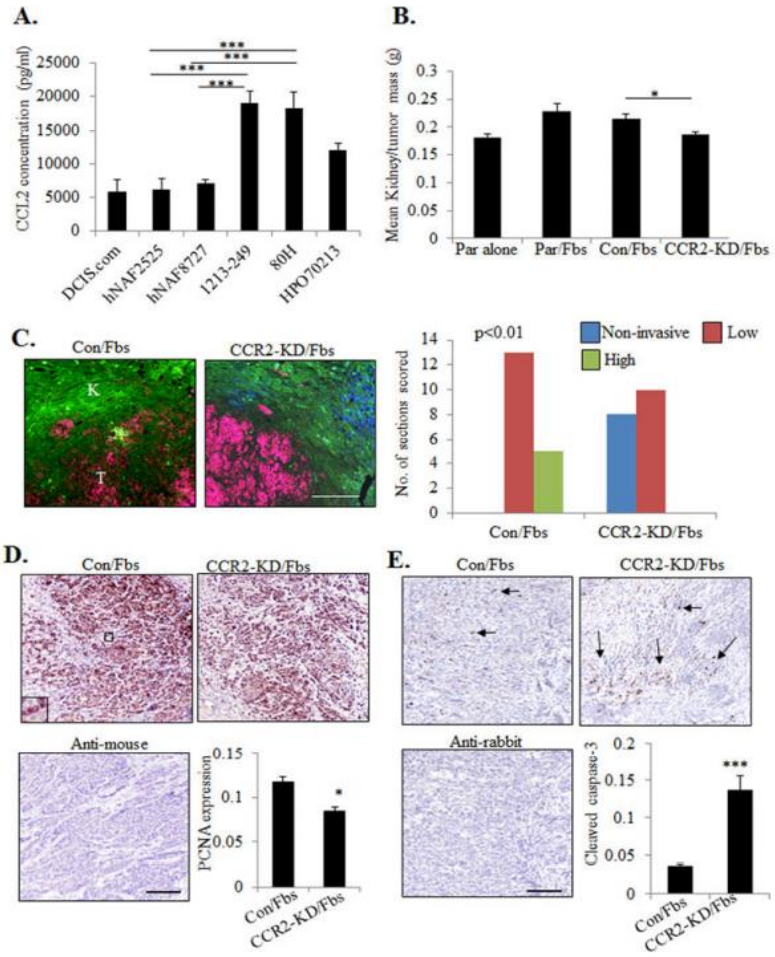

Figure 16. CCR2 knockdown in DCIS.com cells inhibit fibroblast mediated cancer progression. A. CCL2 ELISA of conditioned medium from fibroblasts derived from normal breast (hNAF2525, hNAF8727) or DCIS tissues (1213-249, 80H, HPO70213), in comparison with DCIS.com breast cancer cells. **B-E**. 1213-249 fibroblasts (Fbs) were co-grafted with parental (Par) DCIS.com cells or DCIS.com cells expressing control (Con) or CCR2 shRNAs (CCR2-KD) in the subrenal capsule of NOD-SCID mice for 21 days. Kidney tissues were measured for tumor mass (**B**), scored for tumor invasion into normal kidney by pan-cytokeratin (red) and phalloidin (green) staining (**C**), tumor cell proliferation by PCNA immunostaining (**D**), tumor cell apoptosis by cleaved caspase-3 immunostaining (**E**). Scale bar=400 microns. Magnified insets shown. Arrows point to examples of positive staining. Expression in tissues was quantified by Image J. n=7 mice per group. Statistical analysis was performed using One way ANOVA with Bonferroni *post-hoc* comparison (**B**) or Two tailed *t*-test (**D, E**). Statistical significance was determined by $P<0.05$. *$P<0.05$, ***$P<0.001$. Mean±SEM are shown.

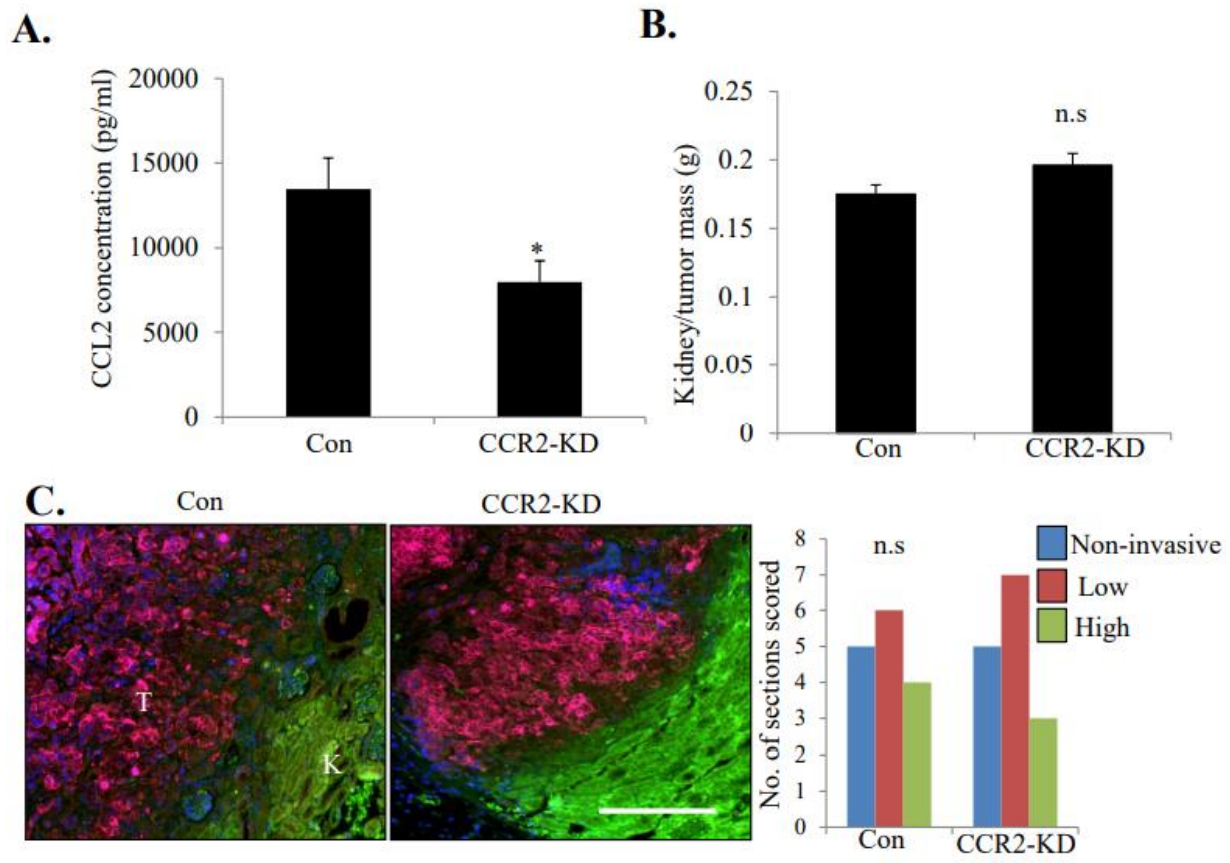

Figure 17. CCR2 knockdown alone does not significantly affect progression of DCIS.com breast cancer cells. **A.** CCL2 ELISA of conditioned medium from Control shRNA (Con) or CCR2 shRNA expressing (CCR2-KD) DCIS.com breast cancer cells **B**. Tumor mass of DCIS.com cells grafted alone in the kidney capsule of NOD-SCID mice. **C.** Scoring of tumor sections immunostained with antibodies to pan-cytokeratin (red) and phalloidin (green). 3 sections/tumor, n=5 samples/group. T=tumor, K=Kidney. Scale bars = 200 microns. Statistical analysis was performed using Two Tailed *t* test. Statistical significance was determined by $P<0.05$. *$P<0.05$, n.s= not significant. Mean±SEM are shown.

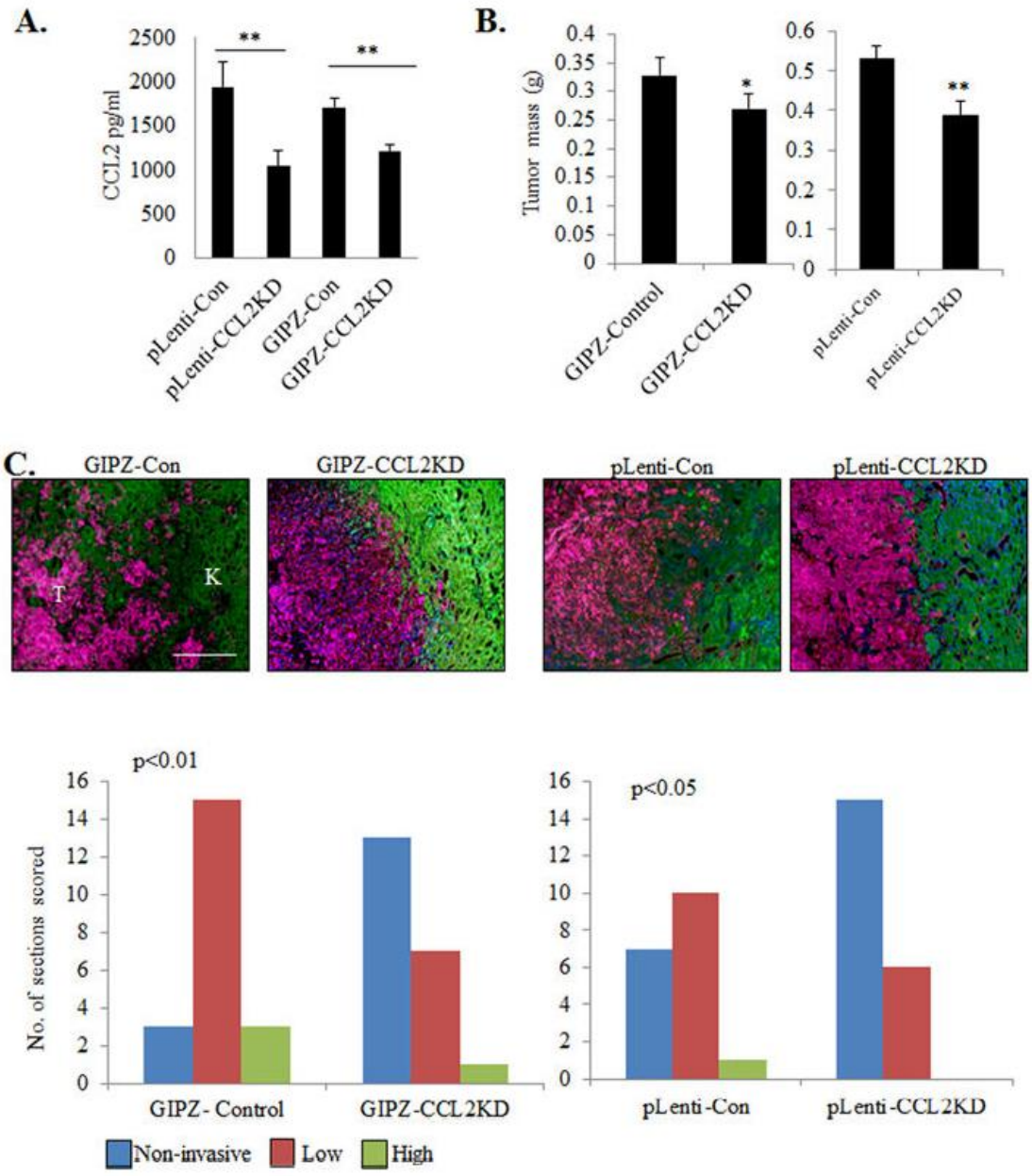

Figure 18. CCL2 derived from DCIS fibroblasts is important for progression of DCIS.com breast cancer cells. A. CCL2 ELISA of 1213-249 fibroblasts expressing control shRNA (Con) or CCL2 shRNAs from pLenti or GIPZ lentivirus systems. **B** and **C,** Control or CCL2 deficient 1213-249 fibroblasts were co-grafted with DCIS.com breast cancer cells in the subrenal capsule and analyzed for changes in tumor growth (**B**), and scored for tumor invasion into normal kidney tissue by pan-cytokeratin (red) and phalloidin (green) staining (**C**). n=7 mice/group. Scale bar=400 microns. K=kidney, T=tumor. Statistical analysis was performed using One-way ANOVA with Bonferroni *post-hoc* comparison. Statistical significance was determined by $p<0.05$. **$p<0.01$. Mean$\pm$SEM are shown.

CCL2/CCR2 mediated invasion is associated with increased ALDHA11 and decreased HTRA2 expression

Lastly, we analyzed the relationship between expression of downstream CCL2/CCR2 signaling proteins and increased breast cancer survival and invasion. Through candidate screening of factors related to breast cancer survival and invasion, we found that CCL2 treatment of DCIS.com breast cancer cells over time increased expression of ALDH1A1, a stem cell and pro-invasive factor [114], and reduced expression of HTRA2, a pro-apoptotic mitochondrial serine protease [115] (Figure 19A-B).

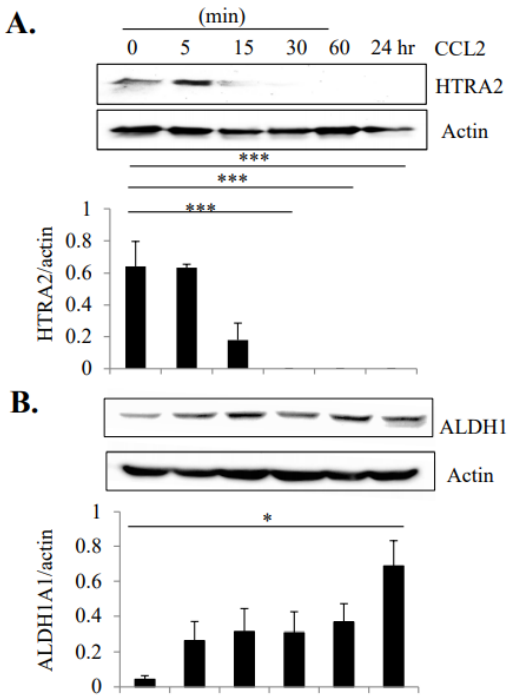

Figure 19. CCL2 treatment of DCIS.com breast cancer cells increase ALDH1 and decreases HTRA2 expression. Immunoblot for **A**. HTRA2 and **B.** ALDH1A1 expression in DCIS.com breast cancer cells treated with 60 ng/ml CCL2 for up to 24 hours. Expression levels were determined by densitometry analysis. Experiments were performed in triplicate. Statistical analysis was performed using One Way ANOVA with Bonferroni *post-hoc* comparison. Statistical significance was determined by $P<0.05$. *$P<0.05$, ***$P<0.001$. Mean±SEM are shown.

CCR2 KD in DCIS.com breast cancer cells decreased expression of ALDH1A1 and increased HTRA2 in MIND xenografts by IHC staining (Figure 21A-B). Conversely, CCR2 overexpression in Sum255 MIND xenografts enhanced ALDH1A1 expression and decreased HTRA2 expression (Figure 20A-B), indicating that epithelial CCR2 was important for regulating ALDH1A1 and HTRA2. Furthermore, CCL2 KD in fibroblasts increased HTRA2 expression and decreased ALDH1 expression in DCIS.com cells in the subrenal capsule model (Figure 21C-D), indicating that paracrine CCL2 signaling from the fibroblastic stroma was important for regulating ALDH1A1 and HTRA2 expression. Through Kaplan – Meier Plotter analysis [137], increased CCR2 and ALDH1A1 and decreased HTRA2 expression were significantly associated with decreased metastasis free survival of breast cancer patients (Figure 21E). These data demonstrate a clinical relevance for CCL2/CCR2 signaling proteins in breast cancer.

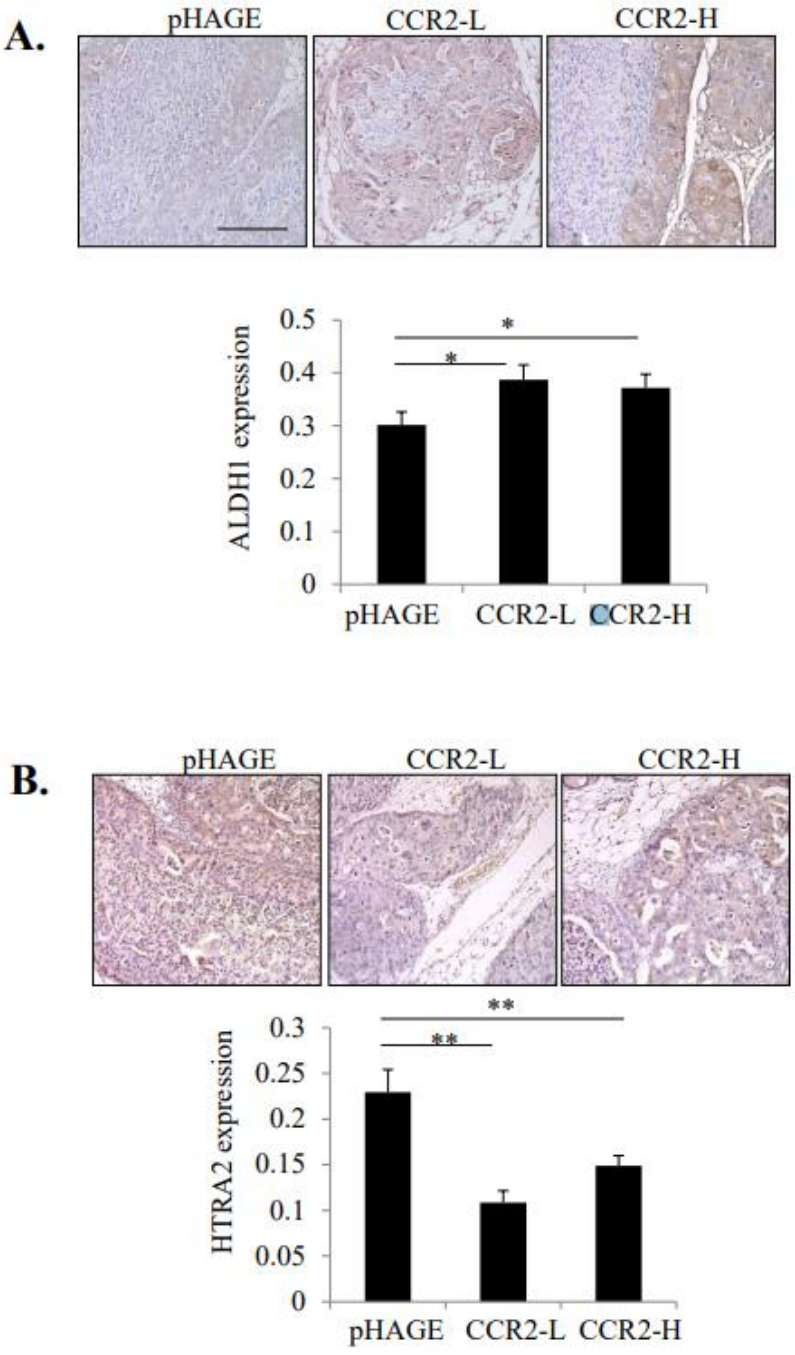

Figure 20. Effect of CCR2 overexpression on ALDH1 and HTRA2 expression in SUM225 MIND xenografts. Sum225 MIND xenografts were immunostained for **A**. ALDH1 or **B**. HTRA2 expression. Expression was measured by Image J (arbitrary units). Statistical analysis was performed using One Way ANOVA with Bonferroni *post-hoc* comparison. Statistical significance was determined by $P<0.05$. *$P<0.05$, ***$P<0.001$. Mean±SEM are shown. n=8 mice per group.

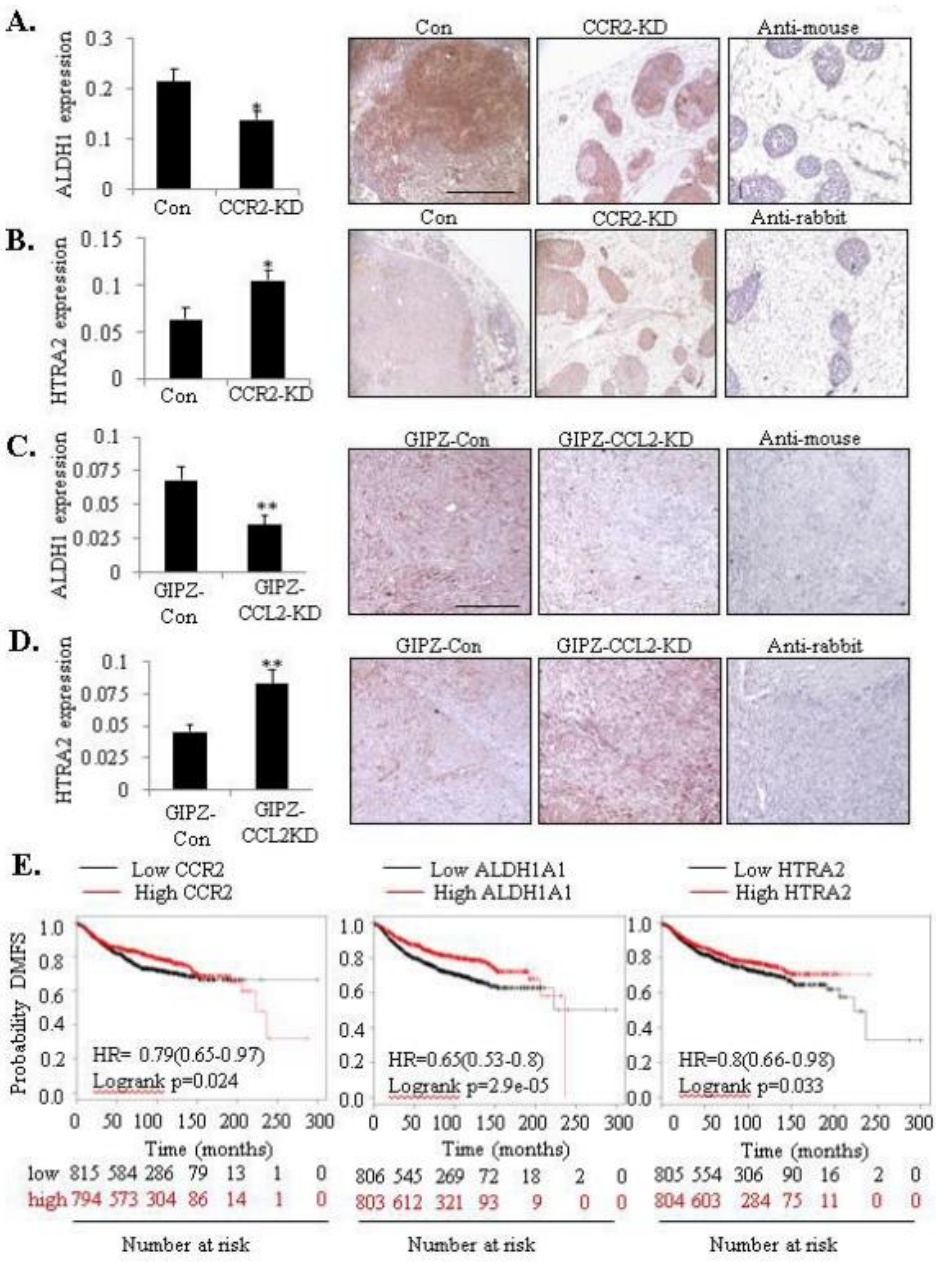

Figure 21. CCL2/CCR2 mediated DCIS progression is associated with increased ALDH1 and decreased HTRA2 expression. A-D. ALDH1 and HTRA2 expression was examined by immunostaining of tumor tissues in the DCIS.com MIND Model (**A** and **B)** and subrenal capsule model (**C** and **D**). Expression in tissues was quantified by Image J. K=kidney tissue; T= tumor. Scale bar= 400 microns. **E**. RNA Expression of CCR2 (Affyid 207794_at), ALDH1A1 (Affyid 212224_at) and HTRA2 (Afftyid 2030809_s_at) were analyzed for associations with Distance Metastasis Free Survival (DMFS) through Kaplan Meier Plotter. Statistical analysis was performed using Two Tailed-T-test (**A** and **B**) or Log-rank Test (**C**). Statistical significance was determined by $P<0.05$. $*P<0.05$, $**P<0.01$. Mean±SEM are shown.

Discussion

The role of fibroblasts in DCIS progression have remained poorly understood. Fibroblasts derived from invasive breast ductal carcinomas promote tumor growth, invasion, metastasis and chemoresistance [132,133]. One study showed that fibroblasts from normal, IDC or arthritic tissues enhanced progression of MCF10A cell lines in a subcutaneous injection model through Transforming Growth Factor-β and Hedgehog dependent mechanisms [138]. For the first time, we show that fibroblasts derived from DCIS patient samples accelerate progression from DCIS to IDC through CCR2 dependent mechanisms. Moreover, CCL2/CCR2 mediated breast cancer progression is associated with increased expression of clinical relevant pro-invasive factors (ALDH1A1) and decreased expression of pro-apoptotic factors (HTRA2).

Here, we noted some complementary and conflicting phenotypes through CCR2 overexpression and knockdown. CCR2 overexpression in SUM225 cells enhanced formation of invasive lesions and increased the presence of CCL2+ fibroblasts, associated with increased ALDH1 and decreased HTRA2. CCR2 KD and knockout in DCIS.com cells inhibited invasive progression and decreased the presence of CCL2+ fibroblasts, associated with decreased ALDH1 and increased HTRA2 expression. However, although CCR2 KD significantly affected mammary tumor mass, CCR2 overexpression did not. Although CCR2 overexpression increased tumor cell proliferation and survival of SUM225 lesions, these levels were still lower than the cell proliferation and survival detected in DCIS.com MIND xenografts. CCR2 expression levels in overexpressing cells did not reach the levels detected in DCIS.com breast cancer cells. Therefore, it is possible that the increase in cell proliferation and survival in

CCR2 overexpressing cells was not sufficient to affect overall mammary tissue mass. The levels of CCR2 expression in DCIS.com cells are consistent with previous studies showing that CCR2 expression levels are higher in basal like breast cancer cells compared to luminal breast cancer cells [113]. Because SUM225 cells are luminal/Her2+, additional oncogenic pathways may be important to DCIS progression of this subtype. Regardless of subtype, by analyzing the effects of CCR2 overexpression in SUM225 cells with CCR2 KD in DCIS.com cells, we demonstrate a critical role for epithelial CCR2 receptor expression in DCIS progression.

Despite a 2-fold increase in the number of CCR2+ cells in the CCR2-H SUM225 cell line, CCR2-H cells did not show increased invasion, proliferation or survival compared to CCR2-L cells. It is possible a threshold of receptor expression modulates cellular activity. Such a threshold has been detected in T cells whereby 8000 T cell receptors/cell are needed for a commitment to proliferate [139,140]. A threshold also exists for EGFR levels in regulating Cbl and Grb2 dependent signaling in epithelial cells [141]. In our studies, CCR2-L cells may have reached a threshold for CCR2 expression in determining cellular invasion. Although more cells expressed CCR2 in the CCR2-H cell line, the level of expression may not have been sufficient to commit these cells to invade. Histogram analysis revealed that while more cells overexpressed CCR2 in the CCR2-H cell line, expression levels did not vary highly between CCR2-L and CCR2-H cells. In addition to a receptor threshold, heterogeneity in expression of intracellular signaling components in breast cancer [142] may also explain why CCR2-H cells did not result in further DCIS progression. As we are unable to control which SUM225 cells express CCR2, it is possible some CCR2 overexpressing cells did not exhibit the

necessary downstream signaling components to induce invasion. As CCR2 overexpression in SUM225 cells did not reach the levels of invasion detected in DCIS.com cells, it is likely that other oncogenic factors would be required to further enhance carcinoma invasion. Several oncogenic signaling pathways including Notch, EGF, and HGF signaling are associated with DCIS progression [143,144]. It would be of interest to further understand how CCL2/CCR2 coordinates DCIS progression with other oncogenic factors.

We also observed that CCR2 overexpression and knockdown affected the levels of fibroblasts in DCIS stroma. We expected that CCR2 signaling in breast cancers modulated fibroblast growth through expression of soluble growth factors such as PDGF and WNT5A, positive regulators of fibroblast proliferation [145,146]. However, cultured DCIS fibroblasts treated with conditioned medium from CCR2 deficient or control DCIS.com control cells showed no significant changes in cell growth (Figure 22).

Furthermore, there were no changes in blood vessel density or macrophage recruitment, indicating that epithelial CCR2 would not regulate fibroblast accumulation indirectly through these stromal cell types. It is possible that epithelial CCR2 acts on other stromal components to indirectly modulate fibroblast growth, including adipocytes or granulocytes. Another possibility may involve the extracellular matrix. Hyaluronan and fibronectin increase fibroblast cell growth, while collagen suppresses fibroblast growth through mechano-signal transduction mechanisms [147,148]. These factors would be present in mammary tissues, but not in conditioned medium. Studies are currently underway to understand how CCL2/CCR2 signaling breast cancer cells modulate the surrounding breast tumor microenvironment.

We show that increased ALDH1 and decreased HTRA2 expression are associated with CCL2/CCR2 mediated DCIS progression. Previous studies have implicated ALDH1 expression in cancer stem cell renewal, invasion, and drug resistance [149]. Emerging studies indicate an important role for HTRA2 in positively regulating mitochondrial dependent apoptosis [150]. The increased expression of HTRA2 in CCR2 deficient lesions is consistent with the increased expression of cleaved caspase 3, as an indicator of apoptosis. CCL2/CCR2 signaling in breast cancer cells may promote DCIS progression by enhancing ALDH1+ tumor initiating cells or activating invasive pathways through ALDH1 activity in breast cancer cells. CCL2/CCR2 signaling may facilitate survival of DCIS lesions through suppression of HTRA2 mediated apoptosis pathways.

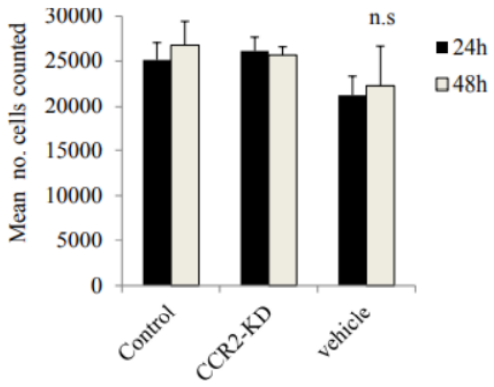

Figure 22. CCR2 deficiency in DCIS.com breast cancer cells does not affect fibroblast growth. Conditioned medium from control shRNA or CCR2-KD DCIS.com cells were used to treat 1213-249 DCIS fibroblasts. Fibroblasts were counted after 24 and 48 hours of treatment by hemocytometer. Serum free medium was used as a vehicle control Statistical analysis was determined by One-way ANOVA with Bonferroni post-hoc comparison test. Statistical significance was determined by $P<0.05$. n.s= not significant. Mean±SEM are shown.

In summary, these studies identify a novel role for CCL2/CCR2 signaling in cancer progression, identify potentially new prognostic factors for DCIS, and potentially new molecular targets for the prevention of invasive breast cancer.

Chapter III. The CCL2/CCR2 chemokine signaling enhances glycolysis in human breast cancer cells by upregulating Hexokinase 2 expression

Abstract

Altered metabolism is a hallmark of cancer cells. In this chapter we discuss how the search to identify additional molecular factors that might cooperate with CCL2/CCR2 chemokine signaling pathway to coordinate DCIS progression, we identified an enhancement in glucose metabolism. By global metabolomic analysis we found that CCL2 enhances glycolysis by increasing glucose uptake and lactate secretion. Additional studies revealed that the CCL2/CCR2 chemokine signaling regulates Hexokinase II expression in vitro and in vivo.

To further evaluate the clinical significance of Hexokinase II expression in DCIS progression, we performed immunostaining on breast tissue microarrays containing matching in situ, invasive ductal carcinomas, and normal adjacent to invasive ductal carcinoma breast tissue. Immunostaining analysis showed increased HKII expression in DCIS and IDC compared to normal adjacent breast tissue.

Taken together, this data indicates that the CCL2/CCR2 chemokine plays a role in regulating glycolysis in part by modulating Hexokinase II expression and with important associations with disease progression. Overall, these studies demonstrate a novel relationship between chemokine signaling altering glucose metabolism with important implications in therapeutic targeting.

Introduction

In breast cancer, CCL2/CCR2 are highly expressed in DCIS compared to normal tissue. In breast cancer cells, epithelial CCR2 corresponds to invasive potential [46,65]. Previous studies have demonstrated that CCL2-induced cell survival, and migration with increased phosphorylation of Smad3 and P-42/44 MAPK proteins [46]. Increased expression of stromal CCL2 has been associated decreased recurrence free survival and with basal like breast cancer subtype [47]. Further characterization of the clinical relevance of the CCL2/CCR2 chemokine signaling pathway related proteins in TMAs containing DCIS, IDC, and normal tissue showed that CCR2 and phospho SMAD-3 expression was significantly higher in IDC compared to DCIS tissues indicating that proteins related to CCL2/CCR2 signaling are highly expressed in DCIS, and further upregulated in IDC (Fang et al, 2020 under review). These data suggest that there is an important association between CCL2/CCR2 related signaling proteins, that corresponds to DCIS progression to invasive disease.

Functional in vivo studies of epithelial CCR2 using the Mammary Intraductal Injection (MIND) as a model of DCIS, demonstrated that CCR2 overexpression was associated with enhanced survival, invasion, and accumulation of CCL2 expressing fibroblast. In contrast, ablating CCR2 function, decreased survival, and formation of invasive lesions [62]. However, targeting CCR2 alone was not sufficient to ablate invasive phenotype which might indicate that other oncogenic factors are necessary to further drive DCIS progression and eventually leading to invasion.

In the search to identify additional molecular factors that might cooperate with CCL2/CCR2 chemokine signaling pathway to coordinate DCIS progression, we identified an enhancement in glucose metabolism. Altered metabolism is a hallmark of cancer cells. By a global metabolomic analysis we found that CCL2 enhances glycolysis by increasing glucose uptake and lactate secretion. Additional studies revealed that the CCL2/CCR2 chemokine signaling regulates Hexokinase II expression in vitro and in vivo. These studies demonstrate a novel relationship between chemokine signaling altering glucose metabolism with important implications in therapeutic targeting.

Materials and Methods

Cell culture

DCIS.com cells which originated from Dr. Fred Miller's laboratory [117] were provided by Dr. Fariba Behbod (University of Kansas Medical Center). MDA-MB-231 were obtained from the American Tissue Culture Collection. These cells were cultured and maintained in DMEM containing 10% FBS, 2mmol/L L-glutamine, and 1% penicillin-streptomycin. HCC1937 cells were provided by Dr. Roy Jensen (University of Kansas Medical Center). The cells were cultured in RPMI containing 10% FBS, 2mmol/L L-glutamine, and 1% penicillin-streptomycin. SUM225 cells were originated at the Medical University of South Carolina, Charleston, SC, at Dr. Steven Ethier's laboratory [118]. These cells were cultured and maintained in Ham F12 media containing 10% FBS, 5ug/mL insulin, 1ug/mL cortisone and 1% penicillin – streptomycin. Cell lines were cultured for no longer than 6 months and analyzed for mycoplasm after thawing using the MycoAlert™ Mycoplasm Detection Kit (Lonza, cat no. LT07-703).

Measurements from the Extracellular acidification rate (ECAR) and oxygen consumption rate (OCR)

Breast cancer cells were evaluated using an extracellular Flux analyzer (XF24; Seahorse Bioscience, Billerica, MA, USA). Cells were seeded in 24-well plates (30,000 cells/well) (using the standard manufacturer .recommended two step seeding procedure. Mitochondrial respiration was evaluated with the XF Cell Mito Stress Kit and glycolytic metabolism with the XF Glycolysis stress test.

To perform the mitochondrial stress test, after plating the cells, the microplate was kept overnight at 37◦C, 5% CO2. incubator, the following day cells were serum starved overnight. Cartridges equipped with Oxygen and pH sensitive probes were hydrated with 1ml of hydrating solution and incubated overnight at 37◦C without CO2. On the day of the assay, cells were treated with CCL2 (100ng/ul) CCL2 was purchased from PeproTech, Inc (cat# 300-04) in complete media for 4 hours. One hour prior the assay, the medium was replaced placed in Agilent XF asay medium with (1mM Pyruvate), (25mM Glucose) and (2mM Glutamine). Each plate was incubated at 37◦C, without CO2 for 1 hour and then transferred to the microplate stage of the Seahose XF24 flux analyzer with the cartrige of probes.

Oxygen consumption rates (OCR) readings were evaluated after injection of the following compounds: 1) oligomycin (1µM final concentration); 2) (FCCP) (carbonyl cyanide-p-(trifluoromethoxy) phenylhydrazone; 0.75µM final concentration); 3) antimycin A + rotenone (1.5µM each final concentration). Three separate readings were taken to ensure stability. The glycolysis stress test was performed as describe aboved, except that the XF SeaHorse Glycolysis Stress Base Medium was used. This media is

supplemented with 2mM L-glutamine, and the readings are evaluated after injection of the following compounds: 1) glucose (10nM final concentration); 2) oligomycin (1µM final concentration); 3) 2-deoxyglucose (2D-G; 100mM final concentration). Data for each experimental condition derived from values obtained from a minimum of six separate wells.

Glucose consumption and lactate secretion

60,000 DCIS.COM breast cancer cells were plated in 24 well plates and serum starved overnight. Cells were treated with DMSO, Merestinib, HGF±Merestinib, and CCL2±Merestinib for 24 hours and another set was plated for assessment at 48 hours treatments. Extracellular glucose consumption was determined by using the Glucose-Glow™ Assay (Cat # J6021 from Promega). This assay includes glucose dehydrogenase which uses glucose and NAD+ to produce NADH. When NADH is present the pro-luciferin reductase substrate is converted to luciferin by reductase. This product is then used by the recombinant luciferase from Ultra-Glo™ to produce light. This assay was performed according to manufacturer's instructions and as previously described [46].

For lactate detection the Lactate- Glo™ Assay (Cat # J5021) was used. This assay includes lactate dehydrogenase which uses lactate and NAD+ to produce NADH and pyruvate. In the presence of NADH, pro-luciferin reductase substrate is converted by Reductase to luciferin. This luciferase reaction produces light in the presence of Ultra-Glo™ that is detected by a luminometer. This assay is specific to L-Lactate which is the

major stereoisomer found in mammalian cells. The assay was performed according to manufacturer's instructions and as previously described [157].

Immunoblot

Breast ductal mammary carcinoma cells were plated in 6-well plates (500,000 cells/well) in DMEM 10%FBS. Cells were serum deprived for 24 hours and incubated with serum free media with or without recombinant CCL2 (100ng/ml) ± Merestinib (203 nM), HGF (100ng/ml) ± Merestinib (203 nM) for 24 hours. Cells were lysed in RIPA buffer containing: 1X PBS, 1% Nonidet P-40, 0.5% sodium deoxycholate, 0.1% SDS with protease and phosphatase inhibitors (Sigma-Aldrich, Cat # P8340). Lysates were sonicated and 20ug of protein were resolved on 8 or 10% SDS-PAGE gels and transferred to nitrocellulose membranes. The membranes were blocked in PBS/0.05% Tween-20 /3% milk and probed with primary antibodies [1:1000] to: Hexokinase II (Cell Signaling Technology®, Cat # 2867). were detected with rabbit secondary antibodies conjugated to horseradish peroxidase (HRP). β-actin Sigma (Cat #A5441) was detected with ani-rabbit-hrp. Membranes were developed with West Pico ECL chemiluminescent substrate and imaged using a Biospectrum Imaging System.

Immunohistochemistry by DAB staining

MIND injection tissues were fixed in 10% neutral formalin buffer and embedded in wax as previously described [120]. Sections were cut 5 microns thick, dewaxed and heated in 10mM sodium Citrate buffer pH 6.0 for 5 minutes. Followed washing the slides, a endogenous peroxidase blocking step was performed with 60% cold methanol/3% H_20_2 in PBS, blocked for at least one hour in 3% FBS in PBS for rabbit antibodies, and

incubated with primary antibodies [1:100] overnight at 4ºC for; Hexokinase II (Cell Signaling Technology®, Cat # 2867). Antigen retrieval for HKII 2M UREA pH 6.8 was used. Slides were incubated with streptavidin peroxidase (Vector Laboratories Cat # PK-6200) for 30 minutes. Slides were developed with 3,3'-diaminobenzidine (DAB) substrate Kit (Vector Laboratories Cat # SK-4100) and counterstained with Mayer's hematoxylin and mounted with cytoseal.

Biospecimens

Patient samples were collected under approval of the Institutional Review Board (IRB) at KUMC. Tissue microarrays (TMAs) consisted of de-identified patient tissue were provided by the Biospecimen Core Repository Facility (BCRF) from the University of Kansas Center (KUMC). TMAs were arrayed in duplicate. Core sections were 1.5 mm in diameter and 5 microns thickness. DCIS tissue was graded using the Van Nuys Prognostic Index (VNPI). Samples were collected between 2007 and 2012, with 3 to 5 year follow up. Tissue microarray pathology information included age, stage, grade, tumor size, expression of KI67, ER, PR and Her2. Additional information included treatment, recurrence, and survival. Clinical pathological features for all breast samples is summarized (Table 1). The mean age of patients was 56 years.

Image Quantification

Images were captured at 10X magnification using the FL-Auto EVOS system (Invitrogen) including 5-10 random fields per section. DAB staining was quantified as previously described [121]. In summary, the images were uploaded in Adobe Photoshop, positive DAB staining was selected by using the Magic wand tool, copied, and saved into

a new layer which makes a separate file. These images were opened in Image J (NIH), converted to gray scale, and adjusted with threshold adjustment to remove nonspecific background. Staining was quantified by using the particle analysis feature. Positive DAB staining values were normalized to total area values which were expressed as arbitrary units. Normalized arbitrary units were subjected to statistical analysis with GraphPad Prism. The same principle was used to quantify the fluorescent staining. The staining of interest was selected and normalized to DAPI.

Statistical Analysis

Experiments involving cell cultures were repeated a minimum of three times. Data is expressed as mean ± standard error of the mean (SEM). Statistical analysis was performed by using GraphPad software. Two-tailed Student *t* test was used to compared two groups. One-way ANOVA with Bonferroni *post hoc* multiple comparisons test was used for normal distributions. For non- Gaussian distributions the Kruskall-Wallis Test with Dunn's *post hoc* comparisons test was used. Statistical significance was determined by $P < 0.05$. $P<0.05$ *, $P<0.01$ **, $P<0.001$ ***, n.s= not significant or $P>0.05$.

Results

CCL2/CCR2 chemokine signaling regulates glycolysis by modulating Hexokinase II expression

By exploring possible molecular mechanisms by which the CCL2/CCR2 chemokine signaling pathway coordinate DCIS progression with other biological processes, we identified an effect on breast cancer cell's metabolism. We first detected

an association between CCL2/CCR2 chemokine signaling and altered metabolism through observational changes in acidity of the media of MDA MB 231 breast carcinoma cells mediated by modulation of CCL2 and CCR2 (data not shown).

To determine how CCL2 treatment specifically affects DCIS.com breast cancer cells metabolite production over time, we performed an unbiased global metabolomic analysis performed by mass spectrometry analysis. DCIS.com parental cells were treated with 100ng/ml of CCL2 at (1, 4, 8h). The global metabolic profile indicated that CCL2 mainly affected the levels of metabolites that are directly associated with glycolysis, TCA cycle, fatty acid synthesis and redox related metabolite production (Figure 23).

The TCA cycle and glycolysis are the two major metabolic pathways that are involved in energy production in the cell. To evaluate the effects of CCL2 on bioenergetic profile of the cells, we performed the cell energy phenotype test with a SeaHorse X24 analyzer instrument (Figure 24A). In this assay both glycolysis and mitochondrial respiration can be assessed in real time in response to metabolic modulators. Treating DCIS.om breast cancer cells with CCL2 increased their glycolytic potential as shown by the significant increase in baseline and stressed Extracellular Acidification Rate (ECAR) between serum free and CCL2 treatment group (Figure 24B).

Upon CCL2 induction, DCIS.com breast cells display a more glycolytic like phenotype compared to untreated cells demonstrated by a significant increase in ECAR, a proxy for glycolysis compared to OCR (Oxygen consumption rate) which reflects

mitochondrial respiration. These results indicate that CCL2 enhances glycolysis but not oxidative phosphorylation (Figure 24 C and D).

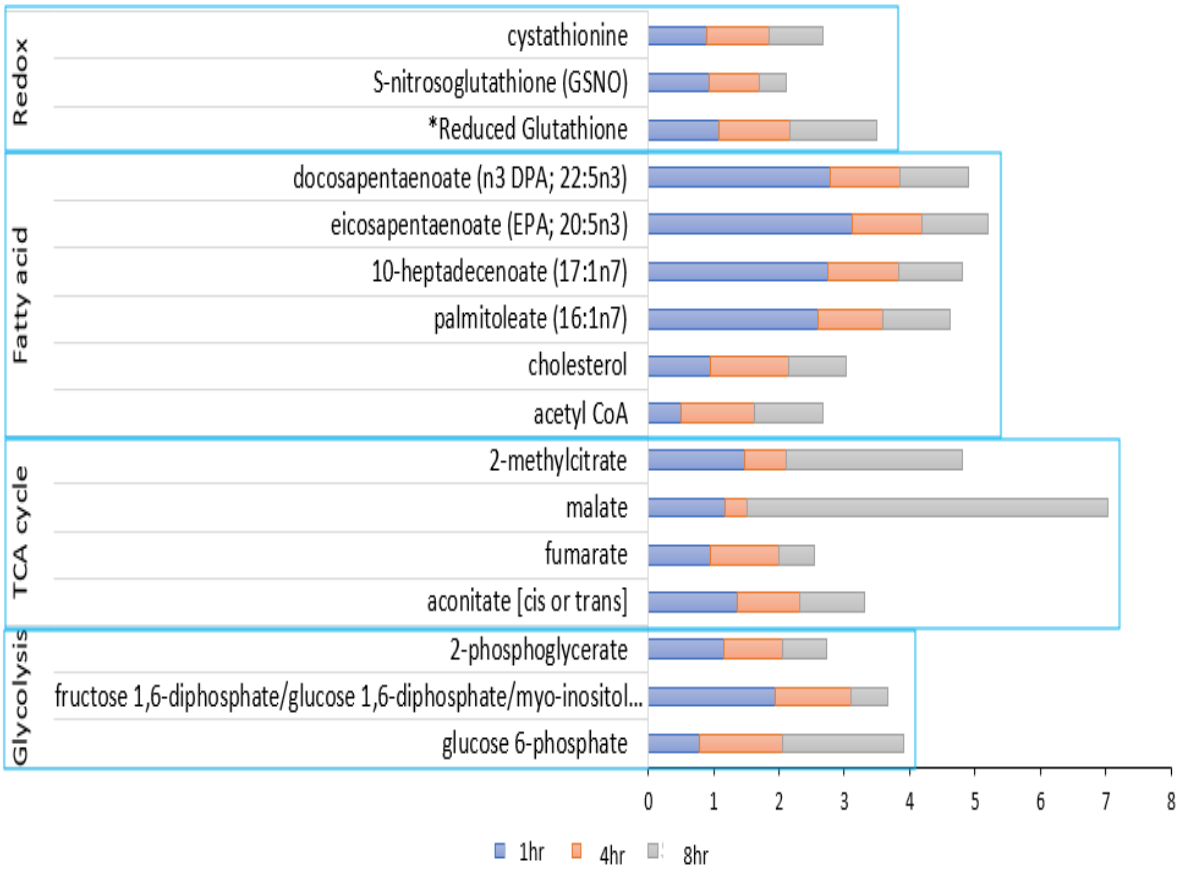

Figure 23. CCL2 modulates TCA cycle, Fatty acid synthesis and Redox related metabolite production in breast cancer cells. DCIS.com breast cancer cells were incubated in serum free media (SF), with/without 100 ng/ml CCL2 for 1, 4h and 8 hours in quadruplicate samples, and analyzed for metabolite production by LC/MS (Metabolon Inc). *glutathione shows increased levels at 8h but not statistically significant Statistical analysis was performed by One Way ANOVA. Statistical significance was determined by $p<0.05$. Statistically significant metabolites are shown.

Next, we decided to investigate the effect of CCL2 and CCR2 on the hallmarks of glycolysis which are glucose consumption and lactate secretion. Therefore, to determine the effect of CCL2 on glucose consumption in breast cancer cells with high levels of CCR2, DCIS.com and HCC1937 cells were treated with CCL2 for 24 hours and evaluated for changes in glucose consumption. Results indicate that CCL2 treatment significantly enhanced glucose consumption in both breast cancer cells compared to SF (Figure 25A). To characterize the importance of CCR2 expression in glucose consumption, we analyzed CCR2 overexpressing cells (CCR2-H) compared to pHAGE control and determined that following CCL2 induction, glucose consumption was significantly higher in CCR2 overexpressing cells compared to pHAGE control (Figure 25B). To investigate the effects of CCL2 on lactate secretion, DCIS.com cells treated with CCL2 in a time course of 24 hours display significant differences in intracellular lactate but not extracellular (Figure 25C and D). These data suggest that both CCL2 and CCR2 influence glycolysis by enhancing glucose consumption and intracellular lactate secretion.

To further identify a potential mechanism by which CCL2/CCR2 regulates glycolysis, we analyzed the expression of glycolytic enzymes and identified that Hexokinase II (HKII), the enzyme in the first concomitant step of glycolysis, was overexpressed in DCIS.com breast cancer cells after CCL2 treatment and downregulated in CCR2 KO breast cancer cells (Figure 26A). To validate the contribution of CCR2 overexpression to Hexokinase 2 expression, we treated SUM225 pHAGE control cells and SUM225 CCR2 overexpressing cells (CCR2-H) with CCL2 for up to 30

min and by immunoblot observed that Hexokinase 2 expression was highly expressed in CCR2 overexpressing cells compared to the pHAGE control (Figure 26B).

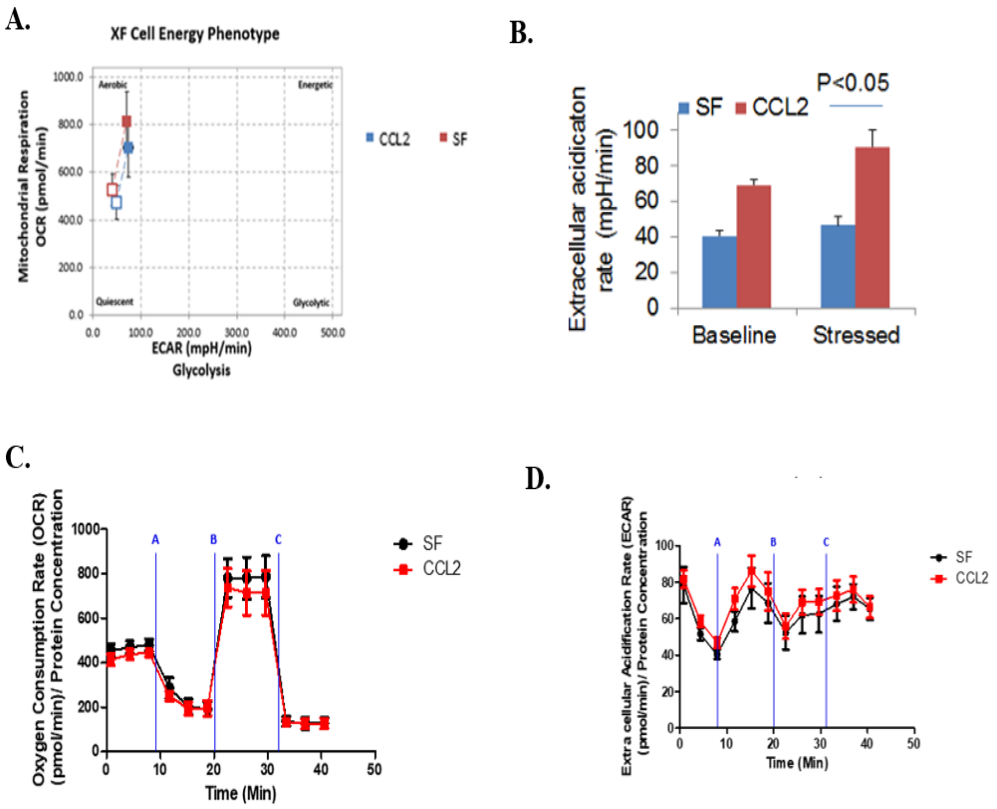

Figure 24. CCL2 significantly increases extracellular acidification rate (ECAR) and decreases oxygen consumption rate (OCR) in DCIS.com breast cancer cells. Cell Energy phenotype test for DCIS.com breast cancer cells induced for 4hrs with CCL2. Open square represents measurements at baseline and full square after the endpoint of the assay **(A)**. Histogram representing the Extracellular Acidification Rate (ECAR) at baseline (before injection of metabolic modulators) and stressed (endpoint of the assay) in DCIS.com breast cancer cells treated with CCL2 **(B).** Real-time respiration stress tests tracings for metabolic profile of DCIS.com breast cancer cells with the mitochondrial stress test DCIS.com breast cancer cells that were incubated in serum free media (SF) with/without CCL2 (100 ng/ml) for 4 hours. Cells were analyzed for rate of oxygen consumption (**D**) and extracellular acidification rate (ECAR) (**E**). Three independent experiments with the Sea Horse XF analyzer**.** Three separate readings were taken to ensure stability. Data for each experimental condition derive from values obtained from a minimum of six separate wells and the data represent readings from three independent plates. Statistical analysis was determined by Two Tailed *t* Test. Statistical significance was determined by $P<0.05$. Cells plated in triplicate. Mean+stdev are shown.

In vivo studies from the MIND model showed that mice injected with generated SUM225 breast cancer cells that overexpress CCR2 which were associated with increased number of invasive lesions, displayed increased HKII expression compared to pHAGE control. In contrast, CCR2 KO MIND lesions which displayed lower number of invasive lesions, showed that HKII expression was downregulated compared to WT control (Figure 26C). These data indicate that Hexokinase expression is modulated by CCL2/CCR2 expression which suggests an important association with DCIS progression in the MIND model.

To further evaluate the clinical significance of Hexokinase II expression in DCIS progression, we performed immunostaining on breast tissue microarrays containing matching in situ, invasive ductal carcinomas, and normal adjacent to invasive ductal carcinoma breast tissue. Immunostaining analysis showed increased HKII expression in DCIS and IDC compared to normal adjacent breast tissue (Figure 27A). Taken together, this data indicates that the CCL2/CCR2 chemokine plays a role in regulating glycolysis in part by modulating Hexokinase II expression and with important associations with disease progression.

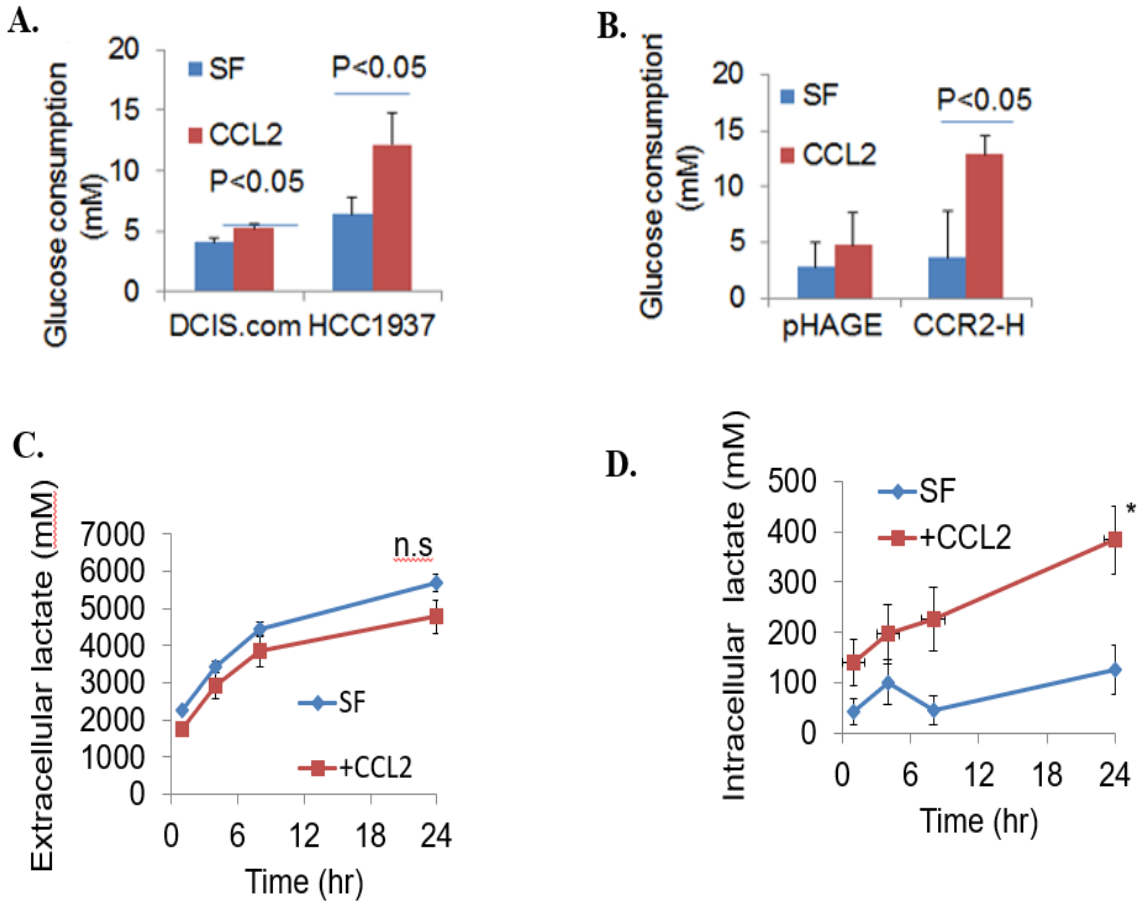

Figure 25. CCL2/CCR2 enhances glycolysis by increases glucose uptake and intracellular lactate secretion. Glucose consumption of DCIS.com, and HCC1937 breast cancer cells treated with CCL2 for 24 hours compared to SF **(A).** Glucose consumption of SUM225 overexpressing cells (CCR2 H) compared to pHAGE control treated with CCL2 and compared to SF **(B).** Extracellular lactate secretion of DCIS.com breast cancer cells treated ±CCL2 for 24 hours **(C).** Measurement of intracellular lactate in DCIS.com breast cancer cells treated with CCL2 at different time intervals up to 1 hour **(D)**. Statistical analysis was determined by Two Tailed *t* Test. Statistical significance was determined by $P<0.05$. n. s. = not significant. Cells plated in triplicate. Mean+stdev are shown.

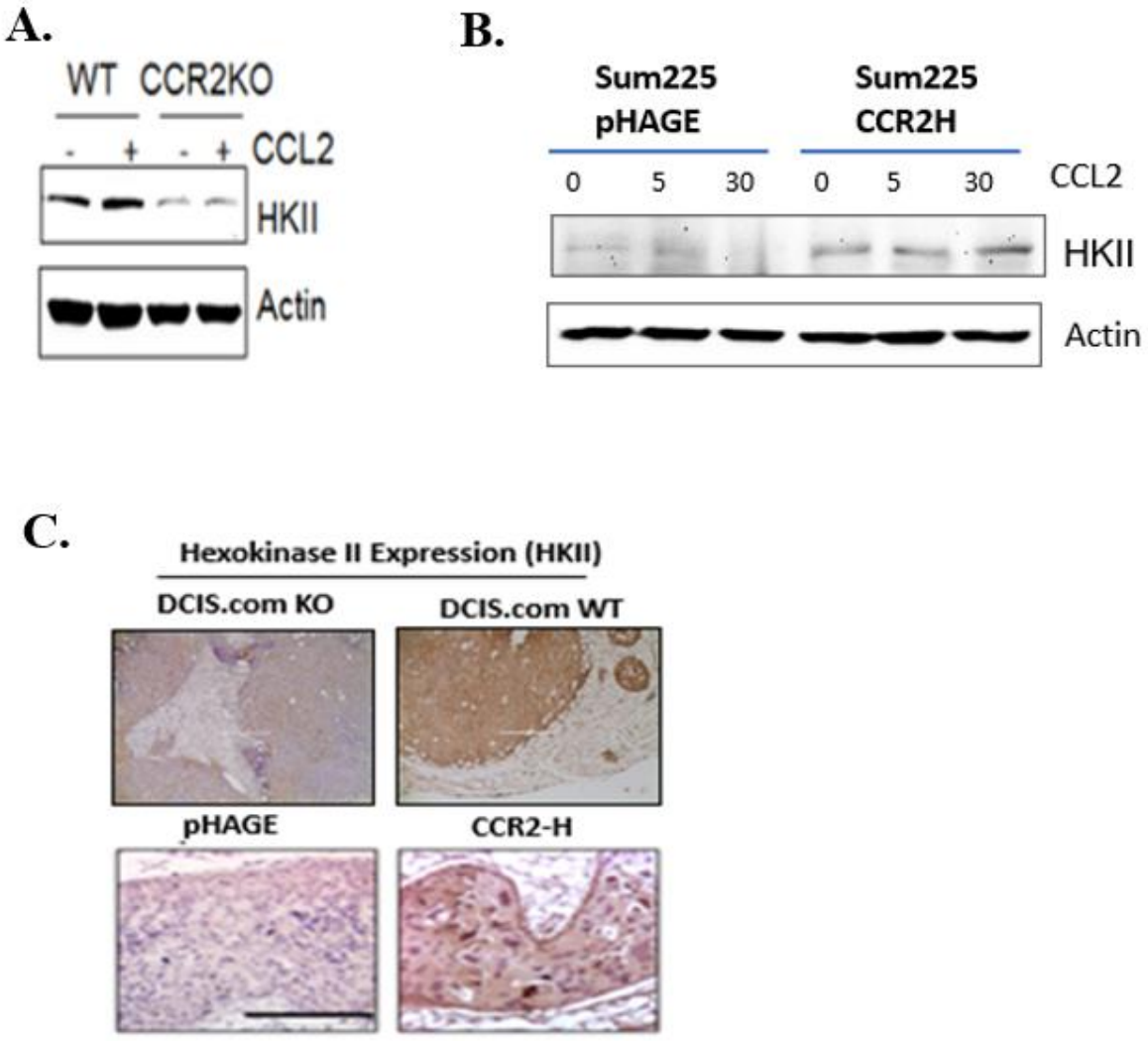

Figure 26. CCR2 expression modulates Hexokinase 2 expression human breast cancer cells. Immunoblot of DCIS.com wildtype (WT) or CCR2 knockout (KO) breast cancer cells for Hexokinase II (HKII) and β-Actin control **(A).** Immunoblot of SUM225 pHAGE Control and CCR2 Overexpressing cells (CCR2-H) for Hexokinase II (HKII) and β-Actin control (**B**). MIND model tissue was analyzed by immunohistochemistry to detect the expression of Hexokinase II in DCIS.com WT, CCR2 KO, SUMM225 (CCR2-H) and pHAGE control **(C).**

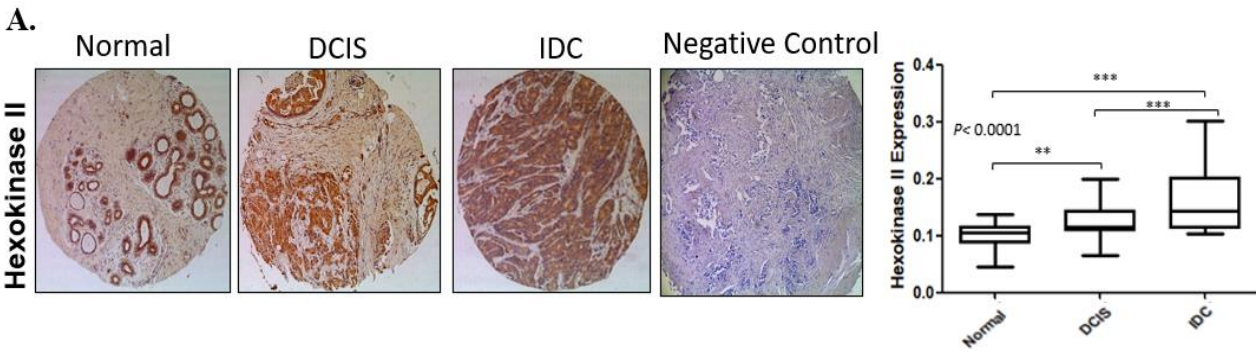

Figure 27. Hexokinase 2 expression increases as DCIS progresses to IDC in human samples. TMAs containing core sections; DCIS (n=45), matching IDC (n=47) and normal adjacent breast tissues to IDC (n=46) were immunostained with antibodies Hexokinase II **(A).** Expression was analyzed by Image J (arbitrary units). Whisker box plots are shown. Whiskers indicate min and max values. Box indicates upper and lower quartile range. Line indicates median Statistical analysis was performed using Two- Way ANOVA. Statistical significance was determined by $P<0.01$, $^{**}P<0.05$, $^{***}P<0.001$, and n.s; not significant. Scale bar=400 microns.

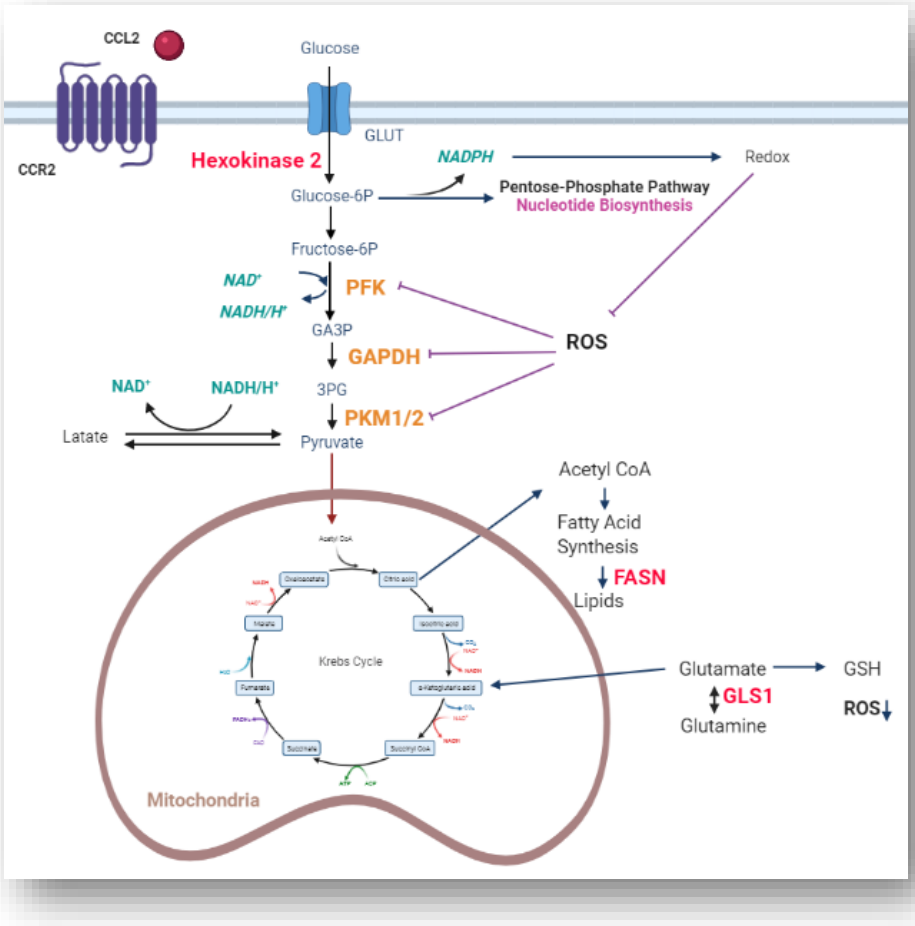

Figure 28. Model for the molecular mechanisms by which CCL2/CCR2 signaling mediates metabolism in breast cancer cells. By a global metabolomic analysis we identified that CCL2 affects glycolysis, TCA cycle, fatty acid synthesis, redox, and glutaminolysis. Metabolic enzymes in red are affected by CCL2/CCR2. Enzymes that regulate glycolysis are in orange. Steps where reactive oxygen species inhibit glycolysis are show in purple.

Factor		(% of total)
	Race	
Black		6%
White		89%
Hispanic/Other		4%
Median Age		56
	<50	30%
	>50	68%
ER		90[a] 99[b] 100[c]
PR		1.5[a] 85[b] 100[c]
HER2		
0		51%
1		38%
2		3%
3		5%
4		1%
Median Ki67		5

Table 1. Clinical Features for patient samples. TMAs with matched DCIS (N=45), IDC (N=45) and normal matched to IDC (N=46). Percent of total are shown with actual number of cases in parentheses. [a]25% percentile, [b]median, [c]75th percentile are shown for Estrogen Receptor (ER) and Progesterone Receptor (PR).

Discussion

By global metabolomic analysis, we demonstrated that the CCL2/CCR2 chemokine pathway directly affects glycolysis by enhancing glucose consumption, lactate secretion, and by modulating hexokinase II expression (Figure 28). Previous studies have reported that other cytokines including CCL5 enhance aerobic glycolysis in breast cancer cells through AMPK dependent mechanisms [158]. Others have identified that there is a strong association and correlation between increase glycolysis as well as genes involved in the MAPK pathway which are known to promote aerobic glycolysis [159]. CCL2 mediated by PKM2 in colorectal cancer cells contribute to an increase in macrophage recruitment [160]. However, to our knowledge, this is the first time that a study focuses on the importance of CCL2/CCR2 chemokine signaling regulating the glycolytic pathway in breast ductal cancer progression.

Some interesting results we observed was that upon CCL2 stimulation there were no significant differences in lactate secretion when compared to serum free but CCL2 increased intracellular lactate concentrations significantly. A possible explanation for the lactate differences could be due to the fact that lactate is released from the cells by the monocarboxylate transporter MCT4 in glycolytic tumor cells and it can be taken up by the cells by the MCT1 transporter [161]. It is possible that there is an influx of lactate into the cells. The importance of intracellular lactate is that the oxidative tumor cells can convert the lactate back to pyruvate mediated by the lactate dehydrogenase enzyme and pyruvate can go back to the mitochondria to feed the TCA cycle through Acetyl CoA enzyme, or can be converted to alanine through a transamination reaction.

Chapter IV. Activation of the c-MET receptor by CCL2/CCR2 chemokine signaling is important for breast cell migration, proliferation, survival, growth, and glycolysis.

Author Contributions: Wei Fang, Ph.D. Performed the experiments and results of figures 30A-C (CO-IP) and PLA assays, generation of MET-KO cell lines, and glycolytic activity assays. Nikki Cheng, Ph.D. Performed the experiments and results of figure 40C. Western blot for glycolytic enzymes in DCIS.com MET KO cell lines.

Abstract

To further understand the potential mechanisms by which CCL2/CCR2 chemokine signaling manages DCIS progression with other oncogenic factors, we identified by reverse phase protein array analysis (RPPA) that in MCF10CA1d WT cells CCL2 induction enhanced c-MET phosphorylation compared to CCR2 knockout (KO) breast cancer cells.

The RPPA results were validated by immunoblot and confirmed that CCL2 induction in DCIS.com breast cancer cells enhanced c-MET phosphorylation in a time and CCR2 dependent manner. This activation was specific at the tyrosine site Y1349, located at the intracellular multifunctional docking site which is the binding site for adaptor proteins and that is important for intracellular signaling. The data suggests that the induction of CCL2 and expression of the CCR2 chemokine receptor correspond to enhanced c-MET activation with potential important roles in signal transduction.

To identify the biological role of c-MET inhibition mediated by CCL2, in biological processes crucial for DCIS progression, we tested three basal like triple negative breast cancer cell lines. Inhibition of c-MET resulted in a significant decrease in collective cell migration, proliferation, survival, and growth across the breast cancer cells. However, MET inhibition resulted in a significant reduction of cell migration induced by CCL2

compared to CCL2 treatment alone across DCIS.com, HCC1937 and MDA-MB-231 breast carcinoma cells. CCL2 treatment enhanced PCNA expression as previously described [34]. Inhibiting c-MET significantly blocked induced CCL2 cell proliferation in DCIS.com. HCC1937 and MDA_MB-231. CCL2 significantly reduced apoptosis and c-Met inhibition blocked CCL2 induced survival of DCIS.com, HCC1937 and MDA-MB-231.

These data indicate that CCL2 has pro-survival effects on different human breast cancer cell lines by blocking apoptosis and that c-MET inhibition mediated by CCL2 blocked breast cancer cell motility, proliferation, and survival in vitro.

Introduction

The lack of assertive diagnoses capable to predict which DCIS lesions will become invasive still represents a major clinical challenge, and a limitation for guiding treatment. It is essential to identify molecular mechanisms that are associated with DCIS progression to identify prognostic markers and potential therapeutic targets. A factor that adds a layer of complexity into guiding treatment is the presence of molecular subtypes. By gene expression analysis five distinct groups of breast cancer types have been identified including, Luminal A/B which express estrogen receptor (ER), progesterone receptor (PR), and or Her2 which are more responsive to endocrine therapy. Another group include Her2 enriched, and the most common and aggressive, the basal like breast cancer subtype also known as triple negative which lacks ER, PR, and Her2 [18] is usually treated with chemotherapy.

Therefore, understanding the molecular mechanisms by which ductal carcinoma in situ lesions from triple negative subtype progresses to invasive disease is essential to identify molecular markers that can predict the malignant nature of the disease. This would help us get closer to detect molecular targets that can be used as alternative tailored therapies for DCIS patients and help them avoid unnecessary and drastic treatment regimes.

We recently identified by RPPA analysis that the CCL2/CCR2 chemokine signaling modulates the activation of the c-MET tyrosine kinase receptor at the multifunctional docking site Y1349 (data not shown). After validation by western blot we confirmed this activation and by PLA and CO-IP, we identified that CCL2/CCR2 modulate c-MET activation through potential Src dependent mechanisms. The c-MET receptor tyrosine kinase is a proto oncogene that regulates mammary gland development [162].

Previous studies have demonstrated that through canonical HGF binding, c-MET regulates mammary gland ductal morphogenesis [163, 164]. Protein and gene expression profiling have identified the c-MET receptor as an emergent biomarker for basal like breast cancers [165, 166] which could make it a promising therapeutic target. However, the role of c-MET activation in the progression of breast ductal carcinoma to invasive disease has not yet been identified.

Inhibiting c-MET activity induced by CCL2 in vitro resulted in blocked cell migration, proliferation, survival, and growth associated with decreased glycolysis in three breast cancer cell lines of basal like subtype. The effects of c-MET inhibition were

validated by ablating MET gene expression by CRISP/R Cas9. The generated cells displayed similar results to the pharmacological inhibition indicating that blocking c-MET activity mediated by CCL2/CCR2 is relevant to halt biological processes related to DCIS progression.

Materials and Methods

Cell culture

DCIS.com cells which originated from Dr. Fred Miller's laboratory [117] were provided by Dr. Fariba Behbod (University of Kansas Medical Center). MDA-MB-231 were obtained from the American Tissue Culture Collection. These cells were cultured and maintained in DMEM containing 10% FBS, 2mmol/L L-glutamine, and 1% penicillin-streptomycin. HCC1937 cells were provided by Dr. Roy Jensen (University of Kansas Medical Center). The cells were cultured in RPMI containing 10% FBS, 2mmol/L L-glutamine, and 1% penicillin-streptomycin. Cell lines were cultured for no longer than 6 months and analyzed for mycoplasm after thawing using the MycoAlert™ Mycoplasm Detection Kit (Lonza, cat no. LT07-703).

Recombinant Proteins/ inhibitors

Recombinant human Hepatocyte Growth Factor (HGF) was obtained from PeproTech, Inc (cat# 100-39H). Recombinant human CCL2 was purchased from PeproTech, Inc (cat# 300-04. For in vitro experiments, the MET inhibitor Merestinib (LY2801653) was kindly provided by E. Lilly and company.

Wound Closure

Wound closure Assays were conducted as follows: human breast carcinoma cells (60,000 cells/well) were seeded in 24 well plates. Upon confluency, the cells were serum starved for 24h and then stimulated with HGF (100ng/ml) as a positive control for c-MET activity ± Merestinib (203 nM) or CCL2 (100ng/ml) ± Merestinib for 24h. A vertical wound was made to the cell monolayer in each well with a sterile pipette tip. Four phase - contrast images per well were taken of each sample at 0 and 24h at 10x magnification using the EVOS imaging system. Wound closure was assessed by five measurements of the wound per image using the NIH ImageJ software analysis as previously described [46].

Proliferation Determination

Cells from the wound closure assay were washed with PBS and fixed with 10% neutral formalin buffer. Fixed cells were washed with PBS and permeabilized with ice-cold methanol for 10 min at -20°C. The cells were washed and blocked with 3% FBS in PBS for at least one hour at room temperature. Cells were immunostained for PCNA from BioLegend (Cat #3 07902) at a dilution of [1:500] overnight at 4°C in blocking buffer. Donkey anti-mouse Alexa Fluor 568 (Cat # A10037) at [1:500] dilution was used to visualize the protein. Samples were counterstained with DAPI at 1:5000 in 50% glycerol/PBS. Four images were captured at 10x magnification using a FL- Auto EVOS microscope.

Cleaved Caspase- 3 Assay

Cells were seeded in 24 well plates at a density of 50,000 cells/well. Apoptosis was induced by serum starvation for a period of 48 h as previously described [167] in the presence or absence of the treatments mentioned above. Cells were washed with PBS and then fixed with 10% neutral formalin buffer. Fixed cells were washed with PBS and permeabilized with ice-cold methanol for 10 min at -20°C. The cells were washed and blocked with 3% FBS in PBS for at least one hour at room temperature. Cells were immunostained for Cleaved Caspase 3 (Asp-175) from Cell Signaling Technologies (Cat # 9661) at a dilution of [1:500] overnight at 4°C in blocking buffer. Donkey anti-rabbit Alexa Fluor 647 (Cat # A-31573) at [1:500] dilution was used to visualize the protein. Samples were counterstained with DAPI at 1:5000 in 50% glycerol/PBS. Four images were captured at 10x magnification using a FL- Auto EVOS microscope.

3D Matrigel: Collagen cell cultures

One million cells were seeded in 10-cm dishes in 10 mL DMEM/10% FBS for 24 hours. Cells were cultured in a Collagen: Matrigel matrix as previously described [168]. Briefly, Rat tail collagen (3.5 mg/ml) Corning, (Cat# 354236) was mixed at a 4:1 ratio with setting solution containing: 1X EBSS, 75 mM NaOH and 290 mM NaHCO3. The rat tail collagen solution was mixed 1:1 with Growth Factor Reduced Matrigel, BD Biosciences (Cat # 354230) in ice. The 96-well plates were coated with 40ul/well of the Collagen: Matrigel mixture for 30 min at 37°C. Breast cancer cells were seeded (2500 cells/well) in 200ul of growth medium: DMEM/10% FBS/ 2.5% Matrigel. For the pharmaceutical inhibition experiments, cells were treated with HGF (100ng/ml) ±

Merestinib (203 nM) or CCL2 (100ng/ml) ± Merestinib (203 nM). For the MET ablation experiments, the cells were treated with HGF (100ng/ml) and CCL2 (100ng/ml). Spheroids were cultured for up to 10 days and the media was replaced every 3 days. Images were captured using the EVOS-FL Auto Imaging System (Invitrogen) at 10x with the Bright Field setting. Four fields per well were captured and the sphere size was quantified using Image J. Growth was compared measured by taking the area of each spheroid and was normalized to the total number of spheroids and compared to untreated control.

Immunofluorescence Staining of 3D cell cultures

At day 10, the 3D cell culture spheroids were fixed with 10% neutral buffered formalin at 4°C overnight. The Matrigel: Collagen plug that contains the samples were carefully removed from each well and triplicate samples were pooled into a 4% agarose onto a glass slide on ice. Samples were placed in embedding cassettes and dehydrated in 70, 90, 100% ethanols and Isopropanol for 1 h each at room temperature. Samples were transferred to isopropanol: paraffin 50:50 for 2h at 60°C and embedded in paraffin blocks. Samples were sectioned at 5µm and de-waxed for detection of proteins by immunofluorescence. As antigen retrieval was performed by heating antibody specific solution for 5 min at low pressure in a pressure cooker. Slides were permeabilized in 10% Methanol in PBS for 20 min. Sections were blocked in 3% FBS in PBS and incubated overnight with antibodies [1:500] to PCNA (BioLegend, Cat# 307902), Cleaved Caspase-3 (Cell Signaling Technologies, Cat # 9661). Sections were counterstained with DAPI and mounted in PBS: Glycerol 1:1. Four fields per section were captured using the

EVOS-FL Auto Imaging system at a 10X magnification. Antibody specificity was determined by omission of primary antibody staining. Protein expression was quantified by Image J. Expression of each protein was normalized to DAPI.

Gene ablation by clustered regularly interspaced short palindromic repeats (CRISP/R)

The c-MET guide RNA was obtained from Addgene (Cat # 76061). The guide RNA sequence was: CCGATCGCACACATTTGTCG. MET gRNA (BRDN0001147560) was a gift from John Doench & David Root (Addgene plasmid #76061; http://n2t.net/addgene:76061; RRID: Addgene_76061) which encodes for the IPT domain ranging from 808 to 827. pLenti-MetGFP was a gift from David Rimm (Addgene plasmid # 37560, http://n2t.net/addgene:37560; from the Homo sapients MET proto-onvogene, receptor tyrosine kinase (MET), transcript variant 2, mRNA. NCBI Reference Sequence: NM_000245.2. DCIS.com, HCC1937, and MDA_MB 231 breast cancer cells were transfected with lentivirus containing Cas9 and a Blasticidin selection marker (Addgene, Cat # 57822). Cells were selected with Blasticidin (4ug/ml-10ug/ml) and transduced with the MET gRNA lentivirus or EGFP vector control and selected with puromycin (5ug/ml). Cells were flow sorted for GFP expression and seeded to allow to reach confluency for downstream applications. The efficiency of the KO was confirmed by western blot.

Measurements from the Extracellular acidification rate (ECAR)

Breast cancer cells were evaluated using an extracellular Flux analyzer (XF24; Seahorse Bioscience, Billerica, MA, USA). Cells were seeded in 24-well plates (30,000

cells/well) (using the standard manufacturer .recommended two step seeding procedure. Glycolytic metabolism was assessed with the XF Glycolysis stress test.

To perform the mitochondrial stress test, after plating the cells, the microplate was kept overnight at 37◦C, 5% CO2. incubator, the following day cells were serum starved overnight. Cartridges equipped with Oxygen and pH sensitive probes were hydrated with 1ml of hydrating solution and incubated overnight at 37◦C without CO2. On the day of the assay, cells were treated with CCL2 (100ng/ul) in complete media for 4 hours. One hour prior the assay, the medium was replaced placed in Agilent XF asay medium with 2mM L-glutamine, and the readings are evaluated after injection of the following compounds: 1) glucose (10nM final concentration); 2) oligomycin (1µM final concentration); 3) 2-deoxyglucose (2D-G; 100mM final concentration). Each plate was incubated at 37◦C, without CO2 for 1 hour and then transferred to the microplate stage of the Seahose XF24 flux analyzer with the cartrige of probes. Three separate readings were taken to ensure stability. Data for each experimental condition derived from values obtained from a minimum of six separate wells.

Proximity Ligation Assay (PLA)

The Duolink™proximity ligation assay (PLA®) was used to perform proximity ligation assays according to the manufacturer's protocol. Briefly, DCIS.com breast carcinoma cells were treated with CCL2 for up to 15 minutes and analyzed for CCR2-MET interactions by proximity ligation assay in 96 well plates. Fixed DCIS.com cells were incubated with CCR2 and MET antibodies. Cells were incubated with Duolink® In Situ PLA®Probe Anti-Mouse MINUS affinity purified Donkey anti-mouse IgG (H+L)

Sigma (Cat # DUO92004) and Duolink® In Situ PLA®Probe Anti-Mouse MINUS affinity purified Donkey anti-rabbit IgG (H+L) Sigma (Cat # DUO92002). A pair of oligo labeled secondary antibodies (PLA probes) Duolink®In Situ PLA®Probe anti-rabbit MINUS Sigma (Cat # DUO92005) and Duolink®In Situ PLA®Probe anti-Mouse PLUS Sigma (Cat # DUO92001) were bound to the primary antibodies. If CCR2 and c-MET are in close proximity, a hybridizing connector would join the PLA probes, forming circle DNA template to be amplified by DNA polymerase. The amplicons were then bound to complementary detection oligos conjugated to fluorochromes and detected by fluorescence microscopy. Technical control including untreated, no secondary control and no antibody controls were included. Whole wells were imaged for fluorescence using EVOS FlAuto Imager.

Determination of enzymatic activities

DCIS.com MET gRNA KO and EGFP controls were seeded and serum starved overnight. On the day of the assay, the cells were treated with CCL2 up to 1 hour and compared to serum free. The enzymatic activity of Hexokinase 2 enzyme assay was determined by using the Hexokinase/ Glucokinase assay kit (Cat # E-111). This assay recognizes all the Hexokinase 2 isoforms.

This assay is based on the reduction of tetrazolium salt INT in a NADH-coupled enzymatic reaction which exhibits an absorption at 492 nm. The assay was performed according to manufacturer's instructions and as previously described [159, 169]. Pyruvate Kinase activity was determined with the assay kit (Cat # E-117). Both assays were obtained from Biomedical Research Service Center (Buffalo, NY, USA). The PK

assay measures luciferase activity in the presence of luciferin that is derived from the PK reaction driven ATP. The PK assay was performed according to manufacturer's description and as previously described [170].

Glucose consumption and lactate secretion

60,000 DCIS.COM breast cancer cells were plated in 24 well plates and serum starved overnight. Cells were treated with DMSO, Merestinib, HGF±Merestinib, and CCL2±Merestinib for 24 hours and another set was plated for assessment at 48 hours treatments. Extracellular glucose consumption was determined by using the Glucose-Glow™ Assay (Cat # J6021 from Promega). This assay includes glucose dehydrogenase which uses glucose and NAD+ to produce NADH. When NADH is present the pro-luciferin reductase substrate is converted to luciferin by reductase. This product is then used by the recombinant luciferase from Ultra-Glo™ to produce light. This assay was performed according to manufacturer's instructions and as previously described [171].

For lactate detection the Lactate- Glo™ Assay (Cat # J5021) was used. This assay includes lactate dehydrogenase which uses lactate and NAD+ to produce NADH and pyruvate. In the presence of NADH, pro-luciferin reductase substrate is converted by Reductase to luciferin. This luciferase reaction produces light in the presence of Ultra-Glo™ that is detected by a luminometer. This assay is specific to L-Lactate which is the major stereoisomer found in mammalian cells. The assay was performed according to manufacturer's instructions and as previously described [172].

Immunoblot

Breast ductal mammary carcinoma cells were plated in 6-well plates (500,000 cells/well) in DMEM 10%FBS. Cells were serum deprived for 24 hours and incubated with serum free media with or without recombinant CCL2 (100ng/ml) ± Merestinib (203 nM), HGF (100ng/ml) ± Merestinib (203 nM) for 24 hours. Cells were lysed in RIPA buffer containing: 1X PBS, 1% Nonidet P-40, 0.5% sodium deoxycholate, 0.1% SDS with protease and phosphatase inhibitors (Sigma-Aldrich, Cat # P8340). Lysates were sonicated and 20ug of protein were resolved on 8 or 10% SDS-PAGE gels and transferred to nitrocellulose membranes. The membranes were blocked in PBS/0.05% Tween-20 /3% milk and probed with primary antibodies [1:1000] to: phospho c-Met Y1234-1235 (Cell Signaling Technology®, Cat # 3077), phospho c-Met Y1349 (Cell Signaling Technology®, Cat # 3121), Met (Cell Signaling Technology®, Cat # 4560), Hexokinase II (Cell Signaling Technology®, Cat # 2867), CCR2 (Cell Signaling Technology®, Cat # 12199), were detected with rabbit secondary antibodies conjugated to horseradish peroxidase (HRP). β-actin Sigma (Cat #A5441) was detected with ani-rabbit-hrp. Membranes were developed with West Pico ECL chemiluminescent substrate and imaged using a Biospectrum Imaging System.

Immunohistochemistry by DAB staining

MIND injection tissues were fixed in 10% neutral formalin buffer and embedded in wax as previously described [121]. Sections were cut 5 microns thick, dewaxed and heated in 10mM sodium Citrate buffer pH 6.0 for 5 minutes. Followed washing the slides, a endogenous peroxidase blocking step was performed with 60% cold methanol/3%

H_20_2 in PBS, blocked for at least one hour in 3% FBS in PBS for rabbit antibodies, and incubated with primary antibodies [1:100] overnight at 4ºC for; phospho c-Met Y1234-1235 (Cell Signaling Technology®, Cat # 3077), phospho c-Met Y1349 (Cell Signaling Technology®, Cat # 3121), and Met (Cell Signaling Technology®, Cat # 4560). Slides were incubated with streptavidin peroxidase (Vector Laboratories Cat # PK-6200) for 30 minutes. Slides were developed with 3,3'-diaminobenzidine (DAB) substrate Kit (Vector Laboratories Cat # SK-4100) and counterstained with Mayer's hematoxylin and mounted with cytoseal.

Biospecimens

Patient samples were collected under approval of the Institutional Review Board (IRB) at KUMC. Tissue microarrays (TMAs) consisted of de-identified patient tissue were provided by the Biospecimen Core Repository Facility (BCRF) from the University of Kansas Center (KUMC). TMAs were arrayed in duplicate. Core sections were 1.5 mm in diameter and 5 microns thickness. DCIS tissue was graded using the Van Nuys Prognostic Index (VNPI). Samples were collected between 2007 and 2012, with 3 to 5 year follow up. Tissue microarray pathology information included age, stage, grade, tumor size, expression of KI67, ER, PR and Her2. Additional information included treatment, recurrence, and survival. Clinical pathological features for all breast samples is summarized (Table 1). Samples sizes include DCIS (n= 81), IDC (n= 82), and normal matching to IDC (n=87). The mean age of patients was 56 years.

Image Quantification

Images were captured at 10X magnification using the FL-Auto EVOS system (Invitrogen) including 5-10 random fields per section. DAB staining was quantified as previously described [47]. In summary, the images were uploaded in Adobe Photoshop, positive DAB staining was selected by using the Magic wand tool, copied, and saved into a new layer which makes a separate file. These images were opened in Image J (NIH), converted to gray scale and adjusted with threshold adjustment to remove nonspecific background. Staining was quantified by using the particle analysis feature. Positive DAB staining values were normalized to total area values which were expressed as arbitrary units. Normalized arbitrary units were subjected to statistical analysis with GraphPad Prism. The same principle was used to quantify the fluorescent staining. The staining of interest was selected and normalized to DAPI.

Statistical Analysis

Experiments involving cell cultures were repeated a minimum of three times. Data is expressed as mean ± standard error of the mean (SEM). Statistical analysis was performed by using GraphPad software. Two-tailed Student *t* test was used to compared two groups. One-way ANOVA with Bonferroni *post hoc* multiple comparisons test was used for normal distributions. For non- Gaussian distributions the Kruskall-Wallis Test with Dunn's *post hoc* comparisons test was used. Statistical significance was determined by $P < 0.05$. $P<0.05$ *, $P<0.01$ **, $P<0.001$ ***, n.s= not significant or $P>0.05$.

Results

CCL2 enhances c-MET phosphorylation through potential interactions with CCR2 and SRC

To further understand the potential mechanisms by which CCL2/CCR2 chemokine signaling manages DCIS progression with other oncogenic factors, we identified by reverse phase protein array analysis (RPPA) that in MCF10CA1d WT cells CCL2 induction enhanced c-MET phosphorylation compared to CCR2 knockout (KO) breast cancer cells (data not shown).

The RPPA results were validated by immunoblot and confirmed that CCL2 induction in DCIS.com breast cancer cells enhanced c-MET phosphorylation in a time dependent manner (Figure 29A). This activation was specific at the tyrosine site Y1349, located at the intracellular multifunctional docking site which is the binding site for adaptor proteins and that is important for intracellular signaling [173].

To evaluate the role of CCR2 in c-MET activation, DCIS.com CCR2 KO and WT were treated with and without CCL2. Immunoblot showed that in DCIS.com WT breast cancer cells treated with CCL2 enhanced c-MET activation compared to SF and abrogation of c-MET phosphorylation in CCR2-KO even after CCL2 stimulation (Figure 29B). The data suggests that the induction of CCL2 and expression of the CCR2 chemokine receptor correspond to enhanced c-MET activation with potential important roles in signal transduction.

To evaluate the protein expression of c-MET and phospho c-MET mediated by CCR2 expression in vivo, we analyzed by immunohistochemistry tissues from the MIND model. Tissues from the parental DCIS.com cells that have high CCR2 levels, displayed enhanced expression of total c-MET compared to parental SUM225 which have lower CCR2 (Figure 29C). The MIND lesions that resulted from SUM225 CCR2 overexpressed injected cells which resulted in lesions that were associated with invasiveness, showed increased expression of phospho and total c-MET compared to the pHAGE control (Figure 29D). In addition, the DCIS.com CCR2 KO MIND model lesions which resulted in fewer number of invasive lesions, displayed a decreased expression of phospho and total c-MET expression compared to WT control (Figure 29E).

Taken together, we have identified an important association between c-MET protein expression and activation that corresponds to increased CCR2 levels. These data indicate that c-MET expression and signaling might be influenced in part by CCL2/CCR2 dependent mechanisms which suggest an important role for CCR2 modulating c-MET activity with an important association in DCIS progression.

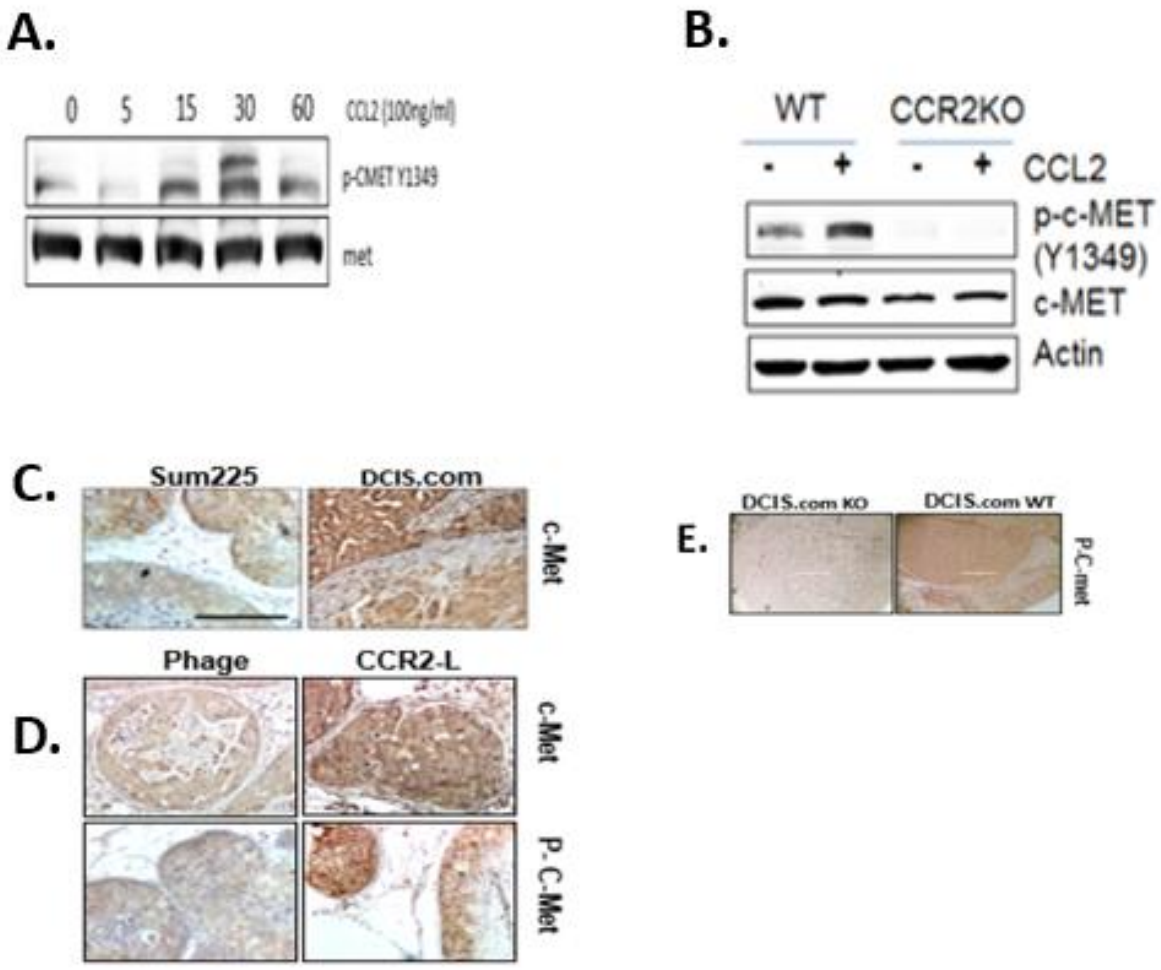

Figure 29. CCL2 and CCR2 modulate c-MET protein expression in cells and MIND model tissue. Parental DCIS.com cells treated with 100ng/ml of CCL2 blotted for phospho or total c-Met expression in a time course of 5, 15, 30 and 60 minutes **(A)**. DCIS.com WT or CCR2 knockout (KO) were treated with 100ng/ml CCL2 and immunoblotted for phospho or total c-Met expression for 1 hour **(B)**. Immunostaining of c-Met in parental SUM225 and DCIS.com MIND model lesions **(C).** Immunostaining of phospho c-Met of DCIS lesions formed from SUM225 control phage cells or CCR2 overexpressing cells (CCR2-L) **(D).** Immunostaining of Phospho c-Met of DCIS lesions formed from DCIS.com CCR2 knockout (KO) or WT control**.** Mean ±SEM **(E).** n=8 mice.

To further examine possible protein protein interactions between CCR2 and c-MET, we performed a Proximity Ligation Assay (PLA) using Duolink ™ PLA probes and antibodies. DCIS.com breast cancer cells were treated with CCL2 for 5 and 15 minutes and incubated with c-MET and CCR2 antibodies. Unstimulated and no antibody treatments were used as negative controls. To control for antibody specificity, MET only and CCR2 only antibody was used respectively. A close association among these two proteins was confirmed with by green fluorescence spots observed by the EVOS FIAuto Imager (Figure 30A). These results suggest that CCR2 and c-MET might have a close interaction.

Previous studies in basal-like breast cancer cells demonstrated that CCL2 enhanced the activity of Src and PKC associated with proliferation and cell-cycle progression [174]. To investigate possible signaling mechanism that could facilitate potential protein interactions induced by CCL2 between CCR2 and c-MET, whole cell protein lysates of DCIS.com cells stimulated with CCL2 for up to 30 minutes were co-immunoprecipitated (Co-IP) with anti c-MET and anti Src antibodies. The IP for c-MET showed a positive signal for CCR2 and Src expression as early as 5 minutes, and even higher at 15 minutes after CCL2 induction (Figure 30B). A reverse IP where Src was pulled down confirmed that CCR2 and c-MET expression were highly up regulated at 5 min. As an assay control, total lysates (input control) were immunoblotted for expression of indicated proteins. These results indicate that there might be a transient but important protein-protein interaction between CCR2 and c-MET through Src dependent mechanisms.

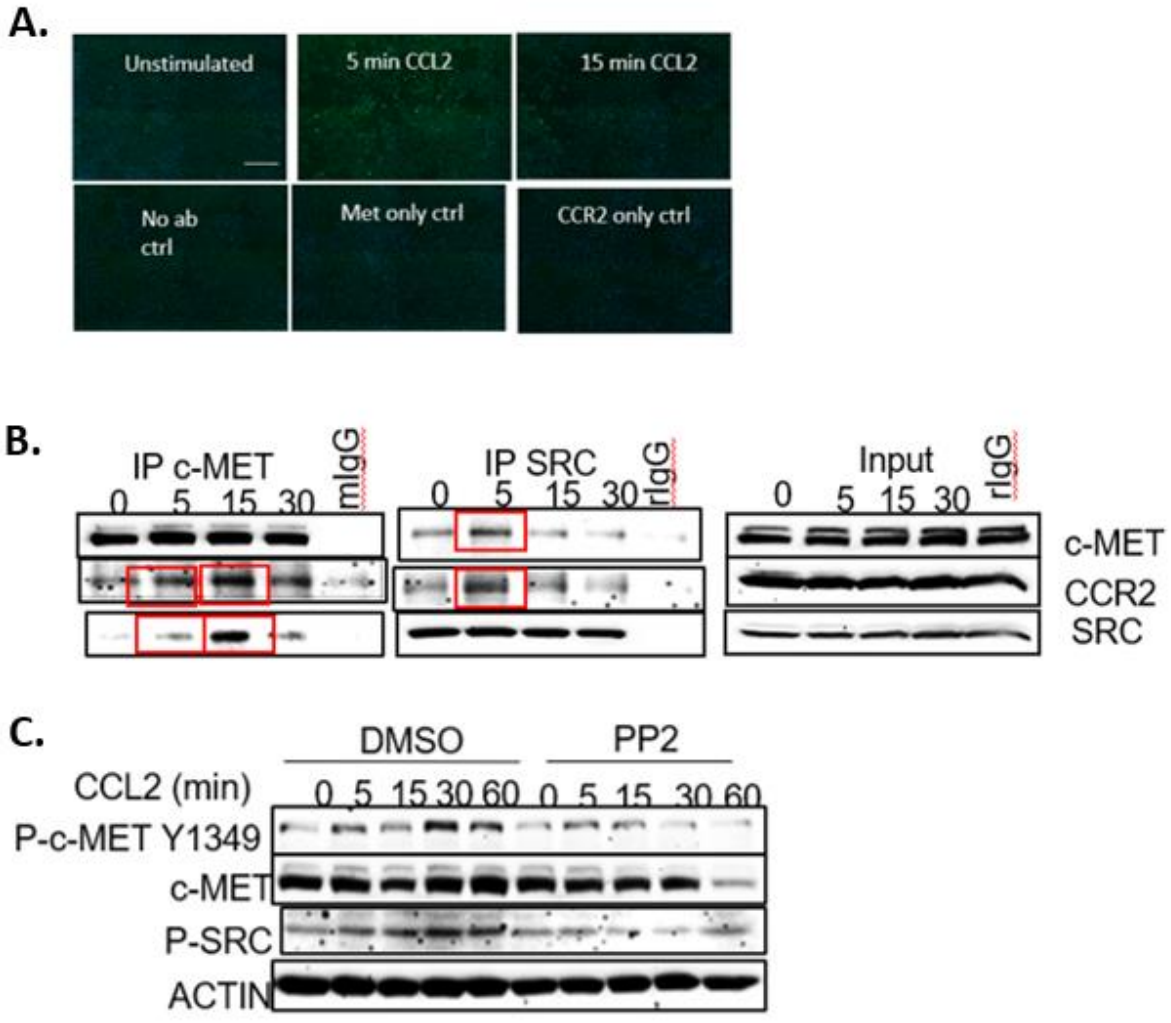

Figure 30. CCL2 enhances c-MET phosphorylation through potential interactions with CCR2 and Src. PLA: DCIS.com cells were treated with CCL2 for up to 15 minutes and analyzed for CCR2-MET interactions by proximity ligation assay in 96 well plates. Fixed DCIS.com cells were incubated with CCR2 and MET antibodies. A pair of oligo labeled secondary antibodies (PLA probes) were bound to the primary antibodies. If CCR2 and c-MET are in close proximity, a hybridizing connector would join the PLA probes, forming circle DNA template to be amplified by DNA polymerase. The amplicons were then bound to complementary detection oligos conjugated to fluorochromes and detected by fluorescence microscopy. Whole wells were imaged for fluorescence using EVOS Fl Auto Imager. Cropped images are shown for clarity. Scale bar=200 microns **(A)**. CO-IP: DCIS.com cells were treated with CCL2 for up to 30 minutes, immunoprecipitated for c-MET or SRC and immunoblotted for expression of indicated proteins. Total lysates (input control) were immunoblotted for expression of indicated proteins **(B).** DCIS.com cells were treated with/without 100 ng/ml CCL2 or 10 mM PP2 (SRC inhibitor) for up to 60 minutes and immunoblotted for expression of the indicated proteins. RIgG =rabbit IgG **(C)**. Experiments were performed in triplicate, repeated three times.

To determine the importance of CCR2 and c-MET protein interaction induced by CCL2 and mediated by Src, DCIS.com breast cancer cells were treated with or without 100ng/ml CCL2 or 10mM PP2, a small molecule inhibitor that targets Src kinase [175] for up to 60 minutes and immunoblotted for c-MET Y1349, c-MET, P-Src and Actin. PP2 inhibition was confirmed by immunoblot which showed a decreased in P-Src expression compared to DMSO. CCL2 induced phosphorylation of c-MET Y1349 overtime but the expression was downregulated in the presence of PP2 in all the time points compared to DMSO treatment. PP2 treatment even in the presence of CCL2 decreased c-MET expression over time with a notable lack of expression at 60 minutes (Figure 30C).

Previous studies have demonstrated that the Src tyrosine kinase protein binds directly to the carboxy terminal docking site of c-MET (Y1349) [176,177]. However, the expression of P-Src is not completely downregulated by PP2 in the presence of CCL2, these results are consistent with previous findings in which breast cancer cells treated with CCL2 and PP2 at [10 and 20μmol/L] showed increased P-Src expression compared to cells treated with PP2 alone [174].

Even though studies that explore the interaction between c-MET and CCR2 and ongoing, these results confirm that CCL2 modulates p-Src activity which could be important for mediating c-MET phosphorylation at Y1349. To our knowledge this is the first time that an alternative signaling mechanism for modulating c-MET phosphorylation at the Y1349 site induced by CCL2 independently of canonical HGF is reported. CCL2 phosphorylated c-MET through Src dependent mechanisms and corresponds to high levels of CCR2 expression. Taken together, this data suggests that c-MET

phosphorylation can be modulated through CCL2/CCR2 dependent and independent mechanisms and mediated through Src.

Targeting c-MET by pharmacological inhibition blocks CCL2 induced collective cell migration, proliferation, survival, and growth in human mammary carcinoma cells.

We next sought to determine the relevance of c-MET activity induced by CCL2 in biological processes that are crucial for DCIS progression. The c-MET receptor was targeted with a pharmacological inhibitor; Merestinib which is a type II ATP competitive inhibitor meaning that it binds to the intracellular kinase portion of the receptor in the inactive form [178, 179]. Merestinib is an FDA approved drug, that has been used to treat non-small cell lung cancer, and acute myeloid leukemia [180, 181]. However, to our knowledge the efficacy of Merestinib to manage breast ductal carcinoma in situ progression has not yet been explored.

Therefore, we used three different human breast cancer cells that by flow cytometry display high levels of CCR2 and c-MET and are highly associated with invasiveness including DCIS.com, HCC1937, and MDA_MB_231. DCIS.com which was originated from a xenotransplantation is a basal like subtype breast cancer cell line that is a model of DCIS [117]. The HCC1937 is a cell line isolated from a primary tumor after surgical resection of a ductal carcinoma of TNB stage IIB, and of triple negative, basal A subtype [182, 183]. MDA_MB_231 is a breast cancer cell line isolated from a pleural effusion of an adenocarcinoma of metastatic origin and of triple negative basal B subtype [184-186].

Cultured DCIS.com, HCC1937 and MDA_MB_231 were treated with HGF (as a positive control for c-MET activity) ± Merestinib or CCL2 ± Merestinib and evaluated for changes in cellular migration, proliferation, survival, and growth. The effect of c-MET inhibition induced by CCL2 on the motility of mammary carcinoma cells was assessed by wound closure assay. CCL2 treatment significantly enhanced migration on all three cell lines over a period of 24 h, consistent with the effects that CCL2 has on migration previously published [46].

However, MET inhibition resulted in a significant reduction of cell migration induced by CCL2 compared to CCL2 treatment alone across DCIS.com breast carcinoma cells (Figure 31A), HCC1937 (Figure 32A), and MDA-MB-231 (Figure 33A). CCL2 treatment enhanced PCNA expression as previously described [174]. Inhibiting c-MET significantly blocked induced CCL2 cell proliferation in DCIS.com. (Figure 31B) HCC1937 (Figure 32B), and MDA_MB-231 (Figure 33B). CCL2 significantly reduced apoptosis and c-Met inhibition blocked CCL2 induced survival of DCIS.com (Figure 31C), HCC1937 (Figure 32C), and MDA-MB-231 (Figure 33C). These data indicate that CCL2 has pro-survival effects on different human breast cancer cell lines by blocking apoptosis, and that c-MET inhibition mediated by CCL2 blocked breast cancer cell motility, proliferation, and survival in vitro.

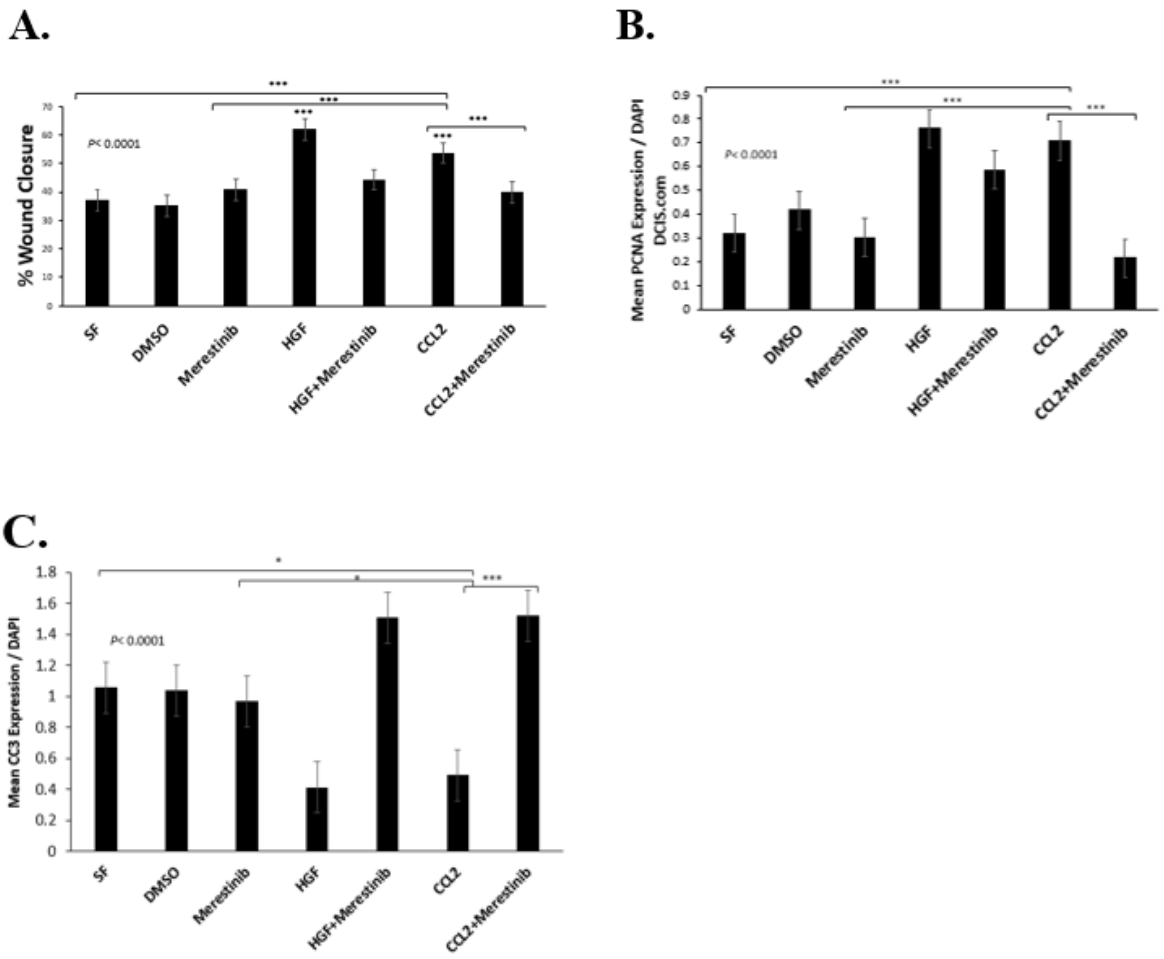

Figure 31. Targeting c-MET by pharmacological inhibition blocks CCL2 induced collective cell migration, proliferation, and survival in DCIS.com human mammary carcinoma cells. DCIS.com parental breast cancer cells were seeded and upon monolayer confluence scratched and treated with 100ng/ml of HGF as a positive control for c-Met, HGF±203nM Merestinib, a c-Met inhibitor, or 100ng/ml of CCL2±203nM Merestinib for 24 hours to assess collective cell migration. Wound closure was analyzed by measuring the distance of the scratch at t=0 and t=24 by Image J software and plotted as % wound closure **(A).** Cells were seeded, and serum deprived for 48 hours to induce apoptosis and treated as above for 24 hours. Cells were analyzed for Cleaved-Caspase 3 expression by immunofluorescence **(B)**. To assess for proliferation, cells were serum starved overnight, treated as above, and evaluated for PCNA expression by immunofluorescence **(C).** Each experimental group was plated in triplicate and experiments were performed three times. Four image fields per slide were taken with an EVOS-FL system. Statistical analysis was performed using a ONE-WAY ANOVA with Bonferroni post-hoc comparison. Statistical significance was determined by *p<0.05, **p<0.01, ***p< 0.0001., n.s. not significant or p>0.05. Mean ± SEM values are shown. Scale bar = 400 microns.

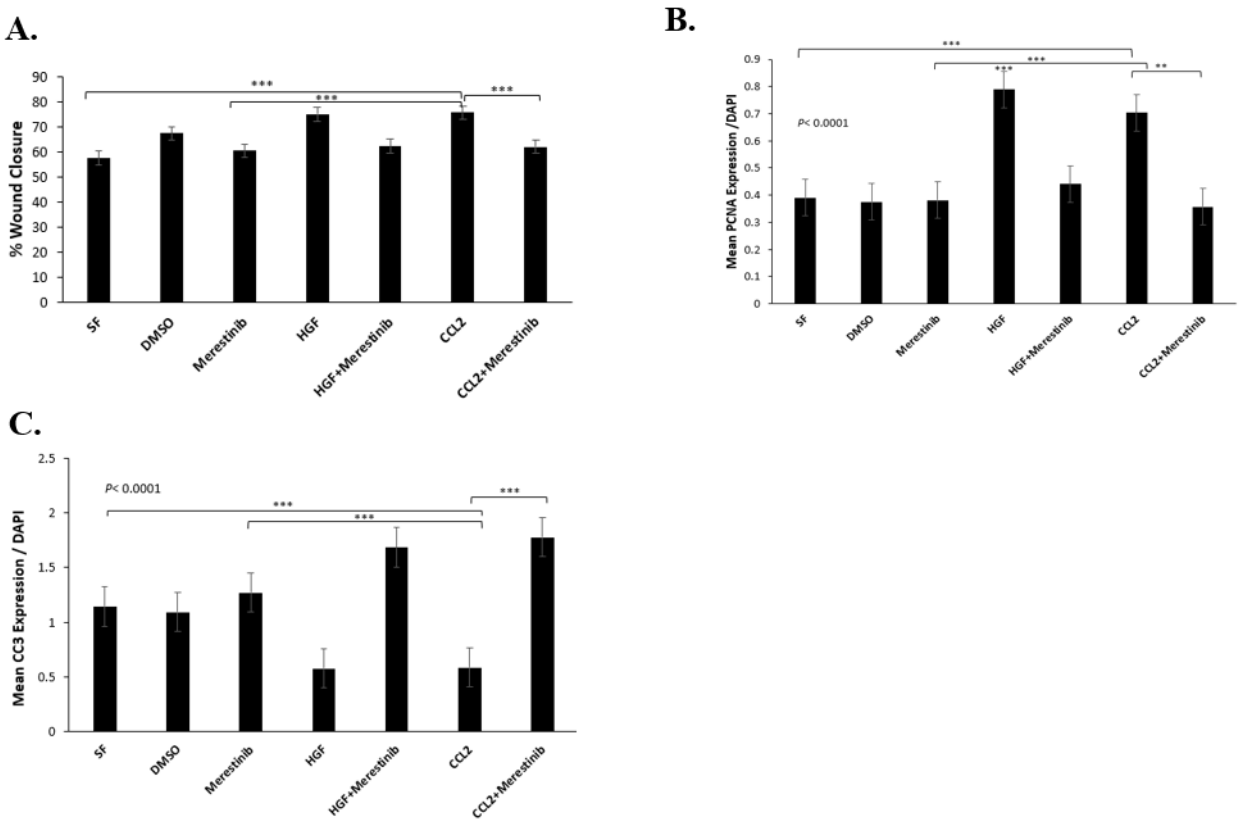

Figure 32. Targeting c-MET by pharmacological inhibition blocks CCL2 induced collective cell migration, proliferation, and survival in HCC1937 human mammary carcinoma cells. HCC1937 parental breast cancer cells were seeded and upon monolayer confluence scratched and treated with 100ng/ml of HGF as a positive control for c-Met, HGF±203nM Merestinib, a c-Met inhibitor, or 100ng/ml of CCL2±203nM Merestinib for 24 hours to assess collective cell migration. Wound closure was analyzed by measuring the distance of the scratch at t=0 and t=24 by Image J software and plotted as % wound closure **(A).** Cells were seeded, and serum deprived for 48 hours to induce apoptosis and treated as above for 24 hours. Cells were analyzed for Cleaved-Caspase 3 expression by immunofluorescence **(B)**. To assess for proliferation, cells were serum starved overnight, treated as above, and evaluated for PCNA expression by immunofluorescence **(C).** Each experimental group was plated in triplicate and experiments were performed three times. Four image fields per slide were taken with an EVOS-FL system. Statistical analysis was performed using a ONE-WAY ANOVA with Bonferroni post-hoc comparison. Statistical significance was determined by *p<0.05, **p<0.01, ***p< 0.0001., n.s. not significant or p>0.05. Mean ± SEM values are shown. Scale bar = 400 microns.

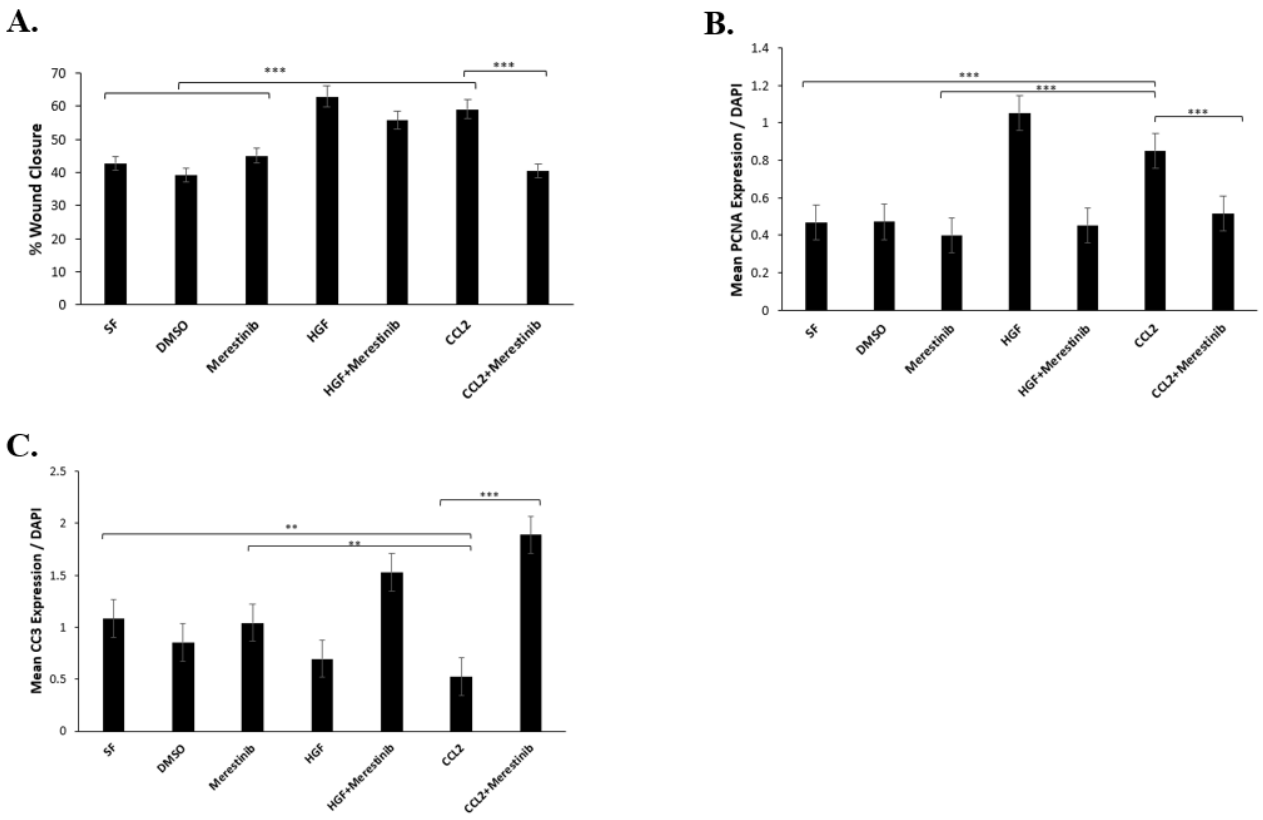

Figure 33. Targeting c-MET by pharmacological inhibition blocks CCL2 induced collective cell migration, proliferation, and survival in MDA_MB_231 human mammary carcinoma cells. MDA_MB_231 parental breast cancer cells were seeded and upon monolayer confluence scratched and treated with 100ng/ml of HGF as a positive control for c-Met, HGF±203nM Merestinib, a c-Met inhibitor, or 100ng/ml of CCL2±203nM Merestinib for 24 hours to assess collective cell migration. Wound closure was analyzed by measuring the distance of the scratch at t=0 and t=24 by Image J software and plotted as % wound closure (A). Cells were seeded, and serum deprived for 48 hours to induce apoptosis and treated as above for 24 hours. Cells were analyzed for Cleaved-Caspase 3 expression by immunofluorescence (B). To assess for proliferation, cells were serum starved overnight, treated as above, and evaluated for PCNA expression by immunofluorescence (C). Each experimental group was plated in triplicate and experiments were performed three times. Four image fields per slide were taken with an EVOS-FL system. Statistical analysis was performed using a ONE-WAY ANOVA with Bonferroni post-hoc comparison. Statistical significance was determined by *p<0.05, **p<0.01, ***p< 0.0001., n.s. not significant or p>0.05. Mean ± SEM values are shown. Scale bar = 400 microns.

To further characterize the molecular mechanisms through which c-Met inhibition regulates CCL2 induced cell growth, we used a 3D Matrigel collagen assay. In this cell culture model, DCIS.com breast cancer cells show abnormal spheres that grow in a period of 10 days [168]. Inhibiting c-Met decreased the growth of CCL2 induced spheroids (Figure 34A). To determine whether differences in spheroid size were related to cell proliferation, we fixed, embedded, and sectioned these spheroids for PCNA analysis by immunofluorescence. Results showed that inhibiting c-Met decreased PCNA expression induced by CCL2 which is associated to decreased spheroid growth (Figure 34B). In summary, these data demonstrated that c-Met inhibition blocks CCL2 induced growth associated with decreased proliferation of DCIS.com mammary carcinoma cells.

Targeting c-MET by gene ablation blocks CCL2 induced collective cell migration, proliferation, survival, and growth in human mammary carcinoma cells.

To further validate the effects of c-MET targeting by pharmacological inhibition with a genetic stable approach, we characterized the significance of *in vitro* c-MET ablation on migration, survival, proliferation, and growth in DCIS progression. The c-MET gene was ablated by CRISP/R Cas9 targeting the extracellular Immunoglobin-Plexin-transcription (IPT) domain in DCIS.com, HCC1937 and MDA_MB_231 breast carcinoma cells (Figure 35A). The knockout gene was compared to EGFP control. Breast cancer cells were treated with HGF, CCL2 and compared to vehicle control.

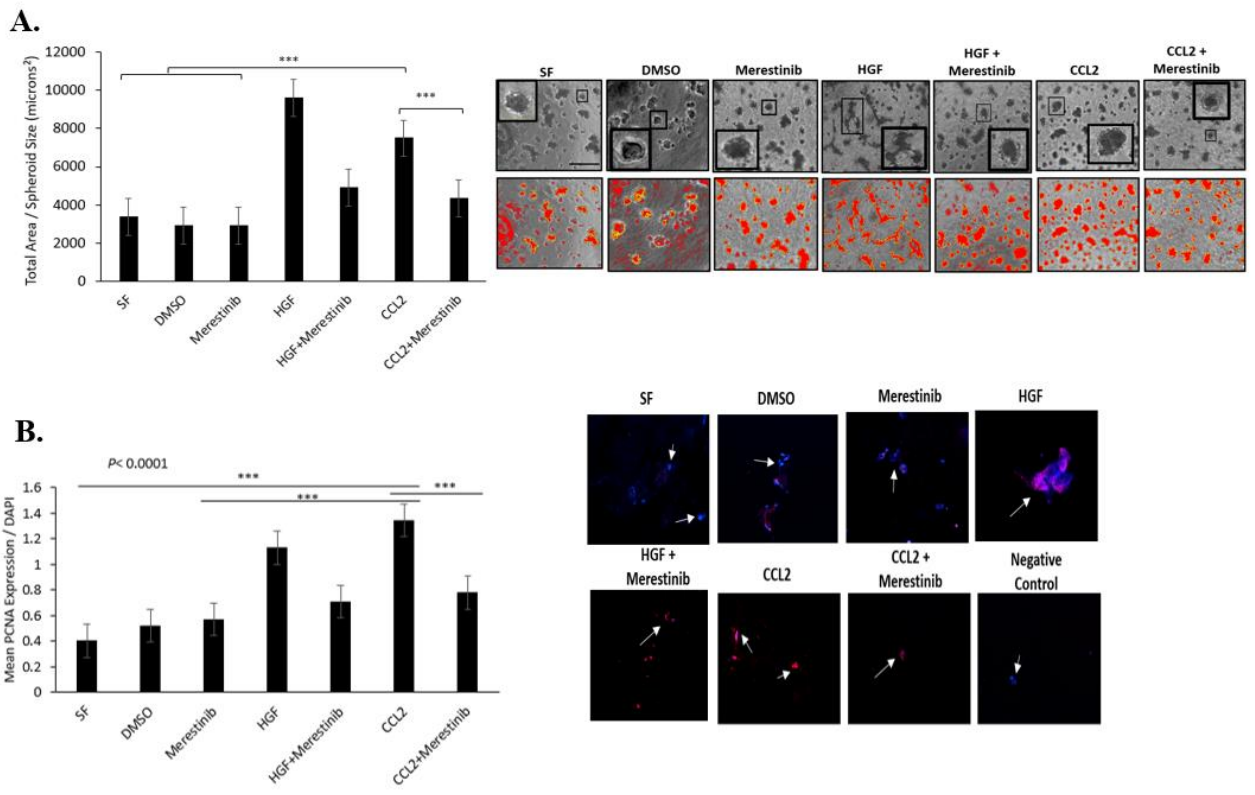

Figure 34. Targeting c-MET by pharmacological inhibition blocks CCL2 induced growth by reducing proliferation in DCIS.com breast carcinoma cells. DCIS.com breast cancer cells were cultured in a Collagen: Matrigel matrix in the presence of the treatments mentioned above. Changes in spheroid size were analyzed for a period of 10 days. Representative images of the spheroids at the end point are shown in the magnified field **(A)**. Spheroid size was calculated using image J and plotted as the total area / spheroid size (microns^3). 3D cell culture sections were immunostained for expression of PCNA and counterstained with DAPI at day 10. White arrows point to positive staining **(B)**. Each experimental group was plated in triplicate and experiments were performed three times. Four image fields per slide were taken with an EVOS-FL system. Statistical analysis was performed using a ONE-WAY ANOVA with Bonferroni post-hoc comparison. Statistical significance was determined by *p<0.05, **p<0.01, ***p< 0.0001., n.s. not significant or p>0.05. Mean ± SEM values are shown. Scale bar = 400 microns.

Consistent with the results obtained from the pharmacological inhibitor, targeting MET by KO in DCIS.com breast cancer cell lines mediated by CCL2 showed a significant decrease in cell migration (Figure 356B), proliferation (Figure 35C), and survival (Figure 35D). To further characterize the effect of c-MET ablation in growth compared to their EGFP controls in DCIS.com. Targeting the c-Met by gene ablation decreased the growth of CCL2 induced spheroids CCL2 (Figure 36A).

The effects of c-MET ablation on HCC1937 breast cancer cells were evaluated. CCL2 treatment enhanced cell migration (Figure 37A), proliferation (Figure 37B), and survival (Figure 37C). These trends are very similar to the ones found in MDA_MB_231 breast cancer cells where targeting c-MET induced by CCL2 blocked migration (Figure 38A), proliferation (Figure 38B), and survival (Figure 38C).

These results are consistent with the results from pharmacological inhibition. Here we have demonstrated by both, pharmacological inhibition, and genetic ablation that targeting c-MET blocks induced CCL2 migration, proliferation, survival, and growth induced by CCL2. These data suggest that c-MET activity induced by CCL2 is very important for modulating biological processes that are crucial for DCIS progression.

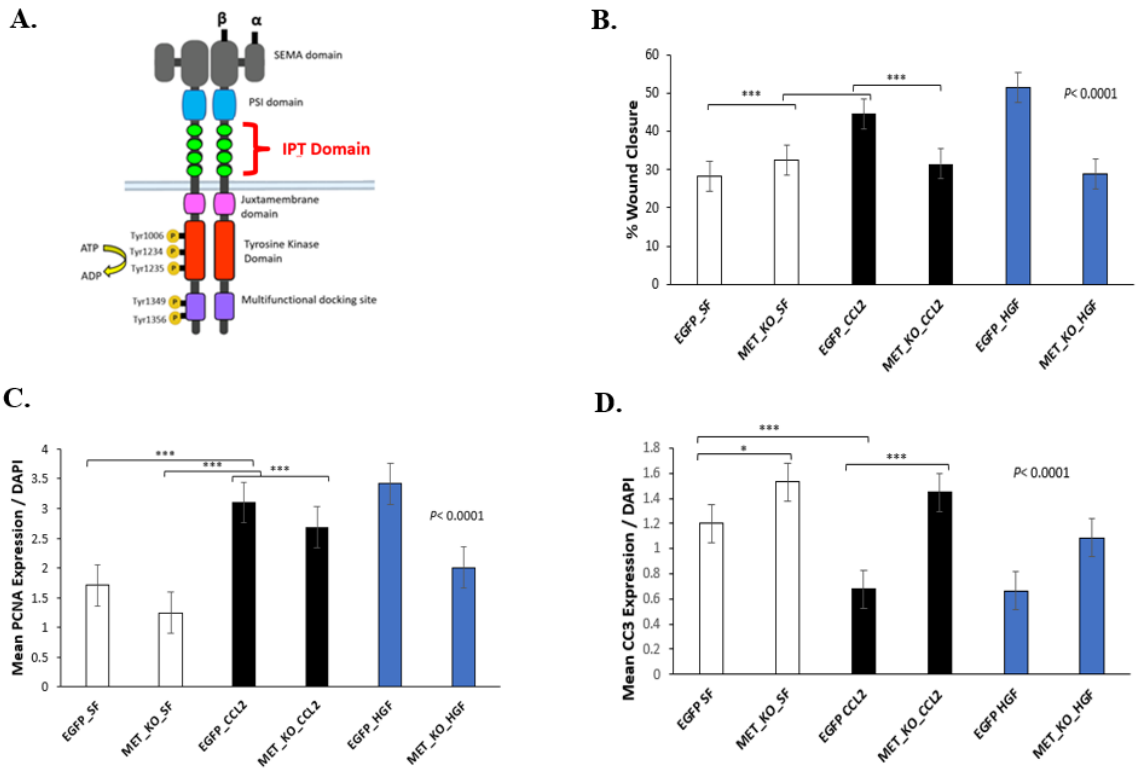

Figure 35. Gene targeting of epithelial c-MET blocks CCL2 induced collective cell migration, proliferation, and survival in DCIS.com human mammary carcinoma cells. The c-MET gene was ablated by CRISP/R Cas9 targeting the extracellular Immunoglobin-Plexin- transcription (IPT) domain (**A**). DCIS.com MET gRNA and EGFP control breast cancer cells were seeded and upon monolayer confluence scratched and treated with 100ng/ml of HGF as a positive control for c-Met or 100ng/ml of CCL2 for 24 hours to assess collective cell migration, wound closure was analyzed by measuring the distance of the scratch at t=0 and t=24 by Image J software. (**B**), Cells were analyzed for proliferation by quantifying the expression of PCNA by immunofluorescence (**C**), Cells were seeded and serum deprived for 48 hours to induce apoptosis and treated with serum free media containing 100ng/ml of HGF as a positive control or 100ng/ml of CCL2 for 24 hours. Cells were analyzed for Cleaved-Caspase 3 expression by immunofluorescence (**D**). Each experimental group was plated in triplicate and experiments were performed three times. Four image fields per slide were taken with an EVOS-FL system. Statistical analysis was performed using a ONE-WAY ANOVA with Bonferroni *post-hoc* comparison. Statistical significance was determined by *p<0.05, **p<0.01, ***p< 0.0001., n.s. not significant or p>0.05. Mean ± values are shown. Scale bar = 400 microns.

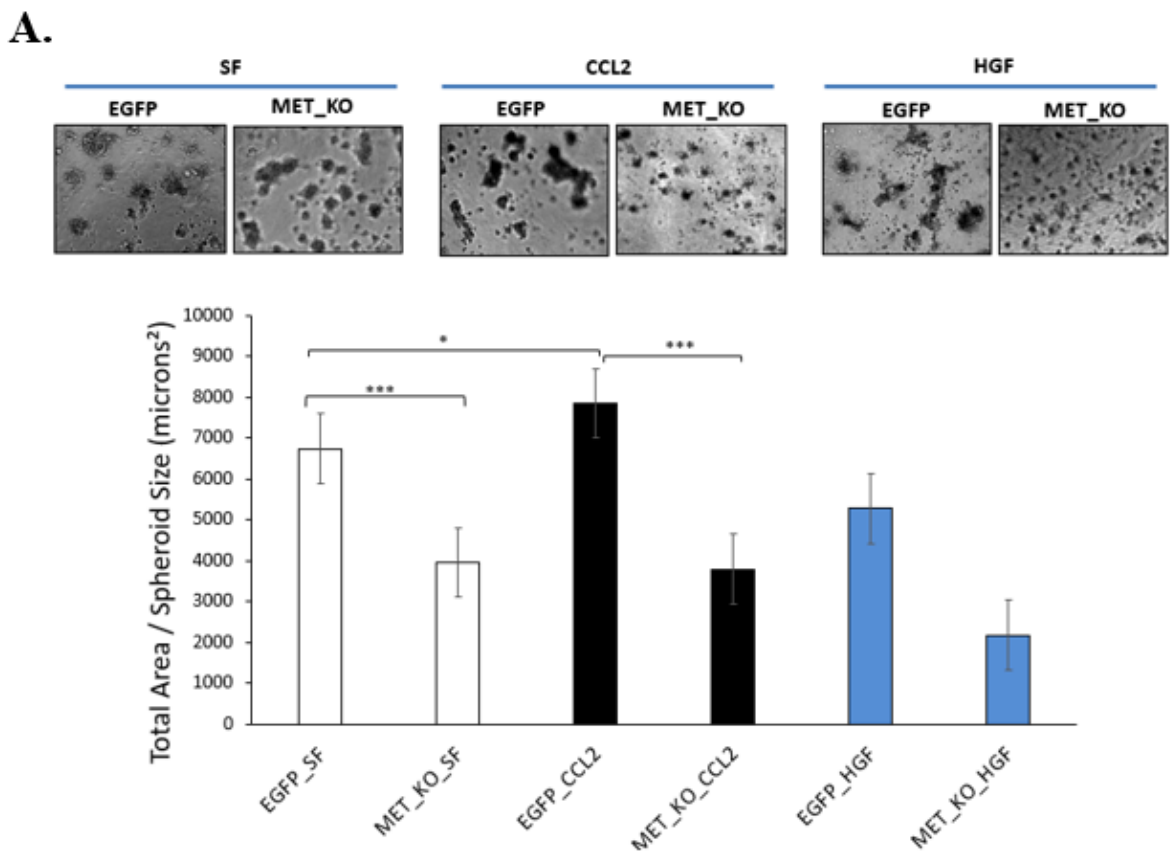

Figure 36. Gene targeting of epithelial c-MET blocks CCL2 induced growth in DCIS.com human mammary carcinoma cells. DCIS.com breast cancer cells were cultured in a Collagen: Matrigel matrix in the presence of the treatments mentioned above. Changes in spheroid size were analyzed for a period of 10 days. Representative images of the spheroids at the end point are shown in the magnified field. Spheroid size was calculated using image J and plotted as the total area / spheroid size (microns^3) **(A)**. Each experimental group was plated in triplicate and experiments were performed three times. Four image fields per slide were taken with an EVOS-FL system. Statistical analysis was performed using a ONE-WAY ANOVA with Bonferroni post-hoc comparison. Statistical significance was determined by *p<0.05, **p<0.01, ***p< 0.0001., n.s. not significant or p>0.05. Mean ± values are shown. Scale bar = 400 microns.

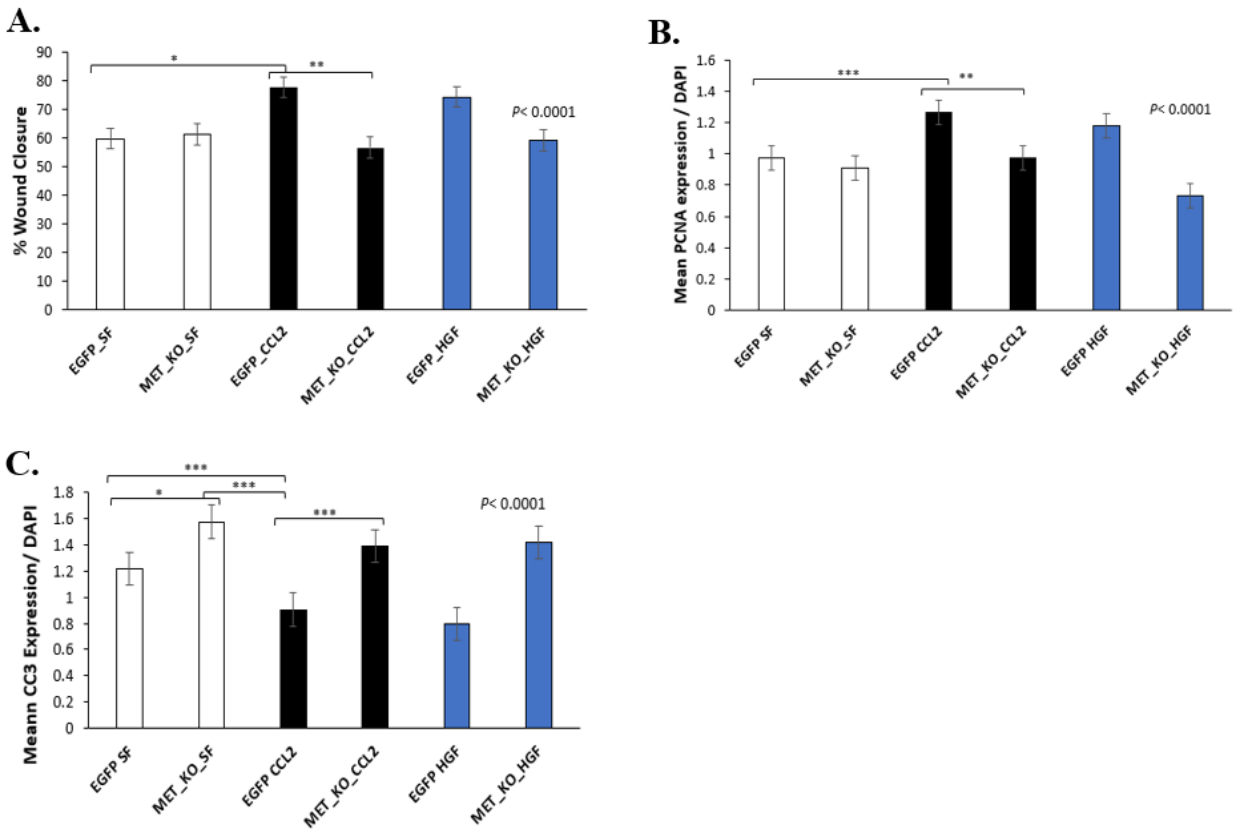

Figure 37. Gene targeting of epithelial c-MET blocks CCL2 induced collective cell migration, proliferation, and survival in HCC1937 human mammary carcinoma cells. HCC1937 MET gRNA and EGFP control breast cancer cells were seeded and upon monolayer confluence scratched and treated with 100ng/ml of HGF as a positive control for c-Met or 100ng/ml of CCL2 for 24 hours to assess collective cell migration, wound closure was analyzed by measuring the distance of the scratch at t=0 and t=24 by Image J software. (**A**), Cells were analyzed for proliferation by quantifying the expression of PCNA by immunofluorescence (**B**), Cells were seeded and serum deprived for 48 hours to induce apoptosis and treated with serum free media containing 100ng/ml of HGF as a positive control or 100ng/ml of CCL2 for 24 hours. Cells were analyzed for Cleaved-Caspase 3 expression by immunofluorescence (**C**). Each experimental group was plated in triplicate and experiments were performed three times. Four image fields per slide were taken with an EVOS-FL system. Statistical analysis was performed using a ONE-WAY ANOVA with Bonferroni *post-hoc* comparison. Statistical significance was determined by *p<0.05, **p<0.01, ***p< 0.0001., n.s. not significant or p>0.05. Mean ± values are shown. Scale bar = 400 microns.

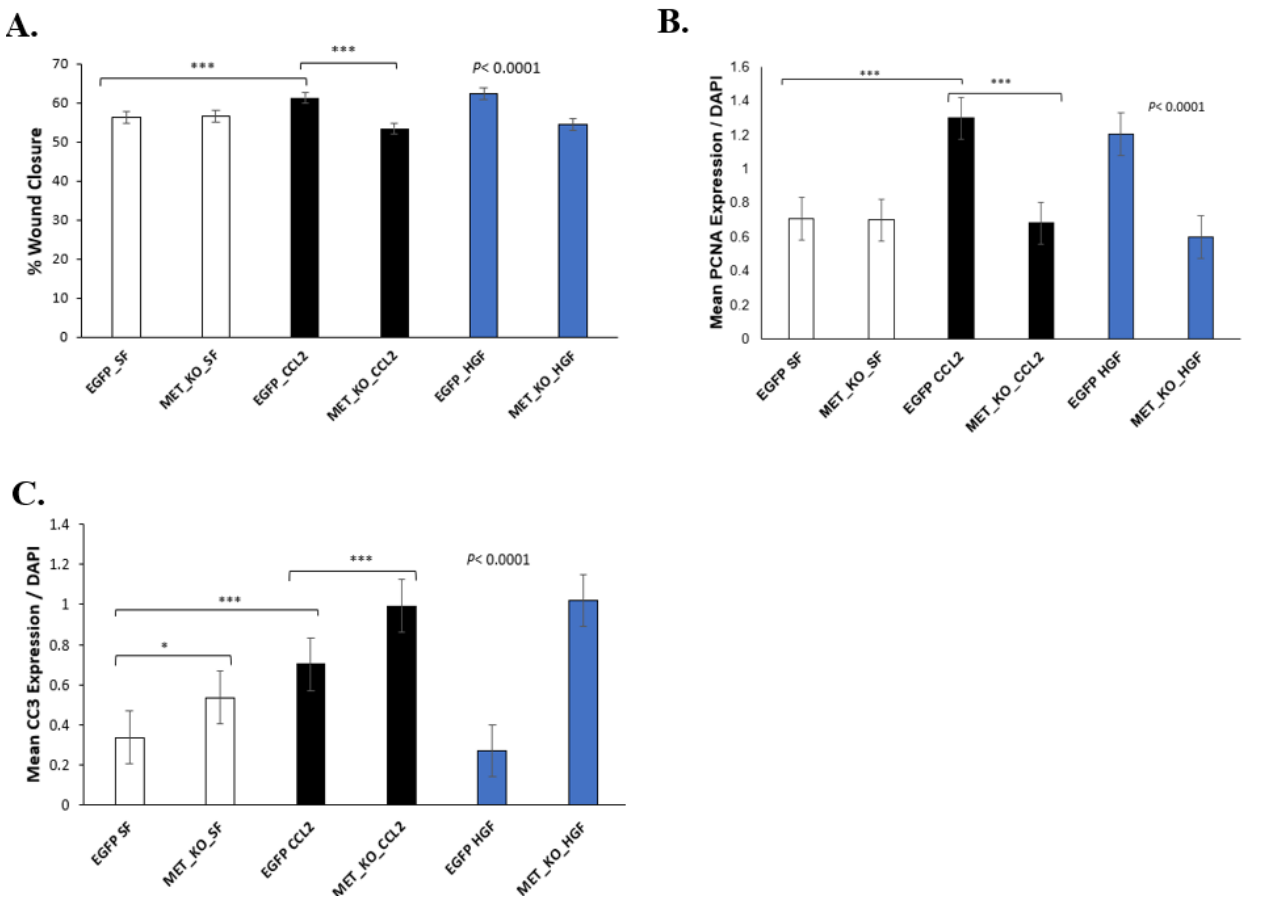

Figure 38. Gene targeting of epithelial c-MET blocks CCL2 induced collective cell migration, proliferation, and survival in MDA_MB_231 human mammary carcinoma cells. MDA_MB_231 MET gRNA and EGFP control breast cancer cells were seeded and upon monolayer confluence scratched and treated with 100ng/ml of HGF as a positive control for c-Met or 100ng/ml of CCL2 for 24 hours to assess collective cell migration, wound closure was analyzed by measuring the distance of the scratch at t=0 and t=24 by Image J software. (**A**), Cells were analyzed for proliferation by quantifying the expression of PCNA by immunofluorescence (**B**), Cells were seeded and serum deprived for 48 hours to induce apoptosis and treated with serum free media containing 100ng/ml of HGF as a positive control or 100ng/ml of CCL2 for 24 hours. Cells were analyzed for Cleaved-Caspase 3 expression by immunofluorescence (**C**). Each experimental group was plated in triplicate and experiments were performed three times. Four image fields per slide were taken with an EVOS-FL system. Statistical analysis was performed using a ONE-WAY ANOVA with Bonferroni *post-hoc* comparison. Statistical significance was determined by *p<0.05, **p<0.01, ***p< 0.0001., n.s. not significant or p>0.05. Mean ± values are shown. Scale bar = 400 microns.

Inhibiting c-MET mediated by CCL2 results in decreased glycolysis and glycolytic flux capacity in human mammary carcinoma cells.

To examine the effects of c-Met inhibition mediated by CCL2 induction in glycolysis, we performed the glycolysis stress test in DCIS.com breast cancer cells. The glycolysis stress test evaluates glycolytic function of the cells by using metabolic inhibitors of energetic pathways. The cells are seeded in base media which is devoid of glucose or pyruvate. At the time of the assay, cells are stimulated with acute injections including, glucose which stimulate the cells to undergo glycolysis.

The uptake of glucose results in pyruvate which can have two fates either be converted to lactate or undergo oxidative decarboxylation and enter the mitochondria as acetyl CoA which eventually leads to oxidative phosphorylation. Therefore, the second acute injection (oligomycin) is an ATPase inhibitor which shuts down oxidative phosphorylation to only account for the glycolysis that results in lactate. The final injection is 2- Deoxy-D-glucose which blocks hexokinase II function by acting as a competitive inhibitor for glucose 6 phosphate thus shutting down glycolysis.

Therefore, the parameters that the glycolysis stress test measures include, non-glycolytic acidification which corresponds to extracellular acidification that is not directly related to glycolysis, glycolysis, glycolytic capacity which is the maximum rate of glycose conversion to exclusively pyruvate, and the glycolytic reserve which refers to the ability of the cell to respond to a demand in energy in response to the metabolic modulators (Figure 39A).

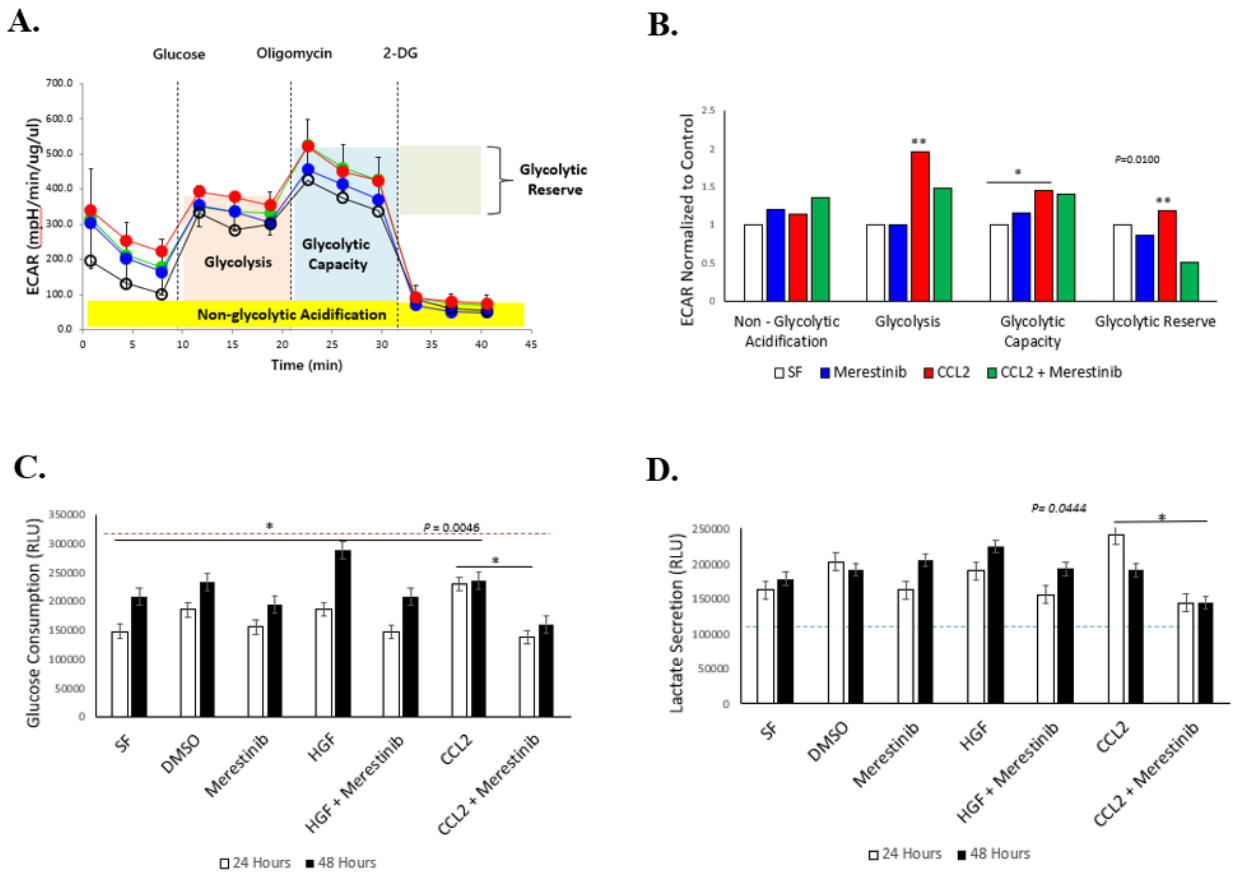

Figure 39. Inhibiting c-MET mediated by CCL2 results in decreased glycolysis and glycolytic flux capacity in human mammary carcinoma cells. Scheme representing different parameters measured in the glycolysis stress test in response to metabolic modulators in real time. Extracellular Acidification Rate (ECAR) is measured prior and after the addition of the following injections: 10nM Glucose, 1µM Oligomycin, 100mM 2-DG, obtained for DCIS.com breast cancer cells treated with CCL2, Merestinib, CCL2+ Merestinib and compared to serum free control **(A).** Area under the curve analysis of non-glycolysis ECAR, glycolysis ECAR, glycolysis flux capacity, and glycolysis flux spare capacity from cells treated for 4 hours with either serum free (white bars), c-Met inhibitor Merestinib (blue bars), 100ug/ul CCL2 (red bars), and CCL2 + Merestinib (green bars). Three separate readings were taken to ensure stability. Data for each experimental condition derive from values obtained from a minimum of six separate wells and the data represent readings from three independent plates **(B).** DCIS.com cells were plated, serum starved overnight and then treated with Merestinib, HGF±Merestinib, CCL2±Merestinib for 4 hours, and compared to serum free. Conditional media was collected and assayed for glucose consumption **(C)** and lactate secretion **(D)** at 24 and 48 hours after treatment. Statistical analysis was determined by One-Way ANOVA with Bonferroni post hoc test. Statistical significance was determined by $p<0.05$. Cells plated in triplicate; experiments repeated 3 times. Mean+Stdev are shown.

Inhibiting c-MET induced by CCL2 resulted in a significant decrease in glycolysis, glycolytic capacity and glycolytic reserved demonstrated by the glycolysis stress test (Figure 39B). To further examine the role of c-MET inhibition mediated by CCL2 on glycolytic flux, we measured glucose consumption and lactate secretion in DCIS.com breast cancer cells. CCL2 induction results in an increase glucose consumption as previously observed. Inhibiting c-MET mediated by CCL2 resulted in a significant decrease in glucose consumption (Figure 39C), and extracellular lactate secretion at 24 and 48 hours (Figure 39D).

c-MET KO mediated by CCL2 abrogates glycolytic enzyme activity and protein expression.

To determine the effect of c-MET ablation on glycolysis, we analyzed the enzymatic activity of Hexokinase II (HK2) and Pyruvate Kinase (PK). These glycolytic enzymes are crucial for regulating glycolytic flux since they are both rate limiting.

Hexokinase 2 is the first enzyme involved in glycolysis, converts glucose to glucose 6 phosphate making it an irreversible step because glucose gets “trapped” in the cell within the cytoplasm. There are four distinct isoforms for hexokinase HK1-4. Hexokinases 1-3 are allosterically regulated by its product glucose 6-phosphate [187]. Hexokinase 4 also known as glucokinase for its high specificity for glucose than other hexoses in humans, is not sensitive to glucose 6 phosphate concentrations [188]. Specifically, in breast cancer hexokinase 2 has been shown to be regulated by miR-155/miR-143 through signal transduction mechanisms [189]. DCIS.com MET KO and

EGFP control breast cancer cells were stimulated with CCL2 for up to 1 hour, compared to unstimulated and evaluated for the activity of Hexokinase 2.

Analysis of the enzymatic activity shows that there is a steady and significant decrease in Hexokinase 2 activity in MET KO cells compared to EGFP control at 5, 15 and 30 minutes followed CCL2 induction. When evaluating Hexokinase 2 activity in CCL2 induced MET-KO and EGFP breast cancer cells compared to untreated controls, there was a significant difference at 15 min on the EGFP CCL2 treated cells only. These data indicate that CCL2 enhances Hexokinase 2 activity that is exclusive in EGFP controls. In addition, by targeting MET by genetic approaches, Hexokinase II activity decreases even in the presence of CCL2 (Figure 40A).

On the other hand, pyruvate kinase (PK), is a glycolytic enzyme in the lower portion of the glycolysis pathway. It catalyzes the conversion of phosphoenolpyruvate (PEP) to pyruvate and ATP by transferring a phosphoryl group from ADP. The activity of PK is allosterically inhibited by different metabolites and co-factors including, long-chain fatty acids, ATP, and acetyl CoA [190]. Pyruvate kinase can be allosterically activated by fructose 1,6-bisphosphate [191]. Pyruvate kinase has four isoforms; PKM1, PKM2, PKL found in liver, and PKR which is found in the red blood cells. In breast cancer, previous studies have identified that the pyruvate kinase isoform M2 is highly expressed in advanced breast cancer patients compared to healthy controls [192]. DCIS.com MET KO and EGFP control were evaluated for the activity of Pyruvate Kinase in a similar fashion as described for Hexokinase II. The enzymatic activity of pyruvate kinase significantly decreased in the MET-KO breast cancer cells compared to the EGFP controls at all time points.

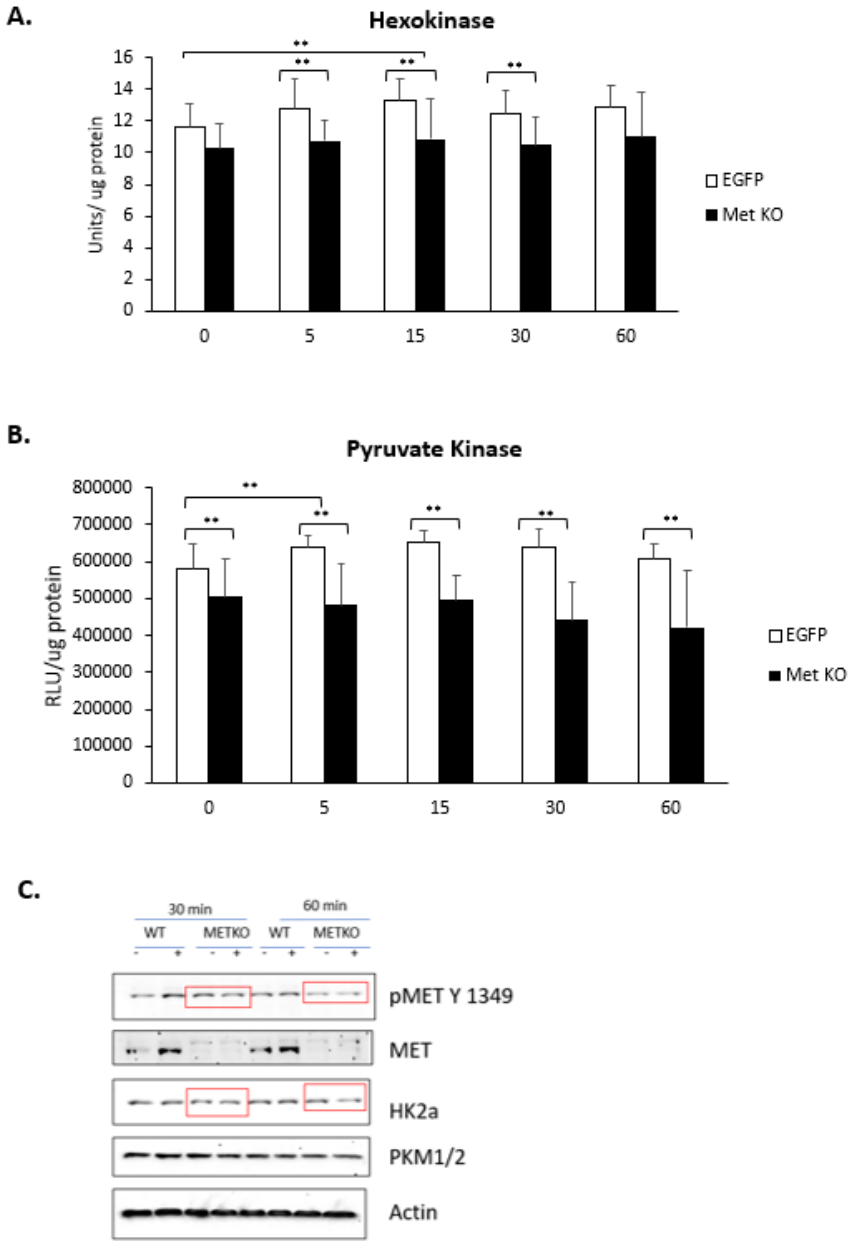

Figure 40. c-MET KO mediated by CCL2 abrogates glycolytic enzyme activity. DCIS.com breast cancer cells targeting c-MET by CRISP/R Cas9 and EGFP controls were treated with CCL2 for up to 60 minutes and compared to untreated. These cells were evaluated for the enzymatic activity of Hexokinase 2 (**A**) and Pyruvate Kinase (**B**). MET KO and EGFP control DCIS.com breast cancer cells were treated ±CCL2 for 30 and 60 minutes. Protein expression of p-MET, MET, HK2, and PKM1/2 were detected by western blot (**C**). Statistical analysis was performed by a student's t test to compare between MET KO and EGFP for each time point. For multiple comparisons, One- WAY ANOVA with Bonferroni post hoc test was used. Statistical significance was determined by $p<0.05$. Cells plated in triplicate; experiments repeated 3 times. Mean+Stdev are shown.

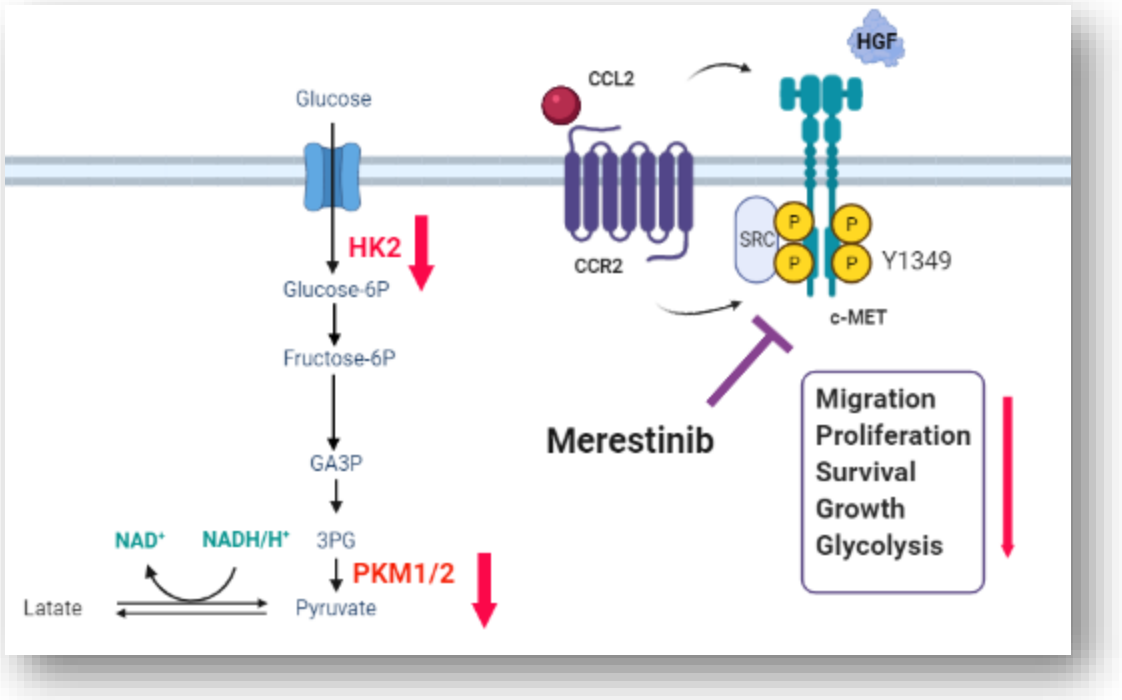

Figure 41. Activation of c-MET by CCL2/CCR2 is important for cell migration, proliferation, survival, growth, and glycolysis in breast cancer cells. CCL2/CCR2 activates the c-MET receptor tyrosine kinase at Y1349 by Src dependent mechanisms independently of canonical HGF binding. Targeting c-MET with the pharmacological inhibitor Merestinib, blocks CCL2 induced cell migration, proliferation, survival, growth, and glycolysis in basal like, triple negative breast cancer cells including DCIS.com, HCC1937, and MDA MB 231. In terms of glycolysis, inhibiting c-MET results in decreased glycolysis, glycolytic capacity, and glycolytic flux. Gene targeting of c-MET results in a decrease in expression and enzymatic activity of Hexokinase 2 and PKM1/2.

When evaluating the effects of CCL2 treatment on the genetically stable cells compared to untreated, results showed that there is a significant increase in pyruvate kinase activity in the EGFP control cells induced with CCL2 at 5 min and in the untreated samples (Figure 40B). These results are very similar to those observed in Hexokinase 2 in which MET KO cells correspond to a decrease in enzyme activity at all time points. Interestingly the decreased in enzyme activity remains in the untreated MET KO cells even when compared to the untreated EGFP. This data indicates that MET ablation acts as a negative regulator of enzymatic activity independently from CCL2 induction and that perhaps due to enzyme kinetics significant differences are found at specific time points. In addition, CCL2 acts as a positive regulator for glycolytic enzyme activity only on the EGFP control cells.

To further evaluate additional mechanisms by which MET ablation mediated by CCL2 regulates glycolysis, we evaluated the protein expression of Hexokinase 2 (HK2) and Pyruvate Kinase isoforms 1 and 2 (PKM1/2). DCIS.com MET KO and EGFP control cells were treated with and without CCL2 for 30 and 60 min and evaluated for protein expression of our glycolytic enzymes of interest by western blot. Hexokinase 2 expression was downregulated by MET KO even in the presence of CCL2 at 30 and 60 minutes (Figure 40C).

These results are consistent with enzyme activity data that was significantly downregulated by MET KO from 5 to 30 minutes. The difference between protein expression and enzymatic activity at 60 minutes could be to kinetic or allosteric mechanisms of the enzyme. When looking at the protein expression of pyruvate kinase, the differences in expression are not as distinct as HK2. However, there is a decrease in

protein expression at 60 min in the MET KO cells compared to EGFP control. This could indicate that the mechanisms of regulation of pyruvate kinase by MET KO are based on allosteric control or alteration at the co- factor level to impact enzyme activity but not necessarily protein expression. Taken together, this data indicates an important relationship in c-MET regulation of glycolysis by decreasing enzymatic activity of Hexokinase 2 and pyruvate kinase 2 in breast cancer cells. The data suggests that the mechanism of enzyme and protein regulation of HK2 and PKM1/2 is CCL2 independent (Figure 41).

Discussion

The CCL2/CCR2 chemokine signaling is overexpressed in breast cancer biopsies and malignant breast cell lines. Here we demonstrated additional molecular factors by which CCL2/CCR2 might drive DCIS progression, by RPPA analysis on DCIS.com breast cancer cells we identified that CCL2 induction phosphorylated c-MET tyrosine kinase. By PLA we confirmed that CCR2 interacts with c-MET and by CO-IP we demonstrated that this interaction is potentially mediated by SRC dependent mechanisms. In vitro studies targeting c-MET induced by CCL2 with the c-MET pharmacological Merestinib, resulted in blocked cellular migration, proliferation, survival, growth, and glycolysis in basal like breast cancer cells.

By RPPA analysis we identified that CCL2/CCR2 chemokine signaling activates the receptor tyrosine kinase c-MET. We provided evidence that CCL2/CCR2 serve as an alternative modulative mechanism for c-MET activation mediated by Src with relevant

clinical implications in DICS progression. Previous studies have demonstrated that followed CCL2 induction in basal- like breast carcinoma cell lines enhanced proliferation, and cell cycle progression by activating PKC and SRC [174].

Receptor tyrosine kinases (RTKs) are a subclass of tyrosine kinases that have high affinity for specific ligands and are involved in biological processes including, cell migration, growth, and metabolism. In cancer, next generation sequence has revealed alterations in genes that encode for receptor tyrosine kinases including EGFR, HER2/Erb2, and MET [193].

The notion that GPCRs activation enhances the signaling activity of RTKs is a molecular mechanism known as transactivation. This term was first described by Daub et al., 1996 and demonstrated by IP in Rat -1 fibroblasts where GPCR was activated by various ligands including thrombin, endothelin- 1, and lysophosphatidic acid which induced the phosphorylation of EGFR [194]. Even though G protein coupled receptors do not directly exert kinase activity, studies in the brain have demonstrated that upon ligand binding GPCRs activate receptor tyrosine kinases (RTKs) including Src, PI3K and Pyk [195].

The mechanism of ligand independent transactivation involves the Gα subunit from GCPR mediating signaling of effector proteins including Src and PKC [196]. By using resonance energy transfer techniques to measure the real – time recruitment of adaptor proteins in transactivation events, protein – protein interactions in live cells have been identified. Studies using Förster Resonance Energy Transfer (FRET) have shown that transactivation of the GCPR β2-AR (Beta 2 adrenergic receptor), transactivates

EGFR by PI3K – dependent phosphorylation of Src at the serine residue 70 (S70) [197]. In PC3 prostate epithelial cells the chemokine CXCL12 induced EGFR activation by mediating ADAM activation and Src phosphorylation at CXCR4 dependent and independent mechanisms demonstrated by IP and Src ELISA [198].

Additionally, recent studies in gastric cancer cells have shown that CXCL12/ CXCR4 induced c-MET activation contributing to EMT phenotype through crosstalk of Cav-1 with c-MET in lipid rafts demonstrated by PLA assay [199]. Our results are consistent with previous studies that indicate that chemokine ligands can result in the transactivation of RTKs mediated by Src dependent mechanisms as we observed by PLA in which CCR2 and MET were found to be in close proximity, and by IP indicating that this protein – protein interaction might be mediated by Src.

We demonstrated by pharmacological inhibition and genetic targeting approaches that c-MET activity induced by CCL2 is important for biological processes that are relevant to DCIS progression. In vitro targeting of c-MET by pharmacological approaches showed that c-MET inhibition induced by CCL2 blocked migration, proliferation, survival, and growth in DCIS.com, HCC1937, and MDA_MB_231 breast carcinoma cells. This data provides a validation of the effectiveness of the inhibitor across the different cell lines. Two important factors to note are first, all these cell lines are triple negative further classified as basal like subtype which is clinically relevant because as this subtype is more aggressive and has the worst prognosis.

Previous studies have identified that gene expression profile of c-MET is enriched and displays high protein expression in triple negative specifically basal like breast

cancers [200, 201]. This demonstrates the clinical and physiological relevance of our studies in targeting c-MET in ductal breast cancer. Another consideration is the evaluation of the effect of inhibiting c-MET dependent of CCL2 autocrine, paracrine signaling, and CCR2 receptor status. Previously, we have identified an association in CCR2 positive cells with invasive potential, and that all the tested cell lines mentioned above display high levels of CCR2 therefore a greater response to CCL2 induction. When we targeted c-MET with the pharmacological inhibitor, we did not see a significant effect of the inhibitor alone, that could mean that autocrine levels of CCL2 on the breast cancer cells are not sufficient to promote c-MET activation mediated by Src.

To validate the effects of inhibiting c-MET, we ablated the gene using CRISPR Cas9 and overall, we saw the same trends in migration, proliferation, and growth. However, we found a conflicting result when we were measuring Cleaved Caspase 3 levels. We saw that targeting MET did not significantly reduced survival. Therefore, it is possible that the mechanisms by which c-MET regulates survival is independent from the ones of the CCL2/CCR2 chemokine signaling. As previously demonstrated, CCL2 binds to CCR2 signaling to MEK, p42/44MAPK pathways to promote survival. An alternative signaling pathway to promote migration and survival is dependent on RhoA mechanisms [46]. On the other hand, studies have demonstrated that c-MET regulates survival dependent of PI3k, ATK and transcriptional factors including p53 [176]. Additionally, the discrepancy of results from in vitro and in vivo can be further explain effects of paracrine secretion in the microenvironment, ROS production and potential changes in hypoxia as disease progresses.

Previous studies have shown that cell apoptosis induced by serum starvation previously reported to have a direct effect in the arrest of G1 phase of the cell cycle on tongue squamous carcinoma cells [167]. Even though all the tested cells were of a basal like subtype, it is possible that they respond different to cell starvation by affecting other phases of the cell cycle different than mentioned above. It is also possible that the genetic background of each cell type influences the response of serum starvation [202].

Chapter V. Targeting c-MET by Merestinib inhibited CCR2 mediated DCIS growth, proliferation, and expression of glycolytic enzymes associated with decreased invasion in vivo

Abstract

In this chapter we evaluate the biological contribution of c-MET to CCL2/CCR2 mediated DCIS progression in the MIND model. By using the SUM225 CCR2 overexpression cells injected via MIND model, we demonstrated that c-MET inhibition mediated by CCL2/CCR2 chemokine resulted in decreased lesion mass, and stromal reactivity associated with decreased expression of markers of proliferation, glycolytic enzymes and fewer number of invasive lesions. By IC-MS we further evaluated the effect of c-MET inhibition on systemic metabolism and identified that compared to normal tissue, MIND model lesions that mimic DCIS progression use more metabolites that are involved in glycolysis and that drug treatment blocks the consumption of such metabolites.

These studies demonstrate that CCL2/CCR2 chemokine signaling modulates early breast cancer progression by enhancing glycolysis and c-MET activity with important implications for potential alternative treatment of basal like breast ductal carcinoma cases that present an increased expression of CCR2 and c-MET.

Introduction

Despite therapeutic improvements, Ductal carcinoma in situ (DCIS) remains the most common type of pre-invasive cancer among women in the United States, with 48,100 new diagnosed cases in 2019 which accounts for 18% of the total of all diagnosed breast tumors [151]. DCIS is a non - invasive heterogeneous group of cells confined in the lumen of the breast duct. In addition, DCIS has been described as a non-obligatory precursor of invasive disease, if left untreated about 40% of the lesions progress to invasive disease [152]. Standard treatment for patients involve lumpectomy with or without radiotherapy or mastectomy [153]. However, about 5- 20% of patients that undergo lumpectomy will still experience disease relapse and one half of the cases will have invasive disease [154, 155]. This presents a clinical conundrum that includes overtreatment reflected in potentially unnecessary surgeries for some patients or undertreatment if these surgeries are not performed in patients that would eventually develop invasive disease.

By developing a molecular approach to evaluate the prognosis of DCIS we can identify therapeutic alternatives for DCIS patients capable of predicting which cases will become invasive and potentially spare women from non-necessary surgeries.

Functional in vivo studies of epithelial CCR2 using the Mammary Intraductal Injection (MIND) as a model of DCIS, demonstrated that CCR2 overexpression was associated with enhanced survival, invasion, and accumulation of CCL2 expressing fibroblast. In contrast, ablating CCR2 function, decreased survival, and formation of invasive lesions [62]. However, targeting CCR2 alone was not sufficient to ablate

invasive phenotype which might indicate that other oncogenic factors are necessary to further drive DCIS progression and eventually leading to invasion.

By using the SUM225 CCR2 overexpression cells injected via MIND model, we demonstrated that c-MET inhibition mediated by CCL2/CCR2 chemokine resulted in decreased lesion mass, and stromal reactivity associated with decreased expression of markers of proliferation, glycolytic enzymes and fewer number of invasive lesions. By IC-MS we further evaluated the effect of c-MET inhibition on systemic metabolism and identified that compared to normal tissue, MIND model lesions that mimic DCIS progression use more metabolites that are involved in glycolysis and that drug treatment blocks the consumption of such metabolites. These studies demonstrate that CCL2/CCR2 chemokine signaling modulates early breast cancer progression by enhancing glycolysis and c-MET activity with important implications for prognosis or treatment of basal like breast ductal carcinoma cases that present an increased expression of CCR2 and c-MET.

Materials and Methods

Mammary Intraductal (MIND) model

In vivo studies were performed at KUMC according to guidelines from the Association for assessment and Accreditation of Laboratory Animal Care. Experiments were approved and in accordance with the Institutional Animal Care and Use Committee guidelines. Briefly, SUM225 breast cancer cells that are overexpressed for CCR2 were injected into NOD-SCID female mice (Non-Obese Diabetic Severe Combined

Immunodeficient interleukin receptor- γ2 null between 8 – 10 weeks of age and purchased from Jackson Laboratories (Bar Harbor, ME). MIND injections were performed as previously described [119, 124] with some modifications. Briefly, 4,000 cells/µL were prepared in 50µL of 0.1% Trypan blue in PBS.

Each mouse was anesthetized with an intraperitoneal injection of Ketamine (100mg/kg body weight) and Xylazine (10mg/kg body weight). Following complete sedation, the hair of the lower abdomen was removed to expose the 4-5 and 9-10 inguinal mammary fat pads. To prepare for surgery, the mouse was placed in a surgical platform and the area close to the inguinal glands was cleaned with 70% ethanol and betadine solution. While holding the base of the nipple with fine forceps the nipple was cut with spring scissors. The mouse was placed at the base of a dissection microscope and the cells were injected in 5µL (20,000) cells/nipple, with a 30-gauge Hamilton syringe with a blunt ended 0.5-inch needle. Successful injection was visually confirmed by the cell/trypan blue in the ductal tree of the mouse. After the injections the mice were placed on a heating pad for recovery and compensate possible loss of body temperature. Post operation mice were injected intraperitoneally with Ketoprofen (5mg/kg body weight) for seven consecutive days. Mice were monitored twice a week and palpated for lesions. Merestinib was solubilized in 20% Captisol in water and formulated in 10% PEG 400/90% (vehicle). Merestinib was obtained from Selleckchem (Cat # S7014). Captisol was obtained from Cydex Pharmaceuticals (Lenexa, Kansas).as previously described [178]. Four weeks following the MIND injection, mice were orally dosed with 12mg/Kg of Merestinib once daily in a 5/2 schedule as previously described for 4 weeks. [203]. Mice were sacrificed at 8 weeks post MIND injection.

Immunohistochemistry by DAB staining

MIND injection tissues were fixed in 10% neutral formalin buffer and embedded in wax as previously described [121]. Sections were cut 5 microns thick, dewaxed and heated in 10mM sodium Citrate buffer pH 6.0 for 5 minutes. Followed washing the slides, a endogenous peroxidase blocking step was performed with 60% cold methanol/3% H_20_2 in PBS, blocked for at least one hour in 3% FBS in PBS for rabbit antibodies, and incubated with primary antibodies [1:100] overnight at 4ºC for; PCNA (BioLegend, Cat # 307902), Cleaved Caspase-3 (Cell Signaling Technologies, Cat # 9661), Hexokinase II (Cell Signaling Technology®, Cat # 2867), PKM1/2 (Cell Signaling Technology®, Cat # 3190S), GLS1 (Proteintech Cat # 20170-1-AP), TWIST (Santa Cruz Cat # 81417), E-Cadherin (BD Transduction Laboratories™(Cat # 610181). Antigen retrieval for CC3 and PCNA was performed by using decloaker. For HKII and PKM1/2, TWIST and E-Cadherin, 2M UREA pH 6.8 was used. For GLS1 10mM of Na Citrate pH 6.0 was used. Slides were incubated with streptavidin peroxidase (Vector Laboratories Cat # PK-6200) for 30 minutes. Slides were developed with 3,3'-diaminobenzidine (DAB) substrate Kit (Vector Laboratories Cat # SK-4100) and counterstained with Mayer's hematoxylin and mounted with cytoseal. PCNA, TWIST and E Cadherin proteins were blocked for and detected using the AffiniPure FAB Fragment Goat Anti-Mouse IgG (H+L) (Jackson immunoResearch Laboratories Inc. Cat # 115-007-003)

Co-immunofluorescence and invasion assessment

Co-staining of cytokeratin and α-sma was performed as previously described [62]. Briefly, slides were heated in 10mM sodium citrate pH 6.0 for 5 minutes and incubated

with solution to quench endogenous peroxidases PBS/60%methanol/3%H202. Slides were washed with PBS, blocked, and incubated with primary antibodies 1:100 overnight at 4ºC to: sma (Cat # SP171, Spring Biosciences), and cytokeratin was detected with (Cat # MS198, Thermo Fisher Scientific). Slides were incubated for 2 hours 1:200 with anti-rabbit- IgG- Alexa Fluor®568 (Cat # A10042, Thermo Fisher Scientific) and anti-mouse IgG Alexa Fluor®488 (Cat # A-11001 Thermo Fisher Scientific). Sections were washed and counterstained with 4', 6-Diamidino-2-Phenylindole, Dihydrochloride (DAPI) and mounted with 50% PBS/Glycerol.

Tissue sections were imaged at 10x, and blinded scored as previously described [62]. Briefly, we score each lesion by the level of the myoepithelial being intact as follows: 1 was assigned for no invasive lesions (DCIS) which corresponded to intact α-sma+myoepithelium and the presence of epithelial cells within the duct; 2 was assigned for lowly invasive lesions (DCIS+Mi) with 50% or less disruption of the α-sma surrounding the duct and/or presence of three or fewer cells invading through the duct; a scoring of 3 described a highly invasive lesion (IDC) which displayed more than 50% α-sma disappearance and the presence of more than three cells invading through the duct and making contact with the periductal stroma.

Analysis of Anionic Metabolites by Ion Chromatography Mass Spectrometry (IC-MS)

MIND model tissue was harvested 24 hours after oral dosage of Merestinib and flashed frozen. Approximately, 10mg of tissue were placed in a pre-weighted cryotube (Bertin # CK28-R). Samples were analyzed for using ion chromatography mass spectroscopy (IC-MS) at the University of Texas MD Anderson Cancer Center's

proteomics and metabolomics core facility. Samples were prepared and analyzed as previously described by reconstituting the polar franctions in 100 µL water and 10 µL used for analysis in the Dionex ICS-5000 (Thermo Fisher Scientific) and operating at a resolution and acquisition as previously described [204, 205].

Image Quantification

Images were captured at 10X magnification using the FL-Auto EVOS system (Invitrogen) including 5-10 random fields per section. DAB staining was quantified as previously described [47]. In summary, the images were uploaded in Adobe Photoshop, positive DAB staining was selected by using the Magic wand tool, copied, and saved into a new layer which makes a separate file. These images were opened in Image J (NIH), converted to gray scale, and adjusted with threshold adjustment to remove nonspecific background. Staining was quantified by using the particle analysis feature. Positive DAB staining values were normalized to total area values which were expressed as arbitrary units. Normalized arbitrary units were subjected to statistical analysis with GraphPad Prism. The same principle was used to quantify the fluorescent staining. The staining of interest was selected and normalized to DAPI.

Statistical Analysis

Experiments involving cell cultures were repeated a minimum of three times. Data is expressed as mean ± standard error of the mean (SEM). Statistical analysis was performed by using GraphPad software. Two-tailed Student *t* test was used to compared two groups. One-way ANOVA with Bonferroni *post hoc* multiple comparisons test was

used for normal distributions. For non- Gaussian distributions the Kruskall-Wallis Test with Dunn's *post hoc* comparisons test was used.

Results

Targeting c-MET with Merestinib inhibited CCR2 mediated DCIS growth, proliferation, and expression of glycolytic enzymes associated with decreased invasion in vivo.

We sought to investigate the biological significance of the c-MET pathway mediated by CCL2/CCR2 chemokine signaling in DCIS progression in vivo. SUM225 breast cancer cells that overexpress CCR2 were injected via MIND model in NOD-SCID mice, 4 weeks post MIND injection, mice were orally dosed with Merestinib for an additional four weeks (Fig. 42A). To determine the effect of disrupting the c-MET pathway by pharmacological inhibition in DCIS progression in vivo, we analyzed lesion mass, proliferation, survival, expression of glycolytic enzymes, and invasion. Inhibiting the c-MET pathway mediated by CCL2/CCR2, significantly reduced lesion mass in the MIND model compared to vehicle control (Fig. 42B).

These results correspond to reduced appearance of stromal reactivity, lesion density shown by H&E (Fig. 42C), and PCNA levels in the mice dosed orally with the pharmacological inhibitor (Fig. 42D). These results are consistent with reduced growth and proliferation observed in the 3D cell culture models. This data indicates that targeting c-Met has a direct effect in cell proliferation and therefore lesion growth arrest. Interestingly, inhibiting c-MET in vivo, did not have a significant effect in cleaved caspase 3 expression which indicates no changes in apoptosis (Fig. 43A). These results could be

due to contributions of the microenvironment in secreting antiapoptotic molecules or changes in hypoxia.

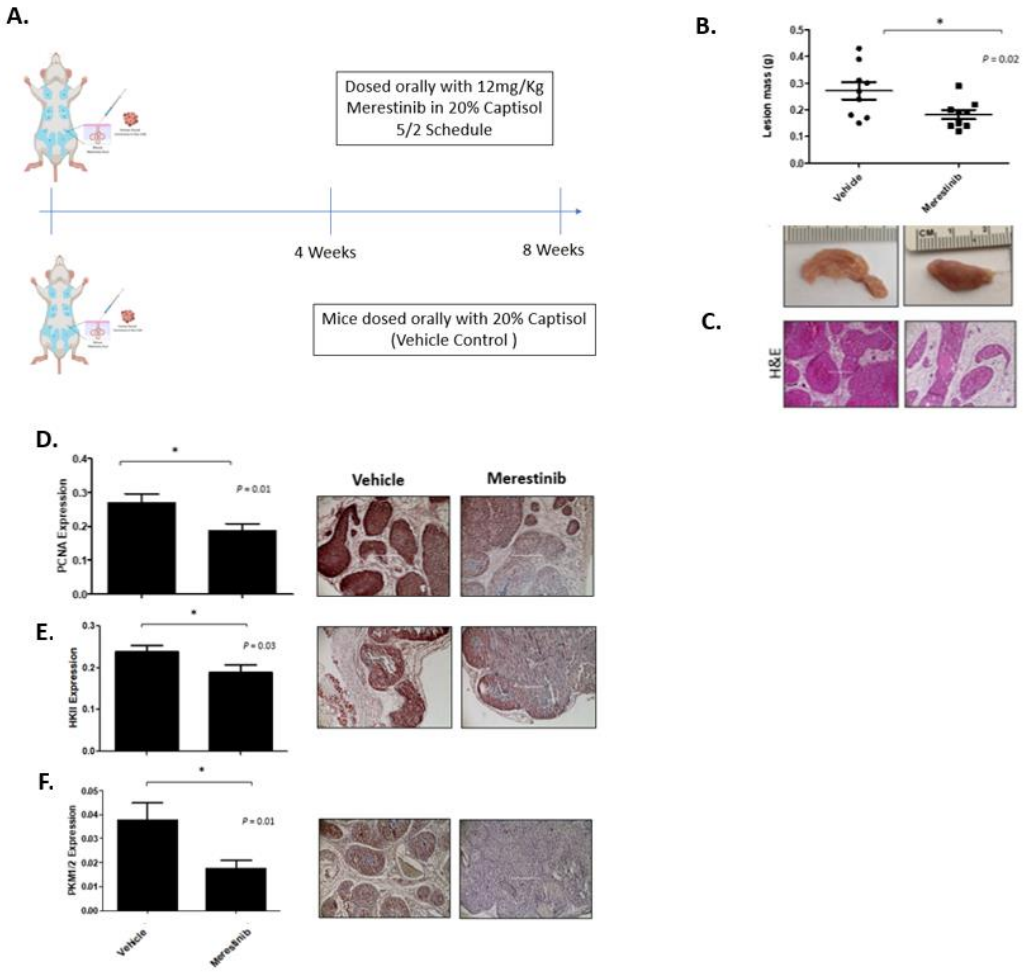

Figure 42. Targeting c-MET by Merestinib inhibited CCR2 mediated DCIS growth, proliferation, and associated with increased expression of glycolytic enzymes in the MIND model. SUMM225 Breast cancer cells overexpressing CCR2 were injected via Mammary Intraductal Model in NOD SCID female mice for 8 weeks. Representative diagram of the experimental design for the MIND model. One group of mice was dosed orally with Merestinib, a c-MET pharmacological inhibitor in a non-continuous dose schedule of 5/2 at a concentration of 12mg/Kg. (**A)**. Tissue mass of SUM225 CCR2-High MIND injected lesions of mice treated with oral dose of Merestinib compared to vehicle control. Representative pictures of each group are shown (**B)**. Histological analysis of the tissue by H&E **(C)**, PCNA **(D)**, HKII **(E),** and PKM1/2 **(F).** Scale bar, 200 μm. Statistical analysis was performed using unpaired student's t-test with Welch's correction **(B, D, E, F)**.Statistical significance was determined by P<0.05.*, P<0.05, P<0.05***; and n.s., not significant. Mean± SEM are shown.

Animals dosed with Merestinib, showed a significantly lower expression of the glycolytic enzymes Hexokinase II (Fig. 42E), and PKM1/2 (Fig. 42F). These results indicate the c-MET receptor tyrosine kinase mediated by CCL2/CCR2 plays an important role in modulating the expression of glycolytic enzymes which might support the growth and proliferation of lesions that are associated with DCIS progression.

We analyzed for the expression of Epithelial to Mesenchymal Transition Markers including E-Cadherin and Twist. Analysis of immunostaining showed that the Merestinib treated group displayed significantly lower E-Cadherin levels compared to vehicle control (Fig 43B). However, a significant difference in twist expression was not identified (Fig. 43C).

One of the characteristics of DCIS progression to IDC is the disappearance of myoepithelia and appearance of invading ductal carcinoma cells that trespass the myoepithelia and invade into the microenvironment [206]. To evaluate the effect of c-MET inhibition mediated by CCL2/CCR2 expression on breast ductal invasion, we co-stained for α-sma to identify the ductal myoepithelium, and to detect the human SUMM225 cells, we used Cytokeratin 19. Lesions were scored for invasiveness based on the extend by which the myoepithelia was intact, and presence of invading cancer cells contacting the periductal stroma as previously described but with minor modifications [62]. Briefly, noninvasive lesions denoted as DCIS, have intact α-sma+ myoepithelial, lowly-invasive lesions (DCIS+Micro invasion), showed low expression of α-sma lining the breast duct, and few invasive cancer cells. Highly invasive lesions (IDC) displayed

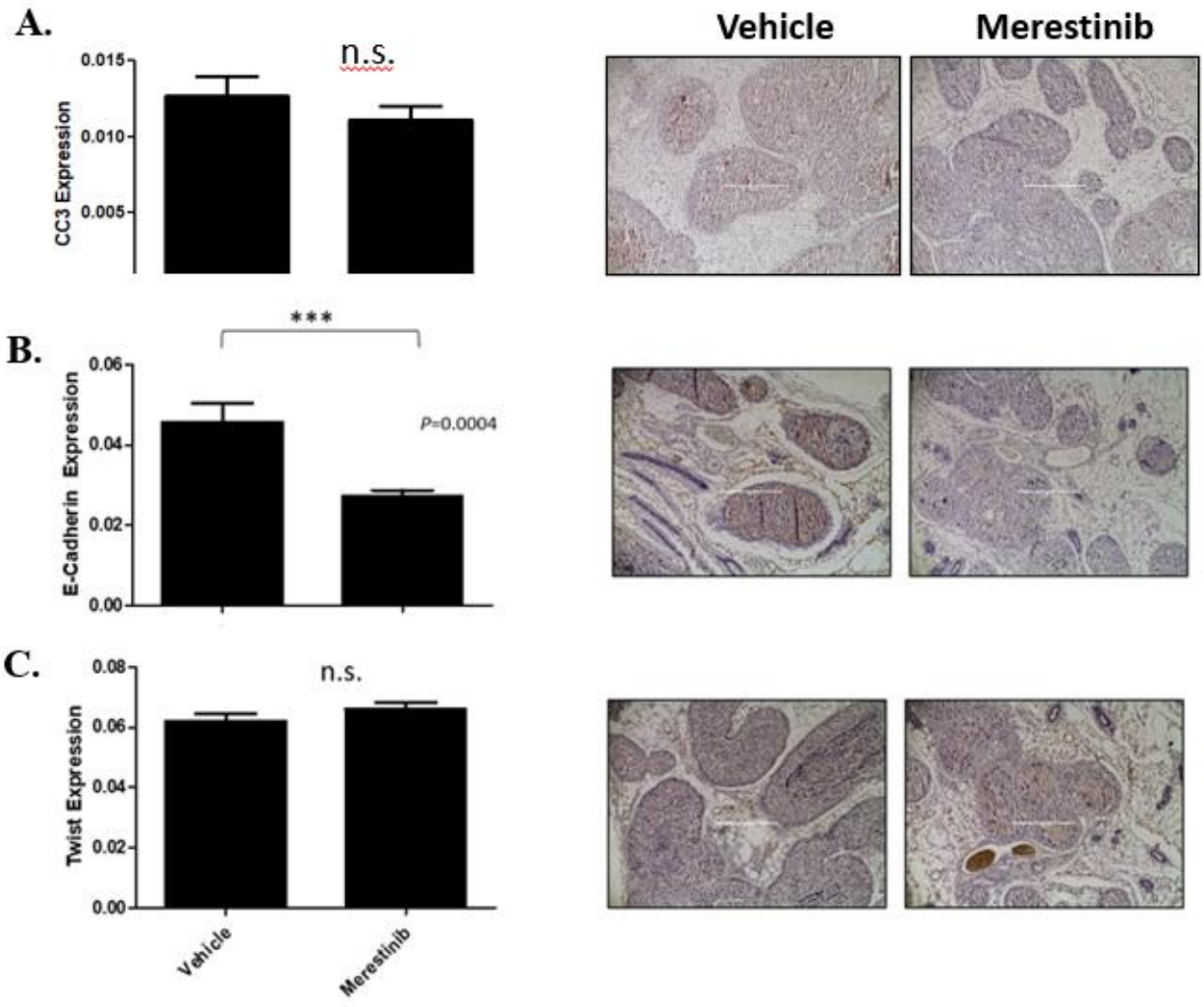

Figure 43. Targeting c-MET decreases E-Cadherin expression but not TWIST or E-Cadherin in the MIND model. SUMM225 Breast cancer cells overexpressing CCR2 were injected via Mammary Intraductal Model in NOD SCID female mice for 8 weeks. Immunohistological analysis for CC3 **(A),** E-Cadherin **(B)**, and twist **(C)**. Scale bar, 200 µm. Statistical analysis was performed using unpaired student's t-test with Welch's correction Statistical significance was determined by P<0.05.*, P<0.05, P<0.05***; and n.s., not significant. Mean± SEM are shown.

reduced α-sma expression, multiple invading cancer cells, and contact with the periductal stroma. In the vehicle control group, 26% of the lesions were DCIS, 56% were DCIS+Mi and 16% were IDC. In the group dosed orally with the c-MET inhibitor, Merestinib, 60% were DCIS, 36% were DCIS+Mi, and 3% IDC (Fig. 44A). Inhibiting c-MET displays more than half DCIS lesions and causes a reduction in the number of IDC lesions. In contrast, the vehicle control group, displayed higher number of DCIS+Mi and IDC lesions. Overall, the mice treated with Merestinib showed a greater number of DCIS lesions compared to vehicle control (Fig. 44B). These data suggest that c-MET inhibition modulated by CCL2/CCR2 expression shifts the invasive phenotype to non- invasive halting DCIS progression in MIND xenografts.

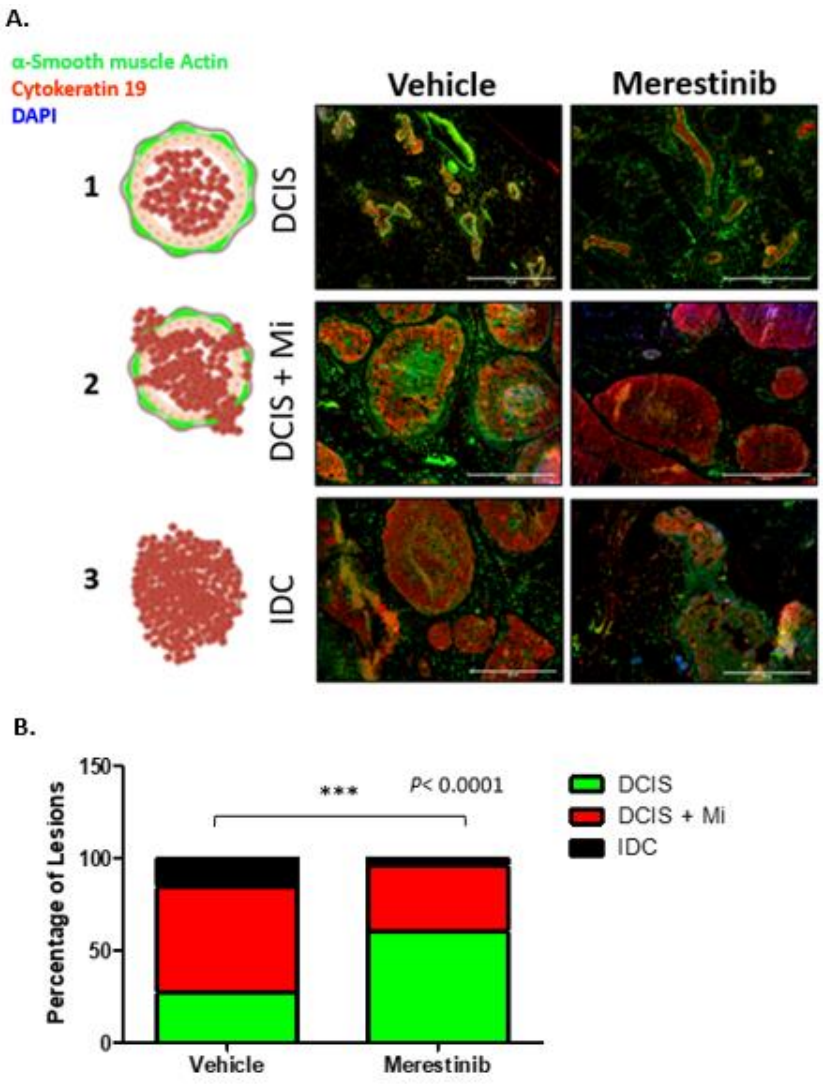

Figure 44. Targeting c-MET by Merestinib inhibited CCR2 mediated DCIS invasion the MIND model. Representative images for DCIS, DCIS with microinvasion and IDC are shown with secondary antibody control of Anti- rabbit 488/anti-mouse-Alexa Fluor 568/DAPI overlay **(A)**. Tissues were co-stained for CK19 (red) and α-sma (green), evaluated for invasiveness and normalized over the total number of lesions n= 427 for vehicle control, 948 for Merestinib. Scale bar, 200 µm. Statistical analysis was performed using unpaired student's t-test with Welch's correction **(B)** Statistical analysis was performed using the χ^2 test. Statistical significance was determined by P<0.05.*, P<0.05, P<0.05***; and n.s., not significant. Mean± SEM are shown.

Targeting c-MET blocks CCL2/CCR2 mediated consumption of glycolytic metabolites in the MIND model

Next, we investigated the effects of inhibiting the c-MET pathway with Merestinib on metabolites involved in the glycolytic pathway in vivo. To have a deeper understanding of how metabolite intermediates from MIND model lesions differ to those in the normal mammary gland, we analyzed both tissue types by Ionic Chromatography Mass Spectroscopy (IC-MS) (Fig.45)

By performing a targeted metabolite analysis, we identified significant changes due to Merestinib treatment in metabolites involved in glycolysis. Alpha – D- glucose 1,6-bisphosphate is low but with no difference between normal, and tumor which indicates that this particular metabolite is being consumed by both tissues in a similar manner. However, 24 hours after the Merestinib dose, there is a drastic difference between normal and tumor tissue which indicates that this metabolite is driven by the tumor and that Merestinib is blocking its consumption (Fig. 46A).

Glucose 6-phosphate, fructose 6-phosphate and fructose 1,6-bisphosphate have a very similar trend, they all display lower levels in the tumor in the vehicle control compared to normal tissue. This indicates that the tumors are more dependent on these metabolites since their consumption is higher than in the normal tissues. After treatment with Merestinib, the metabolites are consumed in the normal tissue compared to vehicle control and the consumption in the tumor is blocked as depicted by the higher levels compared to vehicle control (Figures 46B-D). When looking at metabolites that are involved in the lower portion of the glycolytic pathway, we observed a different trend as

seen on the metabolites above. Glyceric acid and phosphoenolpyruvic acid are highly consumed in the tumors before and after

Figure 45: Experimental Design for determining the effect of Merestinib in vivo

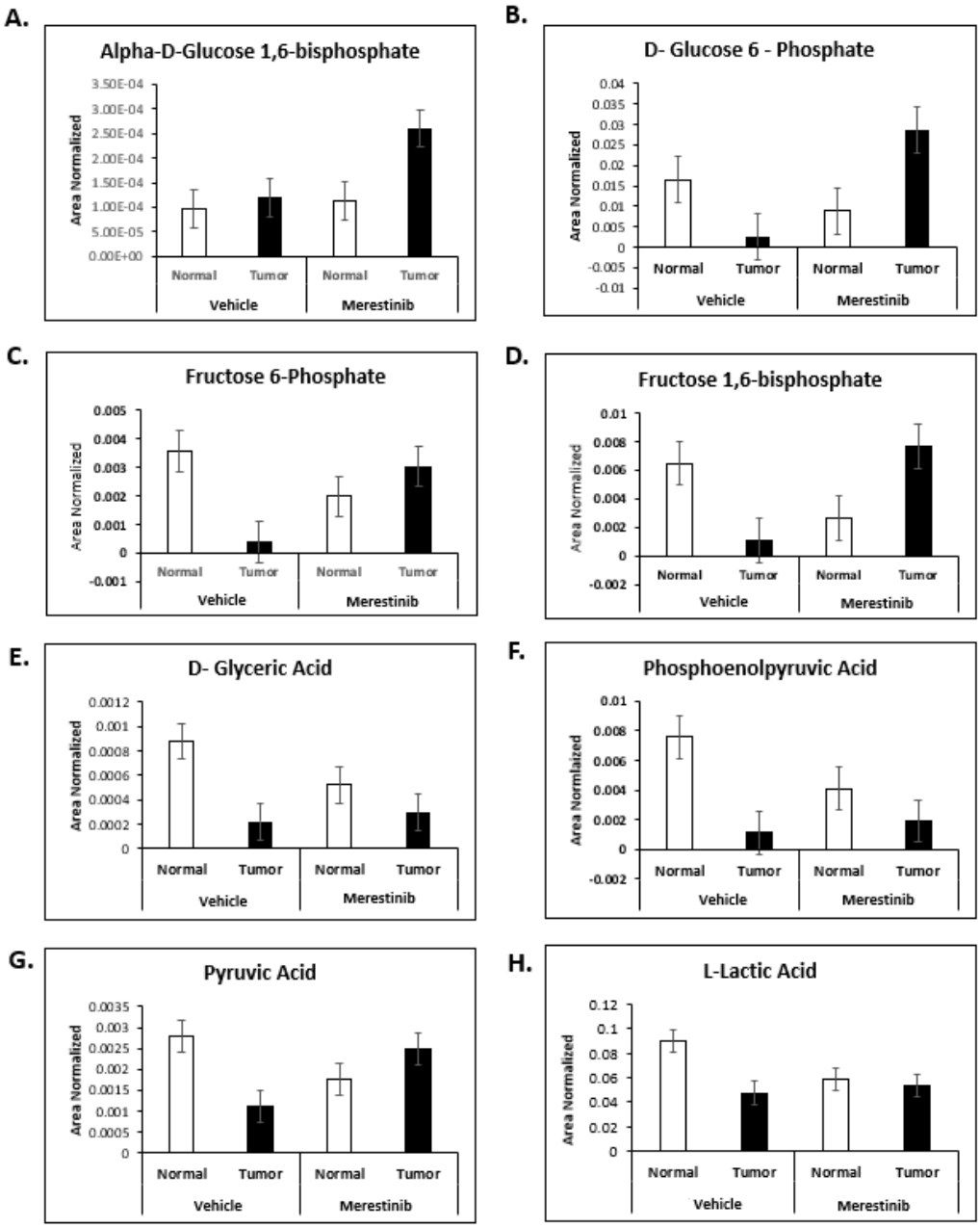

Figure 46. Targeting c-MET blocks CCL2/CCR2 mediated consumption of glycolytic metabolites in the MIND model. Ion chromatography-mass spectrometry (IC-MS) analysis of glycolytic metabolites from the CCR2 High MIND model of normal and malignant ductal breast lesions of mice treated with Merestinib for 24 hours compared to vehicle control (0 hours). Area normalized to total mass of the lesion and normal mammary gland are plotted for glycolytic metabolites including, Alpha-D-Glucose 1,6-bisphosphate **(A),** D-Glucose 6-phosphate **(B)**, Fructose 6-phosphate **(C),** Fructose 1,6-bisphosphate **(D),** D-Glyceric Acid **(E)**, Phosphoenolpruvic Acid **(F)**, Pyruvic Acid **(G)**, Lactic Acid **(H).** n =3 per group.

Merestinib treatment indicating the pharmacological inhibition has no direct effect in blocking the consumption of these metabolites (Fig. 46E and F). In terms of normal tissue, there is a decrease in the abundance of these metabolites 24 hours after Merestinib treatment which indicates that perhaps the treatment has an effect in increasing the consumption of these metabolites in normal tissue. On the other hand, pyruvic and lactic acid have a similar trend in the vehicle group between normal and tumor tissue where these metabolites are highly consumed in the tumor compared to normal tissue (Fig. 46G). Merestinib appears to slightly block the consumption of pyruvic acid in the tumor. However, merestinib treatment does not have a significant change in these metabolites in the normal and tumor tissue in the lactic acid (Fig. 46H).

Since glycolysis, the pentose phosphate shunt, and the TCA cycle are highly interconnected, we evaluated possible effects of Merestinib in these pathways. We identified that metabolites involved in the pentose phosphate pathway are not significantly affected by merestinib treatment (Fig. 47A-D). When evaluating potential effects of metabolites involved in the TCA cycle, no significant differences in metabolite consumption due to merestinib treatment were found (Fig. 47E-H).Taken together, this data indicates that merestinib treatment affects the consumption of metabolites that are upstream of the glycolytic pathway in the tumors. This suggests that the tumors highly rely on these metabolites for growth and progression of DCIS and these results are consistent with the tissue analysis that revealed a decreased lesion mass associated with decreased proliferation, expression of glycolytic enzymes, and invasiveness.

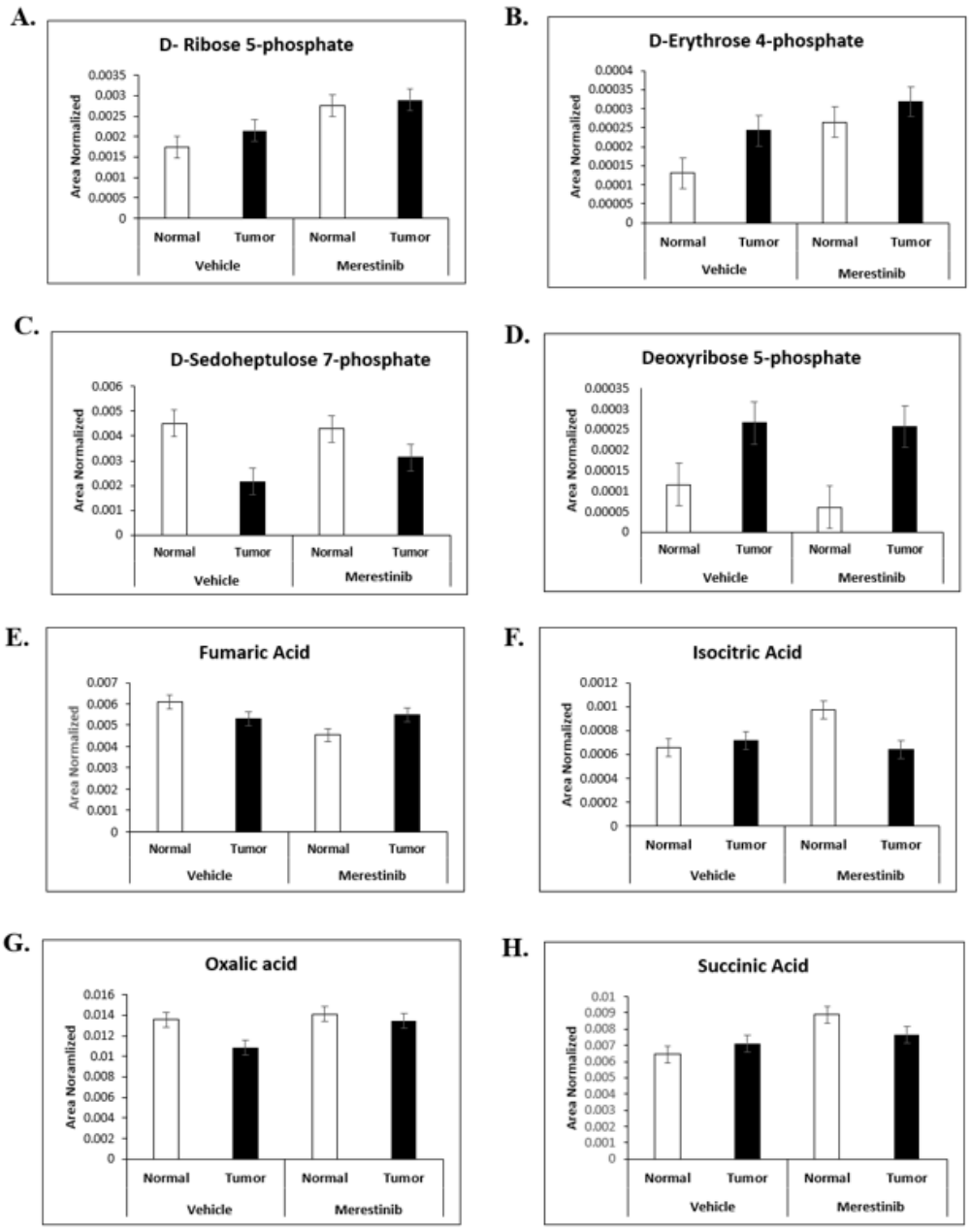

Figure 47. Targeting c-MET in vivo does not have an effect in pentose phosphate pathway and TCA cycle. Ion chromatography-mass spectrometry (IC-MS) analysis of glycolytic metabolites from the CCR2 High MIND model of normal and malignant ductal breast lesions of mice treated with Merestinib for 24 hours compared to vehicle control (0 hours). Area normalized to total mass of the lesion and normal mammary gland are plotted for metabolites involved in the pentose phosphate pathway including D-Ribose 5-phosphate **(A)**, D- Erythrose 4-phosphate **(B),** D-Sedoheptulose 7-phosphate **(C)**, Deoxyribose 5-phosphate **(D)**, and the TCA cycle including Fumaric acid **(E),** Isocitric Acid **(F),** Oxalic Acid **(G)**, Succinic Acid **(H)**. n=3 per group.

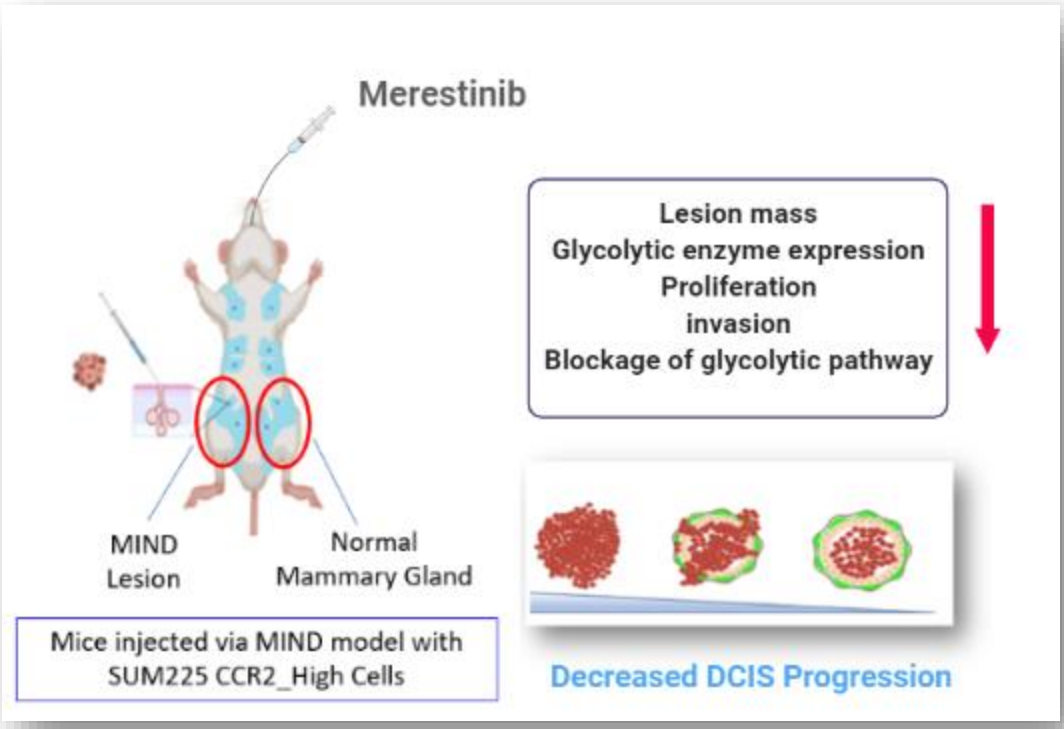

Figure 48. Summary of the effects of inhibiting c-MET in vivo. SUM225 breast cancer cells that overexpress CCR2 were injected via MIND (Mammary Intraductal Injection) model. Four weeks after the MIND injection mice were orally dosed with Merestinib, and FDA approved c-MET inhibitor at 12mg/Kg at a 5/2 schedule for 4 weeks. Upon tissue harvesting, the mice dosed with merestinib resulted with significant decrease in lesion mass, proliferation, expression of glycolytic enzymes associated by fewer number of invasive lesions compared to the vehicle control group. By IC-MS, we identified that mice treated with merestinib showed a blocked consumption of glycolytic metabolites but not those involved in the PPP or TCA cycle.

Discussion

The molecular mechanisms by which DCIS progression occurs and becomes invasive is currently unknown. Previous functional studies on role of epithelial CCR2 in DCIS progression in vivo demonstrated that CCR2 overexpression was associated with enhanced invasiveness and survival. In contrast, ablating CCR2 inhibited invasiveness, and decreased the number of CCL2 expressing fibroblasts [62] but did not completely abrogated invasion. These studies led us to hypothesize that CCR2 was modulating DCIS progression with other oncogenic factors. As previously described on chapter IV, Based on RPPA data, we identify c-MET as a candidate oncogenic factor.

Previous studies have shown that inhibition of RTKs decrease metabolic pathways including glycolysis mediated by PI3K/AKT which promotes AKT dependent Hexokinase 2 activation and membrane translocation of the GLUT1 glucose transporter [207]. Specifically, studies have demonstrated that inhibiting c-MET by pharmacological inhibitor AM7 and the tool compound SU11274 resulted in a decrease in glycolysis mediated by T53- induced Glycolysis and Apoptosis Regulator (TIGAR) by intracellular depletion of NADPH [208]. To examine the effect of c-MET inhibition in vivo, studies have demonstrated in xenograft models of non-small cell lung cancer (NSCLC) in Ncr-nu mice. Xenografts were monitored by FDG-PET (glucose analogue [^{18}F] fluoro-2-deoxy-D-glucose-positron emission tomography) analysis by MRI.

Mice treated with the small molecule MET inhibitor SU11274, resulted in a 45% drop in glucose metabolism compared to untreated controls [209]. Our in vivo studies using Merestinib resulted in a decrease in lesion mass as previously described [178,

203], proliferation, expression of glycolytic enzymes and association with inhibited invasion.

In terms of the effects of Merestinib in glycolytic in vivo, by IC-MS we observed a blockage in the consumption of glycolytic intermediates that was stronger in the upper portion of the glycolysis pathway. Interestingly the effects of Merestinib treatment was found in metabolites involved in glycolysis and not in the TCA cycle or the pentose phosphate pathway (PPP).

One possibility is that Merestinib stimulated TCA cycle or flux, independently from total metabolite levels. For instance, Merestinib could modulate co factors, metabolic intermediates or oncogenes that affect these pathways. Another possibility is that Merestinib could be modulating enzymes involved in glycolysis and glycolytic metabolites and enzymes that produce lactate but not the enzymes or transporters that shuttle pyruvate in the mitochondria where the TCA cycle and the PPP take place. To examine these possibilities, parallel studies that incorporate stable isotope tracing and measurement of metabolite levels could provide more information in regards of possible mechanisms of regulation of the metabolic pathways.

In summary, we demonstrated that CCL2/CCR2 chemokine signaling promotes DCIS progression through an increase in glycolysis, and c-MET activation dependent mechanisms mediated by Src. These studies have the potential to be considered as an alternative therapy for managing the growth and potential progression of DCIS lesions with high CCR2 and c-MET expression (Fig. 48).

Chapter VI. Physiological and clinical relevance of the c-MET tyrosine kinase receptor in DCIS progression to IDC

Abstract

In this chapter, we explore the clinical relevance of c-MET and CCR2 mRNA and protein expression. By examining the TCGA data base and analyzing protein expression for CCR2 and c-MET, we identified a positive and significant correlation in DCIS and IDC samples. This data indicates that both, c-MET and CCR2 are not only highly expressed in DCIS and IDC tissues but that their correlation at the protein level is stronger as disease progresses.

Additionally, we characterized the clinical relevance of breast ductal epithelial c-MET expression with DCIS progression, by immunostaining analysis on matching breast tissue microarrays containing in situ, invasive ductal carcinomas and normal adjacent to invasive tissue we identified that the expression of c-MET in IDC samples was significantly higher in the tumor epithelium compared to normal tissue. There is an expression pattern that increases as the disease progresses indicating that c-MET expression is strongly associated with IDC**.** To determine the clinical significance of c-MET in breast cancer patients, the expression of c-MET was analyzed through Kaplan-Meier Plotter analysis [210] [211] which showed that increased c-MET expression was significantly associated with decreased propability of relapse free survival..

Previous analysis of the clinical relevance of CCR2 by Kaplan- Meier plotter analysis showed that that incresed CCR2 was associated with decreased metastasis-free survival of breast cancer patients [62]. Taken together, these data indicate that CCR2 and c-MET have strong and possitive correlation in DCIS and IDC human tissues in mRNA, and protein expression, demonstrating clinical relevance. Additionally that

both CCR2 and c-MET are markers of poor prognosis that could be use as a biomarker capable of predicting invasive potential of DCIS patients.

Introduction

In breast cancer, CCL2/CCR2 are highly expressed in DCIS compared to normal tissue. In breast cancer cells, epithelial CCR2 corresponds to invasive potential [46, 47] and it is associated with the development of sporadic breast cancer [57].

The CCL2/CCR2 chemokine signaling is highly regulated in breast cancer at different levels including genetic, RNA, protein and signaling via autocrine and paracrine mechanisms. To start, at the genomic levels, single nucleotide polymorphisms of CCL2 (MCP1), have been associated with the risk of breast cancer development. Such variations in the genome exist in the regulatory regions of the MCP-1 gene. Results indicate that independently of initial stage, breast cancer patients that carry at least one G allele were at an increased risk for metastasis [54]. On the other hand, the single nucleotide polymorphism in CCR2 has been implicated with an increased risk for developing Her2+ breast cancer and poor prognosis [55].

Protein and RNA expression level alterations of CCL2 have been implicated in breast cancer. High expression of CCL2 correlates with tumor grade and poor patient prognosis demonstrated by flow cytometry studies of cell suspensions from tumor biopsies [59]. Increased expression of CCL2 in breast tumors by immunohistochemistry in the epithelium and stroma contributes to disease progression and it is highly correlated with increase macrophage recruitment [52].

Analysis of blood serum levels from breast cancer patients revealed that increased CCL2 levels correlated with tumor stage and lymph node involvement [59]. CCL2 has been proposed as a potential alternative target for metastatic breast cancer because high expression of CCL2 correlates with a decrease in survival in breast cancer patients [60, 61]. On the other hand, the CCR2 chemokine receptor is highly upregulated in breast ductal carcinoma in cells in IDC correlates tumor grade and decreased long-term patient survival [46]. These studies indicate that CCL2 plays a role in breast cancer progression by influencing growth and metastatic spread.

Further evidence indicates that stromal CCL2 and epithelial CCR2 expression in breast cancer correlates with poor patient prognosis [62, 63]. CCL2/CCR2 signaling in breast cancer promotes invasion during early stage breast cancer progression. Ex vivo tissue models and in vivo mouse models have demonstrated that CCR2 expression in breast cancer cells is important for DCIS progression, cancer stem cell renewal and breast cancer survival and invasion.

On the other hand, the c-MET receptor tyrosine kinase is a proto oncogene that regulates mammary gland development [162]. Previous studies have demonstrated that through canonical HGF binding, c-MET regulates mammary gland ductal morphogenesis [163, 164]. Protein and gene expression profiling have identified the c-MET receptor as an emergent biomarker for basal like breast cancers [165, 166] which could make it a promising therapeutic target. However, the role of c-MET activation in the progression of breast ductal carcinoma to invasive disease has not yet been identified.

There are several mechanisms of aberrant c-MET regulation in breast cancer including gene mutation, amplification, autocrine and paracrine signaling, and c-MET activation. However, studies have reported that gene mutation and gene amplification are very rare in breast cancer. For instance, studies reported that MET overexpression does not result from mutations in the tyrosine kinase in breast cancer [212]. In terms of MET amplification, it occurs in 0 to 7% in a cohort of 150 patients of breast cancers including lobular, ductal, and infiltrating ductal carcinoma identified by FISH and IHC [213]. Other studies have evaluated correlations between MET copy number and clinical factors in early stage breast cancer. Significant correlations were identified in tumor size >2cm, grade (III), and triple negative breast cancer. Overall, high MET copy number was strongly associated with poorer prognosis estimated by RFS [214].

We demonstrated that there was a positive and significant correlation in mRNA and protein expression in breast cancer patient samples. Further analysis showed that c-MET and CCR2 are highly co- expressed in invasive breast cancer cells compared to non – invasive. Lastly, we identified that in IDC samples, the number of co-expressing cells is higher than in DCIS.

These results indicate that there is a physiological and clinical importance for c-MET and CCR2 co-expression that is associated with invasive disease.

Materials and Methods

Flow Cytometry on live cells

MCF-7, SUM225, DCIS.com and HCC1937 500,000 cells were cultured in their respective complete medium in 10-cm dishes as described above. Cells were washed with PBS twice and detached with Accutase (EMD Millipore, Cat # SCR005) for 10 min at 37˚C. Cells were resuspended in PBS and centrifuged at 1200 rpm for 5 min. The pellet was resuspended in staining buffer containing 1% BSA, 25nM HEPES and 5mM EDTA and incubated with anti-human c-MET (HGFR) FITC diluted 1:10 (eBioscience, Cat # 11-8858-41) and anti-human CCR2 PE diluted 1:50 (Biolegend, Cat# 357205) for 1 hour. All the cells were analyzed using a BD LSRII Flow Cytometer and normalized to their respective unstained controls.

Immunohistochemistry by DAB staining

MIND injection tissues were fixed in 10% neutral formalin buffer and embedded in wax as previously described [121]. Sections were cut 5 microns thick, dewaxed and heated in 10mM sodium Citrate buffer pH 6.0 for 5 minutes. Followed washing the slides, a endogenous peroxidase blocking step was performed with 60% cold methanol/3% H_20_2 in PBS, blocked for at least one hour in 3% FBS in PBS for rabbit antibodies, and incubated with primary antibodies [1:100] overnight at 4ºC for; Met (Cell Signaling Technology®, Cat # 4560). Slides were incubated with streptavidin peroxidase (Vector Laboratories Cat # PK-6200) for 30 minutes. Slides were developed with 3,3'-diaminobenzidine (DAB) substrate Kit (Vector Laboratories Cat # SK-4100) and counterstained with Mayer's hematoxylin and mounted with cytoseal.

Biospecimens

Patient samples were collected under approval of the Institutional Review Board (IRB) at KUMC. Tissue microarrays (TMAs) consisted of de-identified patient tissue including DCIS (n=81), matching IDC (n=82) and normal adjacent breast tissues to IDC (n=87) were provided by the Biospecimen Core Repository Facility (BCRF) from the University of Kansas Center (KUMC). TMAs were arrayed in duplicate. Core sections were 1.5 mm in diameter and 5 microns thickness. DCIS tissue was graded using the Van Nuys Prognostic Index (VNPI). Samples were collected between 2007 and 2012, with 3 to 5 year follow up. Tissue microarray pathology information included age, stage, grade, tumor size, expression of KI67, ER, PR and Her2. Additional information included treatment, recurrence, and survival. Clinical pathological features for all breast samples is summarized (Table 1). The mean age of patients was 56 years.

Image Quantification

Images were captured at 10X magnification using the FL-Auto EVOS system (Invitrogen) including 5-10 random fields per section. DAB staining was quantified as previously described [47]. In summary, the images were uploaded in Adobe Photoshop, positive DAB staining was selected by using the Magic wand tool, copied, and saved into a new layer which makes a separate file. These images were opened in Image J (NIH), converted to gray scale, and adjusted with threshold adjustment to remove nonspecific background. Staining was quantified by using the particle analysis feature. Positive DAB staining values were normalized to total area values which were expressed as arbitrary units. Normalized arbitrary units were subjected to statistical analysis with GraphPad

Prism. The same principle was used to quantify the fluorescent staining. The staining of interest was selected and normalized to DAPI.

Statistical Analysis

Experiments involving cell cultures were repeated a minimum of three times. Data is expressed as mean ± standard error of the mean (SEM). Statistical analysis was performed by using GraphPad software. Two-tailed Student *t* test was used to compared two groups. One-way ANOVA with Bonferroni *post hoc* multiple comparisons test was used for normal distributions. For non- Gaussian distributions the Kruskall-Wallis Test with Dunn's *post hoc* comparisons test was used. The Cancer Genome Atlas datasets (TCGA) were analyzed by Spearman correlation analysis to identify associations between continuous variables. Statistical significance was determined by $P < 0.05$. $P<0.05$ *, $P<0.01$ **, $P<0.001$ ***, n.s= not significant or $P>0.05$.

Results

The receptor tyrosine kinase c-Met correlates to CCR2 mRNA and protein expression in breast cancer tissues.

To examine the clinical relevance of CCR2 and c-MET in breast cancer patients, we investigated the correlation in mRNA and protein expression of CCR2 and c-MET in breast tissues and identified important associations. TCGA database from the breast Invasive carcinoma, firehose legacy in cBioPortal [215, 216] containing data from 1,101 patients out of 1108 samples showed a positive and significant association between CCR2 and MET mRNA expression in 10% of the queried patients and samples (Fig. 49A).

Further analysis of protein expression between c-MET and CCR2 in immunostained DCIS and IDC samples revealed a significant and positive correlation between CCR2 and c-MET in the DCIS cohort (N=58) (Fig. 49B). When IDC (N=67) samples were evaluated, a significant and positive stronger correlation was also found indicated by the R value doubled than the one in the DCIS cohort (Fig. 49C). This data indicates that both, c-MET and CCR2 are not only highly expressed in DCIS and IDC tissues but that their correlation at the protein level is stronger as disease progresses. On the other hand, a positive and significant correlation between CCL2 and c-MET was found in IDC tissues (N=77). but this correlation was not significant in DCIS (Fig. 49D). This data suggests that CCL2 could play a role in the transition from DCIS to IDC but that might not be enough to influence MET expression in early breast ductal carcinoma.

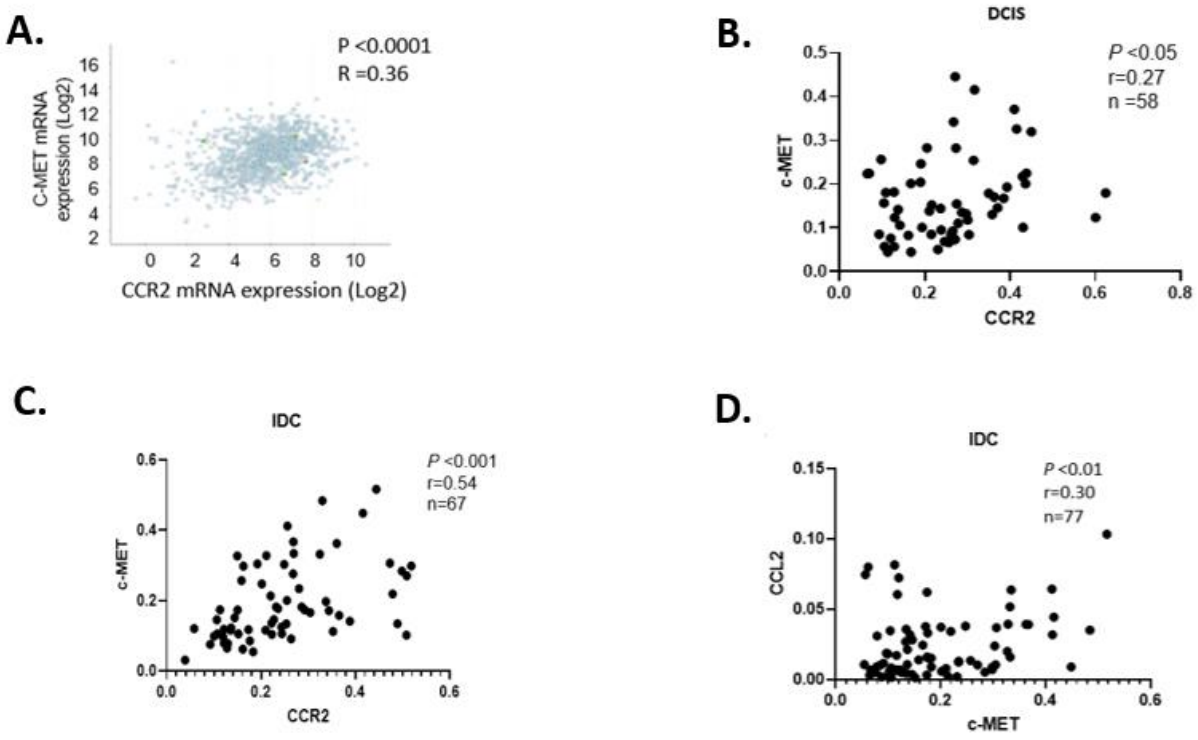

Figure 49. The receptor tyrosine kinase c-Met correlates to CCR2 mRNA expression and it is highly upregulated in DCIS and IDC in human samples. TCGA data set (cbioportal.org, Firehose Legacy, n=1101) was analyzed for CCR2 and MET mRNA expression through RNA seq V2 RSEM. Data are log2 transformed **(A).** Correlation analysis between C-MET and CCR2 protein expression in immunostained samples for DCIS (N=58) **(B)**, IDC (N=67) **(C)**, CCL2 and c-MET correlation in IDC (n=77) **(D).** Correlation analysis was performed using Spearman correlation. Statistical significance was determined by *P*<0.01, ***P*<0.05, ****P*<0.001, and n.s; not significant. Scale bar=400 microns.

To characterize the clinical relevance of breast ductal epithelial c-MET expression with DCIS progression, we performed immunostaining analysis on matching breast tissue microarrays containing in situ, invasive ductal carcinomas and normal adjacent to invasive tissue. The expression of c-MET in IDC samples was significantly higher in the tumor epithelium compared to normal tissue. There is an expression pattern that increases as the disease progresses indicating that c-MET expression is strongly associated with IDC (Fig. 50A). To determine the clinical significance of c-MET in breast cancer patients, the expression of c-MET was analyzed through Kaplan- Meier Plotter analysis [210, 211] which showed that increased c-MET expression was significantly associated with decreased propability of relapse free survival (Fig. 50B).

Previous analysis of the clinical relevance of CCR2 by Kaplan- Meier plotter analysis showed that that incresed CCR2 was associated with decreased metastasis-free survival of breast cancer patients [62]. Taken together, these data indicate that CCR2 and c-MET have strong and possitive correlation in DCIS and IDC human tissues in mRNA, and protein expression, demonstrating clinical relevance. Additionally that both CCR2 and c-MET are markers of poor prognosis that could be use as a biomarker capable of predicting invasive potential of DCIS patients.

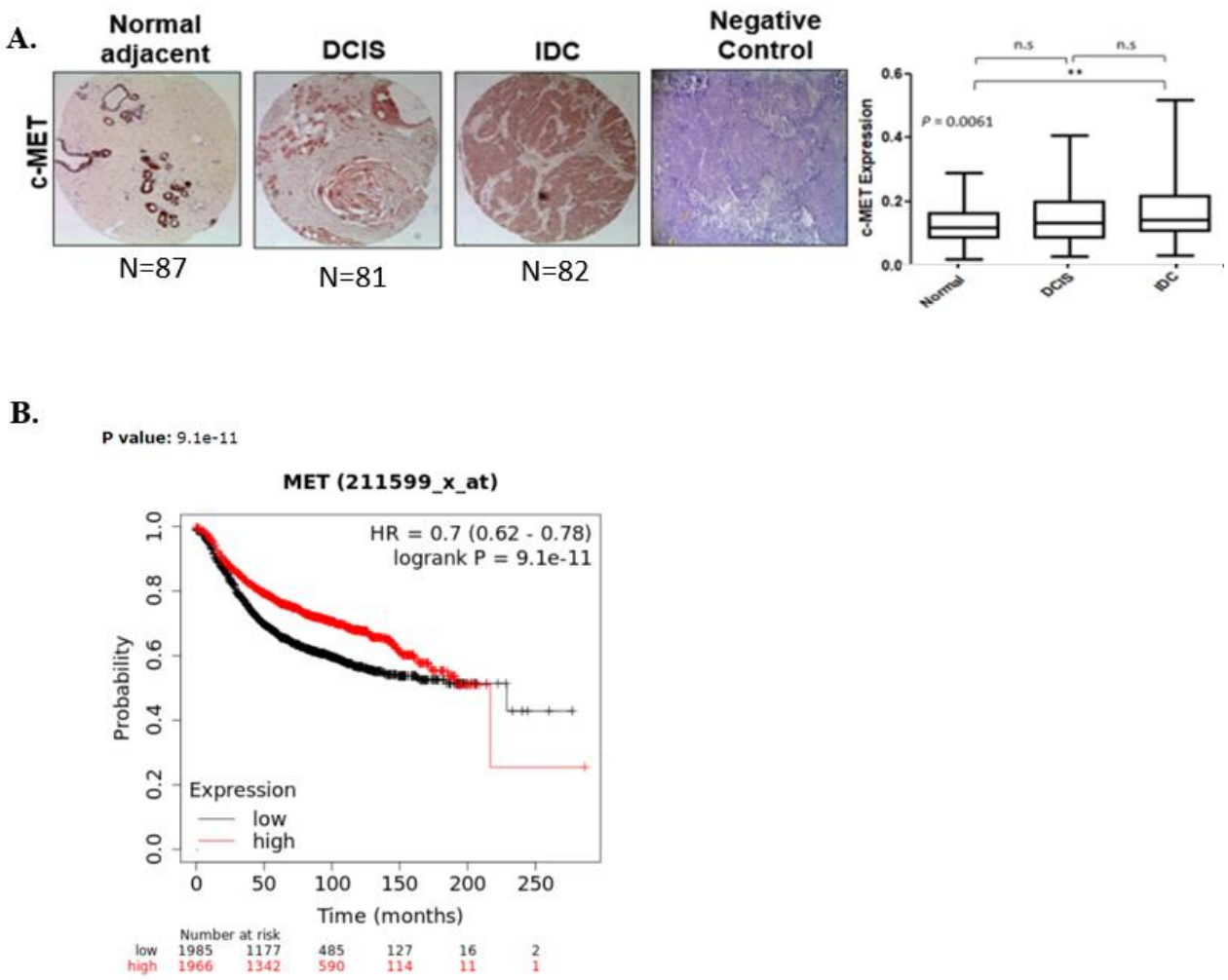

Figure 50. The receptor tyrosine kinase c-Met correlates to CCR2 mRNA expression and it is highly upregulated in DCIS and IDC in human samples. TMAs containing core sections; DCIS (n=65), matching IDC (n=67) and normal adjacent breast tissues to IDC (n=66) were immunostained with antibodies to total c-MET **(A)**. Protein expression was analyzed by Image J (arbitrary units). Whisker box plots are shown. Whiskers indicate min and max values. Box indicates upper and lower quartile range. Line indicates median Statistical analysis was performed using Two- Way ANOVA. RNA expression of c-MET (211599_X_at) was analyzed for associations with Relapse Free Survival (RFS) through KM Plotter for breast cancer **(B).** Statistical significance was determined by $P<0.01$, $^{**}P<0.05$, $^{***}P<0.001$, and n.s; not significant. Scale bar=400 microns.

Co-expression of CCR2 and c-MET correlate with invasiveness in human carcinoma breast cells, and human tissues

To confirm the expression patterns of CCR2, and c-MET in human carcinoma breast cancer cells, we analyzed by flow cytometry co- expression of CCR2/c-MET, CCR2, c-MET, low CCR2/c-MET in lowly invasive (MCF-7, SUM225), and cell lines that model breast ductal carcinoma in Situ (DCIS.com, HCC1937). Results show that highly invasive HCC1937 and DCIS.com cells display greater percentage of CCR2/c-MET co - expressing positive cells than the lowly invasive cell lines SUM225 and MCF7 (Fig. 51A). These data suggest that CCR2 and c-MET co-expression are associated with highly invasive breast cancer cells with important implications in disease progression.

Previous studies have shown that expression of CCL2/CCR2 signaling proteins correlate with DCIS progression to IDC in human tissue (Fang et al, 2021 under revision). To determine the importance of CCR2 and c-MET co-expression in DCIS and IDC samples, co-staining analysis was performed. Results revealed that there is a higher mean expression of CCR2 and c-MET expressing cells in DCIS and IDC tissues compared to normal. Co- expression of CCR2 and c-MET indicated by overlapping fluorophores was higher in DCIS tissues compared to normal, and even greater in IDC tissues (Fig. 51B and C). These results suggest that the protein expression of these two receptors has a clinical relevance that is important for DCIS progression to IDC.

To determine a physiological and genetic relevance for CCL2/CCR2 mediated metabolism, we analyzed associations among CCR2, MET and Hexokinase II (HK2) in breast tissues. By datamining analysis conducted on 3130 samples queried in 8 breast

cancer data bases (cbioportal.org), we identified significant co-occurrences between CCR2 and HK2, MET and CCR2, MET and HK2 (Fig. 51D). Taken together these data indicate that protein co-expression and gene co-occurrence of CCR2 and MET are important in ductal breast carcinoma and are associated with invasive disease.

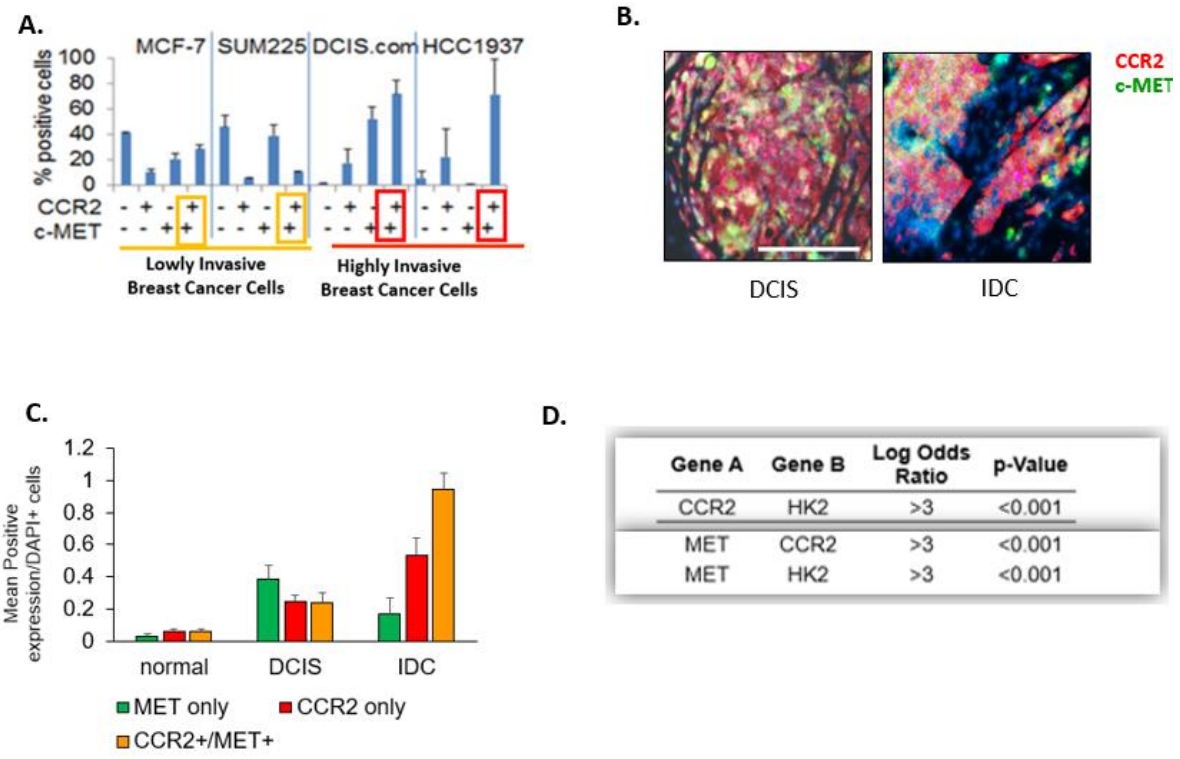

Gene A	Gene B	Log Odds Ratio	p-Value
CCR2	HK2	>3	<0.001
MET	CCR2	>3	<0.001
MET	HK2	>3	<0.001

Figure 51. Co-expression of CCR2 and c-MET correlate with invasiveness in human carcinoma breast cells, and human tissues. Flow cytometry for receptor co-expression of CCR2 and c-MET in lowly invasive breast cancer cells (MCF-7, SUM225) and highly invasive breast cancer cells (DCIS.com and HCC1937). Histogram represents the percentage of positive cells displaying; Low CCR2/c-MET, High CCR2, High c-MET, High CCR2/c-MET **(A).** Co-immunofluorescence staining of DCIS and IDC tissues for CCR2 by anti-CCR2-647, indicated by red, and c-MET by anti c-MET FITC, indicated by green. Overlapping expression indicated by yellow **(B).** The mean of positive expressing cells was normalized to DAPI **(C).** Co-occurrence analysis of CCR2, HK2 and MET conducted on 3130 samples that were queried in 8 breast cancer datasets (cbioportal.org). Gene sets were altered in 326 (10.9%) of queried samples. Statistical analysis was preformed using Fisher's exact test. Statistical significance was determined by $P<0.01$, $^{**}P<0.05$, $^{***}P<0.001$, and n.s; not significant **(D)**. Scale bar=400 microns.

Chapter VII. Concluding remarks and Discussion

Summary of findings and discoveries

In this project we identified that the CCL2/CCR2 chemokine signaling influences breast cancer cell metabolism and cooperates with other oncogenic factors to promote DCIS progression. Specifically, we first detected a relationship in CCL2/CCR2 and metabolism by analyzing the effects of CCL2 shRNA in MDA_MB_231 Breast cancer cells where we observed a change in the media color which lead us to further examine the bioenergetic profile of the cells mediated by CCL2/CCR2. This led us to further investigate the effects of CCL2 on DCIS.com breast cancer cell and by global metabolomic analysis we identified that CCL2 induction had a significant effect on glycolysis, TCA cycle, glutaminolysis, and redox pathways. For the purposes of this dissertation, we decided to focus on the glycolytic pathway, and by performing the energy phenotype test, we identified that CCL2 treatment enhanced a glycolytic phenotype over oxidative phosphorylation.

By analyzing hallmarks of glycolysis including glucose consumption and lactate secretion, results indicated that CCL2 significantly enhanced glucose consumption and lactate secretion. Further evaluation of potential mechanisms by which CCL2/CCR2 modulate glycolysis, we demonstrated by western blot that Hexokinase II expression was upregulated by CCL2 treatment and downregulated in the absence of CCR2 expression.

We confirmed these results by analyzing MIND model tissue from injected cells that display CCR2 overexpression which were associated by increased cell proliferation, survival, and, formation of invasive lesions, showed high levels of Hexokinase II compared to their pHAGE control. Additionally, on CCR2 KO injected lesions that were associated with decreased cell proliferation, survival, and fewer invasive lesions,

Hexokinase II levels were downregulated compared to their WT control These results indicate an important and novel association between CCL2/CCR2 modulating the glycolytic pathway specifically by regulating Hexokinase II expression. The results also highlight an important relationship between proliferation, DCIS progression and glycolysis

We then evaluated the effects of inhibiting c-MET mediated by CCL2 in vitro in biological processes that are important for DCIS progression. By inhibiting c-MET induced by CCL2 with Merestinib, an FDA approved Type II pharmacological inhibitor that has been used in clinical trials for other cancer types including leukemia and non-small lung cancer, we determined that cell migration, proliferation, survival, and growth was blocked.

To determine the effect of c-MET inhibition on glycolysis, we targeted c-MET which resulted in the decrease of glucose consumption and lactate secretion, glycolytic flux and glycolytic reserve. Further studies showed that MET ablation resulted in a significant decrease of Hexokinase II and Pyruvate Kinase II activity and protein expression. These data indicate that c-MET induction by CCL2 is important for modulating migration, proliferation, survival, growth, and glycolysis.

Lastly, to determine the physiological relevance of CCL2/CCR2, c-MET and glycolysis in DCIS progression in vivo, we used the MIND model. We injected SUM225 breast cancer cells that overexpress CCR2, let the lesions grow and four weeks after the MIND injection we dosed a group of mice with the oral inhibitor Merestinib. Results showed that mice dosed with Merestinib resulted in decreased lesion mass, proliferation, expression of metabolic enzymes including Hexokinase II and Pyruvate Kinase II were

associated with fewer number of invasive lesions compared to vehicle control. To further understand how c-MET inhibition affects glycolysis in vivo, we performed IC-MS analysis on the MIND lesions, normal mammary glands and compared them to vehicle control. Data showed that the consumption of metabolites involved in glycolysis are significantly blocked after Merestinib treatment compared to vehicle control. This data indicates that glycolysis is in part driven by CCL2/CCR2 and c-MET in vivo and that DCIS lesions are highly dependent upon this glycolytic pathway.

Limitations

Although the present studies reveal important insights on molecular mechanisms by which CCL2/CCR2 chemokine signaling drives ductal breast cancer progression by enhancing glycolysis and c-MET activation, there are technical limitations worth mentioning.

First, our in vivo studies focused on the epithelial expression of CCR2, c-MET and glycolytic enzymes. However, factors such as interaction of epithelial cells with the immune system need to be addressed. Previous studies from our lab demonstrated in a syngeneic mouse model that in breast cancer cells, CCR2 signaling regulates tumor growth and invasion by mediating angiogenesis, M2 macrophage recruitment, and suppressing CD8+ cytotoxic T cell activation [217].

Additionally, studies have shown that the tumor microenvironment can have drastic metabolic shifts due to lack of Oxygen, leading to hypoxia, nutrient depletion, and accumulation of waste products. These processes have an effect in T cells by inhibiting their metabolism and thus their activity. As a result, effector T cell differentiation and

proper immune response is disrupted which in many cases leads to immune therapy resistance [218]. Therefore, using a humanized animal model would help address the questions regarding the effect of the immune system in response to c-MET inhibition.

As mentioned in the introduction, one of the mechanisms of c-MET regulation in breast cancer is aberrant paracrine signaling. Unfortunately, with our current mouse model system using NOD-SCID female mice (Non-Obese Diabetic Severe Combined Immunodeficient interleukin receptor- γ2 null) impedes the study of paracrine c-MET signaling because murine HGF cannot bind to human c-MET [219]. To overcome these technical challenges, and to maintain the clinical relevance of this studies, a xenograft model that expresses HGF can be used to explore the paracrine signaling mechanism of c-MET and study its effects on ductal breast cancer progression and metabolism as previously published [220].

Another aspect that was not addressed in this study is the effect of hypoxia in metabolism and c-MET expression both in vitro and in vivo. As tumors grow their demand for nutrients and Oxygen changes overtime and it is usually accompanied by malignant transformation. Hypoxia inhibits the respiratory rate downregulating ATP preventing ROS overproduction, and Oxygen depletion [221]. Regarding hypoxia and c-MET expression previous studies have shown that HGF/c-MET expression is enhanced by hypoxia via HIF-1α dependent mechanisms [222]. In addition to overcome hypoxic conditions, studies have demonstrated that HGF regulated the expression of the vascular endothelial cell growth factor (VEGF) through c-MET downstream signaling pathways including PI3K/Akt, MAPK, and STAT 3 in murine colon carcinoma cells, CT26 [223].

Future Directions

CCR2 and c-MET interactions

To further evaluate additional factors or oncogenes that might cooperate with CCL2/CCR2 to promote DCIS progression, we identify by RRPA (data not shown) analysis that CCL2 activates the receptor tyrosine kinase c-MET. We validated those results by immunoblot and confirmed that upon CCL2 induction and in the presence of CCR2, c-MET is phosphorylated at the Y1349 multifunctional docking site of the intracellular domain. To further identify potential mechanisms by which CCL2/CCR2 activate c-MET, we performed a proximity ligation assay that resulted in fluorescent signal at 5 and 15 minutes after CCL2 treatment. This indicated that CCR2 and c-MET were in proximity. To further identify potential protein protein interactions, we performed a CO-IP and demonstrated that CCL2/CCR2 activates c-MET through src dependent mechanisms. These studies are ongoing.

Additionally, we identified a novel association between CCL2/CCR2 and c-MET through src dependent mechanisms which are consistent with previous studies in the brain that have demonstrated that upon ligand binding GPCRs activate receptor tyrosine kinases (RTKs) including Src, PI3K and Pyk.

Future studies will involve the use of BRET techniques to further elucidate the nature of the protein – protein interactions mediated by Src dependent mechanisms.

Other metabolic studies

To better understand the effect of CCL2 on metabolism in human breast cancer cells we performed and unbiased metabolomic study. This study revealed that CCL2 induction had a significant effect on metabolic pathways including glycolysis, TCA cycle, fatty acid synthesis, glutaminolysis and redox reactions. Even though in this study we focused on glycolysis, functional experiments are currently being performed to study the effects of Hexokinase II, FASN, and GLS1 in biological processes that modulate DCIS progression. Therefore, in the future is necessary to further evaluate the other metabolic pathways that are affected by CCL2.

MRS/MRI studies

To understand the biological relevance of CCR2 and c-MET co-expression, and to correlate metabolite concentration to DCIS progression in a non-invasive manner, we will use magnetic resonance spectroscopy (MRS). To address the clinical and physiological relevance of the heterogeneity on breast epithelial CCR2 and c-MET in metabolite production and DCIS progression, DCIS.com parental, HCC1937 breast cancer cells that express various levels of CCR2, and c-MET will be injected via MIND model.

Previous pilot studies from our lab detected in the DCIS.com MIND lesions elevated levels of lipids, choline and glycine compared to non- injected mammary gland using MRI/MRS. Choline (Cho) is an essential nutrient that incorporates into phospholipids and glycine is a target of lipid modification in proteins. [224]. In previous studies, the increase of Cho peak correlates with increase cellular proliferation related to

malignant lesions [39]. We propose that by using MRI/MRS in live animals in a time course we will be able to measure and identify possible changes of these metabolites during DCIS progression in a non- invasive manner. In the future we want to establish a metabolic signature that correlates with DCIS progression and that can be used in the clinical setting to potentially spare women from unnecessary surgeries and guide treatment.

Spatial Profiling

One of the challenges of ductal carcinoma in situ is cell heterogeneity. In vitro studies cannot address biological aspects that influence the epithelial cells by the microenvironment. In vivo studies cannot detect differences between epithelial cells and microenvironment contributions to malignant transformation.

Therefore, to determine the differential expression between tumor and microenvironment we could use the GeoMx DSP platform nanoString. We could develop a clinically relevant molecular signature of CCL2/CCR2 signaling proteins, to DCIS progression.

By spatial mapping, we can identify regions of interest within tissue compartments comparing tumor and stroma focusing on signaling pathways related to chemokine signaling, apoptosis, cell cycle, regulation of cell motility and metabolism. We can potentially use matched breast patient samples of DCIS, IDC stage 2, IDC stage 3, and normal adjacent breast tissue. To distinguish the human epithelia and tumor, the tissue will be stained with Pan Cytokeratin (Red), epithelial CCR2 (Green) and CCL2 (Cyan).

These studies will help us to map out the specific molecular mechanisms of activation of the CCL2/CCR2 signaling pathway and determine how potential changes or interaction with other signaling pathways affect DCIS progression. The positive impact of this study is that it would provide important insights into prognosis by developing a molecular signature able to predict DCIS progression and potentially be used to identify therapeutic targets for alternative and tailored treatments for DCIS patients.

Significance and Innovation

The role of CCL2/CCR2 chemokine signaling in metabolic changes that occur during DCIS progression**:** In terms of cellular metabolism, CCL2/CCR2 has only been studied in tumor free mice and related to obesity and diabetes and studies on metabolism have focused on late stage breast cancer [226, 227]. However, potential metabolic changes that occur during DCIS progression and how chemokines might regulate cancer metabolism are not currently known.

Therefore, this project is based on the conceptual and innovative idea that CCL2/CCR2 mediates metabolic changes in DCIS progression. Here, we demonstrate that c-Met, a tyrosine kinase that regulates ductal breast development and that is highly expressed in invasive breast cancer and activated by CCL2/CCR2.

We suggest that c-Met receptor expression and activity play a role in CCL2 mediated DCIS progression and metabolism. Our studies are novel because they incorporate different approaches that are clinically relevant. Such approaches include: the use of small molecule inhibitors that have been previously used and approved for other cancer types, the development of a metabolic signature that correlates to DCIS

progression and the analysis of blood serum as a potential predictive measure of DCIS progression. The proposed studies seek to explore the role of metabolites that can be altered by CCL2/CCR2 and c-Met expression in an in vitro model and the DCIS MIND model to follow DCIS progression.

To our knowledge, we are the first to report evidence that CCL2/CCR2 directly affects glycolysis on breast cancer cells, in part by modulating Hexokinase II expression with important associations in DCIS progression. Previous studies have reported that other cytokines including CCL5 enhance aerobic glycolysis in breast cancer cells through AMPK dependent mechanisms [23]. Others have identified that there is a strong association and correlation between increased glycolysis as well as genes involved in the MAPK pathway which are known to promote aerobic glycolysis [24]. CCL2 mediated by PKM2 in colorectal cancer cells contribute to an increase in macrophage recruitment [25]. However, to our knowledge, this is the first time that a study focuses on the importance of CCL2/CCR2 chemokine signaling regulating the glycolytic pathway in breast ductal cancer progression.

In this study we have developed and used novel approaches to further understand how the CCL2/CCR2 chemokine signaling pathway cooperates with other molecular and oncogenic factors to promote DCIS progression. Some of this include the generation of genetically stable c-MET CRISP/R Cas9 KO DCIS.com, HCC1937, and MDA_MB_231 triple negative / basal like breast cancer cells. The use of Merestinib, a type II pharmacological c-MET inhibitor that we show to be effective in vitro an in vitro to block migration, proliferation, survival, growth, and a decrease in formation of invasive lesions associate with impaired consumption of glycolytic metabolites. To our knowledge, we are

the first ones to report the use of Merestinib to evaluate the effects of c-MET function, and glycolysis in breast ductal carcinoma in situ. Additionally, we have used different approaches to study metabolism including global metabolomic analysis, IC-MS and assessing metabolic flux in real time by using the SeaHorse XF24 analyzer. Taken together, our studies are both novel and significative and they provide alternative approaches to narrow our knowledge gap regarding the molecular mechanisms by which DCIS progresses. Such approaches include the concept of G-Coupled receptors activating receptor tyrosine kinases, and their effect on metabolic alteration that could drive the progression of the disease.

Concluding remarks

In summary, these results demonstrate that CCL2/CCR2 modulate c-MET activity and glycolysis which fuels biological processes that are crucial for DCIS progression. Therefore, this study elucidates potential novel therapeutic targets for ductal carcinoma in situ cases with high expression of CCR2 and c-MET.

Implication: This project identifies a unique association between CCL2/CCR2 expression, c-MET activity, and enhancement of glycolysis with important implications into prognosis and potential treatment of DCIS progression. These associations can be considered as novel molecular markers to predict DCIS transition to IDC. Additionally, it has the potential to provide alternative therapeutic targets for DCIS patients expressing high levels of CCR2 and c-MET.

References

1. Society, A.C., *American Cancer Society. Breast Cancer Facts & Figures 2017-2018. Atlanta.* American Cancer Society, 2017.
2. DC, A., *Ductal carcinoma in situ: terminology, classification, and natural history.* Journal of the National Cancer Institute . Monographs, 2010(41): p. 134-8.
3. Allred DC, M.S., Fuqua SA., *Histological and biological evolution of human premalignant breast disease.* Endocrine - Related Cancer, 2001. **8**(1): p. 47-61.
4. Allred DC, W.Y., Mao S, Nagtegaal ID, Lee S, Perou CM, Mohsin SK, O'Connell P, Tsimelzon A, Medina D., *Ductal carcinoma in situ and the emergence of diversity during breast cancer evolution.* Clinical Cancer Research, 2008. **14**(2): p. 370-8.
5. Leonard GD, S.S., *Ductal carcinoma in situ, complexities and challenges.* Journal of the National Cancer Institute 2004. **96**(12): p. 906-20.
6. Allred DC, M.S., *Biological features of premalignant disease in the human breast.* Journal of Mammary Gland Biology and Neoplasia, 2000. **5**(4): p. 351-64.
7. Lari, S.A., & Kuerer, H. M. , *Biological Markers in DCIS and Risk of Breast Recurrence: A Systematic Review.* Journal of Cancer, 2011. **2**: p. 232-261.
8. R., B.L.J.a.B.G., *High- Grade Ductal Carcinoma in Situ: An Overview for the Radiologist.* Journal of the American Osteopathic College of Radiology, 2013. **2**(1): p. 18-25.
9. Jansen S A , C.S.D., Fan X , Krausz T, Zamora M, Foxley S, River J, Newstead G M, and Karczmar G S, *Detection of in situ mammary cancer in a transgenic mouse model: in vitro and in vivo MRI studies demonstrate histopathologic correlation.* Phy Med Biol, 2008. **53**(19): p. 5481-5493.
10. Fan, X., et al., *Mammary cancer initiation and progression studied with magnetic resonance imaging.* Breast Cancer Research, 2014. **16**(6): p. 495.
11. Jagannathan NR, S.U., *Breast Tissue Metabolism by Magnetic Resonance Spectroscopy.* Metabolites, 2017. **7**(2).
12. Noguerol Martín, S.-G.J., Martínez Barbero JP, García-Figueiras R, Baleato-González S, Luna A., *Clinical Imaging of Tumor Metabolism with ^{1}H Magnetic Resonance Spectroscopy.* Magnetic Resonance Imaging Clinics of North America, 2016. **24**(1): p. 57-86.
13. Farnie G, C.R., Spence K, Pinnock N, Brennan K, Anderson NG, Bundred NJ., *Novel cell culture technique for primary ductal carcinoma in situ: role of Notch and epidermal growth factor receptor signaling pathways.* Journal of the National Cancer Institute, 2007. **99**(8): p. 616-27.
14. Hu M, Y.J., Carroll DK, Weremowicz S, Chen H, Carrasco D, Richardson A, Violette S, Nikolskaya T, Nikolsky Y, Bauerlein EL, Hahn WC, Gelman RS, Allred C, Bissell MJ, Schnitt S, Polyak K., *Regulation of in situ to invasive breast carcinoma transition.* Cancer Cell, 2008. **13**(5): p. 394-406.
15. Tait LR, P.R., Santner SJ, Heppner GH, Heng HH, Rak JW, Miller FR., *Dynamic stromal-epithelial interactions during progression of MCF10DCIS.com xenografts.* International Journal of Cancer, 2007. **120**(10): p. 2127-34.

16. Charlotte, G.P.B.a.K., *Disease models of breast cancer.* Drug Discovery today: Disease models, 2004. **1**(1): p. 9-16.
17. Sorlie T, Tibshirani R, Parker J, Hastie T, Marron JS, Nobel A, Deng S, Johnsen H, Pesich R, Geisler S, Demeter J, Perou CM, Lonning PE, Brown PO, Borresen-Dale AL, Botstein D. Repeated observation of breast tumor subtypes in independent gene expression data sets. Proc Natl Acad Sci U S A. 2003;100(14):8418-23. Epub 2003/06/28. doi: 10.1073/pnas.0932692100. PubMed PMID: 12829800; PMCID: 166244.
18. Sorlie T, Perou CM, Tibshirani R, Aas T, Geisler S, Johnsen H, Hastie T, Eisen MB, van de Rijn M, Jeffrey SS, Thorsen T, Quist H, Matese JC, Brown PO, Botstein D, Eystein Lonning P, Borresen-Dale AL. Gene expression patterns of breast carcinomas distinguish tumor subclasses with clinical implications. Proc Natl Acad Sci U S A. 2001;98(19):10869-74. Epub 2001/09/13. doi: 10.1073/pnas.191367098. PubMed PMID: 11553815; PMCID: 58566.
19. Cheang MC, Chia SK, Voduc D, Gao D, Leung S, Snider J, Watson M, Davies S, Bernard PS, Parker JS, Perou CM, Ellis MJ, Nielsen TO. Ki67 index, HER2 status, and prognosis of patients with luminal B breast cancer. J Natl Cancer Inst. 2009;101(10):736-50. doi: 10.1093/jnci/djp082. PubMed PMID: 19436038; PMCID: 2684553.
20. Aleskandarany MA, Green AR, Benhasouna AA, Barros FF, Neal K, Reis-Filho JS, Ellis IO, Rakha EA. Prognostic value of proliferation assay in the luminal, HER2-positive, and triple-negative biologic classes of breast cancer. Breast Cancer Res. 2012;14(1):R3. doi: 10.1186/bcr3084. PubMed PMID: 22225836; PMCID: 3496118.
21. Lesurf R, Aure MR, Mork HH, Vitelli V, Oslo Breast Cancer Research C, Lundgren S, Borresen-Dale AL, Kristensen V, Warnberg F, Hallett M, Sorlie T. Molecular Features of Subtype-Specific Progression from Ductal Carcinoma In Situ to Invasive Breast Cancer. Cell reports. 2016;16(4):1166-79. doi: 10.1016/j.celrep.2016.06.051. PubMed PMID: 27396337.
22. Zhou W, Jirstrom K, Amini RM, Fjallskog ML, Sollie T, Lindman H, Sorlie T, Blomqvist C, Warnberg F. Molecular subtypes in ductal carcinoma in situ of the breast and their relation to prognosis: a population-based cohort study. BMC Cancer. 2013;13:512. doi: 10.1186/1471-2407-13-512. PubMed PMID: 24171825; PMCID: PMC4228470.
23. Sharaf Aldeen B, Feng J, Wu Y, Nassar Warzecha H. Molecular subtypes of ductal carcinoma in situ in African American and Caucasian American women: distribution and correlation with pathological features and outcome. Cancer epidemiology. 2013;37(4):474-8. doi: 10.1016/j.canep.2013.03.018. PubMed PMID: 23639792.
24. Behbod F, K.F., LaMarca H, Edwards D, Kerbawy S, Heestand JC, Young E, Mukhopadhyay P, Yeh HW, Allred DC, Hu M, Polyak K, Rosen JM, Medina D., *An intraductal human-in-mouse transplantation model mimics the subtypes of ductal carcinoma in situ.* Breast Cancer Research, 2009. **11**(5).
25. Miller FR, S.S., Tait L, Dawson PJ., *MCF10DCIS.com xenograft model of human comedo ductal carcinoma in situ.* Journal of the National Cancer Institute, 2000. **92**(14): p. 1185-6.

26. Sflomos G, D.V., Metsalu T, Jeitziner R, Battista L, Scabia V, Raffoul W, Delaloye JF, Treboux A, Fiche M, Vilo J, Ayyanan A, Brisken C., *A Preclinical Model for ERα-Positive Breast Cancer Points to the Epithelial Microenvironment as Determinant of Luminal Phenotype and Hormone Response.* Cancer Cell, 2016. **29**(3): p. 407-422.
27. Zabel BA, Z.L., Ohyama T, Allen SJ, Cichy J, Handel TM, Butcher EC., *Chemoattractants, extracellular proteases, and the integrated host defense response.* Experimental Hematology, 2006. **34**(8): p. 1021-32.
28. Laing KJ, S.C., *Chemokines.* Developmental and Comparative immunology, 2004. **28**(5): p. 443-60.
29. Gillitzer R1, G.M., *Chemokines in cutaneous wound healing.* Journal of Leukocite Biology, 2001. **69**(4): p. 513-21.
30. Hembruff SL, C.N., *Chemokine signaling in cancer: Implications on the tumor microenvironment and therapeutic targeting.* Cancer Therapy, 2009. **7**(A): p. 254-267.
31. DeVries ME, K.A., Xu L, Ran L, Robinson J, Kelvin DJ., *Defining the origins and evolution of the chemokine/chemokine receptor system.* Journal of Immunology, 2006. **176**(1): p. 401-15.
32. Roca H, V.Z., Sud S, Craig MJ, Ying C, Pienta KJ., *CCL2 and interleukin-6 promote survival of human CD11b+ peripheral blood mononuclear cells and induce M2-type macrophage polarization.* Journal of Biological Chemistry, 2009. **284**(49): p. 34342-54.
33. Ernst C A, Z.Y.J., Hancock P R, Rutledge B J, Corless C L and Rollins B J, *Biochemical and biologic characterization of murine monocyte chemoattractant protein-1. Identification of two functional domains.* Journal of Immunology, 1994. **152**(7): p. 3541.
34. Huang DR, W.J., Kivisakk P, Rollins BJ, Ransohoff RM., *Absence of monocyte chemoattractant protein 1 in mice leads to decreased local macrophage recruitment and antigen-specific T helper cell type 1 immune response in experimental autoimmune encephalomyelitis.* Journal of Experimental Medicine, 2001. **193**(6): p. 713-26.
35. Fife BT, H.G., Kuziel WA, Karpus WJ., *Cc Chemokine Receptor 2 Is Critical for Induction of Experimental Autoimmune Encephalomyelitis.* Journal of Experimental Medicine, 2000. **192**(6): p. 899-905.
36. Satish L. Deshmane, S.K., Shohreh Amini, and Bassel E. Sawaya, *Monocyte Chemoattractant Protein-1 (MCP-1): An Overview.* Journal of Interferon adn Cytokine Research, 2009. **29**(6): p. 313-326.
37. Tanaka T, T.M., Ariyoshi K, Morimoto K., *Monocyte chemoattractant protein-1/CC chemokine ligand 2 enhances apoptotic cell removal by macrophages through Rac1 activation.* Biochemical and Biophysical Research Communications, 2010. **399**(4): p. 677-82.
38. Raman D, S.-D.T., Richmond A., *Chemokines in health and disease.* Experimental Cell Research, 2011. **317**(5): p. 575-89.
39. Bartoli C, C.M., Pellissier JF, Figarella-Branger D., *CCR2A and CCR2B, the two isoforms of the monocyte chemoattractant protein-1 receptor are up-regulated and*

expressed by different cell subsets in idiopathic inflammatory myopathies. Acta Neuropathol, 2001. **102**(4): p. 385-92.
40. Vlahakis SR, V.-K.A., Gomez T, Vanegas M, Vlahakis N, Paya CV. , *G protein-coupled chemokine receptors induce both survival and apoptotic signaling pathways.* J Immunol., 2002. **15**(10): p. 5546-54.
41. Mellado M, R.-F.J., Aragay A, del Real G, Martín AM, Vila-Coro AJ, Serrano A, Mayor F Jr, Martínez-A C. , *The chemokine monocyte chemotactic protein 1 triggers Janus kinase 2 activation and tyrosine phosphorylation of the CCR2B receptor.* J Immunol. , 1998. **161**(2): p. 805-13.
42. Aragay AM, M.M., Frade JM, Martin AM, Jimenez-Sainz MC, Martinez-A C, Mayor F Jr., *Monocyte chemoattractant protein-1-induced CCR2B receptor desensitization mediated by the G protein-coupled receptor kinase 2.* Proc Natl Acad Sci U S A. , 1998. **95**(6): p. 2985-90.
43. Biswas P, D.F., Bernasconi S, Mengozzi M, Cota M, Polentarutti N, Mantovani A, Lazzarin A, Sozzani S, Poli G. , *Interleukin-6 induces monocyte chemotactic protein-1 in peripheral blood mononuclear cells and in the U937 cell line. .* Blood., 1998. **91**(1): p. 258-65.
44. Hacke, K., et al., *Regulation of MCP-1 chemokine transcription by p53.* Molecular Cancer, 2010. **9**(1): p. 82.
45. Johnson, Z.P., Christine & Weiss-Haljiti, Cornelia & Rintelen, Felix & Ji, Hong & Rückle, Thomas & Camps, M & Wells, Tim & K Schwarz, M & E I Proudfoot, A & Rommel, C, *Chemokine inhibition - Why, when, where, which and how?* Biochemical Society Transactions, 2004. **32**(366-77).
46. Fang WB, J.I., Zou A, Lambert D, Dendukuri P, Cheng N., *CCL2/CCR2 chemokine signaling coordinates survival and motility of breast cancer cells through Smad3 protein- and p42/44 mitogen-activated protein kinase (MAPK)-dependent mechanisms.* Journal of Biological Chemistry, 2012. **287**(43): p. 36593-608.
47. Yao M, Y.E., Staggs V, Fan F, Cheng N., *Elevated expression of chemokine C-C ligand 2 in stroma is associated with recurrent basal-like breast cancers.* Modern Pathology, 2016. **29**(8): p. 810-23.
48. Lim SY, Y.A., Gordon-Weeks AN, Muschel RJ., *Targeting the CCL2-CCR2 signaling axis in cancer metastasis.* Oncotarget, 2016. **7**(19): p. 28697-710.
49. Zhang J, L.Y., Pienta KJ., *Multiple Roles of Chemokine (C-C Motif) Ligand 2 in Promoting Prostate Cancer Growth* Journal of the National Cancer Institute, 2010. **102**(8): p. 522-8.
50. Ueno T, T.M., Saji H, Muta M, Bando H, Kuroi K, Koike M, Inadera H, Matsushima K., *Significance of macrophage chemoattractant protein-1 in macrophage recruitment, angiogenesis, and survival in human breast cancer.* Clinical Cancer Research, 2000. **6**(8): p. 3282-9.
51. Liang Y, B.A., and Gupta N., *CC chemokine receptor-2A is frequently overexpressed in glioblastoma.* Journal of Neuro-Oncology, 2008. **86**(2): p. 153-163.
52. Fujimoto H, S.T., Ishii G, Ikehara A, Nagashima T, Miyazaki M, Ochiai A., *Stromal MCP-1 in mammary tumors induces tumor-associated macrophage infiltration and*

contributes to tumor progression. International Journal of Cancer, 2009. **125**(6): p. 1276-84.
53. Lu Y, C.Z., Xiao G, Liu Y, Keller ET, Yao Z, Zhang J., *CCR2 expression correlates with prostate cancer progression.* Journal of Cellular Biochemistry, 2007. **101**(3): p. 676-85.
54. Ghilardi G, B.M., La Torre A, Battaglioli L, Scorza R. , *Breast cancer progression and host polymorphisms in the chemokine system: role of the macrophage chemoattractant protein-1 (MCP-1) -2518 G allele.* Clin Chem. , 2005. **51**(2): p. 452-5.
55. Banin-Hirata BK, L.-G.R., Oda JM, de Oliveira CE, Campos CZ, Mazzuco TL, Borelli SD, Ceribelli JR, Watanabe MA. , *CCR2-V64I genetic polymorphism: a possible involvement in HER2+ breast cancer.* Clin Exp Med. , 2016. **16**(2): p. 139-45.
56. Jiménez-Sainz, M.C., Fast, B., Mayor, F., Jr, & Aragay, A. M. , *Signaling pathways for monocyte chemoattractant protein 1-mediated extracellular signal-regulated kinase activation.* Molecular pharmacology, 2003. **64**(3): p. 773-782.
57. Zafiropoulos A, C.N., Passam AM, Spandidos DA., *Significant involvement of CCR2-64I and CXCL12-3a in the development of sporadic breast cancer.* Journal of Medical Genetics, 2004. **41**(5): p. 1-5.
58. Chavey C, B.F., Gourgou-Bourgade S, Burlinchon S, Boissière F, Laune D, Roques S, Lazennec G., *Oestrogen receptor negative breast cancers exhibit high cytokine content.* Breast Cancer Research, 2007. **9**(1): p. 1-11.
59. Lebrecht A, G.C., Lantzsch T, Ludwig E, Hefler L, Ulbrich E and Koelbl H. , *Monocyte Chemoattractant Protein-1 Serum Levels in Patients with Breast Cancer.* Tumor Biology, 2004. **25**(1-2): p. 14-7.
60. Wang J, Z.Z., Xu SF, He Q, Shao YG, Ji M, Yang L, Bao W. , *Expression of CCL2 is significantly different in five breast cancer genotypes and predicts patient outcome. .* Int J Clin Exp Med. , 2015. **8**(9): p. 15684-91.
61. Dutta P, S.M., Paico K, Wu Y, Vadgama JV. , *MCP-1 is overexpressed in triple-negative breast cancers and drives cancer invasiveness and metastasis. .* Breast Cancer Res Treat., 2018. **170**(3): p. 477-486.
62. Brummer, G., et al., *Chemokine Signaling Facilitates Early-Stage Breast Cancer Survival and Invasion through Fibroblast-Dependent Mechanisms.* Mol Cancer Res, 2018. **16**(2): p. 296-308.
63. Fang WB, Y.M., Brummer G, Acevedo D, Alhakamy N, Berkland C, Cheng N., *Targeted gene silencing of CCL2 inhibits triple negative breast cancer progression by blocking cancer stem cell renewal and M2 macrophage recruitment.* Oncotarget, 2016. **7**(31): p. 49349-49367.
64. Borsig L, W.M., Roblek M, Lorentzen A, Heikenwalder M., *Inflammatory chemokines and metastasis--tracing the accessory.* Oncogene, 2014. **33**(25): p. 3217-24
65. Hembruff SL, J.I., Yang L, Cheng N., *Loss of transforming growth factor-beta signaling in mammary fibroblasts enhances CCL2 secretion to promote mammary tumor progression through macrophage-dependent and -independent mechanisms.* Neoplasia, 2010. **12**(5): p. 425-33.

66. Fang WB, Y.M., Jokar I, Alhakamy N, Berkland C, Chen J, Brantley-Sieders D, Cheng N., *The CCL2 chemokine is a negative regulator of autophagy and necrosis in luminal B breast cancer cells.* Breast Cancer Research and Treatment 2015. **150**(2): p. 309-20.
67. Qian BZ, L.J., Zhang H, Kitamura T, Zhang J, Campion LR, Kaiser EA, Snyder LA, Pollard JW., *CCL2 recruits inflammatory monocytes to facilitate breast-tumour metastasis.* Nature, 2011. **475**(7355): p. 222-5.
68. Fang WB, J.I., Chytil A, Moses HL, Abel T, Cheng N., *Loss of one Tgfbr2 allele in fibroblasts promotes metastasis in MMTV: polyoma middle T transgenic and transplant mouse models of mammary tumor progression.* Clinical & Experimetnal Metastasis, 2011. **28**(4): p. 351-66.
69. Zhang Y, X.M., Jin K, Wang S, Wei H, Fan C, Wu Y, Li X, Li X, Li G, Zeng Z, Xiong W., *Function of the c-Met receptor tyrosine kinase in carcinogenesis and associated therapeutic opportunities.* Molecular Cancer, 2018. **17**(1).
70. Stoker M, G.E., Perryman M, Gray J., *Scatter factor is a fibroblast-derived modulator of epithelial cell mobility.* Nature, 1987. **327**(6119): p. 239-42.
71. Nakamura T, N.T., Hagiya M, Seki T, Shimonishi M, Sugimura A, Tashiro K, Shimizu S., *Molecular cloning and expression of human hepatocyte growth factor.* Nature, 1989. **342**(6248): p. 440-3.
72. Zarnegar R, M.G., *Purification and biological characterization of human hepatopoietin A, a polypeptide growth factor for hepatocytes.* Cancer Research, 1989. **49**(12): p. 3314-20.
73. Jin L, F.A., Schnitt SJ, Yao Y, Joseph A, Lamszus K, Park M, Goldberg ID, Rosen EM., *Expression of scatter factor and c-met receptor in benign and malignant breast tissue.* Cancer, 1997. **79**(4): p. 749-60.
74. Jedeszko C, V.B., Podgorski I, Sloane BF., *Fibroblast hepatocyte growth factor promotes invasion of human mammary ductal carcinoma in situ.* Cancer Research, 2009. **69**(23): p. 9148-55.
75. Lindemann K, R.J., Nährig J, Kort E, Leeser B, Annecke K, Welk A, Schäfer J, Vande Woude GF, Lengyel E, Harbeck N., *Differential expression of c-Met, its ligand HGF/SF and HER2/neu in DCIS and adjacent normal breast tissue.* Histopathology, 2007. **51**(1): p. 54-62.
76. Lengyel E, P.D., Resau JH, Gauger K, Welk A, Lindemann K, Salanti G, Richter T, Knudsen B, Vande Woude GF, Harbeck N., *C-Met overexpression in node-positive breast cancer identifies patients with poor clinical outcome independent of Her2/neu.* International Journal of Cancer, 2005. **113**(4): p. 678-82.
77. Beviglia L, M.K., Lin CS, Ziober BL, Kramer RH., *Expression of the c-Met/HGF receptor in human breast carcinoma: correlation with tumor progression.* International Journal of Cancer, 1997. **74**(3): p. 301-9.
78. Ho-Yen CM, J.J., Kermorgant S. , *The clinical and functional significance of c-Met in breast cancer: a review. .* Breast Cancer Research, 2015. **17**(1): p. 52.
79. Organ SL, T.M., *An overview of the c-MET signaling pathway.* Therapeutic Advances in Medical Oncology, 2011. **3**(1).
80. Casbas-Hernandez P, D.A.M., Roman-Perez E, Brauer HA, McNaughton K, Miller SM, Chhetri RK, Oldenburg AL, Fleming JM, Amos KD, Makowski L, Troester MA., *Role of HGF in epithelial-stromal cell interactions during progression from*

benign breast disease to ductal carcinoma in situ. Breast Cancer Research, 2013. **15**(5).
81. Graveel CR, T.D., Vande Woude GF. , *MET: a critical player in tumorigenesis and therapeutic target. .* Cold Spring Harb Perspect Biol., 2013. **5**(7): p. a009209.
82. Peschard P, P.M., *From Tpr-Met to Met, tumorigenesis and tubes. .* Oncogene. , 2007. **26**(9): p. 1276-85.
83. Zhang, J. and A. Babic, *Regulation of the MET oncogene: molecular mechanisms.* Carcinogenesis, 2016. **37**(4): p. 345-355.
84. Tuck, A.B., Park, M., Sterns, E. E., Boag, A., & Elliott, B. E. , *Coexpression of hepatocyte growth factor and receptor (Met) in human breast carcinoma.* The American journal of pathology, 1996. **148**(1): p. 225-232.
85. Edakuni G, S.E., Satoh T, Tokunaga O, Miyazaki K. , *Expression of the hepatocyte growth factor/c-Met pathway is increased at the cancer front in breast carcinoma.* Pathol Int., 2001. **51**(3): p. 172-8.
86. Hochgräfe F, Z.L., O'Toole SA, Browne BC, Pinese M, Porta Cubas A, Lehrbach GM, Croucher DR, Rickwood D, Boulghourjian A, Shearer R, Nair R, Swarbrick A, Faratian D, Mullen P, Harrison DJ, Biankin AV, Sutherland RL, Raftery MJ, Daly RJ. , *Tyrosine phosphorylation profiling reveals the signaling network characteristics of Basal breast cancer cells.* Cancer Res., 2010. **70**(22): p. 9391-401.
87. Raghav, K.P., Wang, W., Liu, S., Chavez-MacGregor, M., Meng, X., Hortobagyi, G. N., Mills, G. B., Meric-Bernstam, F., Blumenschein, G. R., Jr, & Gonzalez-Angulo, A. M. , *cMET and phospho-cMET protein levels in breast cancers and survival outcomes. .* Clinical cancer research : an official journal of the American Association for Cancer Research, , 2012. **18**(8): p. 2269–2277.
88. Martínez-Reyes I, C.N., *Mitochondrial TCA cycle metabolites control physiology and disease.* Nat Commun., 2020. **11**(1): p. 102.
89. Liberti, M.V., and Jason W Locasale. , *"The Warburg Effect: How Does it Benefit Cancer Cells?.".* Trends in biochemical sciences, 2016. **41**(3): p. 211-218
90. Warburg, O., Wind, F., & Negelein, E. , *THE METABOLISM OF TUMORS IN THE BODY. .* The Journal of general physiology, 1927. **8**(6): p. 519–530.
91. Richardson, A.D., Yang, C., Osterman, A., & Smith, J. W. , *Central carbon metabolism in the progression of mammary carcinoma. .* Breast cancer research and treatment,, 2008. **110**(2): p. 297–307.
92. Morandi A, C.P.J., *Metabolic implication of tumor:stroma crosstalk in breast cancer. .* Mol Med (Berl). , 2014. **92**(2): p. 117-26.
93. Woo YM, Shin Y, Lee EJ, Lee S, Jeong SH, Kong HK, Park EY, Kim HK, Han J, Chang M, Park JH. Inhibition of Aerobic Glycolysis Represses Akt/mTOR/HIF-1alpha Axis and Restores Tamoxifen Sensitivity in Antiestrogen-Resistant Breast Cancer Cells. PLoS One. 2015;10(7):e0132285. doi: 10.1371/journal.pone.0132285. PubMed PMID: 26158266; PMCID: PMC4497721.
94. Tian C, Yuan Z, Xu D, Ding P, Wang T, Zhang L, Jiang Z. Inhibition of glycolysis by a novel EGFR/HER2 inhibitor KU004 suppresses the growth of HER2+ cancer. Exp Cell Res. 2017;357(2):211-21. doi: 10.1016/j.yexcr.2017.05.019. PubMed PMID: 28532652.

95. Shen L, O'Shea JM, Kaadige MR, Cunha S, Wilde BR, Cohen AL, Welm AL, Ayer DE. Metabolic reprogramming in triple-negative breast cancer through Myc suppression of TXNIP. Proc Natl Acad Sci U S A. 2015;112(17):5425-30. doi: 10.1073/pnas.1501555112. PubMed PMID: 25870263; PMCID: PMC4418882.
96. Lim SO, Li CW, Xia W, Lee HH, Chang SS, Shen J, Hsu JL, Raftery D, Djukovic D, Gu H, Chang WC, Wang HL, Chen ML, Huo L, Chen CH, Wu Y, Sahin A, Hanash SM, Hortobagyi GN, Hung MC. EGFR Signaling Enhances Aerobic Glycolysis in Triple-Negative Breast Cancer Cells to Promote Tumor Growth and Immune Escape. Cancer Res. 2016;76(5):1284-96. doi: 10.1158/0008-5472.CAN-15-2478. PubMed PMID: 26759242; PMCID: PMC4775355.
97. Rattigan YI, Patel BB, Ackerstaff E, Sukenick G, Koutcher JA, Glod JW, Banerjee D. Lactate is a mediator of metabolic cooperation between stromal carcinoma associated fibroblasts and glycolytic tumor cells in the tumor microenvironment. Exp Cell Res. 2012;318(4):326-35. doi: 10.1016/j.yexcr.2011.11.014. PubMed PMID: 22178238; PMCID: PMC3402174.
98. Vander Heiden MG, C.L., Thompson CB., *Understanding the Warburg effect: the metabolic requirements of cell proliferation.* Science, 2009. **324**(5930): p. 1029-33.
99. Li XB, G.J., Zhou QH., *Review of aerobic glycolysis and its key enxymes - new targets for lunh cancer therapy.* Thoracic Cancer, 2015. **6**(1): p. 17-24.
101. Pang, J.M., K.L. Gorringe, and S.B. Fox, *Ductal carcinoma in situ - update on risk assessment and management.* Histopathology, 2016. **68**(1): p. 96-109.
102. Park, T.S. and E.S. Hwang, *Current Trends in the Management of Ductal Carcinoma In Situ.* Oncology (Williston Park), 2016. **30**(9).
103. Virnig, B.A., et al., *Ductal carcinoma in situ of the breast: a systematic review of incidence, treatment, and outcomes.* J Natl Cancer Inst, 2010. **102**(3): p. 170-8.
104. Khan, S., et al., *Are We Overtreating Ductal Carcinoma in Situ (DCIS)?* Ann Surg Oncol, 2016.
105. Goldstein, S.N., *Controversies in pathology in early-stage breast cancer.* Semin Radiat Oncol, 2011. **21**(1): p. 20-5.
106. Kerlikowske, K., et al., *Biomarker expression and risk of subsequent tumors after initial ductal carcinoma in situ diagnosis.* J Natl Cancer Inst, 2010. **102**(9): p. 627-37.
107. Palomino, D.C. and L.C. Marti, *Chemokines and immunity.* Einstein (Sao Paulo), 2015. **13**(3): p. 469-73.
108. Balkwill, F.R., *The chemokine system and cancer.* J Pathol, 2012. **226**(2): p. 148-57.
109. Ansari, A.W., A. Kamarulzaman, and R.E. Schmidt, *Multifaceted Impact of Host C-C Chemokine CCL2 in the Immuno-Pathogenesis of HIV-1/M. tuberculosis Co-Infection.* Front Immunol, 2013. **4**: p. 312.
110. Yao, M., et al., *Elevated expression of chemokine C-C ligand 2 in stroma is associated with recurrent basal-like breast cancers.* Mod Pathol, 2016.
111. Lim, S.Y., et al., *Targeting the CCL2-CCR2 signaling axis in cancer metastasis.* Oncotarget, 2016. **7**(19): p. 28697-710.
112. Borsig, L., et al., *Inflammatory chemokines and metastasis--tracing the accessory.* Oncogene, 2014. **33**(25): p. 3217-24.

113. Fang, W.B., et al., *CCL2/CCR2 chemokine signaling coordinates survival and motility of breast cancer cells through Smad3 protein- and p42/44 mitogen-activated protein kinase (MAPK)-dependent mechanisms.* J Biol Chem, 2012. **287**(43): p. 36593-608.
114. Ginestier C, H.M., Charafe-Jauffet E, Monville F, Dutcher J, Brown M, Jacquemier J, Viens P, Kleer C, Liu S, Schott A, Hayes D, Birmbaum D, Wicha MS, Dontu G., *ALDH1 is a marker of normal and malignant human mammary stem cells and a predictor of poor clinical outcome.* Cell Stem Cell, 2007. **1**(5): p. 555-67.
115. Jeyaraju, D.V., et al., *Hax1 lacks BH modules and is peripherally associated to heavy membranes: implications for Omi/HtrA2 and PARL activity in the regulation of mitochondrial stress and apoptosis.* Cell Death Differ, 2009. **16**(12): p. 1622-9.
116. O'Hare, M.J., et al., *Conditional immortalization of freshly isolated human mammary fibroblasts and endothelial cells.* Proc Natl Acad Sci U S A, 2001. **98**(2): p. 646-51.
117. Miller, F.R., et al., *MCF10DCIS.com xenograft model of human comedo ductal carcinoma in situ.* J Natl Cancer Inst, 2000. **92**(14): p. 1185-6.
118. Ethier, S.P., C.A. Ammerman, and M.L. Dziubinski, *Isolation and Culture of Human Breast Cancer Cells from Primary Tumors and Mestases*, in *Methods in Mammary Gland Biology and Breast Cancer Research*, B.B.A. Margot M. Ip, Editor. 2000, Kluwer Academic /Plenum Publishers: New York.
119. Behbod, F., et al., *An intraductal human-in-mouse transplantation model mimics the subtypes of ductal carcinoma in situ.* Breast Cancer Res, 2009. **11**(5): p. R66.
120. Cheng, N. and D.L. Lambert, *Mammary transplantation of stromal cells and carcinoma cells in C57BL/6J mice.* J Vis Exp, 2011(54).
121. Cheng, N., et al., *Loss of TGF-beta type II receptor in fibroblasts promotes mammary carcinoma growth and invasion through upregulation of TGF-alpha-, MSP- and HGF-mediated signaling networks.* Oncogene, 2005. **24**(32): p. 5053-68.
122. Mardekian, S.K., A. Bombonati, and J.P. Palazzo, *Ductal carcinoma in situ of the breast: the importance of morphologic and molecular interactions.* Hum Pathol, 2016. **49**: p. 114-23.
123. Sambade, M.J., et al., *Lapatinib in combination with radiation diminishes tumor regrowth in HER2+ and basal-like/EGFR+ breast tumor xenografts.* Int J Radiat Oncol Biol Phys, 2010. **77**(2): p. 575-81.
124. Valdez, K.E., et al., *Human primary ductal carcinoma in situ (DCIS) subtype-specific pathology is preserved in a mouse intraductal (MIND) xenograft model.* J Pathol, 2011. **225**(4): p. 565-73.
125. Damiani, S., et al., *Myoepithelial cells and basal lamina in poorly differentiated in situ duct carcinoma of the breast. An immunocytochemical study.* Virchows Arch, 1999. **434**(3): p. 227-34.
126. Lazard, D., et al., *Expression of smooth muscle-specific proteins in myoepithelium and stromal myofibroblasts of normal and malignant human breast tissue.* Proc Natl Acad Sci U S A, 1993. **90**(3): p. 999-1003.
127. Patarroyo, M., K. Tryggvason, and I. Virtanen, *Laminin isoforms in tumor invasion, angiogenesis and metastasis.* Semin Cancer Biol, 2002. **12**(3): p. 197-207.

128. Ioachim, E., et al., *Immunohistochemical expression of extracellular matrix components tenascin, fibronectin, collagen type IV and laminin in breast cancer: their prognostic value and role in tumour invasion and progression.* Eur J Cancer, 2002. **38**(18): p. 2362-70.
129. Park, S.Y., H.M. Kim, and J.S. Koo, *Differential expression of cancer-associated fibroblast-related proteins according to molecular subtype and stromal histology in breast cancer.* Breast Cancer Res Treat, 2015. **149**(3): p. 727-41.
130. Sugimoto, H., et al., *Identification of fibroblast heterogeneity in the tumor microenvironment.* Cancer Biol Ther, 2006. **5**(12): p. 1640-6.
131. Carvalho, I., et al., *Overexpression of platelet-derived growth factor receptor alpha in breast cancer is associated with tumour progression.* Breast Cancer Res, 2005. **7**(5): p. R788-95.
132. Bussard, K.M., et al., *Tumor-associated stromal cells as key contributors to the tumor microenvironment.* Breast Cancer Res, 2016. **18**(1): p. 84.
133. Fang, W.B., M. Yao, and N. Cheng, *Priming cancer cells for drug resistance: role of the fibroblast niche.* Front Biol (Beijing), 2014. **9**(2): p. 114-126.
134. Zhang, C., et al., *Advancing bioluminescence imaging technology for the evaluation of anticancer agents in the MDA-MB-435-HAL-Luc mammary fat pad and subrenal capsule tumor models.* Clin Cancer Res, 2009. **15**(1): p. 238-46.
135. Cheng, N., et al., *Enhanced hepatocyte growth factor signaling by type II transforming growth factor-beta receptor knockout fibroblasts promotes mammary tumorigenesis.* Cancer Res, 2007. **67**(10): p. 4869-77.
136. Livasy, C.A., et al., *Phenotypic evaluation of the basal-like subtype of invasive breast carcinoma.* Mod Pathol, 2006. **19**(2): p. 264-71.
137. Szasz, A.M., et al., *Cross-validation of survival associated biomarkers in gastric cancer using transcriptomic data of 1,065 patients.* Oncotarget, 2016.
138. Hu, M., et al., *Regulation of in situ to invasive breast carcinoma transition.* Cancer Cell, 2008. **13**(5): p. 394-406.
139. Kimachi, K., M. Croft, and H.M. Grey, *The minimal number of antigen-major histocompatibility complex class II complexes required for activation of naive and primed T cells.* Eur J Immunol, 1997. **27**(12): p. 3310-7.
140. Viola, A. and A. Lanzavecchia, *T cell activation determined by T cell receptor number and tunable thresholds.* Science, 1996. **273**(5271): p. 104-6.
141. Capuani, F., et al., *Quantitative analysis reveals how EGFR activation and downregulation are coupled in normal but not in cancer cells.* Nat Commun, 2015. **6**: p. 7999.
142. Norton, N., et al., *Assessment of Tumor Heterogeneity, as Evidenced by Gene Expression Profiles, Pathway Activation, and Gene Copy Number, in Patients with Multifocal Invasive Lobular Breast Tumors.* PLoS One, 2016. **11**(4): p. e0153411.
143. Jedeszko, C., et al., *Fibroblast hepatocyte growth factor promotes invasion of human mammary ductal carcinoma in situ.* Cancer Res, 2009. **69**(23): p. 9148-55.
144. Farnie, G., et al., *Novel cell culture technique for primary ductal carcinoma in situ: role of Notch and epidermal growth factor receptor signaling pathways.* J Natl Cancer Inst, 2007. **99**(8): p. 616-27.

145. Grotendorst, G.R. and M.R. Duncan, *Individual domains of connective tissue growth factor regulate fibroblast proliferation and myofibroblast differentiation.* FASEB J, 2005. **19**(7): p. 729-38.
146. Vuga, L.J., et al., *WNT5A is a regulator of fibroblast proliferation and resistance to apoptosis.* Am J Respir Cell Mol Biol, 2009. **41**(5): p. 583-9.
147. Meran, S., et al., *Hyaluronan facilitates transforming growth factor-beta1-mediated fibroblast proliferation.* J Biol Chem, 2008. **283**(10): p. 6530-45.
148. Mariggio, M.A., et al., *Enhancement of fibroblast proliferation, collagen biosynthesis and production of growth factors as a result of combining sodium hyaluronate and aminoacids.* Int J Immunopathol Pharmacol, 2009. **22**(2): p. 485-92.
149. Rodriguez-Torres, M. and A.L. Allan, *Aldehyde dehydrogenase as a marker and functional mediator of metastasis in solid tumors.* Clin Exp Metastasis, 2016. **33**(1): p. 97-113.
150. Kilbride, S.M. and J.H. Prehn, *Central roles of apoptotic proteins in mitochondrial function.* Oncogene, 2013. **32**(22): p. 2703-11.
151. DeSantis CE, M.J., Gaudet MM, Newman LA, Miller KD, Goding Sauer A, Jemal A, Siegel RL. , *Breast cancer statistics, 2019.* CA Cancer J Clin. 2019 2019. **69**(6): p. 438-451.
152. Cowell CF, W.B., Sakr RA, Ng CK, Hicks J, King TA, Reis-Filho JS. , *Progression from ductal carcinoma in situ to invasive breast cancer: revisited. .* Mol Oncol., 2013. **7**(5): p. 859-69.
153. Virnig BA, T.T., Shamliyan T, Kane RL. J *Ductal carcinoma in situ of the breast: a systematic review of incidence, treatment, and outcomes. .* Natl Cancer Inst. , 2010. **102**(3): p. 170-8.
154. Rakovitch E, N.-M.S., Hanna W, Narod S, Thiruchelvam D, Saskin R, Spayne J, Taylor C, Paszat L. , *HER2/neu and Ki-67 expression predict non-invasive recurrence following breast-conserving therapy for ductal carcinoma in situ. .* Br J Cancer. , 2012. **13**(6): p. 1160-5.
155. Lari SA, K.H., *Biological Markers in DCIS and Risk of Breast Recurrence: A Systematic Review.* J Cancer. , 2011. **1**(2): p. 232-61.
156. Sørlie T, P.C., Tibshirani R, Aas T, Geisler S, Johnsen H, Hastie T, Eisen MB, van de Rijn M, Jeffrey SS, Thorsen T, Quist H, Matese JC, Brown PO, Botstein D, Lønning PE, Børresen-Dale AL. , *Gene expression patterns of breast carcinomas distinguish tumor subclasses with clinical implications.* Proc Natl Acad Sci U S A. , 2001. **11**(19): p. 10869-74.
157. Gershon, T.R., Crowther, A. J., Tikunov, A., Garcia, I., Annis, R., Yuan, H., Miller, C. R., Macdonald, J., Olson, J., & Deshmukh, M. , *Hexokinase-2-mediated aerobic glycolysis is integral to cerebellar neurogenesis and pathogenesis of medulloblastoma.* Cancer & metabolism, 2013. **1**(2): p. 1-17.
158. Lin S., S.L., Lyu X., Ai X., Du D., Su N., Li H., Zhang L., Yu J., Yuan S., *Lactate-activated macrophages induced aerobic glycolysis and epithelial-mesenchymal transition in breast cancer by regulation of CCL5-CCR5 axis: a positive metabolic feedback loop. .* Oncotarget, 2017. **8**: p. 110426-110443.
159. Gillies RJ, R.I., Gatenby RA., *Causes and consequences of increased glucose metabolism of cancers.* J Nucl Med. , 2008. **2**: p. 24S-42S.

160. Zou K, W.Y., Hu Y, Zheng L, Xu W, Li G. , *Specific tumor-derived CCL2 mediated by pyruvate kinase M2 in colorectal cancer cells contributes to macrophage recruitment in tumor microenvironment. .* Tumour Biol., 2017. **39**(3): p. 1010428317695962.
161. Draoui N, F.O., *Lactate shuttles at a glance: from physiological paradigms to anti-cancer treatments.* Dis Model Mech., 2011. **4**(6): p. 727-32.
162. Niranjan B, B.L., Yant J, Perusinghe N, Atherton A, Phippard D, Dale T, Gusterson B, Kamalati T. 1995 Sep;121(9):2897-908. PMID: 7555716., *HGF/SF: a potent cytokine for mammary growth, morphogenesis and development. .* Development., 1995. **121**(9): p. 2897-908.
163. Berdichevsky F, A.D., D'Souza B, Taylor-Papadimitriou J. , *Branching morphogenesis of human mammary epithelial cells in collagen gels. .* J Cell Sci. , 1994. **107**: p. 3557-68.
164. Soriano JV, P.M., Nakamura T, Orci L, Montesano R. , *Hepatocyte growth factor stimulates extensive development of branching duct-like structures by cloned mammary gland epithelial cells. .* J Cell Sci. , 1995. **108**: p. 413-30.
165. Charafe-Jauffret E, G.C., Monville F, Finetti P, Adélaïde J, Cervera N, Fekairi S, Xerri L, Jacquemier J, Birnbaum D, Bertucci F, *Gene expression profiling of breast cell lines identifies potential new basal markers.* Oncogene., 2006. **25**(15): p. 2273-84.
166. Gonçalves, A., Charafe-Jauffret, E., Bertucci, F., Audebert, S., Toiron, Y., Esterni, B., Monville, F., Tarpin, C., Jacquemier, J., Houvenaeghel, G., Chabannon, C., Extra, J. M., Viens, P., Borg, J. P., & Birnbaum, D. , *Protein profiling of human breast tumor cells identifies novel biomarkers associated with molecular subtypes. .* Molecular & cellular proteomics, 2008. **7**(8): p. 1420–1433.
167. Huang, Y., Fu, Z., Dong, W., Zhang, Z., Mu, J., & Zhang, J. , *Serum starvation-induces down-regulation of Bcl-2/Bax confers apoptosis in tongue coating-related cells in vitro. .* Molecular Medicine Reports, 2018. **17**: p. 5057-5064.
168. Hu, Q., Myers, M., Fang, W., Yao, M., Brummer, G., Hawj, J., Smart, C., Berkland, C., & Cheng, N. , *Role of ALDH1A1 and HTRA2 expression in CCL2/CCR2-mediated breast cancer cell growth and invasion. .* Biology open, 8(7), 2019. **8**(7).
169. Martin, P.L., Yin, J. J., Seng, V., Casey, O., Corey, E., Morrissey, C., Simpson, R. M., & Kelly, K. , *Androgen deprivation leads to increased carbohydrate metabolism and hexokinase 2-mediated survival in Pten/Tp53-deficient prostate cancer.* Oncogene,, 2017. **36**: p. 525–533.
170. Zhu L, B.S., Shahein A, Choudhury S, Liu W, Bhatia T, Baker RD, Lee T. , *Upregulation of non-canonical Wnt ligands and oxidative glucose metabolism in NASH induced by methionine-choline deficient diet. .* Trends Cell Mol Biol. , 2018. **13**: p. 47-56.
171. Leippe, D., Sobol, M., Vidugiris, G., Cali, J. J., & Vidugiriene, J. , *Bioluminescent Assays for Glucose and Glutamine Metabolism: High-Throughput Screening for Changes in Extracellular and Intracellular Metabolites.* SLAS discovery : advancing life sciences R & D, 2017. **22**(4): p. 366-377.
172. Obara-Michlewska, M., Ding, F., Popek, M., Verkhratsky, A., Nedergaard, M., Zielinska, M., & Albrecht, J. , *Interstitial ion homeostasis and acid-base balance*

are maintained in oedematous brain of mice with acute toxic liver failure. . Neurochemistry international, 2018. **118**(286-291).
173. Organ, S.L., & Tsao, M. S. , *An overview of the c-MET signaling pathway. .* Therapeutic advances in medical oncology, 2011. **3**: p. S7–S19.
174. Yao, M., et al., *CCR2 Chemokine Receptors Enhance Growth and Cell-Cycle Progression of Breast Cancer Cells through SRC and PKC Activation.* Molecular Cancer Research, 2019. **17**(2): p. 604-617.
175. Hanke, J.H., Gardner, J. P., Dow, R. L., Changelian, P. S., Brissette, W. H., Weringer, E. J., Pollok, B. A., & Connelly, P. A. , *Discovery of a novel, potent, and Src family-selective tyrosine kinase inhibitor. Study of Lck- and FynT-dependent T cell activation. .* The Journal of biological chemistry, 1996. **271**: p. 695–701.
176. Birchmeier, C., Birchmeier, W., Gherardi, E., & Vande Woude, G. F. , *Met, metastasis, motility and more.* Nature reviews. Molecular cell biology,, 2003 **4**(12): p. 915-925.
177. Stefan, M., Koch, A., Mancini, A., Mohr, A., Weidner, K. M., Niemann, H., & Tamura, T. , *Src homology 2-containing inositol 5-phosphatase 1 binds to the multifunctional docking site of c-Met and potentiates hepatocyte growth factor-induced branching tubulogenesis.* The Journal of biological chemistry, 2001. **276**(5): p. 3017-3023.
178. Yan SB, P.V., Ajamie R, Buchanan SG, Graff JR, Heidler SA, Hui YH, Huss KL, Konicek BW, Manro JR, Shih C, Stewart JA, Stewart TR, Stout SL, Uhlik MT, Um SL, Wang Y, Wu W, Yan L, Yang WJ, Zhong B, Walgren RA., *LY2801653 is an orally bioavailable multi-kinase inhibitor with potent activity against MET, MST1R, and other oncoproteins, and displays anti-tumor activities in mouse xenograft models.*
Investigational New Drugs, 2013. **31**(4): p. 833-44.
179. Konicek BW, C.A., Credille KM, Ebert PJ, Falcon BL, Heady GL, Patel BKR, Peek VL, Stephens JR, Stewart JA, Stout SL, Timm DE, Um SL, Willard MD, Wulur IH, Zeng Y, Wang Y, Walgren RA, Betty Yan SC. , *Merestinib (LY2801653) inhibits neurotrophic receptor kinase (NTRK) and suppresses growth of NTRK fusion bearing tumors.* Oncotarget, 2018. **9**(17): p. 13796-13806.
180. Kosciuczuk, E.M., Saleiro, D., Kroczynska, B., Beauchamp, E. M., Eckerdt, F., Blyth, G. T., Abedin, S. M., Giles, F. J., Altman, J. K., & Platanias, L. C. , *Merestinib blocks Mnk kinase activity in acute myeloid leukemia progenitors and exhibits antileukemic effects in vitro and in vivo.* Blood, 2016. **128**(3): p. 410-414.
181. Wu, W., Bi, C., Credille, K. M., Manro, J. R., Peek, V. L., Donoho, G. P., Yan, L., Wijsman, J. A., Yan, S. B., & Walgren, R. A. , *Inhibition of tumor growth and metastasis in non-small cell lung cancer by LY2801653, an inhibitor of several oncokinases, including MET. .* Clinical cancer research : an official journal of the American Association for Cancer Research, 2013. **19**(20): p. 5699-5710.
182. Gazdar, A.F., Kurvari, V., Virmani, A., Gollahon, L., Sakaguchi, M., Westerfield, M., Kodagoda, D., Stasny, V., Cunningham, H. T., Wistuba, I. I., Tomlinson, G., Tonk, V., Ashfaq, R., Leitch, A. M., Minna, J. D., & Shay, J. W. , *Characterization of paired tumor and non-tumor cell lines established from patients with breast cancer. .* International journal of cancer, 1998. **78**(6): p. 766-774.

183. Kao, J., Salari, K., Bocanegra, M., Choi, Y. L., Girard, L., Gandhi, J., Kwei, K. A., Hernandez-Boussard, T., Wang, P., Gazdar, A. F., Minna, J. D., & Pollack, J. R., *Molecular profiling of breast cancer cell lines defines relevant tumor models and provides a resource for cancer gene discovery.* PloS one, , 2009. **4**(7): p. e6146.
184. Cailleau, R., Olivé, M., & Cruciger, Q. V., *Long-term human breast carcinoma cell lines of metastatic origin: preliminary characterization.* In vitro, , 1978. **14**(11): p. 911-915.
185. Dai, X., Cheng, H., Bai, Z., & Li, J. , *Breast Cancer Cell Line Classification and Its Relevance with Breast Tumor Subtyping.* Journal of Cancer, , 2017. **8**(16): p. 3131-3141.
186. Charafe-Jauffret, E., et al., *Gene expression profiling of breast cell lines identifies potential new basal markers.* Oncogene, 2006. **25**(15): p. 2273-2284.
187. TeSlaa T, T.M., *Techniques to monitor glycolysis. .* Methods Enzymol., 2014. **542**: p. 91-114.
188. JE., W., *Hexokinases. Rev.* Physiol Biochem Pharmacol., 1995: p. 126:65-198.
189. Jiang, S., Zhang, L. F., Zhang, H. W., Hu, S., Lu, M. H., Liang, S., Li, B., Li, Y., Li, D., Wang, E. D., & Liu, M. F. , *A novel miR-155/miR-143 cascade controls glycolysis by regulating hexokinase 2 in breast cancer cells. .* The EMBO journal, 2012. **31**(8): p. 1985–1998.
190. Nelson, D.L., & Cox, M. M. (2017), *Lehninger principles of biochemistry*, ed. W.H. Freeman. 2017.
191. Dombrauckas JD, S.B., Mesecar AD. , *Structural basis for tumor pyruvate kinase M2 allosteric regulation and catalysis.* Biochemistry., 2005. **44**(27): p. 9417-29.
192. Lüftner D, M.J., Akrivakis C, Geppert R, Petrides PE, Wernecke KD, Possinger K., *Tumor type M2 pyruvate kinase expression in advanced breast cancer.* Anticancer Res., 2000. **20**(6D): p. 5077-82.
193. Du, Z., Lovly, C.M. , *Mechanisms of receptor tyrosine kinase activation in cancer.* Mol Cancer, 2018. **17**(58): p. 12943-018-0782-4.
194. Daub, H., Weiss, F. U., Wallasch, C., & Ullrich, A. , *Role of transactivation of the EGF receptor in signalling by G-protein-coupled receptors. .* Nature, 1996. **379**(6565): p. 557-560.
195. Di Liberto, V., Mudò, G., & Belluardo, N. , *Crosstalk between receptor tyrosine kinases (RTKs) and G protein-coupled receptors (GPCR) in the brain: Focus on heteroreceptor complexes and related functional neurotrophic effects.* Neuropharmacology, 2019. **152**(67-77).
196. Kilpatrick, L.E., and Hill, Stephen J., *Transactivation of G protein-coupled receptors (GPCRs) and receptor tyrosine kinases (RTKs): Recent insights using luminescence and fluorescence technologies,* , in *Current Opinion in Endocrine and Metabolic Research,*. 2021. p. 102-112.
197. Watson, L.J., Alexander, K. M., Mohan, M. L., Bowman, A. L., Mangmool, S., Xiao, K., Naga Prasad, S. V., & Rockman, H. A. , *Phosphorylation of Src by phosphoinositide 3-kinase regulates beta-adrenergic receptor-mediated EGFR transactivation.* Cellular signalling, , 2016. **28**(10): p. 1580–1592.
198. Kasina, S., Scherle, P. A., Hall, C. L., & Macoska, J. A., *ADAM-mediated amphiregulin shedding and EGFR transactivation. .* Cell proliferation, 2009. **42**(6): p. 799–812.

199. Cheng, Y., Song, Y., Qu, J., Che, X., Song, N., Fan, Y., Wen, T., Xu, L., Gong, J., Wang, X., Zhang, C., Qu, X., & Liu, Y., *The Chemokine Receptor CXCR4 and c-MET Cooperatively Promote Epithelial-Mesenchymal Transition in Gastric Cancer Cells.* Translational oncology, , 2018. **11**(2): p. 487-497.
200. Linklater, E.S., Tovar, E. A., Essenburg, C. J., Turner, L., Madaj, Z., Winn, M. E., Melnik, M. K., Korkaya, H., Maroun, C. R., Christensen, J. G., Steensma, M. R., Boerner, J. L., & Graveel, C. R. , *Targeting MET and EGFR crosstalk signaling in triple-negative breast cancers.* Oncotarget, 2016. **7**(43): p. 69903–69915. .
201. Lehmann, B.D., Bauer, J. A., Chen, X., Sanders, M. E., Chakravarthy, A. B., Shyr, Y., & Pietenpol, J. A., *Identification of human triple-negative breast cancer subtypes and preclinical models for selection of targeted therapies. .* The Journal of clinical investigation, 2011. **121**(7): p. 2750-2767.
202. Barnabas, N., & Cohen, D. , *Phenotypic and Molecular Characterization of MCF10DCIS and SUM Breast Cancer Cell Lines.* International journal of breast cancer, 2013. **2013**.
203. Yan, S.B., Um, S. L., Peek, V. L., Stephens, J. R., Zeng, W., Konicek, B. W., Liu, L., Manro, J. R., Wacheck, V., & Walgren, R. A. , *MET-targeting antibody (emibetuzumab) and kinase inhibitor (merestinib) as single agent or in combination in a cancer model bearing MET exon 14 skipping.* Investigational new drugs, 2018. **36**(4): p. 536-544.
204. Sun, R.C., Fan, T. W. M., Deng, P., Higashi, R. M., Lane, A. N., Le, A.-T., Scott, T. L., Sun, Q., Warmoes, M. O., & Yang, Y. , *Noninvasive liquid diet delivery of stable isotopes into mouse models for deep metabolic network tracing.* Nature Communications, 2017. **8**(1): p. 1646.
205. Sun Y, B.M., Lofton T, Smith M, Bristow CA, Carugo A, Rogers N, Leonard P, Chang Q, Mullinax R, Han J, Shi X, Seth S, Meyers BA, Miller M, Miao L, Ma X, Feng N, Giuliani V, Geck Do M, Czako B, Palmer WS, Mseeh F, Asara JM, Jiang Y, Morlacchi P, Zhao S, Peoples M, Tieu TN, Warmoes MO, Lorenzi PL, Muller FL, DePinho RA, Draetta GF, Toniatti C, Jones P, Heffernan TP, Marszalek JR. , *Functional Genomics Reveals Synthetic Lethality between Phosphogluconate Dehydrogenase and Oxidative Phosphorylation. .* Cell Reports, 2019. **26**(2): p. 469-482.e5.
206. Mardekian, S.K., Bombonati, A., & Palazzo, J. P. , *Ductal carcinoma in situ of the breast: the importance of morphologic and molecular interactions.* Human pathology, 2016. **49**: p. 114-123.
207. Rahman, M., & Hasan, M. R. , *Cancer Metabolism and Drug Resistance.* metabolites 2015. **5**(4): p. 571–600.
208. Lui, V.W., Wong, E. Y., Ho, K., Ng, P. K., Lau, C. P., Tsui, S. K., Tsang, C. M., Tsao, S. W., Cheng, S. H., Ng, M. H., Ng, Y. K., Lam, E. K., Hong, B., Lo, K. W., Mok, T. S., Chan, A. T., & Mills, G. B. , *Inhibition of c-Met downregulates TIGAR expression and reduces NADPH production leading to cell death.* Oncogene, 2011. **30**(9): p. 1127–1134.
209. Tang, Z., Du, R., Jiang, S., Wu, C., Barkauskas, D. S., Richey, J., Molter, J., Lam, M., Flask, C., Gerson, S., Dowlati, A., Liu, L., Lee, Z., Halmos, B., Wang, Y., Kern, J. A., & Ma, P. C. , *Dual MET-EGFR combinatorial inhibition against T790M-*

EGFR-mediated erlotinib-resistant lung cancer. . British journal of cancer, 2008. **99**(6): p. 911–922
210. Nagy Á, M.G., Győrffy B. , *Pancancer survival analysis of cancer hallmark genes.* Sci Rep. , 2021. **15**(1): p. 6047.
211. Szász, A.M., Lánczky, A., Nagy, Á., Förster, S., Hark, K., Green, J. E., Boussioutas, A., Busuttil, R., Szabó, A., & Győrffy, B. , *Cross-validation of survival associated biomarkers in gastric cancer using transcriptomic data of 1,065 patients.* Oncotarget,, 2016. **7**(31): p. 49322–49333.
212. Bièche I, C.M., Lidereau R. , Infrequent mutations of the MET gene in sporadic breast tumours. Int J Cancer., 1999. **82**(6): p. 908-10.
213. Carracedo A, E.K., Salido M, Rojo F, Corominas JM, Arumi M, Corzo C, Tusquets I, Espinet B, Rovira A, Albanell J, Szollosi Z, Serrano S, Solé F. , *FISH and immunohistochemical status of the hepatocyte growth factor receptor (c-Met) in 184 invasive breast tumors. .* Breast Cancer Res. , 2009. **11**(2): p. 402.
214. Gonzalez-Angulo, A.M., Chen, H., Karuturi, M. S., Chavez-MacGregor, M., Tsavachidis, S., Meric-Bernstam, F., Do, K. A., Hortobagyi, G. N., Thompson, P. A., Mills, G. B., Bondy, M. L., & Blumenschein, G. R., Jr., *Frequency of mesenchymal-epithelial transition factor gene (MET) and the catalytic subunit of phosphoinositide-3-kinase (PIK3CA) copy number elevation and correlation with outcome in patients with early stage breast cancer.* Cancer,, 2013. **119**(1): p. 7-15.
215. Ethan Cerami, J.G., Ugur Dogrusoz, Benjamin E. Gross, Selcuk Onur Sumer, Bülent Arman Aksoy, Anders Jacobsen, Caitlin J. Byrne, Michael L. Heuer, Erik Larsson, Yevgeniy Antipin, Boris Reva, Arthur P. Goldberg, Chris Sander and Nikolaus Schultz, *The cBio Cancer Genomics Portal: An Open Platform for Exploring Multidimensional Cancer Genomics Data.* Cancer Discovery, 2012. **2**(5): p. 401-404.
216. Gao J, A.B., Dogrusoz U, Dresdner G, Gross B, Sumer SO, Sun Y, Jacobsen A, Sinha R, Larsson E, Cerami E, Sander C, Schultz N., *Integrative analysis of complex cancer genomics and clinical profiles using the cBioPortal.* Sci Signal. , 2013. **2**(6): p. 269.
217. Brummer G, F.W., Smart C, Zinda B, Alissa N, Berkland C, Miller D, Cheng N. , *CCR2 signaling in breast carcinoma cells promotes tumor growth and invasion by promoting CCL2 and suppressing CD154 effects on the angiogenic and immune microenvironments.* Oncogene., 2020. **39**(11): p. 2275-2289.
218. Lim, A.R., Rathmell, W. K., & Rathmell, J. C., *The tumor microenvironment as a metabolic barrier to effector T cells and immunotherapy.* eLife,, 2020. **9**: p. e55185.
219. Wang, R., Ferrell, L. D., Faouzi, S., Maher, J. J., & Bishop, J. M., *Activation of the Met receptor by cell attachment induces and sustains hepatocellular carcinomas in transgenic mice. .* The Journal of cell biology, 2001. **153**(5): p. 1023–1034.
220. Francone TD, L.R., Chen CT, Sun MY, Kuntz EJ, Zeng Z, Dematteo RP, Paty PB, Weiser MR. , *Novel xenograft model expressing human hepatocyte growth factor shows ligand-dependent growth of c-Met-expressing tumors. .* Mol Cancer Ther., 2007. **6**(4): p. 1460-6.

221. Wheaton, W.W., & Chandel, N. S., *Hypoxia. 2. Hypoxia regulates cellular metabolism. .* American journal of physiology., 2011. **300**(3): p. C385–C393.
222. Hara S, N.K., Klosek SK, Ishikawa T, Shintani S, Hamakawa H. , *Hypoxia enhances c-Met/HGF receptor expression and signaling by activating HIF-1alpha in human salivary gland cancer cells.* Oral Oncol., 2006. **42**(6): p. 593-8.
223. Matsumura, A., Kubota, T., Taiyoh, H., Fujiwara, H., Okamoto, K., Ichikawa, D., Shiozaki, A., Komatsu, S., Nakanishi, M., Kuriu, Y., Murayama, Y., Ikoma, H., Ochiai, T., Kokuba, Y., Nakamura, T., Matsumoto, K., & Otsuji, E. , *HGF regulates VEGF expression via the c-Met receptor downstream pathways, PI3K/Akt, MAPK and STAT3, in CT26 murine cells. .* International journal of oncology,, 2013. **42**(2): p. 535–542.
224. Jagannathan NR, S.U., *Breast Tissue Metabolism by Magnetic Resonance Spectroscopy.* Metabolites, 2017. **7**(2).
225. Martín Noguerol T, S.-G.J., Martínez Barbero JP, García-Figueiras R, Baleato-González S, Luna A., *Clinical Imaging of Tumor Metabolism with ¹H Magnetic Resonance Spectroscopy.* Magnetic Resonance Imaging Clinics of North America, 2016. **24**(1): p. 57-86.
226. Kanda H, Tateya S, Tamori Y, Kotani K, Hiasa K, Kitazawa R, Kitazawa S, Miyachi H, Maeda S, Egashira K, Kasuga M. MCP-1 contributes to macrophage infiltration into adipose tissue, insulin resistance, and hepatic steatosis in obesity. J Clin Invest. 2006;116(6):1494-505. PubMed PMID: 16691291.
227. Huang R, Zong X. Aberrant cancer metabolism in epithelial-mesenchymal transition and cancer metastasis: Mechanisms in cancer progression. Critical reviews in oncology/hematology. 2017;115:13-22. doi: 10.1016/j.critrevonc.2017.04.005. PubMed PMID: 28602165.